Improving real-time fast-scan cyclic voltammetry serotonin detection to understand different antidepressant and genetic effects in *Drosophila melanogaster*

Kelly Dunham

Cookeville, Tennessee, United States

Bachelor of Science,

Tennessee Technology University,

Cookeville, Tennessee, United States, 2018

A Dissertation Presented to the Graduate Faculty of the University of Virginia in Candidacy for the Degree of Doctor of Philosophy

Department of Chemistry

University of Virginia

April 2023

Abstract

Depression is a common mental illness. However, current treatment options are extremely variable from person to person. The main neurochemical target of interest for common selective serotonin reuptake inhibitors (SSRIs) is the serotonin transporter (SERT) on serotonin neurons. SSRIs bind to SERT and cause extracellular serotonin concentrations to increase. However, it is not clear if all antidepressants share this mechanism of action. Further, it is not understood how different genetic polymorphisms to the gene that encodes SERT affect its structure and function, which impacts antidepressant activity. Currently, it is difficult to study depression because of a lack of biological models and accurate analytical techniques that measure real-time serotonin changes. Fast-scan cyclic voltammetry (FSCV) is a common electrochemical technique that measures neurotransmitters in brain tissue with rapid temporal resolution, however it possesses unique issues with serotonin because it polymerizes onto electrodes and ruins accurate measurements. Also, *Drosophila melanogaster*, the fruit fly, has not been previously investigated to explore serotonin changes with antidepressants. Thus, this dissertation aims to improve fast-scan cyclic voltammetry (FSCV) detection of serotonin to understand different antidepressant and genetic effects in *Drosophila* brain tissue.

In this thesis, Chapter 1 introduces the current literature surrounding depression, current treatments, real-time electrochemical serotonin measurement techniques, and *Drosophila melanogaster*. Chapter 2 explores different FSCV waveforms to understand electrode fouling to serotonin and its major metabolite, 5- hydroxindoleacetic acid, to improve real-time serotonin detection. Chapter 3 uses these new techniques and compares serotonin concentration and reuptake changes with common SSRIs: fluoxetine, escitalopram, paroxetine, and citalopram, to understand their individual mechanisms of action. Chapter 4 explores changes in serotonin with ketamine compared to SSRIs to determine differences in their serotonin mechanisms, as well as downstream effects with feeding and locomotion behaviors. Finally, Chapter 5 covers initial data from different genetic mutations to SERT compared to data collected in Chapters 3-4. Two *Drosophila* SERT mutant lines were used with specific point mutations or partial gene knock-outs, and FSCV and optogenetics will be used in the future to compare serotonin release and reuptake changes for SSRIs and micro-dose ketamine therapies.

Overall, my dissertation improves analytical detection of serotonin in brain tissue with FSCV, and applies these techniques to understand biological differences between several antidepressant drugs. We show that serotonin release and reuptake changes are unique for different antidepressants and cause dose-dependent behavior changes. This work benefits others in analytical chemistry and neurochemistry who will use these techniques and models to explore new antidepressant therapies or other neurotransmitters, like dopamine and glutamate, to help design and implement successful treatments for those who suffer from depression.

Professional Acknowledgements

We thank Dr. Mimi Shin and Dr. Pumidech (Max) Puthongkham (University of Virginia, Chemistry) for their time training with FSCV instrumentation and *Drosophila* techniques (Chapter 2). We thank Dr Jeffery Copeland (Eastern Mennonite University, Biology) for his guidance on *Drosophila* genetic manipulations (Ch. 2-4). We also thank Dr. Jay Hirsh (University of Virginia, Biology) for the tph-Gal4 fly line (Ch. 2) and advice on *Drosophila* larvae feeding and locomotion assays (Ch. 4). MAE Rapid Prototyping and Machine Labs (University of Virginia, Engineering) was used for 3D-printing (Ch.4). Undergraduates Leah Weizman and Kani Khaled assisted with optogenetic and feeding experiments (Ch. 4). This work was funded by NIH R01MH085159.

This thesis produced two published articles: Chapter 2) Improving serotonin fast-scan cyclic voltammetry detection: new waveforms to reduce electrode fouling. 2020. *Analyst*. DOI: 10.1039/d0an01406k and Chapter 3) SSRI antidepressants differentially modulate serotonin reuptake and release in *Drosophila*. 2022. *Journal of Neurochemistry*. DOI: 10.1111/jnc.15658.

Sappy Acknowledgments

I would like to thank my mom and dad, Amy and Jim Dunham. I owe all of my successes to their hard work, endless encouragement, and support. I am eternally grateful to my sister, Kiki Dunham, and life-long friends, Phuong Truong and Debra Rios, for bringing so much joy to my life and reminding me to take a moment and live a little. I also dedicate this work to my dogs: Roxy, Elvis, and Gigi, and my cats: Xander, Maggie, Lucy, and Suzie. Thanks for hanging out with me through all the late nights studying and writing over the years.

Thank you to my mentor, Dr. Mimi Shin, for her patience and wisdom, and for teaching me everything in lab. I also thank Drs. Qun Cao, Yuanyu Chang, Malli Ganesana, Pumidech (Max) Puthongkham, and Zijun Shao, as well as Greatness Olaitan, Kailash Shrestha, Zhixi (Joy) Xu, and He (Oliver) Zhao, for all the happy memories we created over the years.

Thank you, too, to our undergraduate researchers, Leah Weizman, Kani Khaled, Courtney Vetter, and Sam Hanser, whose brilliance, excitement, and determination inspire me to be a better mentor and scientist. I know you will do great things.

Thank you to my committee members: Drs. David Cafiso, Jay Hirsh, James Landers, and Rebecca Pompano for your knowledge, guidance, and assistance that helped me improve this thesis.

Finally, I thank my advisor, Dr. Jill Venton, for her invaluable mentorship. I am grateful for all the life advice she has given me and everything she has taught me over the last five years. Thank you for making me a better scientist, writer, and teacher.

Table of Contents

Improving real-time fast-scan cyclic voltammetry serotonin detection to understand different antidepressant and genetic effects in *Drosophila melanogaster* 1

Abstract 2

Professional Acknowledgements 3

Sappy Acknowledgments 3

Chapter 1: Introduction 7

1.1 Serotonin and Depression 8

1.1.1 Serotonin neurobiology and neurochemistry 8

1.1.2 Depression 12

1.1.3 SSRI antidepressants 13

1.1.4 Genetic effects with depression and SSRIs 15

1.1.5 Treatment resistant depression and micro-dosing ketamine 17

1.2 Electrochemical Methods for Serotonin Detection 20

1.2.1 Electrochemical detection of neurotransmitters 20

1.2.2 Common sampling and electrochemical methods 20

1.2.3 Fast-scan cyclic voltammetry 23

1.2.4 Issues with serotonin FSCV detection 25

1.2.5 Previous FSCV and electrochemical serotonin research in mammals 27

1.3 *Drosophila melanogaster* 28

1.3.1 *D. melanogaster* as a model organism 28

1.3.2 *D. melanogaster* genetic tools 31

1.3.3 *D. melanogaster* as a model for neuroscience research 34

1.3.4 *D. melanogaster* locomotion and feeding behavioral assays in larvae and adults 37

1.3.5 Previous real-time serotonin electrochemical research with *D. melanogaster* 41

1.4 Overview of Dissertation 43

1.5 References 45

Chapter 2: Improving serotonin FSCV detection: new waveforms to reduce electrode fouling 56

2.1 Introduction 58

2.2 Experimental Methods 60

2.2.1 Chemicals 60

2.2.2 Microelectrode Preparation 60

2.2.3 Electrochemical Instrumentation 60

2.2.4 Waveform Parameters 62

2.2.5 *Drosophila melanogaster* Experiments 62

2.2.6 Serotonin Imaging in Larvae Ventral Nerve Cords 63

2.2.7 Statistics 63

2.3 Results and Discussion 64
2.3.1 Waveform Characteristics 64
2.3.2 Repeated serotonin measurement fouling 66
2.3.3 Fouling after long exposure to 5-hydroxyindoleacetic acid 68
2.3.4 Waveform sensitivity and selectivity determination 71
2.3.5 Characterization of optogenetically-stimulated serotonin release…in *Drosophila* ventral nerve cords 73
2.3.6 Comparison of serotonin waveforms and future applications 75
2.4 Conclusions 77
2.5 References 77
Chapter 3: SSRI antidepressants differentially modulate serotonin reuptake and release in *Drosophila* 80
3.1 Introduction 82
3.2 Experimental Methods 84
3.2.1 Chemicals 84
3.2.2 Microelectrode Preparation 85
3.2.3 Electrochemical Instrumentation 85
3.2.4 Tissue Preparation for *in vitro* Experiments 85
3.2.5 Optogenetic Serotonin Release 86
3.2.6 Serotonin GFP Imaging in Larvae Ventral Nerve Cords 86
3.2.7 Statistics 87
3.3 Results 87
3.3.1 Characterization of SSRI antidepressants in *Drosophila* with fast-scan cyclic voltammetry 87
3.3.2 Escitalopram increases serotonin reuptake and concentration more than citalopram 89
3.3.3 Paroxetine elicits high serotonin concentration changes, but less change in reuptake 92
3.3.4 Fluoxetine slows serotonin reuptake, but does not affect serotonin concentration 93
3.3.5 SSRIs show differences in serotonin concentration, reuptake, and SERT affinity 94
3.4 Discussion 101
3.4.1 SSRIs differ in their effects on serotonin reuptake 101
3.4.2 Serotonin concentration changes are coupled with reuptake for some SSRIs, but independent for others 104
3.4.3 Comparison of SSRIs 104
3.4.4 Future applications in *Drosophila* to understand genetic effects on SSRI efficacy 105
3.5 Conclusions 106
3.6 References 106
Chapter 4: Microdosing ketamine increases locomotion and feeding in *Drosophila*, but does not affect serotonin like SSRIs 111
4.1 Introduction 113
4.2 Experimental Methods 115
4.2.1 Chemicals 115
4.2.2 Microelectrode preparation 115

4.2.3 Electrochemical instrumentation 115
4.2.4 Ventral nerve cord tissue preparation for optogenetic *in vitro* experiments 116
4.2.5 Optogenetic serotonin release 116
4.2.6 Feeding antidepressants to larvae for FSCV optogenetic experiments 117
4.2.7 UV-Vis dye tracer food consumption determination with different antidepressants 118
4.2.8 Real-time *Drosophila* larvae locomotion tracking 118
4.2.9 Statistics and data analysis 118
4.3 Results 119
4.3.1 Ketamine and SSRIs show differences in serotonin release, reuptake, and dSERT affinity 119
4.3.2 Ketamine does not affect serotonin release or reuptake at low doses compared to SSRIs after 24 hours 122
4.3.3 Ketamine mainly affects serotonin release at mid-doses, while SSRIs affect reuptake after 24 hours 124
4.3.4 High doses of ketamine and fluoxetine inhibit SERT to increase serotonin after 24 hours 125
4.3.5 Low doses of ketamine and escitalopram increase feeding behaviors 126
4.3.6 Low doses of ketamine, escitalopram, and fluoxetine increase locomotion behaviors 127
4.4 Discussion 129
4.4.1 Ketamine and SSRIs show different serotonin changes that are dose-dependent 129
4.4.2 Ketamine and SSRIs change feeding and locomotion similarly, even though serotonin changes are different 130
4.4.3 Comparison of ketamine and SSRI behavioral data to the literature 131
4.4.4 Future applications in *Drosophila* to understand serotonin receptor and dSERT effects with antidepressants 133
4.5 Conclusions 133
4.6 References 134
Chapter 5: Conclusions and future directions 138
5.1 Contributions of this dissertation to the field 139
5.1.1 Improved fast-scan cyclic voltammetry waveforms for serotonin and dopamine detection 139
5.1.2 Using serotonin FSCV detection to elucidate different antidepressant mechanisms of action and their downstream effects on behaviors 140
5.2 Challenges and future directions 141
5.2.1 Investigating *D. melanogaster* serotonin transporter mutations to understand genetic and behavior effects with ketamine and SSRIs 141
5.2.2 Using *in vivo* FSCV serotonin detection and glutamate genetic sensors to explore SERT and serotonin receptor genetic effects with ketamine and SSRIs 143
5.3 Final Remarks 146
5.4 References 147
Appendix 150
List of publications for this dissertation 150
List of fly lines used in this dissertation 150

Chapter 1

Introduction

1.1 Serotonin and Depression

1.1.1 Serotonin neurobiology and neurochemistry

Serotonin is a monoamine neurotransmitter that regulates many physiological functions and neurological behaviors, such as sleep, mood, and appetite,[1–3] and is also phylogenetically conserved in several species including fruit flies, mice, and humans. Historically, serotonin was first discovered in blood serum more than 70 years ago.[3] More than 95% of serotonin in the human body is located in enterochromaffin cells in the digestive system, however, most serotonin research focuses on its role in neurobiology in the brain.[2,4] Serotonin is synthesized from the diet-derived amino acid tryptophan, and Figure 1A shows the biosynthesis pathway from tryptophan to serotonin. The initial and rate determining step is the conversion of tryptophan to 5-hydroxy-tryptophan (5-HTP) by tryptophan hydroxylase (Trh)[5] Amino acid decarboxylase then converts 5-HTP into serotonin (5-hydroxytryptophan or 5-HT). Serotonin also acts as a precursor to melatonin, which is important for sleep regulation with circadian rhythms (Fig. 1B).[2,4,6] Similar to other monoamine neurotransmitters, monoamine oxidase controls serotonin concentrations in the brain by converting serotonin to 5-hydroxyindole acetic acid (5-HIAA, Fig. 1C).[7] 5-HIAA is approximately 1000x more concentrated than serotonin in brain tissue in mammals.

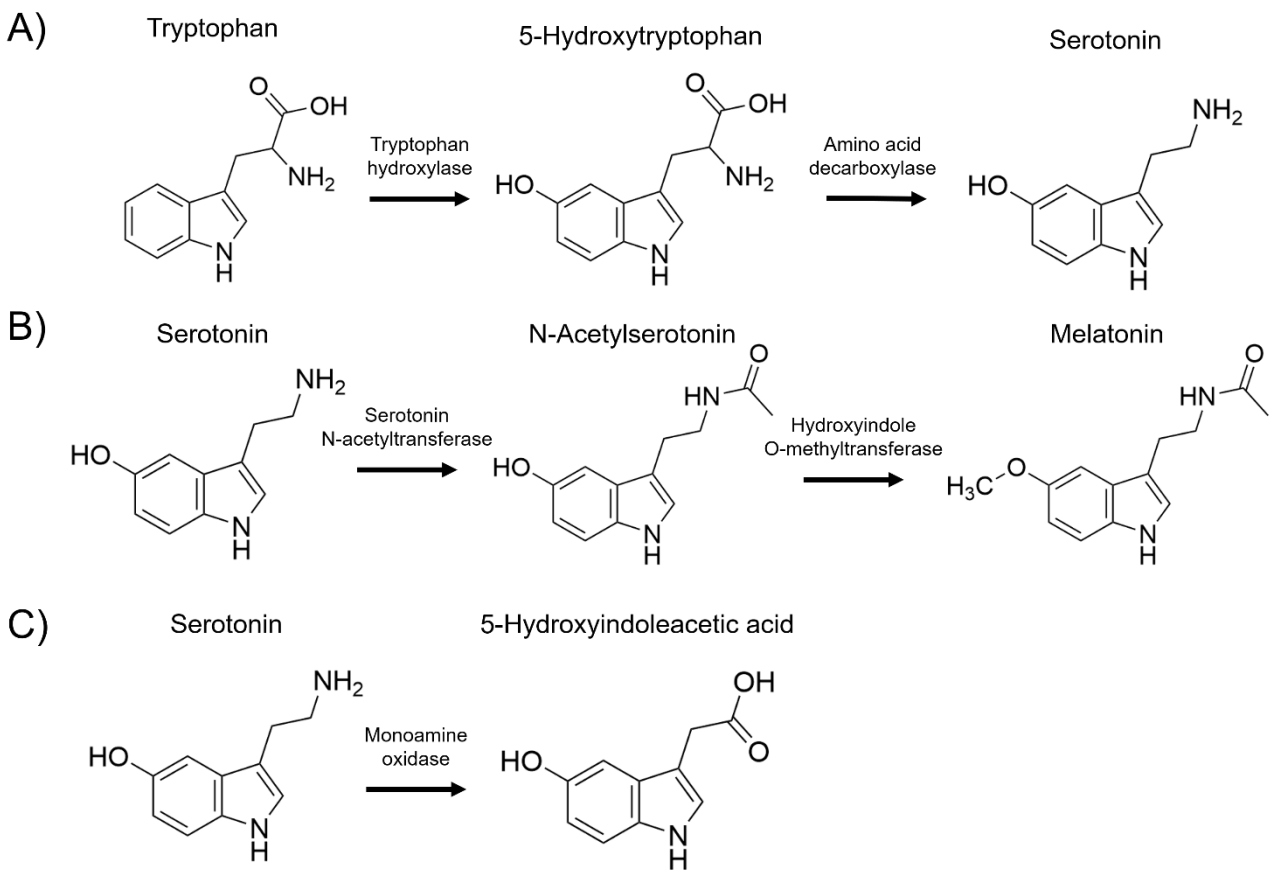

Figure 1. Serotonin formation and byproduct synthesis. **A.** Serotonin is derived from the amino acid tryptophan by the enzyme tryptophan hydroxylase, which produces 5-hydroxytryptophan (5-HTP). Amino acid decarboxylase then removes a carboxyl group from 5-HTP to form serotonin. **B.** Serotonin is a precursor to the monoamine neurotransmitter melatonin. Serotonin N-acetlytransferase and hydroxyindole o-methyltransferase are used to convert serotonin to N-acetylserotonin and then melatonin, respectively. **C.** The metabolic byproduct of serotonin is 5-hydroxyindoleacetic acid (5-HIAA), and it is catalyzed by monoamine oxidase.

When serotonin is released from the digestive system into the blood stream, it is be taken up by platelets where it plays a role in aggregation and vasodilation with clotting and wound healing.[4,8] Tryptophan in the blood travels to the brain where it concentrates in the dorsal raphe nuclei (DRN) of the brain stem, which is illustrated in Figure 2.[4,9] Primarily, serotonin cell bodies radiate from the DRN and other raphe nuclei to the substantia nigra (S), hypothalamus (Hyp), nucleus accumbens (ACN), and medial prefrontal cortex (mPFC). Some serotonin neurons also branch into the thalamus (Tha) and caudate putamen (Cpu).[2,9] These diverse signaling pathways allow serotonin to regulate different behaviors like sleep, mood, memory, and appetite.[2,3,6,10] Serotonin neural circuitry is also similar to dopamine circuitry, and these neurons are found together in several brain regions including the substantia nigra (SN) and CPu.[8,10] In serotonin neurons, serotonin is synthesized from tryptophan intracellularly and is stored in vesicles that are loaded by

the vesicular monoamine transporter (VMAT).[9] For serotonin release, different SNARE complex proteins like SCAMP2, synaptotagmin, synaptobrevin, SNAP-25, and others dock and fuse serotonin vesicles to the intracellular surface that are then emptied into the synaptic cleft between neurons through exocytosis.[4,11]

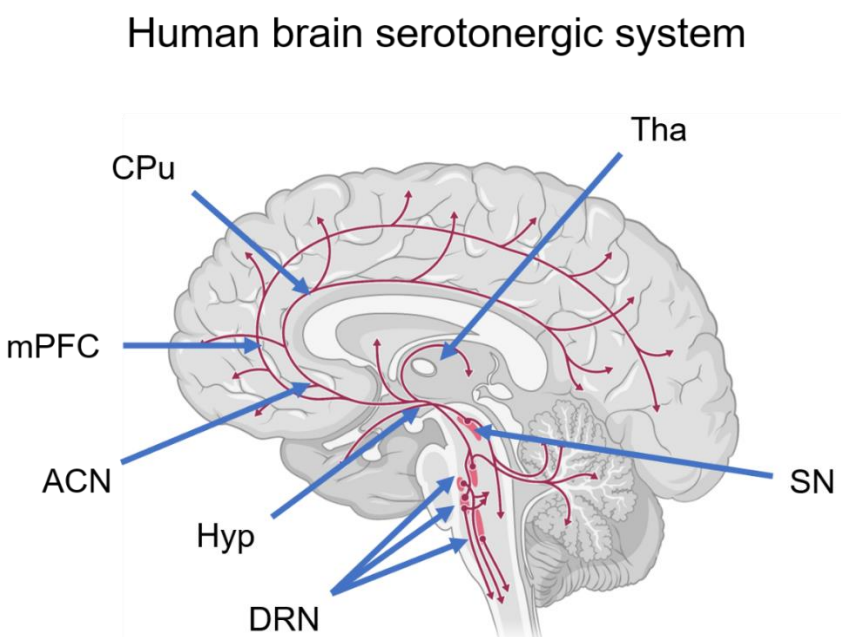

Figure 2. Schematic shows pathways of serotonin neurons in the human brain. The dorsal raphe nuclei (DRN) are located in the brain stem and contain the majority of the serotonin neurons. Axons are colored in red. The axons radiate and branch from the DRN as illustrated. For identification, Hyp = hypothalamus, ACN = nucleus accumubens, mPFC = medial prefrontal cortex, CPu = caudate putamen, Tha = thalamus, and SN = substantia nigra. Serotonin neuron pathways also overlap with dopamine neurons in the ACN, CPu, and SN. Figure created in BioRender.

In order to regulate serotonin exocytosis in presynaptic neurons, the serotonin transporter (SERT) uses a negative feedback loop to reuptake extracellular serotonin back into the neuron to stop serotonin release, which is shown in Figure 3.[1,2,12] SERT is classified as a neurotransmitter sodium symporter transport protein, and shares 50% sequence identity to the norepinephrine transporter (NET) and dopamine transporter (DAT).[4,13] These transporters contain 12 transmembrane helices and rely on the active transport of sodium with an Na+/K+ pump and adenosine triphosphatase to break down ATP.[4,12] This allows serotonin and sodium to translocate into the neuron, and potassium to be translocated out. After reuptake, excess serotonin is either re-packaged into vesicles for release again or destroyed by lysosomes.[4] Ultimately, this process regulates serotonin exocytosis, and SERT's dysfunction is theorized to affect mood and cause depression.

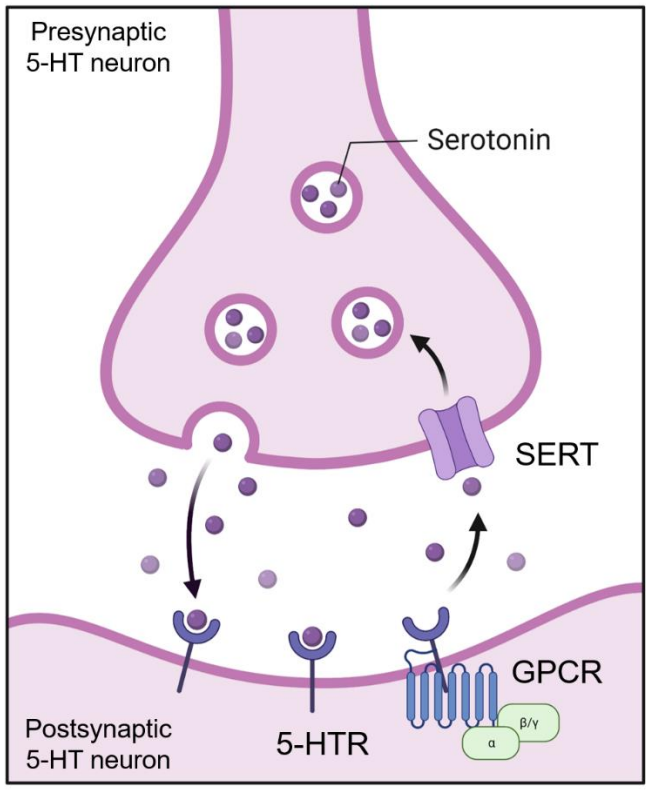

Figure 3. Overview of the molecular mechanisms of 5-HT reuptake in the brain. SERT is found in presynaptic neurons, whereas 5-HT receptors are G-protein coupled receptors that are located on pre- and postsynaptic neurons. In the absence of SSRIs, 5-HT binds to SERT and is recycled to the interior of the presynaptic neuron where it can be repackaged into a vesicle for exocytosis or degraded. Figure created in BioRender.

There are seven classes of serotonin receptors in mammals that regulate serotonin neuron activation and inhibition in the brain that are classified in Table 1.[1,2,14] With the seven receptor classes, all are G-protein coupled receptors (GPCRs), except 5-HT-3 receptors, which are ligand-gated ion channel receptors. The GPCR serotonin receptors are also illustrated in Figure 3.[1,2,4] These receptors act as either autoreceptors or heteroreceptors. Autoreceptors are located on presynaptic neurons and attenuate serotonin release with a negative feedback loop, while heteroreceptors are on post-synaptic neurons and regulate serotonin or other neurotransmitters pre-synaptically or through postsynaptic feedback.[1,2,15] In addition to mammals, *Drosophila melanogaster*, the fruit fly, also possess SERT and serotonin receptors. dSERT contains 51% sequence homology to human SERT (hSERT) and serotonin 1A, 1B, 2A, and 2B receptors that are similar to mammals in structure and function.[16–19] Since SERT and serotonin receptors control serotonin signaling in the brain, their dysfunction causes depression, anxiety, and aggression that are not well understood.[14,15]

Table 1. Serotonin (5-HT) receptor classification, types, and action in humans

Family	Sub-receptor class	Receptor type	Action
5-HT1	A, B, D, E, F	GPCR	Inhibitory
5-HT2	A, B, C	GPCR	Excitatory
5-HT3	-	Ligand-gated ion channel	Excitatory
5-HT4	-	GPCR	Excitatory
5-HT5	A, B	GPCR	Inhibitory
5-HT6	-	GPCR	Excitatory
5-HT7	-	GPCR	Excitatory

1.1.2 Depression

Depression is a common mental illness that affects hundreds of millions of people in the world; 1/16 adults in the United States currently have or have had depression.[1,20] Depression causes overwhelming feelings of sadness and loss of interest that manifest in a range of symptoms with adverse changes to sleep, appetite, and energy. Thoughts of suicide are also common.[21] Historically, depression was not described in the Diagnostic and Statistical Manual of Mental Disorders (DSM) until the 1950s.[22] At that time, antidepressant treatments were not regulated or well understood, so arbitrary drugs were commonly prescribed, like tranquilizers, tricyclic amines, anti-tuberculosis therapies, and thalidomide.[22] The latter of which was discontinued in the 1960s because of severe birth defects in children from pregnant women who took the drug for anxiety. From autopsies of suicide patients, scientists found that their dorsal raphe nuclei were smaller compared to patients that had no committed suicide, and the hippocampus had atrophied.[21] This phenomenon led researchers to develop the monoamine hypothesis of depression that suggests low concentrations of serotonin in the brain create depression symptoms.[20]

The monoamine hypothesis stimulated early research to create antidepressants that change serotonin concentrations in the brain.[20,22] Tricyclic amines (TCAs) were first introduced in the 1950s,[20,22] and decades later, it was discovered that they block serotonin and norepinephrine reuptake and increases their concentrations in the brain to alleviate depression symptoms.[20] However, TCAs cause extremely variable side effects, including heart issues that cause death with high doses.[23,24] Likewise, monoamine

oxidase inhibitors (MAOIs) were also introduced in the 1950s by accident to treat tuberculosis and inhibited the breakdown of serotonin by monoamine oxidase.[20] However, these drugs also cause extremely dangerous side effects and require a strict diet.[23] In the early 1970s, scientists at Eli Lilly designed a new antidepressant that would increase serotonin in the brain by targeting serotonin neurons.[22,25] This led to the discovery of fluoxetine hydrochloride (Prozac), and through two decades of clinical trials, they found that Prozac inhibited SERT to block serotonin reuptake, which was later classified as a selective serotonin reuptake inhibitor (SSRI).[20,25] Still, the exact mechanism of action for Prozac is not currently understood. Other similar drugs were developed soon after, since Prozac showed less severe side effects compared to TCAs and MAOIs, but positive effects were still variable from person to person.[20]

1.1.3 SSRI antidepressants

Fluoxetine hydrochloride (Prozac) was the first SSRI antidepressant marketed in North America in 1986. Created by Eli Lilly, Prozac underwent 16 years of clinical trials to understand its side effects in depressed patients.[25] Through radioligand binding assays of [^{3}H]-5-HT, several initial studies determined that fluoxetine binds to SERT to inhibit serotonin reuptake.[25] Shaskan and Snyder determined Michaelis-Menten kinetics for serotonin and several other antidepressants[25,26] Prozac had less severe side effects compared to TCAs and MAOIs, but showed extremely variable efficacies between patients.[20,25] After fluoxetine (Prozac), the second generation of SSRIs were introduced in the 1990s and early 2000s and include paroxetine (Paxil), and sertraline (Zoloft), citalopram (Celexa), escitalopram (Lexapro), and fluvoxamine (Luvox), which all bind to SERT and inhibit serotonin reuptake and are illustrated in Figure 4 A-G.[27] However, similar to Prozac, these drugs were still variable from person to person.[1]

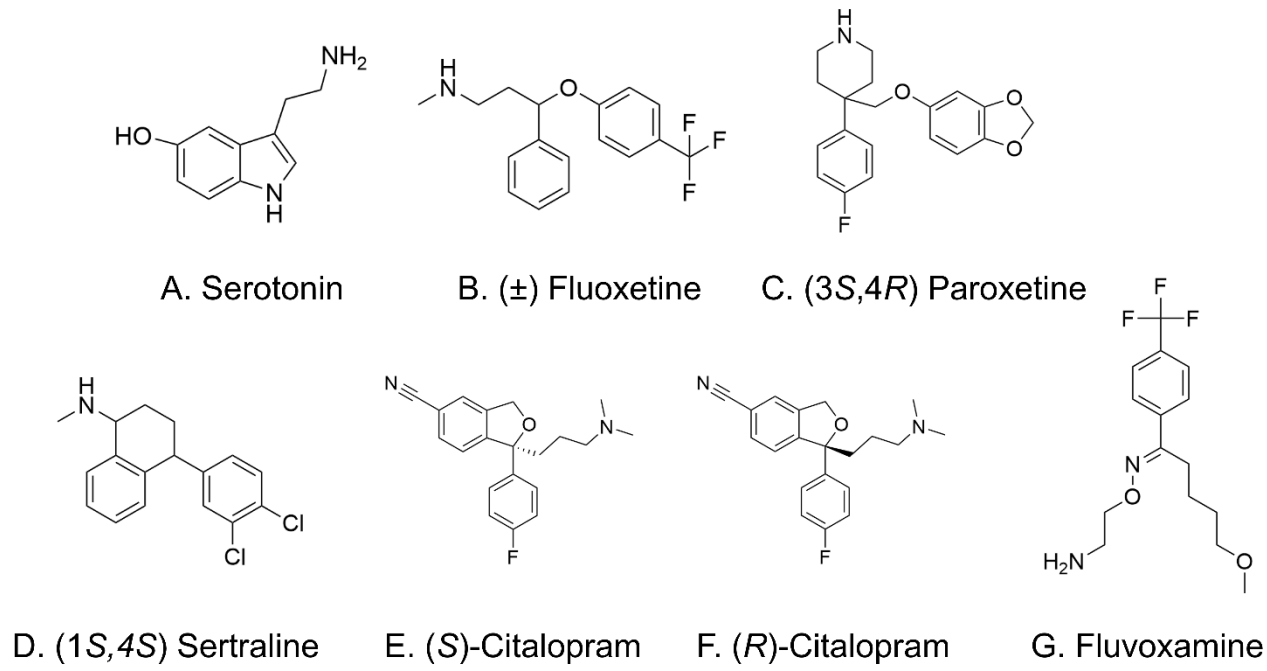

Figure 4. SSRI antidepressants have different chemical structures that cause differences in binding to SERT. **A.** Serotonin is an indolamine monoamine neurotransmitter whose precursor is the amino acid tryptophan. **B.** Fluoxetine (Prozac) is a racemic mixture of (*S*) and (*R*)-fluoxetine. Fluoxetine shares a similar chemical structure to diphenhydramine (Benadryl) and is very different compared to the other SSRIs. **C.** Paroxetine (Paxil) contains a benzodioxole group on a piperdine ring that bears substitutes at the 3 and 4 positions for a (3*S*,4*R*)-diastereomer. **D.** Sertraline (Zoloft) is a tetraline that is substituted at positions 1 and 4 by methylamino and (3*S*,4*S*)-dichlorophenyl groups. **E.** (*S*)-citalopram is the S-enantiomer of citalopram and is exclusively produced as the escitalopram (Lexapro). **F.** (*R*)-citalopram is the (R)-enantiomer of citalopram. Citalopram (Celexa) is a racemic mixture of the (*S*) and (*R*)-enantiomers. **G.** Fluvoxamine (Luvox) is also unique compared to other SSRIs. It is a 2-aminoethyl oxime ether of aralkylketones.

All SSRIs block reuptake of serotonin, but it is not understood if they share the same downstream mechanisms of action.[12,28] Each SSRI possesses vastly different chemical structures that do not share many specific chemical motifs, which are shown in Figure 4. Besides benzene ring structures, SSRIs usually contain halogen groups like fluoride and chloride that create electrostatic interactions to specific amino acids on SERT.[28,29] Several previous molecular modeling and docking simulations found that SSRIs bind to SERT with different affinities because of their different structures.[28,30,31] Historically, dSERT was also used in these molecular modeling studies until the structure of human SERT (hSERT) was discovered in 2016.[32,33] Several of these studies found that drugs like paroxetine (Fig. 4C) and escitalopram (4E) bind to SERT with higher affinity because their ring structures more closely resemble the indole ring structure in serotonin (4A).[12,28,31] Interestingly, fluoxetine has a very different chemical structure compared to other SSRIs, and historically, diphenhydramine (Benadryl) was used a precursor when it was initially designed.[25] It has the lowest binding affinity to SERT and requires higher doses compared to the others.[30] In addition to binding affinity, SERT possesses two binding sites, a primary site and an allosteric site.[12,28] Each SSRI binds to SERT's primary site, but only some bind to its allosteric site, which

affects reuptake inhibition differently. After an SSRI binds to SERT, it also activates different downstream pathways that could increase or decrease serotonin release or SERT expression on the cell surface.[12]

1.1.4 Genetic effects with depression and SSRIs

Although SSRIs bind to SERT with different affinities and may elicit different downstream effects that impact serotonin reuptake and release, another hypothesis focuses on different genetic effects with SERT and 5-HT receptors mutations that result in variable SSRI efficacies in different individuals.[13,34–36] In 1991, the gene that encodes SERT was identified for the first time and this discovery launched new research into how its genetic mutations affect different antidepressant responses and correlate to illnesses like depression.[13,34,37] Figure 5 shows the organization of the human SERT gene and the locations of its common polymorphisms.[38] Figure 5A-C shows the gene map for human SERT with exons (coding regions) colored in blue.[38] Additionally, alternative splicing sites upstream near the promoter region or alternate polyadenylation sites downstream can impact how and what parts of the gene are transcribed through recombination.[13] In the promoter region, the 5HTTLPR mutation is labeled in Figure 5A.[38] The 5HTTLPR allele mutations are composed of either a “short” allele, known as an “S” allele of 14 repeated elements or a “long, L” allele of 16 repeated elements (each 20-23 base pairs).[34] The S and L 5HTTLPR variants differentially modulate transcriptional activity of the SERT promoter, which changes the amount of SERT mRNA and protein expressed (Fig. 5C). This mutation directly affects the amount of serotonin reuptake in the brain.[13] The S allele is also associated with lower SERT expression, and the homozygous SS phenotype is implicated in anxiety and depression-related behaviors.[13] Additionally, a variable number of tandem repeats (VNTR) in the coding region of the gene can possess 9, 10, or 12 copies of 16 to 17-base pair repeats in this domain, which is another common mutation.[13] The longer 12 copies in the VNTR are correlated with upregulated SERT expression than the 9 and 10 copies.[13] Along with these mutations, other common single nucleotide polymorphisms (SNPs) have also been explored. Since mice and *Drosophila* do not have an ortholog for the short and long promoter polymorphisms, mutations can be created by inserting a neo cassette (Fig. 5B) or premature stop codon (5C) to understand these changes to SERT expression.

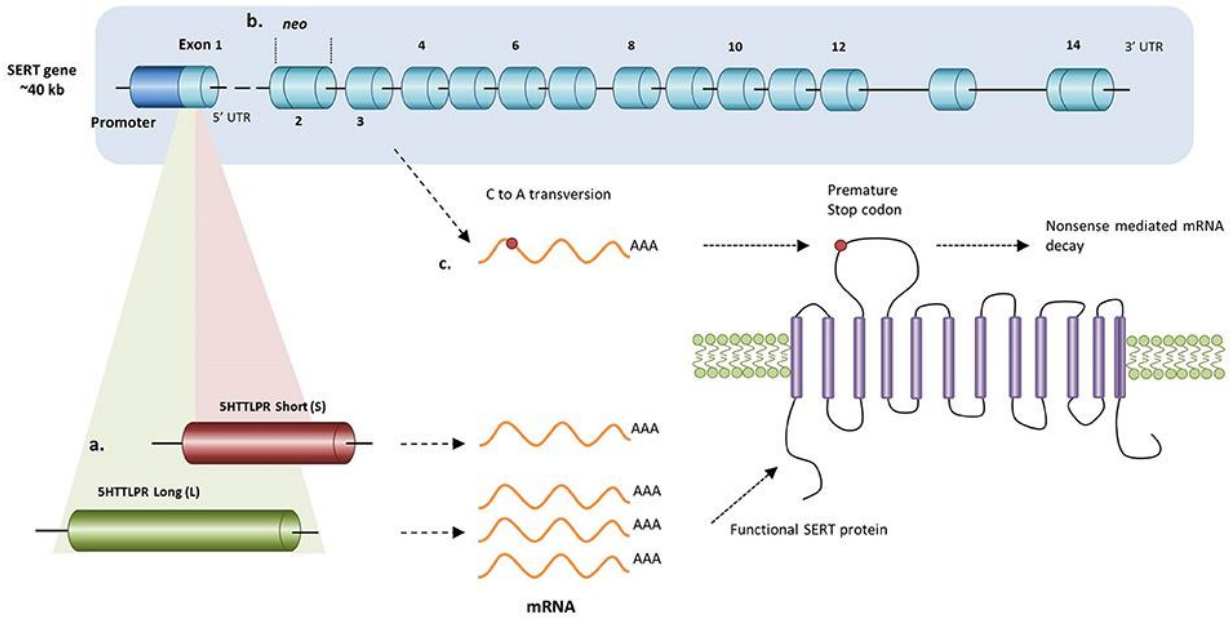

Figure 5. Different alterations in SERT gene expression result in changed transcription levels. **A.** In humans, either a short or long allele for the 5-HTTLPR results in either lower or higher transcription levels respectively. Since rodents and *Drosophila* do not carry an orthologue of this polymorphism, knockout of the SERT can be achieved by (**B**) replacing exon 2 with a neo cassette or by (**C**) inducing a premature stop codon in exon 3 results in the absence of a functional SERT protein. Taken from Houwing, D. J.; Buwalda, B.; Van Der Zee, E. A.; De Boer, S. F.; Olivier, J. D. A. The Serotonin Transporter and Early Life Stress: Translational Perspectives. *Front. Cell. Neurosci*. 2017, 11 (April), 1–16. https://doi.org/10.3389/fncel.2017.00117.

SERT is comprised of 630 amino acids that forms a 12-transmembrane spanning protein, which is illustrated in Figure 5C. A single nucleotide polymorphism (SNPs) is a substitution of a single nucleotide at a specific position on gene, which can produce a mutation when the gene is transcribed and translated. These SNPs are categorized as either synonymous or non-synonymous. Synonymous SNPs are nucleotide codons that code for the same amino acid, while non-synonymous SNPs do not code for the same amino acid and will alter SERT's shape and function when it is translated. When SERT's structure is altered from these mutations, it changes the S1 and S2 binding sites that SSRIs bind to, which will change how they inhibit serotonin reuptake. Molecular modeling and docking simulation studies show that several charged amino acids, including Tyr95, Asp 98, Ser 336, and Ser 438 are important with binding SSRIs to the S1 and S2 binding sites.[28,30,31] Mutations from SNPs in these regions could change how the SSRIs bind and affect serotonin reuptake, which will probably impact the efficacies of these drugs.[13] However, real-time characterization of serotonin reuptake and concentration changes have not been characterized with any of these SERT mutations.

1.1.5 Treatment resistant depression and micro-dosing ketamine

Depression is used as an umbrella term to include serval types of depression, including major depressive disorder (MDD), bipolar depression, postpartum depression, and seasonal affective disorder.[22] Usually, when a patient is diagnosed with depression, he or she may enter into talk therapy and/or start taking an antidepressant, such as an SSRI.[22,39] If the patient does not respond to these treatments over time, this illness progresses into treatment resistant depression.[40,41] It is difficult to diagnose treatment resistant depression because of variable responses to antidepressants from person to person.[40] Generally, a depressed patient can start one SSRI antidepressant, and if they do not see positive responses after several weeks, their medical professional will either prescribe higher doses of the same medication, or prescribe another SSRI.[40] In fact, about one-third of people with MDD and ~50% of people who take SSRIs go into remission for depression after unsuccessfully trying two SSRIs.[39] People with treatment resistant depression fail to positively respond to at least two antidepressants, and are marked as high risk for suicide.[40] Although treatment resistant depression is difficult to diagnose and alleviate, new experimental drug therapies with ketamine suggest that future antidepressants may rely on other neurotransmitter systems besides serotonin, like glutamate, which enables new research to understand different antidepressant responses.[40,41]

In the 1960s, ketamine was first introduced as a safer anesthetic to phencyclidine (PCP).[41,42] Today, ketamine is considered an essential medicine and is commonly used as an anesthetic for humans and animals in surgery.[41,43] It has also been used to treat severe pain after surgeries or with different chronic illnesses.[41] Although ketamine is considered harmless, it is classified as a Schedule III drug because of its abuse potential and diverse psychoactive effects, since sub-anesthetic doses cause transient, dissociative effects that are similar to schizophrenia.[41] In neuroscience, ketamine is known as a “dirty” drug because it binds to a variety of neurotransmitter receptors and transporters in the brain, including serotonin and dopamine.[20,41,44] Formally, though, it is classified as a noncompetitive N-methyl-D-aspartate (NMDA) antagonist, which is part of the glutamatergic system.[20,41–43] In the last three decades, several groups have explored the extent to which ketamine or other NMDA antagonists function as antidepressants at sub-anesthetic doses for patients that suffer with MDD and treatment resistant depression that do not respond to SSRIs.[41]

In 1990, Trullas and Skolnick were the first to suggest NMDA antagonists could be used as antidepressants.[45] They hypothesized a link between depression and the glutamatergic system since stress can cause depression symptoms and pro-longed depression can disrupt long-term potentiation in the hippocampus, which is usually regulated by NMDA receptor activation.[41,45] Thus, they reasoned that NMDA antagonists could inhibit this disruption and act as antidepressants.[41] In the 2000s, early clinical trials showed sub-anesthetic doses of ketamine alleviated depression symptoms when given intravenously.[41,46,47] However, these positive

results for clinical ketamine use were not taken seriously until they were replicated in 2013 in larger, placebo-controlled trials.[41,47] Interestingly, patients showed rapid-onset positive effects with ketamine within 2 hours that were persistent for up to 7 days, which is remarkably different than positive effects reported with conventional SSRIs that take many weeks.[43] Since this discovery, several studies over the last decade have tried to elucidate ketamine's downstream cellular signaling cascades to understand the differences in action mechanisms between ketamine and SSRI antidepressants, and how other new antidepressants can similarly target the glutamatergic system, which shows prolonged effects.[41]

A drug's efficacy is usually determined by its dose-response dependency to a specific molecular target (i.e., SSRIs to the serotonin transporter).[41,48,49] Ketamine shows the highest antagonism affinity to NMDA receptors (~2 μM),[41] however it also has high affinity for AMPA receptors, which also bind glutamate and elicit faster excitatory transmission responses compared to NMDA receptors.[41,42] Additionally, ketamine also shows weak agonism to μ, δ, and κ opioid receptors, and one recent study suggested μ-opiate receptor antagonism could prolong ketamine's antidepressant responses.[41,42] Ketamine's effect on the opiate system also validates it's use as a safer treatment for opioid addiction.[41] Ketamine also affects other neurotransmitter systems, like dopamine and serotonin because it shows antagonism to the D_2 dopamine receptor and 5-$HT_{1A,2A,2C}$ serotonin receptors.[20,41] It has also been found to inhibit dopamine, serotonin, and norepinephrine reuptake with their respective transporters.[41,44] Some initial studies found that after ketamine binds to one of these targets, different signaling cascades could be initiated, which are illustrated in Figure 6.[41] Regardless of the exact cascade (i.e., AKT/ERK, MAPK, HOMER/ SHANK, or RAS/ RAF) the major downstream effects are similar.[42] Specifically, these cascades result in rapid translation of brain-derived neurotrophic factor (BDNF) that causes dendritic spine density formation in the crucial cortical region and prefrontal cortex to increase,[20,41,50] which is thought to alleviate symptoms in MDD by returning plasticity in these regions.[41] These cascades can also lead to cytoskeletal reconfiguration and neurogenesis, which could also help patients with MDD and treatment resistant depression.[41]

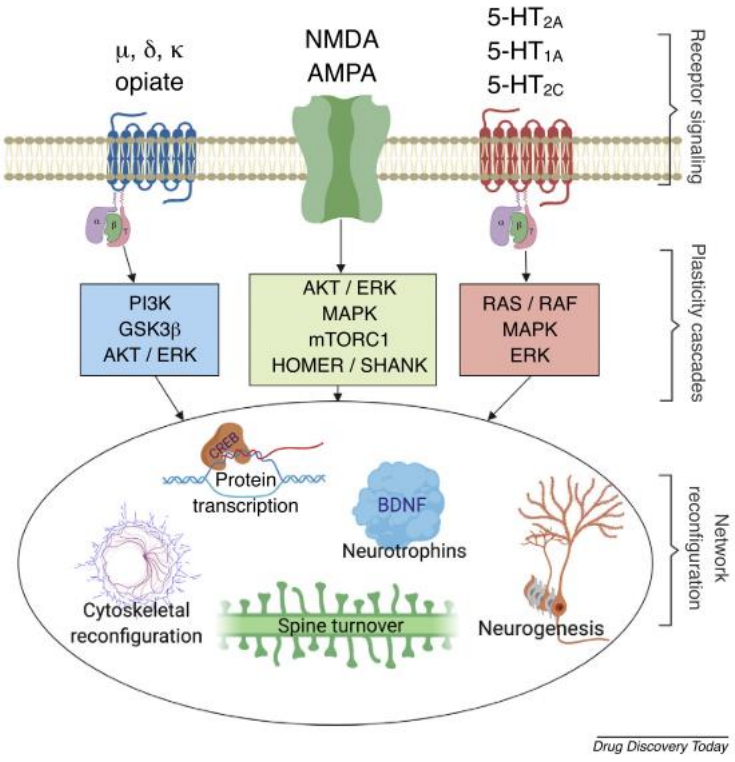

Figure 6. Shared antidepressant mechanisms in three different neurotransmitter systems. Opioid, glutamatergic and serotonergic receptors are linked to intracellular signaling cascades that target shared neurobiological mechanisms of network reconfiguration. Notably, rapid-acting antidepressant effects occurring within days to 1 week have, so far, only been shown for glutamatergic and serotonergic drugs. Abbreviations: NMDA, N-methyl-D-aspartate receptor; AMPA, a-amino-3- hydroxy-5-methyl-4-isoxazolepropionic acid receptor; 5-HT1/2A, serotonin-1A receptor, serotonin-2A receptor; 5-HT2C, serotonin-2C receptor; PI3K, phosphoinositide 3-kinase; GSK3b, glycogen synthase kinase 3 beta; AKT, protein kinase B; ERK, extracellular signal-regulated kinase; MAPK, mitogen-activated protein kinase; mTORC1, mammalian target of rapamycin complex 1; HOMER, homer protein homolog 1; SHANK, SH3 and multiple ankyrin repeat domain 3; RAS/RAF, GTPase protein coupling calcium influx to forms of synaptic plasticity; BDNF, brain-derived neurotrophic factor; d, delta; k, kappa; m, mu; CREB, cyclic adenosine. Taken from Kraus, C.; Wasserman, D.; Henter, I. D.; Acevedo-Diaz, E.; Kadriu, B.; Zarate, C. A. The Influence of Ketamine on Drug Discovery in Depression. *Drug Discov. Today* **2019**, *24* (10), 2033–2043. https://doi.org/10.1016/j.drudis.2019.07.007.

Although this research elucidates some intercellular processes for ketamine's mechanism of action, more research is needed to clarify how different genetic effects impact dynamic glutamate changes, as well as ketamine's effects on the serotonin and dopamine transporters and their receptors.[20,44,47,51] Specifically, real-time measurements of serotonin, dopamine, and glutamate need to explored with these long-term ketamine experiments and genetic effects.[44,51] Additionally, another current issue is that new ketamine delivery systems may need to be considered because mainstream intravenous ketamine use will be difficult to employ in non-clinical situations.[41] However, there are new biotech companies, like Bexson Biomedical, that have prototyped a small pod-shaped device, similar to an insulin pump, that can deliver buffered, sub-anesthetic doses of ketamine into the abdomen over long periods of time.[52,53] Bexson Biomedical has received special authorization from the FDA to fast-track their device, which can be used for opioid treatment, after painful surgeries, and for treatment resistant depression.[41,52,53] Here, my thesis work explores the effects of ketamine

on serotonin in a model system, and compares it to SSRIs to understand their effects on concentration and reuptake dynamics in the brain and with different genetic effects.[41,44,51]

1.2 Electrochemical Methods for Serotonin Detection

1.2.1 Electrochemical detection of neurotransmitters

Neurotransmission is the chemical exchange of information between neurons.[54–57] As previously stated, neurotransmitters, such as serotonin, are packaged into vesicles in neurons and released through exocytosis.[55,56] Neurotransmitter release occurs quickly, in sub-second time intervals, and the distance between two neurons is approximately 20-100 nm.[54–56] Therefore, fast techniques are required to monitor real-time neurotransmitter changes.[55–57] Additionally, these techniques must be sensitive to detect low concentrations (0.1-1 µM) of neurotransmitters and selective for specific neurotransmitters, such as serotonin detection over dopamine, in areas of the brain where their pathways overlap.[54–56] Fortunately, there are several electrochemical and analytical techniques available to measure real-time serotonin release in brain tissue, but each has their own advantages and disadvantages.[55–57]

1.2.2 Common sampling and electrochemical methods

In the 1960s, Ralph Adams was the first to theorize that small, electroactive biogenic amines could be easily oxidized and reduced when electrochemical potentials were applied to an electrode, and showed in a fundamental experiment that a carbon paste electrode could detect neurotransmitters in rat brain tissue. However, through the 1970s, the most common technique used to label and quantify neurotransmitters on and near neurons was radioimmunoassays.[58] However, this technique lacked real-time measurement and was difficult to apply *in vivo*. Over the past five decades, sampling and electrochemical techniques have significantly improved in order to quantitatively measure real-time, dynamic, neurochemical fluctuations that can be correlated with pharmacology, behavior, and disease in real-time. Figure 7 shows a few of these techniques, including microdialysis, cyclic voltammetry, and amperometry.

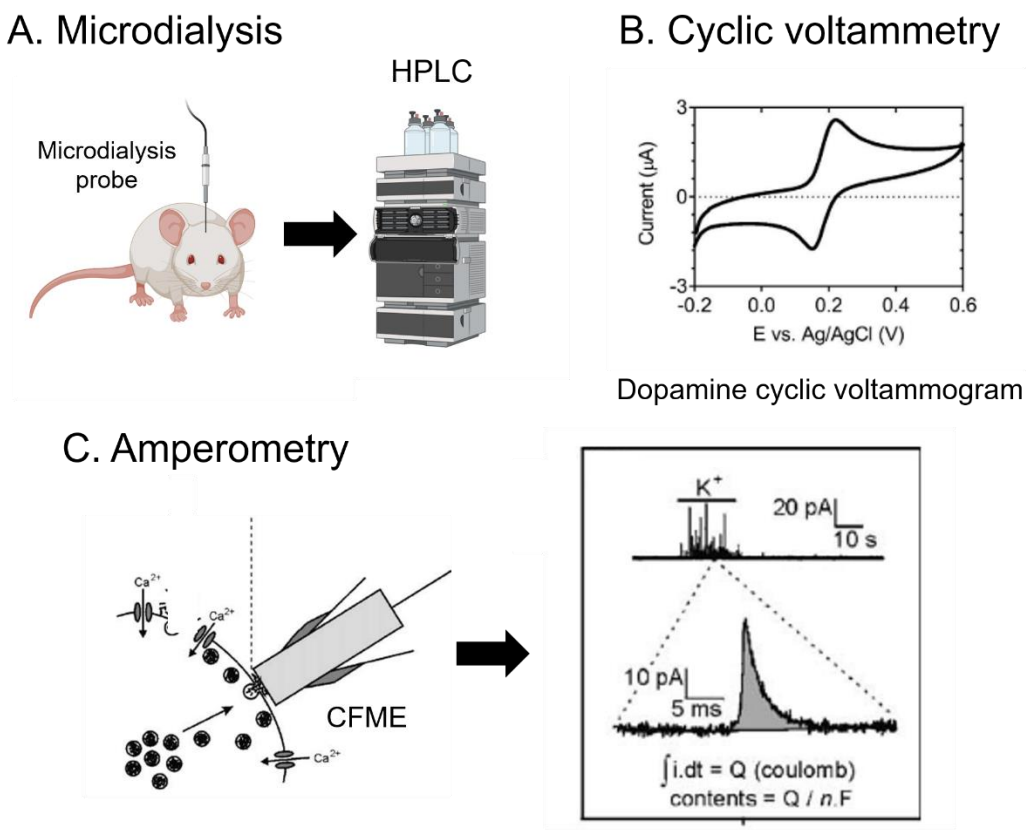

Figure 7. Common sampling and electrochemical techniques to measure neurotransmitters in brain tissue. Microdialysis is a common sampling where a probe collects fluid from tissue that is analyzed and identified with a separation instrument. **A.** Microdialysis probe inserted into mouse brain tissue collects fluid that is analyzed for neurotransmitter composition with HPLC. Figure created in BioRender. **B.** Cyclic voltammogram of 100 µM dopamine at a glassy carbon electrode. Scan rate is 100 mV/s and scan range is -0.2 V to 0.6 V. Voltages are measured vs. a Ag/AgCl reference electrode. Taken from Venton, B. J.; Cao, Q. Fundamentals of Fast-Scan Cyclic Voltammetry for Dopamine Detection. *Analyst* 2020. https://doi.org/10.1039/c9an01586h. **C.** Amperometric recording of catecholamine content from a PC12 cell measured with a carbon fiber microelectrode (CFME). The bar on top indicates the period of superfusion with high K^+ saline. A single current peak, corresponding to the release of the contents of one single vesicle, is shown on an extended time scale. The integral of the current peak corresponds with the charge (Q) transferred during the event, which is a measure for the amount of neurotransmitter secreted. Taken from Westerink, R. H. S. Exocytosis: Using Amperometry to Study Presynaptic Mechanisms of Neurotoxicity. *Neurotoxicology* 2004, 25 (3), 461–470. https://doi.org/10.1016/j.neuro.2003.10.006.

Microdialysis is a common sampling and collection technique where a 200-400 µm probe is placed into tissue to collect fluid that is analyzed for specific neurotransmitters with a separation instrument, such as LC-MS or HPLC (Figure 7A).[55,59–61] The shaft of the probe contains an inlet tube and outlet tube with a semipermeable membrane. This membrane allows small molecules, like neurotransmitters, to pass through the inlet, while large biomolecules, like proteins, are blocked.[55,61] Microdialysis allows ample collection of multiple neurotransmitters at one time that are easily identifiable and quantifiable with a separation instrument.[55] However, it has several limitations with temporal and spatial resolution.[55] With temporal resolution, the microdialysis probe collects

fluid on the order of minutes, so fast, real-time measurements cannot correlate with pharmacology, behavior, or disease.[55] Additionally, the 200-400 µm probe can cause tissue damage by breaking blood vessels, which causes immune responses that confound measurements *in vivo*.[55] However, over the last decade, the Kennedy group has tried to fix these issues by microfabricating smaller microdialysis probes that are about ~45 µm in diameter.[59,61] Although this research improves spatial resolution, microdialysis does not have the capabilities to measure dynamic neurotransmitter changes in real-time.

With electrochemistry, some of the most common techniques used to measure neurotransmitters are cyclic voltammetry and amperometry.[54,55,58,62,63] Cyclic voltammetry (CV) is commonly used in research and industry settings.[62] With CV, a sweeping voltage potential is applied with a potentiostat to a three-electrode system (working, counter, and reference) in a sample solution.[62,63] The current response from the sample is measured at the working electrode and plotted against applied voltage to create a cyclic voltammogram, where the anodic current response is usually located on the forward scan and the cathodic response is located on the reverse scan.[62] These cyclic voltammograms act as fingerprints for each neurotransmitter, which is illustrated in Figure 7B. Although CV can detect neurotransmitters, it applies the ramp potentials with 1-100 mV/s scan rates, which requires tens of seconds to several minutes to complete a cycle.[64] CV is more well-suited to measure reactive oxygen species or oxygen changes in biological samples that do not require millisecond temporal resolution.[62] In industry, it is also used to measure drug quality for pharmaceuticals or phenolics and antioxidants for food and wine.[62]

Another common electrochemical technique, constant-potential amperometry (or amperometry), applies a constant potential to an electrode that is able to oxidize or reduce an analyte of interest (i.e. to detect dopamine a voltage of 0.6 V is applied to an electrode), which is illustrated in Figure 7C.[44,55,58,65] The currents generated are mass transport limited,[58] and if the potential is constant throughout an experiment, no charging currents are generated.[58,66] Instead, direct integration from the currents detected can be used to calculate the amount of analyte present with Faraday's law (Fig. 7C).[58,65] Further, amperometry measures redox reactions in real-time, and is only limited by the data acquisition rate.[58,64] Thus, amperometry has been used to measure the neurotransmitter contents of a cell or a synaptic vesicle.[65,67] Even though amperometry shows incredible real-time neurotransmitter detection, it cannot distinguish between neurotransmitters that have the same oxidation potential,[58] and if a high potential is applied, many neurotransmitters can oxidize at that one potential.[58,64,66] Because of these issues with cyclic voltammetry and amperometry, fast-scan cyclic voltammetry is often used because it combines the selectivity of CV with the fast, real-time measurements of amperometry.[64,66]

1.2.3 Fast-scan cyclic voltammetry

Fast-scan cyclic voltammetry (FSCV) is a popular electrochemical technique that applies a linear ramp potential, known as a waveform, with high scan rates of 100-1000 V/s.[57,64,66] These faster scan rates allow real-time neurotransmitter electrochemical detection with millisecond temporal resolution. Potentials are ramped positively to oxidize neurotransmitters and then negatively to reduce them. For example, the popular FSCV dopamine waveform (-0.4 V, 1.3 V, -0.4 V, 400 V/s) starts at -0.4 V and ramps to 1.3 V and back to -0.4 V at a scan rate of 400 V/s and frequency of 10 Hz, where a single waveform cycle is applied every 9.8 ms, which is shown in Figure 8A.[66] FSCV is 1000x faster than conventional CV.[64,68] In Figure 8A-E, an example neurotransmitter, dopamine, adsorbs onto an electrode surface where it oxidizes and then reduces as a waveform is applied. Dopamine then desorbs and returns to the bulk solution around the electrode. FSCV is a differential technique because when a voltage is applied to an electrode, a double layer (also known as Helmholz layer) of ions covers the electrode surface and creates a capacitance on the electrode.[69] This causes a background current that is stable throughout an FSCV measurement, and is subtracted to produce a cyclic voltammogram used to identify dopamine, which is illustrated in Figure 8B and 8C.[66] Dopamine can be identified by its oxidation and reduction potentials at approximately 0.6 V and -0.2 V, respectively (Fig. 8C). Figure 8D and 8E also show FSCV data plotted in a false color plot in 3-dimensions: potential, time, and current detected.[66] Additionally in Figure 8E, above the color plot is an *i* vs. t plot, which shows the current detected over time and is commonly used to compare changes to the half max decay (t_{50}) to determine reuptake changes of neurotransmitters when specific drugs are applied.[66,70,71]

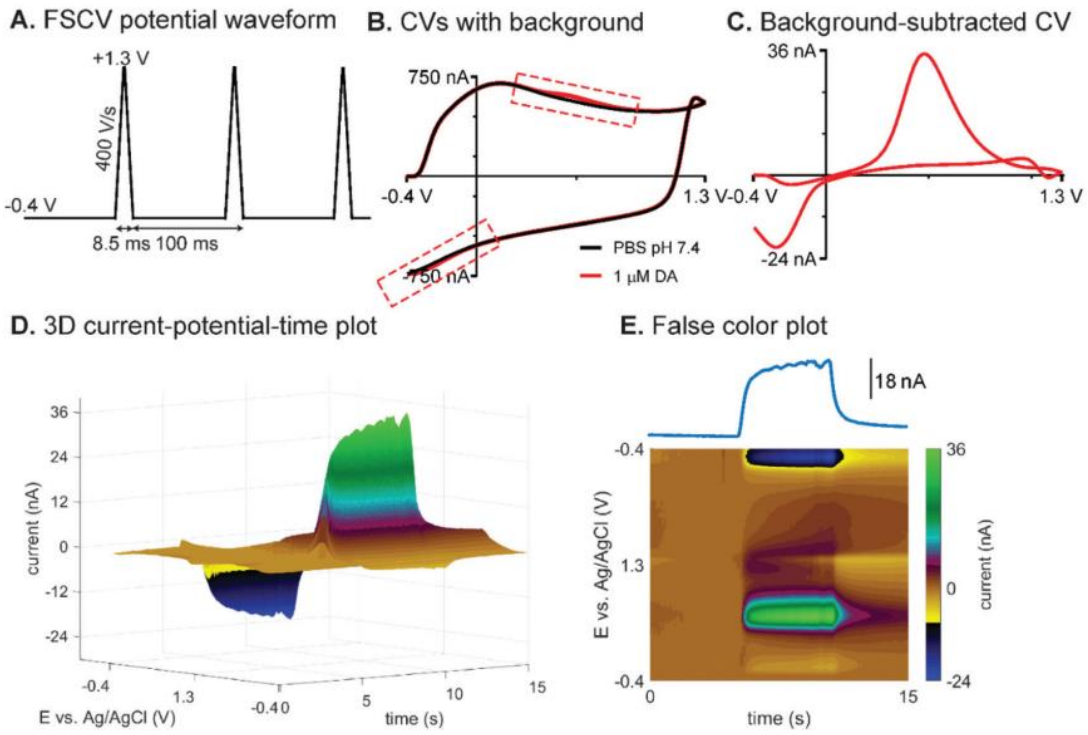

Figure 8. FSCV of dopamine. **A.** Applied potential waveform using -0.4 V holding potential, +1.3 V switching potential, 400 V/s, and 10 Hz repetition rate. **B.** Example CVs with background (PBS pH 7.4) (black) and buffer with 1 µM dopamine (red). Dashed boxes emphasize the difference between them. **C.** Background-subtracted CV of 1 µM dopamine. **D.** Three-dimensional current-potential-time plot and **(E)** conventional false color plot with anodic peak current-time trace of 5 s bolus injection of 1 µM dopamine. Taken from Puthongkham, P.; Venton, B. J. Recent Advances in Fast-Scan Cyclic Voltammetry. *Analyst* 2020. https://doi.org/10.1039/c9an01925a.

FSCV is often coupled to carbon fiber microelectrodes (CFMEs) that are inserted into brain tissue to detect real-time neurotransmitter changes. CFMEs have a diameter of approximately 7 µM and a smooth surface composed of T-650 graphitic carbon that contains both basal and edge plan carbon, which is illustrated in Figure 9.[68,72] CFs are a decent electrode material because they show high biocompatibility and the small diameter limits tissue destruction during *in vivo* experiments. Although CFMEs are commonly used with FSCV, they possess issues with electrode fouling from neurotransmitters like serotonin and tissue because of their smooth surface.[66,68,72] Other carbon electrode materials, like carbon nanotubes (CNTs) and carbon nanospikes (CNSs) contain more edge-plane sites that improve neurotransmitter adsorption, which increases sensitivity.[68] CNTs and CNSs also improve electrode fouling because of their rougher surface area.[68] Although other carbon electrode materials like CNTs and CNSs increase sensitivity and decrease electrode fouling, they are difficult to mass produce, while CFMEs are cheap and are easily mass produced.[68,72]

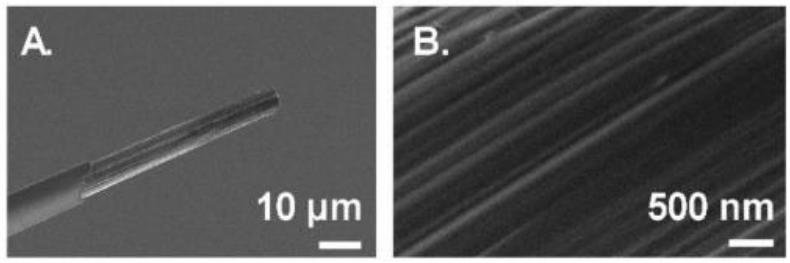

Figure 9. SEM images of a cylindrical carbon fiber microelectrode (CFME) sealed in glass capillary at **(A)** 1000x and **(B)** 25000x magnification. Taken from Puthongkham, P.; Venton, B. J. Recent Advances in Fast-Scan Cyclic Voltammetry. *Analyst* 2020. https://doi.org/10.1039/c9an01925a.

Although FSCV is an advantageous electrochemistry technique, it possesses limitations. Because FSCV is a differential technique, it can only identify dynamic changes in neurotransmitters and cannot detect basal concentrations. Additionally, most FSCV studies focus on improving dopamine detection to understand neurological diseases affected by dopamine dysregulation, like Parkinson's disease.[10,57,66,69,73] Other neurotransmitters, like serotonin, have unique issues that hinder successful FSCV detection and biological applications with CFME fouling. This has limited research on neurological diseases and illnesses affected by serotonin such as depression.[7,74]

1.2.4 Issues with serotonin FSCV detection

Wightman's lab was the first to detect serotonin with FSCV in Jackson et al. 1995.[74] Before this, most previous studies focused on dopamine detection. Initially, FSCV serotonin detection was more difficult because when serotonin oxidizes, it forms radicals that dimerize and polymerize onto CFMEs that build up overtime to form films.[7,74–76] These films passivate the electrode and make it difficult for serotonin to adsorb onto the electrode surface.[7] This causes the current detected to decrease, which is known as electrode fouling. Additionally, neurotransmitters require more time to adsorb onto the electrode because of these films, which ruins kinetic determination. In order to combat these issues, Jackson et al. optimized a new FSCV waveform for serotonin detection that scans from 0.2 V to 1.0 V to -0.1 V and back to 0.2 V with a fast scan rate of 1000 V/s (known as the Jackson waveform) to "outrun" polymerized film formation, which is illustrated in Figure 10A.[74] The Jackson waveform limits electrode fouling over short measurement, however long-term fouling with serotonin and its downstream metabolite, 5-HIAA, are still significant issue with this waveform.[7]

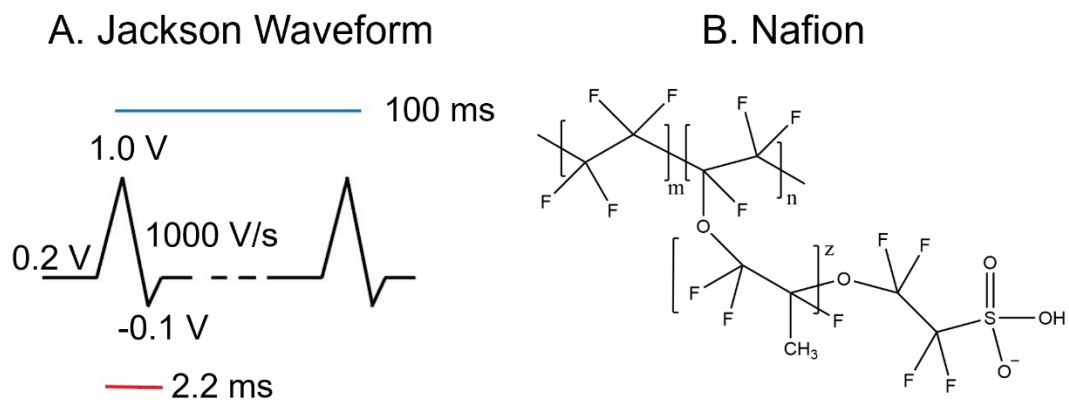

Figure 10. Traditional methods used to detect serotonin with FSCV. **A.** Traditional serotonin "Jackson" waveform that scans from a holding potential of 0.2 V to a 1.0 V switching potential to -0.1 V back to 0.2 V at 1000 V/s. The 1000 V/s scan rate was optimized to limit electrode fouling to serotonin's oxidation byproducts, but electrodes still foul with long-term measurements. **B.** Nafion is a negatively charged polymer that shields serotonin oxidation byproducts from polymerizing onto CFMEs, which fouls the electrode. Nafion also increases sensitivity to positively charged neurotransmitters, but does not improve selectivity between serotonin and dopamine. Thick layers of Nafion also slow down adsorption, which ruins accurate kinetic determination.

In Hashemi et al. 2009, the Wightman lab improved serotonin electrode fouling by Nafion-coating carbon fiber disk electrodes.[7] Nafion is a negatively charged, sulfonated polymer that coats the electrode and shields it from negatively charged radicals and is depicted in Figure 10B.[68] It also shields polymerized serotonin from adsorbing to the electrode surface because it cannot diffuse through the polymer network.[68] Only small biomolecules, like neurotransmitters, pass through. Additionally, the negative charge repels the negatively charged 5-HIAA, which also eliminates electrode fouling.[7,68] The negative charge also attracts positively charged neurotransmitters, like serotonin and dopamine, to the surface of the electrode, which increases sensitivity.[7,68] Although Nafion eliminates electrode fouling to serotonin and 5-HIAA, it does not improve selectivity for serotonin over dopamine. However, the authors did find that the Jackson waveform was selective for serotonin over dopamine, and could not detect concentrations ≥ 10 μM dopamine, which is above physiological concentrations.[7] In addition to these sensitivity issues, thick layers of Nafion cause diffusion rates to be 400x slower than bare carbon fibers, which limits accurate kinetic information.[68,74,77] Still, the FSCV Jackson waveform with Nafion-coated CFMEs allowed new research to understand depression and antidepressant mechanisms in mammals. However, *Drosophila melanogaster* may be a better model to detect serotonin with bare CFMEs because they do not possess the monoamine oxidase-A (MAOI-A) enzyme that catalyzes the breakdown of serotonin into 5-HIAA,[78] which limits electrode measurements over long-term experiments.[79]

1.2.5 Previous FSCV and electrochemical serotonin research in mammals

Previously, several groups have used FSCV and amperometry to determine serotonin kinetic changes with SSRIs and other drugs in mammals.[7,44,80–83] Historically, Shaskan and Snyder were the first to suggest two reuptake mechanisms for serotonin with antidepressants, slow and fast, in their work with radioligand-binding assays in the 1970s.[25,26,84] They coined these mechanisms "Uptake 1," which is high affinity and low efficiency uptake and "Uptake 2," which is low affinity and high efficiency uptake.[26] The Daws group further elaborated on this research with amperometry and found with pharmacology experiments that Uptake 1 primarily relied on SERT, while Uptake 2 relied on other neurotransmitter transporters like the dopamine transporter (DAT) and norepinephrine transporter (NET).[84] Although this work is helpful for determining serotonin kinetics, it has not been successfully investigated with SERT genetic mutations or newer ketamine therapies for treatment resistant depression, which would be easier to investigate in *Drosophila melanogaster* because of its short life cycle and easily accessible genome.[85] In Bowman et al., the Daws group also tried to investigate dynamic serotonin changes to ketamine with SERT KO mice, however, serotonin reuptake did not significantly change in the SERT KO mice in their controls, which implies compensation by other neurotransmitter systems and confounds the study.[44]

Using FSCV, the Hashemi group also demonstrated citalopram and escitalopram increase extracellular serotonin in mice *in vivo* by dramatically slowing reuptake of serotonin.[26,81] They also showed that fluoxetine increases serotonin concentrations and reuptake, but requires higher concentrations because of its lower affinity to SERT.[86] They further elaborated on Daws' work with serotonin kinetics and proposed hybrid clearance of serotonin with SSRIs, like escitalopram, that show initial fast uptake that then slows.[26] From this work, the Hashemi lab also created an online modeling software, known as the Analysis Kid, that uses raw FSCV color plots and *i* versus *t* plots to determine serotonin kinetic changes to different pharmacological and genetic applications.[87] However, like the Daws group, this work has not been investigated in SERT genetic mutants and newer ketamine therapies, which is difficult to accomplish with mice and rat models.

In addition to serotonin kinetics, Wightman's group also used FSCV to explore serotonin vesicular transport and exocytosis in mammals.[7,74,88] In Kile et al., they compared the role of synapsins in dopamine versus serotonin release with triple knock-out (TKO) mice that lacked all three synapsin genes.[88] They found no differences in serotonin release with the TKO mice versus control, but dopamine release doubled in the mutant. Their work found through pharmacology experiments that synapsins differentially regulate dopamine and serotonin release. They suggested dopamine neurons probably rely on synapsins for dopamine release, however serotonin release seems to be independent of synapsin activity. Instead, they suggest serotonin release may rely on primed serotonin storage in dense core vesicles.[89–91] In addition to this research in mice, *Drosophila melanogaster* also contain synapsin

genes that could be easily mutated to understand the effects of dopamine or serotonin with other more current antidepressant treatments.[89–92]

The Hashemi lab also showed serotonin can co-release with histamine,[93] an important neurotransmitter that causes vasodilation and inflammation for immune responses.[93–95] Their work also suggests that serotonin release is unique compared to other neurotransmitters, and contributes to the cytokine hypothesis for depression,[20,96–99] which states that over-active immune responses from serotonin and histamine signaling can cause depression.[20,96–98] Although these studies help explain fundamentals on serotonin signaling and release, more exocytosis proteins, such as SCAMP-2 and syntaxin-1A, can also be explored with genetics manipulations to discern their effects on serotonin changes, since these proteins have been implicated in previous SSRI mechanism research.[11,12,89,90] Because these genetic manipulations are tedious and time-consuming to make in mammals, *Drosophila melanogaster*, may be a better model to explore these genetic manipulations and effects with depression.

1.3 *Drosophila melanogaster*

1.3.1 D. melanogaster as a model organism

Drosophila melanogaster, commonly known as the fruit fly, is a small invertebrate in the order Diptera and family Drosophilidae that subsists on the decaying matter of rotten fruit.[100] Similar to humans, *Drosophila* first originated in Sub-Saharan Africa and migrated to Europe some 15,000 years ago.[100–103] Eventually, humans also helped fruit flies colonize the Americas in the last few hundred years through the trade of fruit.[100] Although they are considered a nuisance pest in everyday life, *Drosophila* has been continuously used in scientific experiments for more than 100 years.[100–103] In 1910, Thomas Hunt Morgan's lab at Columbia University was the first to confirm the chromosome theory of inheritance with fruit flies.[100,101,103] Since then, *Drosophila* has been cultivated and continuously used in thousands of labs throughout the world.[100,101] Compared to mammalian models, fruit flies are easily cultivated and maintained in a lab setting and live in small conical tubes with a plug of food media that contains cornmeal, yeast, and agar.[100,101] Flies have proven to be a steadfast model that have been used to understand different genetic effects, immune responses, and molecular signaling cascades.[100,104–108] Although genome sequencing and genetic editing techniques have enhanced the creation of mammal models in the last few decades, *Drosophila* has many beneficial characteristics that expedite this process and allow genetic experiments to be performed faster than other models.[100,101]

A major advantage for using *Drosophila* is their short life cycle, which allows for the fast generation of a large number of progenies to use in multiple genetic experiments.[85,100,109] With *Drosophila*, a fertilized egg develops into an adult in only 9-10 days at room temperature (25°C), which is illustrated in Figure 11.[85,100] After fertilization, embryogenesis is completed within 24 hours and is followed by three larval stages that are termed first, second, and third instar with a molting event in between each stage transition.[100,109] The first two instars each last approximately 1 day, while the third instar requires 2 days.[100] So, 5 days after fertilization, larval development is complete and a fly goes through metamorphosis by producing a hard, chitin-based pupal case.[100,109] A fly will remain in the pupal case for 4-5 days where the larval tissue will break down and adult features and structures will develop.[100,109] An adult fly will emerge from the pupal case in a process called eclosion and become sexually mature within 12 hours, which allows the fruit fly life cycle to rapidly repeat itself.[100]

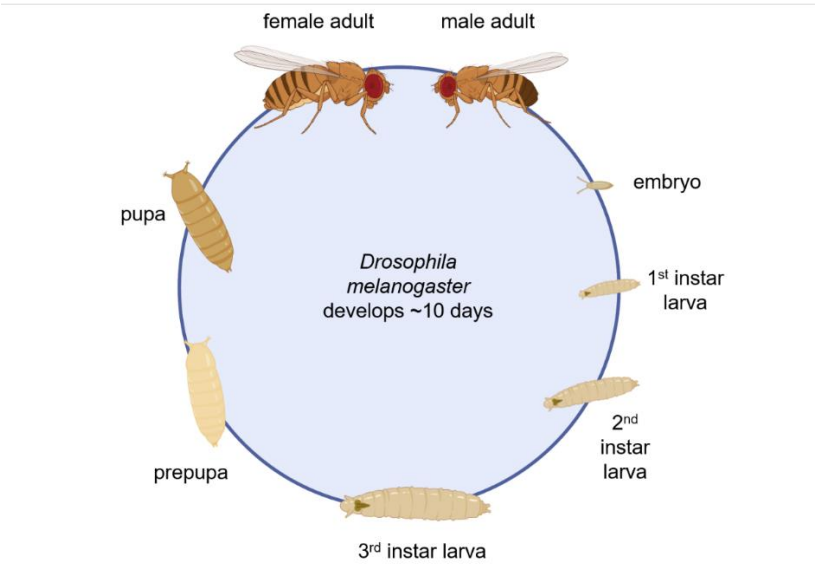

Figure 11. *Drosophila melanogaster* life cycle. From clockwise, *Drosophila* develops in about 10 days and moves through the embryo and three larval stages in 6 days. It then produces a hard, chitin pupal case and spends 4 days in the pupal stage. Around day 10, the adult will emerge from the pupal case in a process called eclosion. Adult fruit flies become sexually mature within 12 hours of eclosion, causing the life cycle to repeat. Figure created in BioRender.

In addition to their short life cycle, fruit flies are also advantageous because of their small, compact genome that is easily accessible with gene editing techniques, which is described in Figure 12.[100,110,111] *Drosophila* was the second organism to have its genome sequenced, after *C. elegans*, and is commonly used to verify novel whole genome sequencing techniques.[100,101] Their entire genome is estimated to be only ~180 Mb, with ~120 Mb being euchromatin that includes approximately 13,900 protein-coding genes.[100] *Drosophila* only possess 4 chromosome pairs with the first chromosomes used for sex determination.[100] Unlike mammals, a Y chromosome is not solely used for male sex determination. Instead, each fly has a copy of an X chromosome, and two X

chromosomes (XX) result in a female fly, while one copy of an X chromosome (XO) results in a male fly. The sex chromosomes are usually highly compact and transcriptionally silent with DNA and are not usually used for gene editing experiments.[100,110,111] The remaining chromosomes are autosomes.[100] Chromosomes 2 and 3 are the largest and their left (L) and right (R) arms are termed 2L, 2R, 3L, and 3R, respectively, while chromosome 4 is referred to as the “dot chromosome” and is small in size.[100] With genetic techniques, most mutations are introduced on chromosome 2 and 3 because of their large size.[100] Because of their small, compact genome, it is relatively easy to introduce genetic material into flies with common techniques like transposable elements or CRISPR/Cas9.[104,110,111] Additionally, *Drosophila* is also advantageous because of the public databases and centers that allow scientists to easily share mutant fly lines to other labs around the world.[100] FlyBase is a database that catalogues genetic mutations created by different labs and allows users to BLAST DNA or RNA sequences, browse specific mutations mapped out on the fly genome, and quick search for a specific fly line used in a publication.[100,105,112–114] It also directly links to fly stock centers where you can directly purchase these flies. The two largest fly centers are the Bloomington Drosophila Stock Center (BDSC) at the University of Indiana and the Vienna Drosophila Resource Center (VDRC).[100,105,113,114]

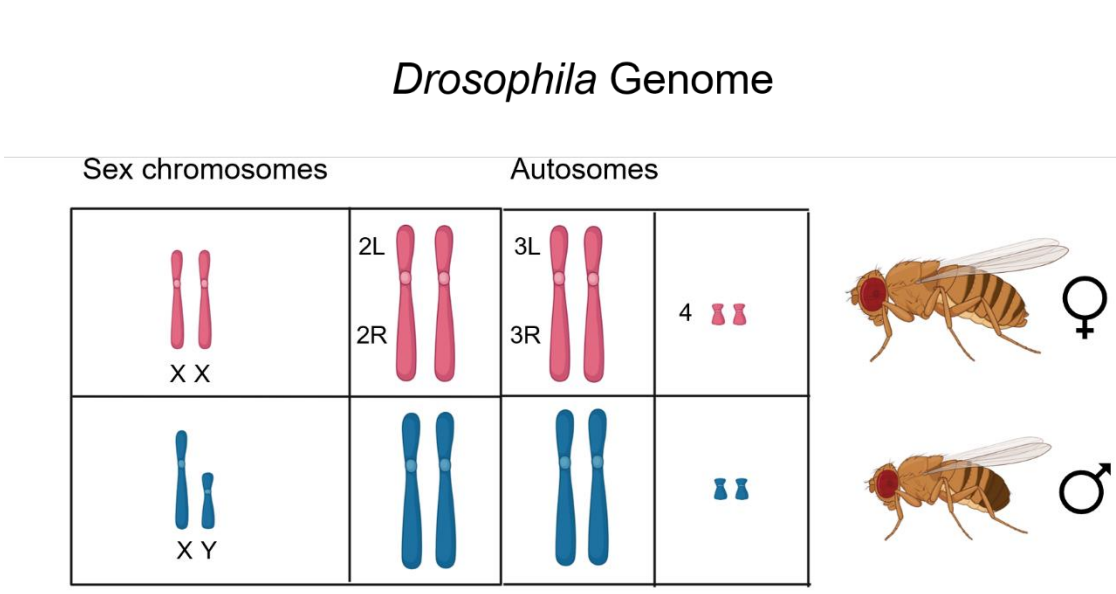

Figure 12. *Drosophila melanogaster* genome with labeled chromosomes. The *Drosophila* genome is estimated to be 180 Mb with approximately 13,900 protein-coding genes. *Drosophila* possesses only 4 chromosomes. The first are sex chromosomes, where XX results in the female phenotype, while XY results in the male phenotype. Chromosome 2 and 3 are the largest autosomes, and most gene editing techniques mutate genes on these chromosomes. Chromosome 4 is referred to as the “dot” chromosome, and is not commonly used in gene editing experiments. Figure created in BioRender.

1.3.2 D. melanogaster genetic tools

Creating mutations with genetic tools is essential to understand gene function.[85,100,104,111] With *Drosophila*, the dependable and reliable method to create genetic mutations is with transposable elements.[100,104,111,115] A transposon, or transposable element, is a DNA sequence that can change its position within a genome.[115] First engineered in the late 1980s and early 1990s, transposable elements allow for insertional mutagenesis of a gene.[115,116] The P-transposon element, commonly known as a P-element, is the most widely used vehicle to insert genes in *Drosophila* because it transposes at high rates, depends on exogenous transposase, inserts in heterochromatic and euchromatic regions, and transposes near promoter regions.[104,115] Usually, a p-element with the transgene of choice is inserted into a vector, such as a plasmid, and is inserted into a fertilized fly egg, which is then screened with PCR for the gene of interest as the fly ages.[100,104,111] Transposons act as insert mutations, stop codons, nonsense mutations, or can be used to make RNAi knockdown mutations that disrupt a gene to understand its function.[104,105,113,117] Whole genome disruption projects have been spearheaded in several labs throughout the United States using transposons, including at Baylor University and Harvard Medical School.[104,105,112,113,118] Transposons have also been used to create genetic markers, such as dominant visible characteristics, like curly wings and stubbly hair on chromosome 2 and 3, respectively.[100,104] Further, they were also initially used to drive UAS/Gal4 production to turn on and off transgenes in progeny flies.[100,116] Transposons are still frequently used today, however, CRISPR/Cas9 is starting to also be used to mutate the *Drosophila's* genome.[110]

CRISPR/Cas9, short for clustered regularly interspaced short palindromic repeat system, is a newer genetic engineering technique that is able to find and insert or delete genes in a system with a guide RNA that is illustrated in Figure 13.[110,119] Usually, CRISPR acts as an immunological defense system against invading viruses and plasmids in many bacterial species.[110] The most studied CRISPR/Cas9 system in bacteria is from *Streptococcus pyogenes*, where the Cas9 endonuclease is targeted to a sequence from the invading pathogen by a guide crRNA, or CRISPR RNA.[110] The guide crRNA provides better specificity to the endonuclease by pairing with a 20 nucleotide complimentary sequence within the DNA. A trans-acting crRNA, or tracrRNA, also forms a complex with the crRNA and incorporates into the Cas9 complex.[110] However, this process has been simplified with the fusion of the crRNA and tracrRNA into a 100 nucleotide synthetic single guide RNA (sgRNA), which now only requires Cas 9 and the sgRNA to be expressed.[110] With CRISPR/Cas9, the Cas9/sgRNA complex acts as a pair of scissors that can cut into DNA and cause single or double strand breaks. Single cuts result in short deletions (1-100 nt) or insertions (1-20 nt), while double breaks cause longer deletions (many kb) that are repaired by non-homologous end joining or homologous recombination.[110,119] With homologous repair, the desired DNA template can be inserted after a double break and is used to edit the genome in a myriad of ways.[110] Specifically with *Drosophila*, CRISPR/Cas9 has been successfully used to edit its genome since 2013.[110,114,119–121] CRISPR/Cas9 is used in

several ways, such as creating new UAS/GAL4 and RNAi lines, tagging genes with green fluorescent protein (GFP), or upregulating or downregulating transcription of a gene.[105,113,114] For example, Deng et al. 2019 used CRISPR/Cas9 to develop numerous knockout and knockin fly lines that targeted *Drosophila's* chemoconnectome, which is its entire set of genes that affect neurotransmitters, neuromodulators, neuropeptides, and their receptors and transporters.[114] CRISPR/Cas9 is also used to design more accurate depression models that genetically alter SERT or the glutamatergic system to understand genetic effects with SSRIs and ketamine, which could be accomplished more quickly in *Drosophila* compared to mammals.[17,41,85,100,122]

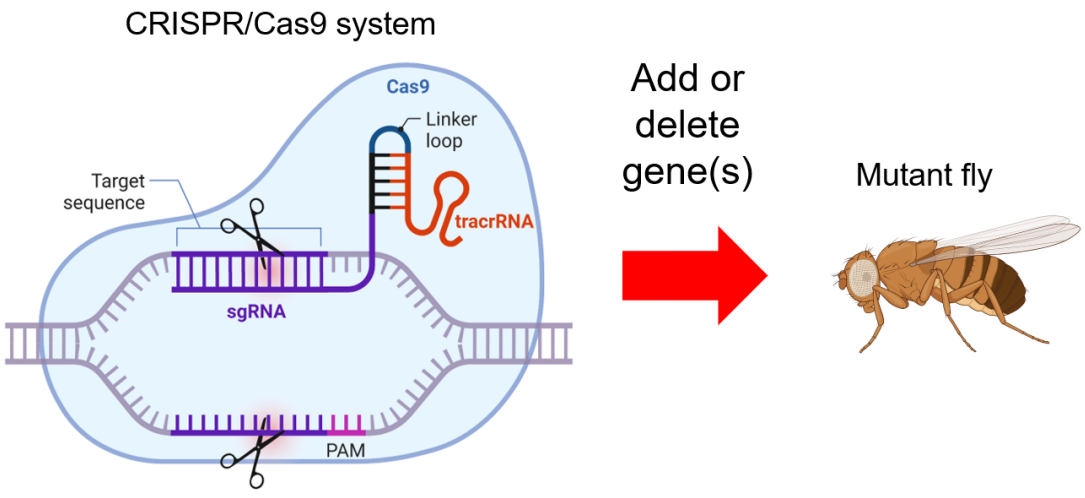

Figure 13. CRISPR/Cas9 gene editing tool used to create mutations in *Drosophila melanogaster*. CRISPR usually acts as an immunological defense system in bacteria. The Cas9 endonuclease targets a sequence with a guide crRNA, or CRISPR RNA. A tans-acting crRNA, or tracrRNA, also forms a complex with the crRNA and incorporates into the Cas9 complex.[110] However, the crRNA and tracrRNA have been fused into one synthetic single guide RNA (sgRNA) for simplicity, which now only requires Cas 9 and the sgRNA to be expressed. The Cas9/sgRNA complex acts like a pair of scissors and can cut single or double stranded breaks into DNA. Single cuts result in short deletions (1-100 nt) or insertions (1-20 nt), while double breaks cause longer deletions (kb) that are repaired by non-homologous end joining or homologous recombination.[110,119] With homologous repair, a DNA template can be inserted. CRISPR/Cas9 can be used to create new UAS/GAL4 and RNAi lines, or green fluorescent protein (GFP) markers. Figure created in BioRender.

In Brand and Perrimon 1993, they took the P-element insertional mutagenesis technique and used it to create a gene expression system that allows users to express any gene of interest in any tissue within the fly, which they termed the Gal4/UAS system that is shown in Figure 14.[85,100,104,111,116] In the study, they cloned the yeast transcription factor, Gal4, into a P-element vector and showed that a defined promoter could be placed in the genome upstream of the Gal4 and act as an enhancer trap to express Gal4.[100,116] To drive this gene expression, they created an accompanying P-element vector that contained the upstream activating sequence (UAS) that binds the Gal4 protein.[100,116] The UAS sequences are connected to a promoter that allow for insertion in any

gene of interest.[85,100,116] Since its inception, the GAL4/UAS system has been improved by introducing landing sites, such as attB and attP that help place the UAS into the correct location in the genome. The GAL4/UAS system has become widely used by *Drosophila* scientists because of its great versatility, and large collections of publicly available stocks have been created that target different tissues and developmental stages.[85,104,105,114] Additionally, reporter genes, like GFP, have been integrated into the system to label specific cells and tissue to understand Drosophila's neurobiology and immune system.[85,106,114,123,124]

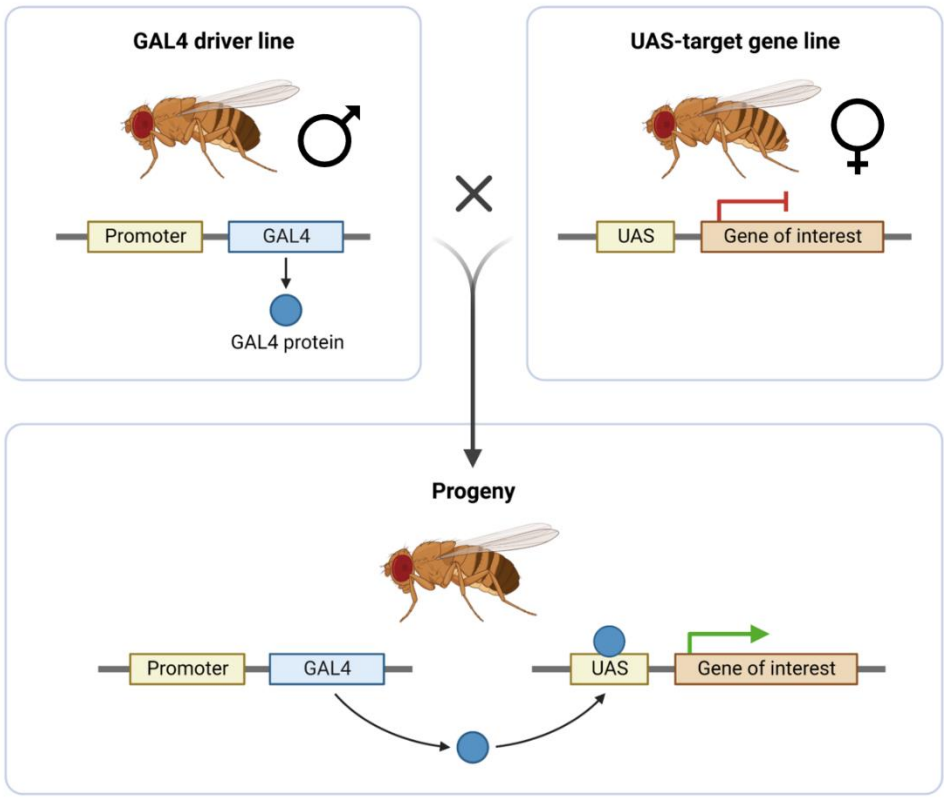

Figure 14. UAS/Gal4 system in *Drosophila melanogaster*. The Gal4/UAS system allows for the specific expression of a transgene in cells that express Gal4 from the tissue specific promoter in the Gal4 gene. Figure created in BioRender.

With the GAL4/UAS system and CRISPR/Cas9 editing technology, whole libraries of fly strains have been created that use RNA interference (RNAi) to target and knockdown a gene of interest to understand its function using *Drosophila*.[85,100,125] RNAi is a cellular mechanism that degrades messenger RNA transcripts with a double stranded RNA (dsRNA).[100,117,126] Although this mechanism was original found in *C. elegans*, *Drosophila* was mainly used to perform mechanistic studies to understand RNAi, which is conserved throughout different eukaryotic organisms.[117,126] In the RNAi biochemical pathway, once exogenous dsRNA is introduced, a complex forms that consists of Dicer-2 and R2D2, which cuts the duplex RNAs into short 21-nt long fragments.[117] After, a series of proteins

stabilize the complex, which then unwinds the duplex and then cleaves and ejects the passenger RNA strand. Following, the full RNA-induced silencer complex (RISC) is formed, which identifies sequence-homologous endogenous RNAs through homology-seeking activity that leads to their cleavage and degradation. Because of *Drosophila's* small, easily accessible genome, whole genome-wide screens with transgenic libraries have been introduced to understand the loss of function of a majority of its protein-coding genes.[85,117,126] The *Drosophila* Transgenic RNAi Project (TRiP) at Harvard Medical School is the largest creator of these transgenic lines that have been made to use the GAL4/UAS system.[105] Some of these lines include SERT and serotonin receptor RNAi knockdowns, which have not been fully investigated to understand how serotonin changes in real-time or how their loss of function will affect the action of different antidepressants.[15]

1.3.3 D. melanogaster as a model for neuroscience research

Drosophila melanogaster is a simple, controllable model in neuroscience research that can be used to understand changes in behavior, brain development, and neurological diseases more easily than mammals.[85] Although *Drosophila* are invertebrates, they share the same assortment of neurotransmitters (i.e., dopamine, serotonin, histamine, glutamate, GABA, and acetylcholine) and major neurological systems, like the optical and olfactory systems.[85,127–130] Additionally, *Drosophila* is easier to genetically manipulate to understand changes in neurotransmitters or neural circuitry, which can be used for various experimental applications.[85,100,102]

Figure 15 shows brain structures in *Drosophila* larvae and adults. Figure 15 A shows a third-instar larva, and its ventral nerve cord (VNC) dissected out inset. The larval central nervous system contains ~2000 neurons and is organized into the VNC and protocerebrum with motor neurons that radiate from the center of the larva to its lateral edges.[85,127,131,132] Figure 15B also shows serotonin and dopamine neuron location in a larva VNC with GFP expression from a Ddc-Gal4 driver.[85] Immunohistochemistry staining also depicts where serotonin neurons (red) and serotonin neuron GFP expression overlap,[133] which appears yellow. Serotonin and dopamine neurons both innervate the optic lobes, but in the VNC, serotonin neurons cluster along the midline while dopamine neurons cluster lateral to the midline and by the outermost edges of the larva's body near motor neurons that help the larva crawl.[15,127,134] Compared to larvae, the *Drosophila* adult's brain is larger in size (Fig 15C) and contains more than 100,000 neurons.[85,135] Figure 15D depicts a 3D construct of the adult fly brain, which has 41 anatomical regions and 58 interregional tracts, and figure 15E illustrates some of these major anatomical regions.[133] Much like mammalian brains, *Drosophila* uses neurotransmitters to communicate chemical information between neurons, which varies from region to region.[85] Drosophila possess ~ 280 dopamine neurons located in 18 clusters in the adult brain that have been implicated in movement, sleep, learning, and male

courtship behaviors, and are located in the mushroom body (Fig. 15D, brown).[85] Likewise, there are 10 major clusters of serotonin neurons that mediate depression behaviors, memory, and aggression that radiate from the mushroom body to the central complex (Fig. 15D, green) and to the olfactory and optical systems.[85,130,132,135] Unlike mammals, however, *Drosophila* do not possess epinephrine or norepinephrine, and instead use the neurotransmitters octopamine and tyramine, respectively, which serve similar "fight or flight" functions seen in mammals.[109,121,136–138] Specifically, octopamine is known to regulate aggression and locomotion.[85] In addition to similar brain structures that use the same neurotransmitters, 75% of human disease genes are orthogonal to genes in fruit flies, which have been used to understand the genetic and molecular basis of several neurological diseases.[85,135]

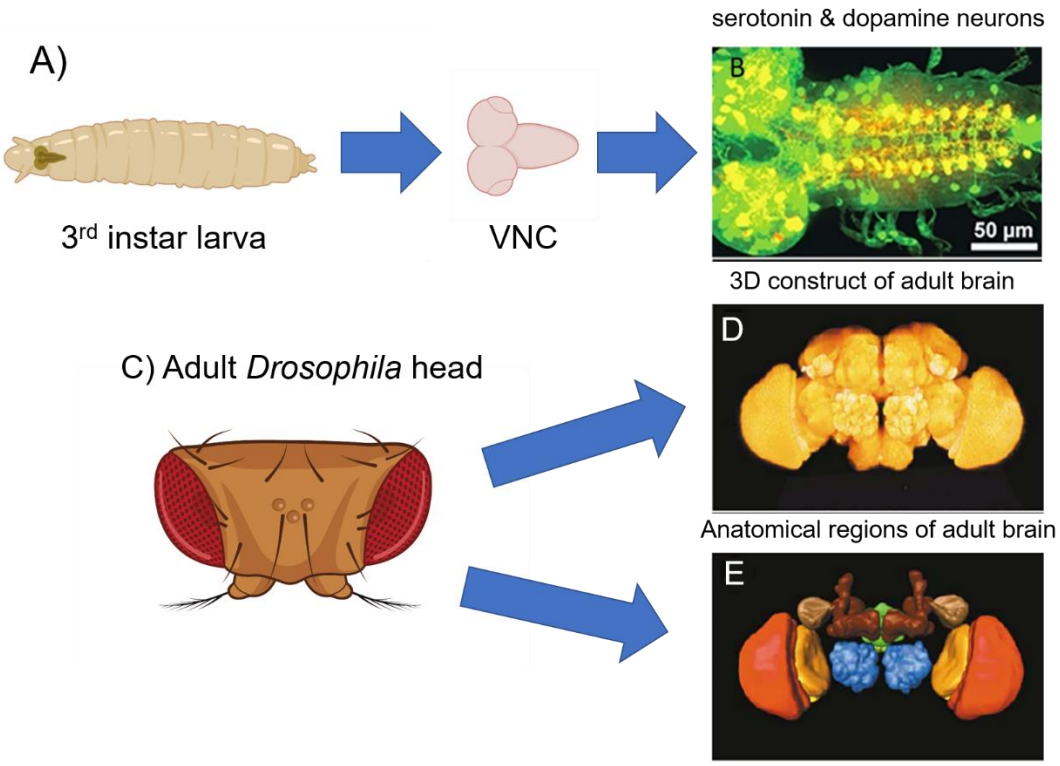

Figure 15. *Drosophila melanogaster* neural circuitry and brain structures in larvae and adults. **A.** Drosophila 3rd instar larva with dissected out ventral nerve cord (VNC) tissue. B. Ddc-GAL4 drives GFP expression (green) in dopamine and serotonin neurons in VNC. Immunohistochemistry shows serotonin neurons with red antibodies, and the overlap makes them appear yellow. C. Adult Drosophila head. D. 3D imaging of the adult brain. E. Anatomical regions in the adult brain. Dark brown = mushroom body; blue = antennal lobe; green = central complex; red = medulla; orange = lobula. Taken from Shin, M.; Copeland, J. M.; Venton, B. J. Drosophila as a Model System for Neurotransmitter Measurements. ACS Chem. Neurosci. 2018, 9 (8), 1872–1883. https://doi.org/10.1021/acschemneuro.7b00456 and Rein, K.; Zöckler, M.; Mader, M. T.; Grübel, C.; Heisenberg, M. The Drosophila Standard Brain. Curr. Biol. 2002, 12 (3), 227–231. https://doi.org/10.1016/S0960-9822(02)00656-5. Parts of figure created in BioRender.

In the 1970s, *Drosophila* was initially found to have similar circadian rhythms compared to humans that are responsible for sleep-wake cycles.[135,139] Their sleep behaviors led to the discovery of a *period* gene that is responsible for regulating sleep through an

autoregulatory feedback loop, and its dysfunction led to different insomnia phenotypes and other sleep disorders.[135,140] It took 20 years for the *period* gene to be discovered in mammals, but the core molecular mechanisms that control the "core clock" in circadian rhythms was found to be phylogenetically conserved across invertebrates and vertebrates.[135] This initial work in circadian rhythms was a touchstone for neurological disease research in *Drosophila*, which expanded over the past few decades to include neurodegenerative diseases, like Parkinson's and Alzheimer's disease,[85,141–145] as well as addiction and mental illnesses like depression.[127,132,135,146] For Parkinson's disease, *Drosophila* has been instrumental in elucidating it's genetic (i.e., *parkin*, *pink1*, *LRRK2* genes) and environmental causes, and locomotion changes over time are easily tractable with this model when dopamine neurons are lost.[10,141–144,147] Additionally, flies have also been used to understand amyloid-β toxicity and tau accumulation in Alzheimer's disease[145] and to isolate genes of interest in addiction.[135] *Drosophila* is a beneficial model to understand compulsive drug seeking behavior through substance abuse and dependance, especially with alcohol.[135] Further, *Drosophila* has also been developed into a model to understand genetic causes of depression, specifically with SERT and serotonin receptor mutants.[15,146,148,149] With depression, *Drosophila* shows changes in feeding and locomotion behaviors similar with mammals,[15,127,146,148,150] and they have also been used in neuropharmacology drug screenings to understand genetic effects to different antidepressant treatments.[132,135]

Historically, dSERT and dDAT (dopamine transporter) were used in substrate binding or molecular modeling and docking simulation studies to understand the binding affinities of SSRIs and other psychoactive drugs until the structure of hSERT was determined with x-ray crystallography in 2016.[16,19,32,122,151] Previous studies from the Barker and Blakely labs found that dSERT and human SERT (hSERT) show 51% sequence identity and similar structures with active sites.[16–18,122,152] They also explored hSERT/dSERT chimeras where they used site-specific mutagenesis to understand genetic differences to citalopram.[16] Additionally, the Krantz group also created genetic screens to test neuropsychiatric drugs that target monoamine neurotransmitters with this model.[153] Specifically, they were able to introduce a mutation in the *Drosophila* vesicular monoamine transporter (dVMAT) to perform suppressor screens with ~1000 known drugs to understand their effects on larval locomotion.[153] In addition to these examples, a majority of *Drosophila* neuroscience research focuses on understanding genetic effects with behavioral assays, like locomotion or feeding, but real-time characterizations of serotonin changes and antidepressants effects have not been explored in this model.[146,148,154,155]

1.3.4 D. melanogaster locomotion and feeding behavioral assays in larvae and adults

Initially, *Drosophila* was first used to understand changes in behavior with alcohol addiction.[132,135] Specifically, when alcohol vapors were applied to adult flies, it was found that they exhibited similar locomotion changes to humans where low doses caused activation and disinhibition, while higher doses caused sedation and loss of righting reflex.[135] Since then, *Drosophila* has been used to understand locomotion changes with different genetic mutations and drugs in both larvae and adults.[148,155,156] Originally, the cheapest and easiest method used to measure fly locomotion was with a Petri dish above graph paper, where a scientist would count how many squares a larva or adult crossed in a specific amount of time.[157] Another popular locomotion test is a climbing assay for adults, where a tube is inverted and the time required for a fly to climb to the top is recorded to understand changes in its physiological motor function with neurodegenerative diseases or depression.[144,146] With larvae, their main locomotion behaviors include forward and backward crawling, body turns, head sweeps, hunching, burrowing, and rolling (escape).[156] Besides monitoring these crawling movements, another popular locomotion test for larvae includes counting their body wall contractions (BWCs) with a microscope and Petri dish.[155,156,158] Although these tests are cheap and easy to carry out, human measurements can lead to error and bias, so over the past 20 years, real-time tracking of *Drosophila* with video recording technology has been developed to study locomotion changes in adults and larvae.[159]

Historically, Rothenfluh and Heberlein were the first to use video recording technology in the early 2000s to compare adult fly locomotion with drugs of abuse, including ethanol and cocaine.[159] Since then, there locomotion tracking video technology has become common in *Drosophila* labs.[146,148,159] Usually, a camera is able to record a larva or adult fly in a 100 ms time frame over a 20-30 s period.[159] The animal's movements are stitched together, and computer software is able to draw its movements around an "arena," which is usually a Petri dish. Although these techniques seem rudimentary, they eliminate human error, and computer software also analyzes large replicates of flies for genetic screens or drug assays very easily.[148,159] However, over the past few years, new real-time locomotion tracking systems have also been developed that investigate neural circuitry in locomotion using virtual reality experiences in fruit flies.[160,161]

The newest fruit fly locomotion-tracking systems use virtual reality to simulate visual or olfactory conditioning that elicit moving behaviors, which is linked to specific neurotransmitters or neural circuits using genetic tools.[160,162,163] With virtual reality experiments, opotogenetics is frequently used to provoke a certain behavior with light in fruit flies.[85,137,164,165] Using the GAL4/UAS system, a genetically-encoded, light-sensitive cation channel (CsChrimson) are targeted to a tissue-specific driver for a neurotransmitter, neural circuit, or anatomical region (i.e. Trh-Gal4 targets tryptophan hydroxylase in serotonin neurons).[49,79,166] With CsChrimson, a red light

(617 nm) activates the cation channel in a tissue from the Gal4 driver.[85,165] With these techniques, there are several locomotion-tracking systems currently available.[160,161] In Flores-Valle and Seelig, they developed the locomotion-tracking virtual reality system with an arena surrounding a rotating ball.[160] A camera is focused on a tethered fly, pinned to the rotating ball, and the surrounding arena enables visual cues and optogenetic light stimulations. This system allows for experiments that investigate guided memory and learning through place memory, and the arena also allows for direct imaging of specific neurons or neuronal circuits *in vivo*.[160,167–169] Although this ball locomotion-tracking system is exquisite, it only records adult fruit fly movements. Tadres and Louis created the PiVR system, which is a closed-loop, tracking platform that monitors the locomotion changes for fruit fly larvae or adults.[161] The PiVR system uses a Raspberry Pi computer connected to a hand-made platform made of cheap materials (<$500), including acrylic sheets and infrared and red lights used for optogenetics, which are illustrated in Figure 16.[161] A camera records the animal's movement in the arena, and the PiVR software creates different stimulations with virtual reality patterns in the arena to elicit behavior changes in the animal.[161] In addition to being inexpensive, the PiVR system also allows for odor diffusion, which can be utilized for memory, reward, or aversion behavior experiments.[150,161,162,170] Although both of these virtual reality, locomotion-tracking systems enable better behavioral data collection, they have not been used yet to understand different genetic or antidepressant effects with depression.

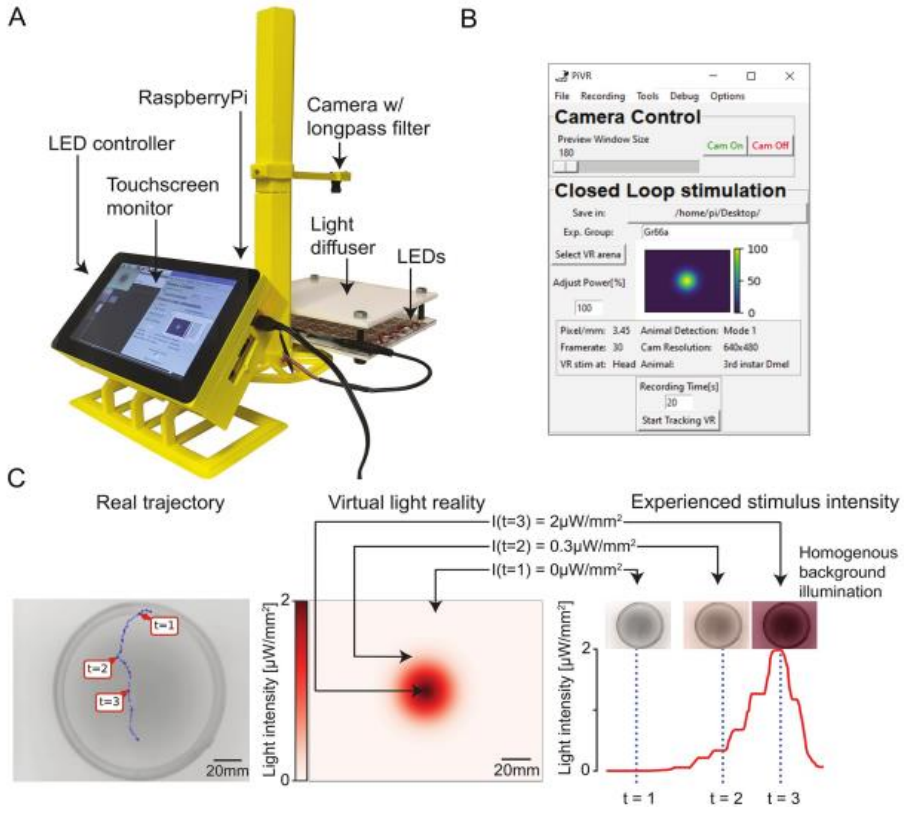

Figure 16. Virtual realities created by PiVR. (A) Picture of the standard PiVR setup. The animal is placed on the light diffuser and illuminated from below using infrared LEDs and recorded from above. The Raspberry Pi computer and the LED controller are attached to the touch screen, which permits the user to interface with the PiVR setup. (B) Screenshot of the GUI while running a virtual reality experiment. The GUI has been designed to be intuitive and easy to use while presenting all important experimental parameters that can be modified. (C) Virtual realities are created by updating the intensity of a homogeneous light background based on the current position of a tracked animal mapped onto a predefined landscape shown at the center. (Center) Predefined virtual gradient with a Gaussian geometry. (Left) Trajectory of an unconstrained animal moving in the physical arena. (Right) The graph indicates the time course of the light intensity experienced by the animal during the trajectory displayed in the left panel. Depending on the position of the animal in the virtual-light gradient, the LEDs are turned off (t = 1) or turned on at an intermediate (t = 2) or maximum intensity (t = 3). GUI, graphical user interface; LED, light-emitting diode; PiVR, Raspberry Pi Virtual Reality. Taken from Tadres, D.; Louis, M. PiVR: An Affordable and Versatile Closed-Loop Platform to Study Unrestrained Sensorimotor Behavior. *PLoS Biol.* **2020**, *18* (7), 1–25. https://doi.org/10.1371/journal.pbio.3000712.

With *Drosophila*, depression has been found to affect locomotion behaviors with serotonin receptor and dSERT genetic mutations, as well as antidepressants.[146,148,155] In Majeed et al., they compared BWC changes in serotonin receptor RNAi knockdowns and serotonin biosynthesis-inhibited larvae compared to a control.[155] They found that serotonin 2A and 2B receptors play a modulatory role in the larvae sensory motor circuit. They also fed larve different drugs, including fluoxetine, which inhibited locomotion compared to the control.[155] In Hidalgo et al., they also investigated larvae locomotion changes for a new dSERT mutant and antidepressant, 4-methylthioamphetamine (4-MTA), where the larva's movements were tracked with a camera across a Petri dish when an aversive odor, benzaldehyde (Bz), was applied to one side of the arena.[148] Normally, a larva will crawl away from the Bz odor. Although they found the dSERT mutants did not show different aversion behaviors compared to the wild type (wt) group,

mutants that were fed 4-MTA did not show similar aversion behaviors compared to the control. Both works show that antidepressant treatments affect locomotion behaviors in larvae.[148,155] In addition to larvae, Ries et al. were able to investigate climbing behavior changes in adult fruit flies with serotonin receptor 1A and 1B RNAi knockdowns. They used a novel induced vibrational stress model to replicate depression in adult flies, and performed climbing assays to show their motivation to move. Interestingly, they found that the 5-HT1A RNAi knockdown did not seek sugar relief after climbing, which showed a change in motivation from depression symptoms.[146] Although these studies showed locomotion changes with dSERT and serotonin receptor mutation, as well as antidepressants, new real-time locomotion tracking systems like the walking tethered fly ball or PiVR have not been explored.[160,161]

Drosophila are also used to understand changes in feeding behavior.[155,163,171–173] Previously, the most common method to measure changes in *Drosophila* feeding was to manually count mouth hook movements (MHMs) with a larva under a microscope.[155] In Majeed et al., they counted MHMs with receptor 5-HT 1A, 1B, and 7 RNAi knockdowns, and found that the receptor 5-HT 1A and 1B knockdowns exhibited decreased mouth hook movements compared to a control.[155] Although this work shows a correlation between feeding behavior and serotonin receptor mutations, manually counting MHMs can introduce human error and bias. To circumvent this issue, several labs have pioneered a consumption-excretion dye tracer method that analytically measures the amount of food fruit flies consume and excrete with common Ultraviolet-Visible (UV-Visible) spectrophotometers.[174–177] In Shell et al., they used common food dyes, like FD&C Blue No. 1, to stain food media that adult fruit flies consume, which is shown in Figure 17.[174] After a period of time, the flies can be collected and homogenized with a centrifuge to make a tissue aggregate that expels the dye tracer. Upon eating colored food, the fly's stomach tissue will become the color of the dye tracer.[174–176] Additionally, special feeding tubes can be used to collect the waste the flies excrete.[174,177] The consumed and excreted food dye are analytically measured with a UV-Vis, and the concentration of food consumed is calculated from a calibration curve.[174,177] Although the con-ex measurement method eliminates human bias and error, it is a relatively new technique that has not been used to measure differences with genetics or antidepressants for depression in *Drosophila*. Still, the method is slowly becoming more mainstream, and new dye tracers with more colors have been created.[175,176]

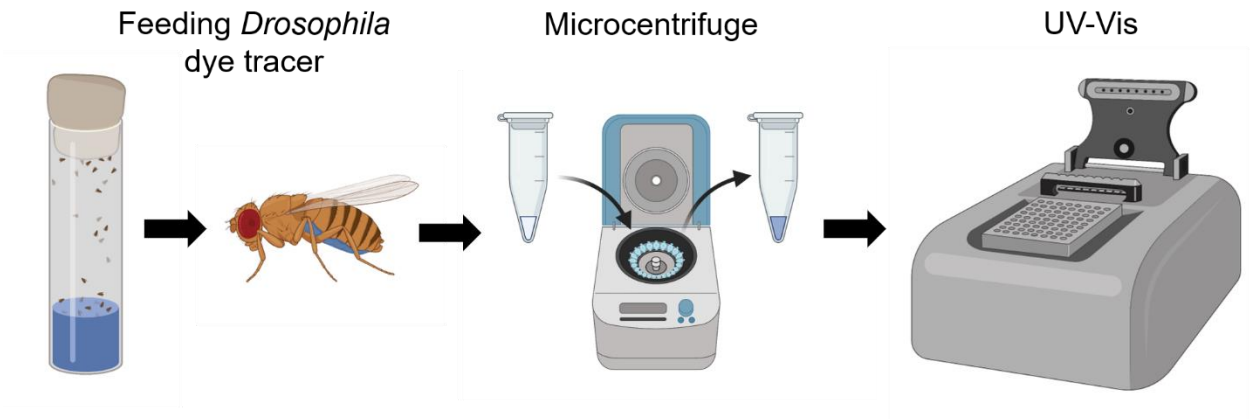

Figure 17. Schematic diagram of consumption method to quantify food intake in *Drosophila.* Food media is mixed with 10% v/w FD&C Blue No. 1, which turns food blue in color. Adult fruit flies consume the food for a specific period of time (i.e. 24 hours), and the dye makes their abdomens appear blue. Dye tracer is expelled from adult flies by creating a tissue homogenate with a microcentrifuge. Dye tracer is quantified by measuring absorbance of sample at 630 nm and comparing the sample's absorbance to a calibration curve. Figure created in BioRender.

1.3.5 Previous real-time serotonin electrochemical research with D. melanogaster

With depression research in fruit flies, very few researchers have used electrochemical techniques to understand how serotonin changes in real-time, or its impact on behavioral changes. Initially, separation techniques, like CE, HPLC, or MS were primarily used to identify neurotransmitters and their concentrations in *Drosophila* tissue homogonates of both larvae and adults.[178] For example, in Denno et al., they found that serotonin content in *Drosophila* brain tissue was not significantly different between the life stages (larva, pupa, and adult) or by sex.[109] Over the past 10 years, however, there has been an influx of researchers who use real-time electrochemical techniques to understand serotonin changes. In Majeed et al., they recorded excitatory postsynaptic potentials using amperometry to understand how muscle fibers were affected with different 5-HT receptor RNAi knockdowns. They found that 5-HT-2A and 2B play a modulatory role in the larvae sensory motor circuit, and that fluoxetine, slows locomotion compared to a control.[155] Additionally, the Campusano group also explored how bioamine neurotransmitters (serotonin, dopamine, and octopamine) were affected with a novel dSERT mutant with fluoxetine using chronoamperometry.[148] The dSERT mutant displayed increased body movements and that fluoxetine increased biogenic amine reuptake.[148] The Venton lab has mainly focused on using FSCV to measure real-time serotonin changes in *Drosophila* larvae, but changes with different antidepressant and genetic effects, as well as behavioral effects, have not been explored.[70,71,109,164]

With FSCV, the Venton lab has pioneered real-time serotonin characterization in *Drosophila* using optogenetics to stimulate its release.[49,70,71,79,164] However, most of this work focused on method development. In Borue and Venton 2009, they used Channelrhodopsin-2 (ChR2), a form of optogenetics that is activated with blue light, to stimulate serotonin release and the FSCV

Jackson waveform to measure it (Figure 18A).[71] They also explored how serotonin detection was affected with different stimulation parameters (stim. length and number) and before and after drugs like PCPA were applied. Additionally, in Borue and Venton 2010, they further characterized serotonin release and vesicle re-packaging by applying different drugs (cocaine and PCPA) with repeated optogenetic stimulations.[70] Here, they found that the releasable pool of serotonin takes between 2-5 minutes to replenish itself with repeated stimulations. Further, in Xiao et al., they continued to investigate how serotonin FSCV detection was affected with different pulsed stimulations, varied frequencies, and ChR2 optogenetic stimulations. Here, they also compared how serotonin concentration and reuptake were affected with 100 µM fluoxetine, which is illustrated in Figure 18B-C. Ultimately, they used this information to compare serotonin and dopamine kinetics and found that serotonin's V_{max} was 0.54 ± 0.07 µM/s and K_m was 0.61 ± 0.04 µM, while dopamine's V_{max} was 0.12 ± 0.03 µM/s and K_m was 1.6 ± 0.3 µM. Although these works pioneered method development to explore how real-time serotonin changes with FSCV in a single *Drosophila* larva, they have not been applied to understand different antidepressant effects with SSRIs or micro-dosing ketamine, or genetic mutations to SERT and 5-HT receptors.

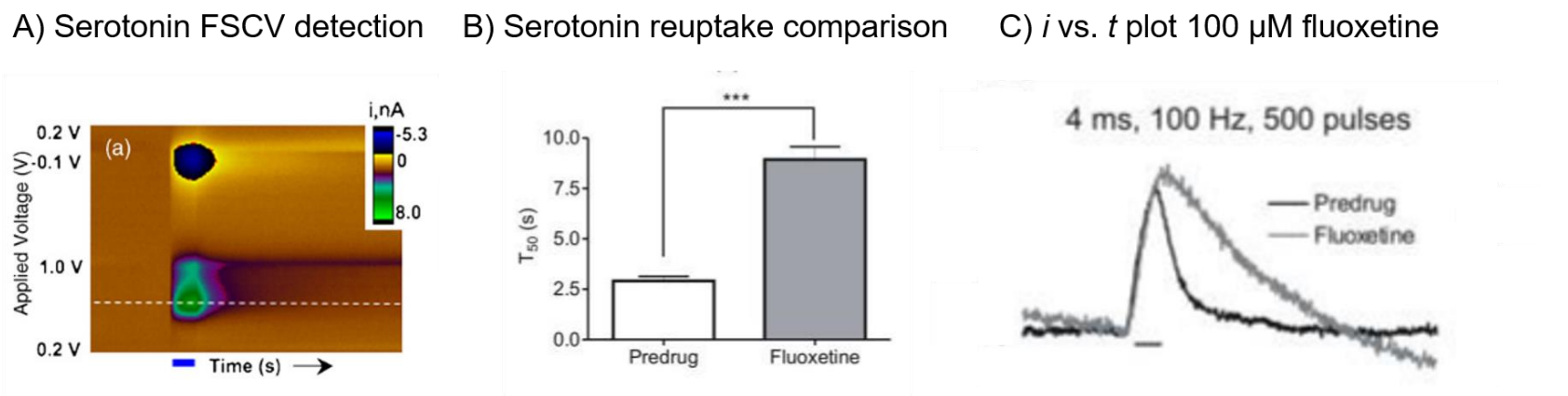

Figure 18. Real-time FSCV serotonin detection and changes with fluoxetine in *Drosophila* larvae VNC tissue. **A.** Serotonin is detected using the FSCV Jackson waveform at a CFME inserted into VNC tissue. A 2-second optogenetic stimulation (ChR2) was applied. FSCV can be used to determine serotonin concentrations when compared to a post-calibration factor. **B.** SSRIs, like fluoxetine, inhibit serotonin reuptake. Here, 100 µM fluoxetine slows serotonin clearance significantly compared to pre-drug after 15 minutes (***$p < 0.001$, paired *t* test, n = 15). **C.** An *i*-vs *t* plot shows how serotonin concentrations change before and after 100 µM fluoxetine was applied (2 second stim). Current slightly increases, which is proportional to concentration, and reuptake is slower. Taken from Borue, X.; Cooper, S.; Hirsh, J.; Condron, B.; Venton, B. J. Quantitative Evaluation of Serotonin Release and Clearance in Drosophila. J. Neurosci. Methods 2009, 179 (2), 300–308. https://doi.org/10.1016/j.jneumeth.2009.02.013 and Xiao, N.; Privman, E.; Venton, B. J. Optogenetic Control of Serotonin and Dopamine Release in Drosophila Larvae. *ACS Chem. Neurosci.* **2014**, *5* (8), 666–673. https://doi.org/10.1021/cn500044b.

1.4 Overview of Dissertation

Depression is a common mental illness. However, current treatment options are extremely variable from person to person. The main neurochemical target of interest for common selective serotonin reuptake inhibitors (SSRIs) is the serotonin transporter (SERT) on serotonin neurons. SSRIs bind to SERT to inhibit a negative feedback loop that causes extracellular serotonin concentrations to increase. However, it is not clear if all antidepressants share this mechanism of action. Further, it is not understood how different genetic polymorphisms to the gene that encodes SERT affect its structure and function, which impacts antidepressant activity. Currently, it is difficult to study depression because of a lack of biological models that replicate SERT genetic differences and accurate analytical techniques that measure real-time serotonin changes *in vivo*. This dissertation aims to improve fast-scan cyclic voltammetry (FSCV) detection of serotonin and use new analytical techniques to understand different antidepressant and genetic effects on serotonin in *Drosophila* brain tissue.

In Chapter 2, I explore different FSCV waveforms to understand electrode fouling to serotonin and its major metabolite, 5-hydroxindoleacetic acid (5-HIAA), to improve real-time serotonin detection. In previous FSCV research, modified Dopamine waveforms with extended switching potentials (≥ 1.3 V) and extended holds (≥ 1 ms) increased dopamine sensitivity and reduced electrode fouling. However, the Jackson waveform, that is used for serotonin detection, has not been revisited in more than 25 years to reduce electrode fouling to serotonin. In this chapter, I analyze repeated measurement and long-term electrode fouling to serotonin and 5-HIAA with four waveforms: the Jackson waveform (0.2 V, 1.0 V, -0.1 V, 0.2 V, 1000 V/s), the dopamine waveform (-0.4 V, 1.3 V, -0.4 V, 400 v/s), the extended serotonin waveform (0.2 V, 1.3 V, -0.1 V, 0.2 V, 1000 V/s), and the extended hold serotonin waveform (0.2 V, 1.3 V (1 ms), -0.1 V, 0.2 V, 1000 V/s). Electrode sensitivity and selectivity for serotonin and dopamine will also be compared with each waveform. I find that extending the switching potential to 1.3 V decreases electrode fouling by 50% for both analytes. However, the dopamine waveform eliminates electrode fouling because of its negative holding potential and 1.3 V switching potential. Additionally, all extended switching potential waveforms increase serotonin and dopamine sensitivity, but the Jackson waveform is the most selective for serotonin. I also characterize serotonin detection *in vitro* in fruit fly larvae VNC tissue and find that electrodes do not foul with repeated optogenetic stimulations, which shows that *Drosophila melanogaster* may be a beneficial model to measure serotonin. This work provides a tool-box of serotonin waveforms that can be used to measure serotonin in different experiments where high sensitivity or selectivity may be needed, or no electrode fouling.

Chapter 3 uses FSCV with the new extended serotonin waveform (ESW) and optogenetics to compare serotonin concentration and reuptake changes with four common SSRIs: fluoxetine, escitalopram, paroxetine, and citalopram. The goal of the study is to understand individual mechanisms of SSRI in *Drosophila* larvae. SSRIs are assumed to have the same mechanism of action, where they bind to SERT to inhibit serotonin reuptake. However, many do not share the same chemical structural motifs, and they are known to bind to SERT with different affinities. In this chapter, we investigate real-time serotonin concentration and reuptake changes after applying various doses (0.1-100 µM) of SSRIs to *Drosophila* larvae VNC tissue. I find that fluoxetine increases reuptake from 1-100 µM, but serotonin concentrations only increase at 100 µM. Thus, fluoxetine occupies dSERT and slows clearance, but does not affect concentration. Escitalopram and paroxetine increase serotonin concentrations at all doses, but escitalopram increases reuptake more. Citalopram shows lower concentration changes and faster reuptake profiles compared to escitalopram, so the racemic mixture of citalopram does not change reuptake as much as the *S*-isomer. I also construct dose response curves to compare dSERT affinities and paroxetine shows the highest affinity and fluoxetine the lowest. These data demonstrate SSRI mechanisms are complex, with separate effects on reuptake or release. I also compare our data to previous FSCV data collected in mammals and find that serotonin changes are similar in both models. This work establishes how antidepressants affect serotonin in real-time, which is useful for future studies that will investigate pharmacological effects of SSRIs with different genetic mutations in *Drosophila*

Chapter 4 explores changes in real-time serotonin dynamics with ketamine compared to SSRIs to determine differences in serotonin regulation that may contribute to their different mechanisms of action. Ketamine is considered an essential drug for anesthesia, and the FDA approved micro-dosing ketamine for treatment resistant depression in 2019. Formally, ketamine is classified as an NMDA antagonist, but it has unclear effects on the serotonergic system. It is not understood how serotonin changes in real-time with ketamine versus common SSRIs, or how real-time locomotion and feeding behaviors change with these treatments. In this chapter, I measure and characterize serotonin changes with FSCV, and track real-time locomotion and feeding behaviors in *Drosophila* larvae with Raspberry Pi Virtual Reality (PiVR) and Ultraviolet-Visible (UV-Vis) Spectroscopy. I fed larvae various doses (1 – 100 mM) of antidepressants (fluoxetine (Prozac), escitalopram (Lexapro), paroxetine (Paxil), and ketamine) for 24 hours, and find that ketamine does not affect serotonin concentrations or release at low doses. However, it does increases serotonin release at mid-doses and inhibits serotonin reuptake at higher, anesthetic doses. Additionally, all SSRIs affect serotonin reuptake, but yield different concentration changes because of their different SERT affinities that are similar to our previous bath-applications. There are also dose-dependent effects were low doses of escitalopram and fluoxetine inhibited SERT, but did not affect serotonin concentrations. I also show that low doses of ketamine, escitalopram, and fluoxetine significantly increase feeding and locomotion

behaviors. These data suggest ketamine's mechanism of action is complex and different from SSRI antidepressants. Specifically, ketamine does not rely on serotonin at micro-doses or SERT inhibition. Additionally, the locomotion and feeding behavior changes with ketamine, escitalopram, and fluoxetine suggest different downstream effects with glutamate, 5-HT receptors, or SERT, since their profiles are so different. Future studies should also investigate real-time, multiplexed changes in glutamate and serotonin for these antidepressants. However, this work shows that *Drosophila* is a good model system to study complex mechanisms of different types of antidepressants.

Chapter 5 explores future directions of this research with different genetic mutations to SERT compared to control data collected in Chapters 2-3. Two *Drosophila* SERT mutant lines will be investigated with specific point mutations or whole gene knock-outs created with CRISPR-Cas9. FSCV and optogenetics will be also be used to compare serotonin release and reuptake changes for SSRIs and ketamine. Additionally, novel *in vivo Drosophila* adult experiments will be explored to multiplex serotonin FSCV detection with glutamate genetic sensors to understand how they change using 5-HT-1A and 1B RNAi knockdowns with micro-dosing ketamine treatments.

In summary, my dissertation improves analytical detection of serotonin *in vitro* in brain tissue with FSCV, and applies these techniques to understand biological differences between several antidepressant drugs and individual genetic effects. I show that serotonin release and reuptake changes are unique for different antidepressant drugs and with genetic mutations. This work benefits others in analytical chemistry and neurochemistry who will use these techniques and models to explore new antidepressant therapies or other neurotransmitters, like dopamine and glutamate, to help design and implement successful treatments for depression.

1.5 References

(1) Fakhoury, M. Revisiting the Serotonin Hypothesis: Implications for Major Depressive Disorders. *Mol. Neurobiol.* **2016**, *53* (5), 2778–2786. https://doi.org/10.1007/s12035-015-9152-z.

(2) Fidalgo, S.; Ivanov, D. K.; Wood, S. H. Serotonin: From Top to Bottom. *Biogerontology* **2013**, *14* (1), 21–45. https://doi.org/10.1007/s10522-012-9406-3.

(3) Berger, M.; Gray, J. A.; Roth, B. L. The Expanded Biology of Serotonin. *Annu. Rev. Med.* **2009**, *60*, 355–366. https://doi.org/10.1146/annurev.med.60.042307.110802.

(4) Siegel, George; Albers, Wayne; Brady, Scott; Price, D. Serotonin. In *Basic Neurochemistry: Molecular, Cellular, and Medical Aspects*; American Society for Neurochemistry: Burlington, Massachusetts, 2006; pp 227–248.

(5) Xiao, N.; Privman, E.; Venton, B. J. Optogenetic Control of Serotonin and Dopamine Release in Drosophila Larvae. *ACS Chem. Neurosci.* **2014**, *5* (8), 666–673. https://doi.org/10.1021/cn500044b.

(6) Hensley, A. L.; Colley, A. R.; Ross, A. E. Real-Time Detection of Melatonin Using Fast-Scan Cyclic Voltammetry. *Anal. Chem.* **2018**, *90* (14), 8642–8650. https://doi.org/10.1021/acs.analchem.8b01976.

(7) Hashemi, P.; Dankoski, E. C.; Petrovic, J.; Keithley, R. B.; Wightman, R. M. Voltammetric Detection of 5-Hydroxytryptamine Release in the Rat Brain. *Anal. Chem.* **2009**, *81* (22), 9462–9471. https://doi.org/10.1021/ac9018846.

(8) Kundys, M.; Adamiak, W.; Jönsson-Niedziółka, M. Rotating Droplet as a New Alternative for Small Volume Electrochemical Measurements. *Electrochem. commun.* **2016**, *72*, 46–49. https://doi.org/10.1016/j.elecom.2016.08.025.

(9) Charnay, Y.; Leger, L. Brain Serotonergic Circuitries. *Dialogues Clin. Neurosci.* **2010**, *12* (4), 471–487. https://doi.org/10.31887/dcns.2010.12.4/ycharnay.

(10) Moran, R. J.; Kishida, K. T.; Lohrenz, T.; Saez, I.; Laxton, A. W.; Witcher, M. R.; Tatter, S. B.; Ellis, T. L.; Phillips, P. E.; Dayan, P.; Montague, P. R. The Protective Action Encoding of Serotonin Transients in the Human Brain. *Neuropsychopharmacology* **2018**, *43* (6), 1425–1435. https://doi.org/10.1038/npp.2017.304.

(11) Liao, H.; Ellena, J.; Liu, L.; Szabo, G.; Cafiso, D.; Castle, D. Secretory Carrier Membrane Protein SCAMP2 and Phosphatidylinositol 4,5-Bisphosphate Interactions in the Regulation of Dense Core Vesicle Exocytosis. *Biochemistry* **2007**, *46* (38), 10909–10920. https://doi.org/10.1021/bi701121j.

(12) Zhong, H.; Sánchez, C.; Caron, M. G. Consideration of Allosterism and Interacting Proteins in the Physiological Functions of the Serotonin Transporter. *Biochem. Pharmacol.* **2012**, *83* (4), 435–442. https://doi.org/10.1016/j.bcp.2011.09.020.

(13) Murphy, Dennis L.; Lerner, Alicja; Rudnick, Gary; Lesch, K.-P. Serotonin Transporter: Gene, Genetic Disorders, and Pharmacogenetics. *Mol. Interv.* **2004**, *4* (2), 1–6. https://doi.org/10.1016/B978-008055232-3.60442-8.

(14) Best, J.; Duncan, W.; Sadre-Marandi, F.; Hashemi, P.; Nijhout, H. F.; Reed, M. Autoreceptor Control of Serotonin Dynamics. *BMC Neurosci.* **2020**, *21* (1), 1–21. https://doi.org/10.1186/s12868-020-00587-z.

(15) Silva, B.; Goles, N. I.; Varas, R.; Campusano, J. M. Serotonin Receptors Expressed in Drosophila Mushroom Bodies Differentially Modulate Larval Locomotion. *PLoS One* **2014**, *9* (2). https://doi.org/10.1371/journal.pone.0089641.

(16) Barker, E. L.; Perlman, M. A.; Adkins, E. M.; Houlihan, W. J.; Pristupa, Z. B.; Niznik, H. B.; Blakely, R. D. High Affinity Recognition of Serotonin Transporter Antagonists Defined by Species-Scanning Mutagenesis. An Aromatic Residue in Transmembrane Domain I Dictates Species-Selective Recognition of Citalopram and Mazindol. *J. Biol. Chem.* **1998**, *273* (31), 19459–19468. https://doi.org/10.1074/jbc.273.31.19459.

(17) Rodriguez, G. J.; Roman, D. L.; White, K. J.; Nichols, D. E.; Barker, E. L. Distinct Recognition of Substrates by the Human and Drosophila Serotonin Transporters. *J. Pharmacol. Exp. Ther.* **2003**, *306* (1), 338–346. https://doi.org/10.1124/jpet.103.048751.

(18) Demchyshyn, L. L.; Pristupa, Z. B.; Sugamori, K. S.; Barker, E. L.; Blakely, R. D.; Wolfgang, W. J.; Forte, M. A.; Niznik, H. B. Cloning, Expression, and Localization of a Chloride-Facilitated, Cocaine-Sensitive Serotonin Transporter from Drosophila Melanogaster. *Proc. Natl. Acad. Sci. U. S. A.* **1994**, *91* (11), 5158–5162. https://doi.org/10.1073/pnas.91.11.5158.

(19) Roman, D. L.; Saldaña, S. N.; Nichols, D. E.; Carroll, F. I.; Barker, E. L. Distinct Molecular Recognition of Psychostimulants by Human and Drosophila Serotonin Transporters. *J. Pharmacol. Exp. Ther.* **2004**, *308* (2), 679–687. https://doi.org/10.1124/jpet.103.057836.

(20) Li, Y. F. A Hypothesis of Monoamine (5-HT) – Glutamate/GABA Long Neural Circuit: Aiming for Fast-Onset Antidepressant Discovery. *Pharmacol. Ther.* **2020**, *208*, 107494. https://doi.org/10.1016/j.pharmthera.2020.107494.

(21) Van Heeringen, K.; Mann, J. J. The Neurobiology of Suicide. *The Lancet Psychiatry* **2014**, *1* (1), 63–72. https://doi.org/10.1016/S2215-0366(14)70220-2.

(22) Davis, J. E. The Biologization of Everyday Suffering. In *Chemically Imbalanced*; The University of Chicago Press: Chicago, Illinois, United States, 2020; pp 42–69. https://doi.org/https://doi.org/10.7208/chicago/9780226686714.001.0001.

(23) Sun-edelstein, C.; Tepper, S. J.; Shapiro, R. E. Syndrome : A Review. **2008**.

(24) Taylor, D. J. E.; Braithwaite, R. A. Cardiac Effects of Tricyclic Antidepressant Medication a Preliminary Study of Nortriptyline. *Heart* **1978**, *40* (9), 1005–1009. https://doi.org/10.1136/hrt.40.9.1005.

(25) Wong, D. T.; Perry, K. W.; Bymaster, F. P. The Discovery of Fluoxetine Hydrochloride (Prozac). *Nature Reviews Drug Discovery*. December 2005, p 950. https://doi.org/10.1038/nrd1821.

(26) Wood, K. M.; Zeqja, A.; Nijhout, H. F.; Reed, M. C.; Best, J.; Hashemi, P. Voltammetric and Mathematical Evidence for Dual Transport Mediation of Serotonin Clearance in Vivo. *J. Neurochem.* **2014**, *130* (3), 351–359. https://doi.org/10.1111/jnc.12733.

(27) Owens, M. J.; Knight, D. L.; Nemeroff, C. B. Second-Generation SSRIs: Human Monoamine Transporter Binding Profile of Escitalopram and R-Fluoxetine. *Biol. Psychiatry* **2001**, *50* (5), 345–350. https://doi.org/10.1016/S0006-3223(01)01145-3.

(28) Zeppelin, T.; Ladefoged, L. K.; Sinning, S.; Schiøtt, B. Substrate and Inhibitor Binding to the Serotonin Transporter: Insights from Computational, Crystallographic, and Functional Studies. *Neuropharmacology* **2019**, *161* (December 2018), 107548. https://doi.org/10.1016/j.neuropharm.2019.02.030.

(29) Staroń, J.; Pietruś, W.; Bugno, R.; Kurczab, R.; Satała, G.; Warszycki, D.; Lenda, T.; Wantuch, A.; Hogendorf, A. S.; Hogendorf, A.; Duszyńska, B.; Bojarski, A. J. Tuning the Activity of Known Drugs via the Introduction of Halogen Atoms, a Case Study of SERT Ligands – Fluoxetine and Fluvoxamine. *Eur. J. Med. Chem.* **2021**, *220*. https://doi.org/10.1016/j.ejmech.2021.113533.

(30) Andersen, J.; Stuhr-Hansen, N.; Zachariassen, L. G.; Koldsø, H.; Schiøtt, B.; Strømgaard, K.; Kristensen, A. S. Molecular Basis for Selective Serotonin Reuptake Inhibition by the Antidepressant Agent Fluoxetine (Prozac). *Mol. Pharmacol.* **2014**, *85* (5), 703–714. https://doi.org/10.1124/mol.113.091249.

(31) Rannversson, H.; Andersen, J.; Bang-Andersen, B.; Strømgaard, K. Mapping the Binding Site for Escitalopram and Paroxetine in the Human Serotonin Transporter Using Genetically Encoded Photo-Cross-Linkers. *ACS Chem. Biol.* **2017**, *12* (10), 2558–2562. https://doi.org/10.1021/acschembio.7b00338.

(32) Coleman, J. A.; Green, E. M.; Gouaux, E. X-Ray Structures and Mechanism of the Human Serotonin Transporter. *Nature* **2016**, *532* (7599), 334–339. https://doi.org/10.1038/nature17629.

(33) Coleman, J. A.; Gouaux, E. Structural Basis for Recognition of Diverse Antidepressants by the Human Serotonin Transporter. *Nat. Struct. Mol. Biol.* **2018**, *25* (2), 170–175. https://doi.org/10.1038/s41594-018-0026-8.

(34) Murphy, D. L.; Li, Q.; Engel, S.; Wichems, C.; Andrews, A.; Lesch, K. P.; Uhl, G. Genetic Perspectives on the Serotonin Transporter. *Brain Res. Bull.* **2001**, *56* (5), 487–494. https://doi.org/10.1016/S0361-9230(01)00622-0.

(35) Murphy, S. E.; Norbury, R.; Godlewska, B. R.; Cowen, P. J.; Mannie, Z. M.; Harmer, C. J.; Munafò, M. R. The Effect of the Serotonin Transporter Polymorphism (5-HTTLPR) on Amygdala Function: A Meta-Analysis. *Mol. Psychiatry* **2013**, *18* (4), 512–520. https://doi.org/10.1038/mp.2012.19.

(36) Hariri, A. R.; Holmes, A. Genetics of Emotional Regulation: The Role of the Serotonin Transporter in Neural Function. *Trends Cogn. Sci.* **2006**, *10* (4), 182–191. https://doi.org/10.1016/j.tics.2006.02.011.

(37) Ogilvie, A. D.; Battersby, S.; Bubb, V. J.; Fink, G.; Harmar, A. J.; Goodwin, G. M.; Smith, C. A. D. Polymorphism in Serotonin Transporter Gene Associated with Susceptibility to Major Depression. *Lancet* **1996**, *347* (9003), 731–733. https://doi.org/10.1016/S0140-6736(96)90079-3.

(38) Houwing, D. J.; Buwalda, B.; Van Der Zee, E. A.; De Boer, S. F.; Olivier, J. D. A. The Serotonin Transporter and Early Life Stress: Translational Perspectives. *Front. Cell. Neurosci.* **2017**, *11* (April), 1–16. https://doi.org/10.3389/fncel.2017.00117.

(39) Coplan, J. D.; Gopinath, S.; Abdallah, C. G.; Berry, B. R. A Neurobiological Hypothesis of Treatment-Resistant Depression-Mechanisms for Selective Serotonin Reuptake Inhibitor Non-Efficacy. *Front. Behav. Neurosci.* **2014**, *8* (MAY), 1–16. https://doi.org/10.3389/fnbeh.2014.00189.

(40) Ruberto, V. L.; Jha, M. K.; Murrough, J. W. Pharmacological Treatments for Patients with TRD. *Pharmaceuticals* **2020**, *13*, 116.

(41) Kraus, C.; Wasserman, D.; Henter, I. D.; Acevedo-Diaz, E.; Kadriu, B.; Zarate, C. A. The Influence of Ketamine on Drug Discovery in Depression. *Drug Discov. Today* **2019**, *24* (10), 2033–2043. https://doi.org/10.1016/j.drudis.2019.07.007.

(42) Stahl, S. M. Mechanism of Action of Ketamine. *CNS Spectr.* **2013**, *18* (4), 171–174. https://doi.org/10.1017/S109285291300045X.

(43) Zanos, P.; Thompson, S. M.; Duman, R. S.; Zarate, C. A.; Gould, T. D. Convergent Mechanisms Underlying Rapid Antidepressant Action. *CNS Drugs* **2018**, *32* (3), 197–227. https://doi.org/10.1007/s40263-018-0492-x.

(44) Bowman, M. A.; Vitela, M.; Clarke, K. M.; Koek, W.; Daws, L. C. Serotonin Transporter and Plasma Membrane Monoamine Transporter Are Necessary for the Antidepressant-like Effects of Ketamine in Mice. *Int. J. Mol. Sci.* **2020**, *21* (20), 1–22. https://doi.org/10.3390/ijms21207581.

(45) Trullas, R.; Skolnick, P. Functional Antagonists at the NMDA Receptor Complex Exhibit Antidepressant Actions. *Eur. J. Pharmacol.* **1990**, *185* (1), 1–10. https://doi.org/10.1016/0014-2999(90)90204-J.

(46) Berman, R. M.; Cappiello, A.; Anand, A.; Oren, D. A.; Heninger, G. R.; Charney, D. S.; Krystal, J. H. Antidepressant Effects of Ketamine in Depressed Patients. *Biol. Psychiatry* **2000**, *47* (4), 351–354. https://doi.org/10.1016/S0006-3223(99)00230-9.

(47) Mathew, S. J.; Zarate, C. A. Ketamine for Treatment-Resistant Depression: The First Decade of Progress. *Ketamine Treat. Depress. First Decad. Prog.* **2016**, 1–155. https://doi.org/10.1007/978-3-319-42925-0.

(48) Currie, G. M. Pharmacology, Part 1: Introduction to Pharmacology and Pharmacodynamics. *J. Nucl. Med. Technol.* **2018**, *46* (2), 81–86. https://doi.org/10.2967/jnmt.117.199588.

(49) Dunham, K. E.; Venton, B. J. SSRI Antidepressants Differentially Modulate Serotonin Reuptake and Release in Drosophila. *J. Neurochem.* **2022**, No. June, 1–13. https://doi.org/10.1111/jnc.15658.

(50) Pham, T. H.; Mendez-David, I.; Defaix, C.; Guiard, B. P.; Tritschler, L.; David, D. J.; Gardier, A. M. Ketamine Treatment Involves Medial Prefrontal Cortex Serotonin to Induce a Rapid Antidepressant-like Activity in BALB/CJ Mice. *Neuropharmacology* **2017**, *112*, 198–209. https://doi.org/10.1016/j.neuropharm.2016.05.010.

(51) Can, A.; Zanos, P.; Moaddel, R.; Kang, H. J.; Dossou, K. S. S.; Wainer, I. W.; Cheer, J. F.; Frost, D. O.; Huang, X. P.; Gould, T. D. Effects of Ketamine and Ketamine Metabolites on Evoked Striatal Dopamine Release, Dopamine Receptors, and Monoamine Transporters. *J. Pharmacol. Exp. Ther.* **2016**, *359* (1), 159–170. https://doi.org/10.1124/jpet.116.235838.

(52) Wallach, J.; Gamrat, J.; Jauhola-Straight, R.; Becker, J.; Eckrich, T. Three Birds, One Excipient: Development of an Improved PH, Isotonic, and Buffered Ketamine Formulation for Subcutaneous Injection. *Pharmaceutics* **2022**, *14* (3). https://doi.org/10.3390/pharmaceutics14030556.

(53) Peritore, C. S. The Promise of Psychedelic Research. *Futur. Drug Discov.* **2022**, *4* (1). https://doi.org/10.4155/fdd-2021-0012.

(54) Lama, R. D.; Charlson, K.; Anantharam, A.; Hashemi, P. Ultrafast Detection and Quantification of Brain Signaling Molecules with Carbon Fiber Microelectrodes. *Anal. Chem.* **2012**, *84* (19), 8096–8101. https://doi.org/10.1021/ac301670h.

(55) Ganesana, M.; Lee, S. T.; Wang, Y.; Venton, B. J. Analytical Techniques in Neuroscience: Recent Advances in Imaging, Separation, and Electrochemical Methods. *Anal. Chem.* **2017**, *89* (1), 314–341. https://doi.org/10.1021/acs.analchem.6b04278.

(56) Shin, M.; Wang, Y.; Borgus, J. R.; Venton, B. J. Electrochemistry at the Synapse. *Annual Review of Analytical Chemistry*. 2019, pp 297–321. https://doi.org/10.1146/annurev-anchem-061318-115434.

(57) Venton, B. J.; Wightman, R. M. Psychoanalytical Electrochemistry: Dopamine and Behavior. *Anal. Chem.* **2003**, *75* (19).

(58) Bucher, E. S.; Wightman, R. M. Electrochemical Analysis of Neurotransmitters. *Annu. Rev. Anal. Chem.* **2015**, *8* (1), 239–261. https://doi.org/10.1146/annurev-anchem-071114-040426.

(59) Lee, W. H.; Ngernsutivorakul, T.; Mabrouk, O. S.; Wong, J. M. T.; Dugan, C. E.; Pappas, S. S.; Yoon, H. J.; Kennedy, R. T. Microfabrication and in Vivo Performance of a Microdialysis Probe with Embedded Membrane. *Anal. Chem.* **2016**, *88* (2), 1230–1237. https://doi.org/10.1021/acs.analchem.5b03541.

(60) Schultz, K. N.; Kennedy, R. T. Time-Resolved Microdialysis for In Vivo Neurochemical Measurements and Other Applications. *Annu. Rev. Anal. Chem.* **2008**, *1* (1), 627–661. https://doi.org/10.1146/annurev.anchem.1.031207.113047.

(61) Kennedy, R. T. Emerging Trends in in Vivo Neurochemical Monitoring by Microdialysis. *Curr. Opin. Chem. Biol.* **2013**, *17* (5), 860–867. https://doi.org/10.1016/j.cbpa.2013.06.012.

(62) Wang, H.-W.; Bringans, C.; Hickey, A. J. R.; Windsor, J. A.; Kilmartin, P. A.; Phillips, A. R. J. Cyclic Voltammetry in Biological

Samples: A Systematic Review of Methods and Techniques Applicable to Clinical Settings. *Signals* **2021**, *2* (1), 138–158. https://doi.org/10.3390/signals2010012.

(63) Harnisch, F.; Freguia, S. A Basic Tutorial on Cyclic Voltammetry for the Investigation of Electroactive Microbial Biofilms. *Chem. - An Asian J.* **2012**, *7* (3), 466–475. https://doi.org/10.1002/asia.201100740.

(64) Venton, B. J.; Cao, Q. Fundamentals of Fast-Scan Cyclic Voltammetry for Dopamine Detection. *Analyst* **2020**. https://doi.org/10.1039/c9an01586h.

(65) Westerink, R. H. S. Exocytosis: Using Amperometry to Study Presynaptic Mechanisms of Neurotoxicity. *Neurotoxicology* **2004**, *25* (3), 461–470. https://doi.org/10.1016/j.neuro.2003.10.006.

(66) Puthongkham, P.; Venton, B. J. Recent Advances in Fast-Scan Cyclic Voltammetry. *Analyst* **2020**. https://doi.org/10.1039/c9an01925a.

(67) Phan, N. T. N.; Li, X.; Ewing, A. G. Measuring Synaptic Vesicles Using Cellular Electrochemistry and Nanoscale Molecular Imaging. *Nat. Rev. Chem.* **2017**, *1*, 1–18. https://doi.org/10.1038/s41570-017-0048.

(68) Cao, Q.; Puthongkham, P.; Venton, B. J. Review: New Insights into Optimizing Chemical and 3D Surface Structures of Carbon Electrodes for Neurotransmitter Detection. *Anal. Methods* **2019**, *11* (3), 247–261. https://doi.org/10.1039/c8ay02472c.

(69) Venton, B. J.; Cao, Q. Fundamentals of Fast-Scan Cyclic Voltammetry for Dopamine Detection. *Analyst* **2020**, *145*, 1158–1168. https://doi.org/10.1039/C9AN01586H.

(70) Borue, X.; Condron, B.; Venton, B. J. Both Synthesis and Reuptake Are Critical for Replenishing the Releasable Serotonin Pool in Drosophila. *J. Neurochem.* **2010**, *113* (1), 188–199. https://doi.org/10.1111/j.1471-4159.2010.06588.x.

(71) Borue, X.; Cooper, S.; Hirsh, J.; Condron, B.; Venton, B. J. Quantitative Evaluation of Serotonin Release and Clearance in Drosophila. *J. Neurosci. Methods* **2009**, *179* (2), 300–308. https://doi.org/10.1016/j.jneumeth.2009.02.013.

(72) Huffman, M. L.; Venton, B. J. Carbon-Fiber Microelectrodes for in Vivo Applications. *Analyst* **2009**, *134* (1), 18–24. https://doi.org/10.1039/b807563h.

(73) Robinson, D. L.; Venton, B. J.; Heien, M. L. A. V.; Wightman, R. M. Detecting Subsecond Dopamine Release with Fast-Scan Cyclic Voltammetry in Vivo. In *Clinical Chemistry*; 2003. https://doi.org/10.1373/49.10.1763.

(74) Jackson, B. P.; Dietz, S. M.; Wightman, R. M. Fast-Scan Cyclic Voltammetry of 5-Hydroxytryptamine. *Anal. Chem.* **1995**, *67* (6), 1115–1120. https://doi.org/10.1021/ac00102a015.

(75) Wrona, M. Z.; Dryhurst, G. Electrochemical Oxidation of 5-Hydroxytryptamine in Aqueous Solution at Physiological PH. *Bioorg. Chem.* **1990**. https://doi.org/10.1016/0045-2068(90)90005-P.

(76) Anne, A.; Lemordant, D.; Dryhurst, G.; Wrona, M. Z. Mechanism and Products of Electrochemical Oxidation of 5, 7-Dihydroxytryptamine. *J. Am. Chem. Soc.* **1989**, *111* (2), 719–726. https://doi.org/10.1021/ja00184a050.

(77) Ross, A. E.; Venton, B. J. Nafion-CNT Coated Carbon-Fiber Microelectrodes for Enhanced Detection of Adenosine. *Analyst* **2012**, *137* (13), 3045–3051. https://doi.org/10.1039/c2an35297d.

(78) Dewhurst, S. A.; Croker, S. G.; Ikeda, K.; Mccaman, R. E. METABOLISM OF BIOGENIC NERVOUS TISSUE IN DROSOPHILA E Metabolism in Insect Tissues Has Received Little Attention Compared with Acetylcholine Metabolism (Metcalf & March , 1950 ; Colhoun , 1958 ; Dewhurst et Al ., 1970). In 1954 Adrenalin , Noradrenalin. *Comp. Biochem. Physiol.* **1972**, *43* (1966), 975–981.

(79) Dunham, K. E.; Venton, B. J. Improving Serotonin Fast-Scan Cyclic Voltammetry Detection: New Waveforms to Reduce Electrode Fouling. *Analyst* **2020**, *145* (22), 7437–7446. https://doi.org/10.1039/d0an01406k.

(80) Abdalla, A.; Atcherley, C. W.; Pathirathna, P.; Samaranayake, S.; Qiang, B.; Peña, E. A.; Morgan, S. L.; Heien, M. L.; Hashemi, P. In Vivo Ambient Serotonin Measurements at Carbon-Fiber Microelectrodes. *Anal. Chem.* **2017**, *89* (18), 9703–9711. https://doi.org/10.1021/acs.analchem.7b01257.

(81) Wood, K. M.; Hashemi, P. Fast-Scan Cyclic Voltammetry Analysis of Dynamic Serotonin Reponses to Acute Escitalopram. *ACS Chem. Neurosci.* **2013**, *4* (5), 715–720. https://doi.org/10.1021/cn4000378.

(82) Saylor, R. A.; Hersey, M.; West, A.; Buchanan, A. M.; Berger, S. N.; Nijhout, H. F.; Reed, M. C.; Best, J.; Hashemi, P. In Vivo Hippocampal Serotonin Dynamics in Male and Female Mice: Determining Effects of Acute Escitalopram Using Fast Scan Cyclic Voltammetry. *Front. Neurosci.* **2019**, *13* (APR), 1–13. https://doi.org/10.3389/fnins.2019.00362.

(83) Hashemi, P.; Dankoski, E. C.; Lama, R.; Wood, K. M.; Takmakov, P.; Wightman, R. M. Brain Dopamine and Serotonin Differ in Regulation and Its Consequences. **2012**, *109* (29), 1–6. https://doi.org/10.1073/pnas.1201547109.

(84) Daws, L. C.; Koek, W.; Mitchell, N. C. Revisiting Serotonin Reuptake Inhibitors and the Therapeutic Potential of “Uptake-2” in Psychiatric Disorders. *ACS Chem. Neurosci.* **2013**, *4* (1), 16–21. https://doi.org/10.1021/cn3001872.

(85) Shin, M.; Copeland, J. M.; Venton, B. J. Drosophila as a Model System for Neurotransmitter Measurements. *ACS Chem. Neurosci.* **2018**, *9* (8), 1872–1883. https://doi.org/10.1021/acschemneuro.7b00456.

(86) Ribaudo, G.; Bortoli, M.; Witt, C. E.; Parke, B.; Mena, S.; Oselladore, E.; Zagotto, G.; Hashemi, P.; Orian, L. ROS-Scavenging Selenofluoxetine Derivatives Inhibit In Vivo Serotonin Reuptake. *ACS Omega* **2021**. https://doi.org/10.1021/acsomega.1c05567.

(87) Mena, S.; Dietsch, S.; Berger, S. N.; Witt, C. E.; Hashemi, P. Novel, User-Friendly Experimental and Analysis Strategies for Fast Voltammetry: 1. The Analysis Kid for FSCV . *ACS Meas. Sci. Au* **2021**, *1* (1), 11–19. https://doi.org/10.1021/acsmeasuresciau.1c00003.

(88) Kile, B. M.; Guillot, T. S.; Venton, B. J.; Wetsel, W. C.; Augustine, G. J.; Wightman, R. M. Synapsins Differentially Control Dopamine and Serotonin Release. *J. Neurosci.* **2010**, *30* (29), 9762–9770. https://doi.org/10.1523/JNEUROSCI.2071-09.2010.

(89) Hammarlund, M.; Watanabe, S.; Schuske, K.; Jorgensen, E. M. CAPS and Syntaxin Dock Dense Core Vesicles to the Plasma Membrane in Neurons. *J. Cell Biol.* **2008**, *180* (3), 483–491. https://doi.org/10.1083/jcb.200708018.

(90) Liu, Y.; Schirra, C.; Stevens, D. R.; Matti, U.; Speidel, D.; Hof, D.; Bruns, D.; Brose, N.; Rettig, J. CAPS Facilitates Filling of the Rapidly Releasable Pool of Large Dense-Core Vesicles. *J. Neurosci.* **2008**, *28* (21), 5594–5601. https://doi.org/10.1523/JNEUROSCI.5672-07.2008.

(91) Nurrish, S. Dense Core Vesicle Release: Controlling the Where as Well as the When. *Genetics* **2014**, *196* (3), 601–604. https://doi.org/10.1534/genetics.113.159905.

(92) Renden, R.; Berwin, B.; Davis, W.; Ann, K.; Chin, C. T.; Kreber, R.; Ganetzky, B.; Martin, T. F. J.; Broadie, K. Drosophila CAPS Is an Essential Gene That Regulates Dense-Core Vesicle Release and Synaptic Vesicle Fusion. *Neuron* **2001**, *31* (3), 421–437. https://doi.org/10.1016/S0896-6273(01)00382-8.

(93) Hashemi, P.; Dankoski, E. C.; Wood, K. M.; Ambrose, R. E.; Wightman, R. M. In Vivo Electrochemical Evidence for Simultaneous 5-HT and Histamine Release in the Rat Substantia Nigra Pars Reticulata Following Medial Forebrain Bundle Stimulation. *J. Neurochem.* **2011**, *118* (5), 749–759. https://doi.org/10.1111/j.1471-4159.2011.07352.x.

(94) Best, J.; Buchanan, A. M.; Nijhout, H. F.; Hashemi, P.; Reed, M. C. Mathematical Models of Serotonin, Histamine, and Depression. *IntechOpen* **2021**, 13. https://doi.org/http://dx.doi.org/10.5772/intechopen.96990 in.

(95) Puthongkham, P.; Lee, S. T.; Venton, B. J. Mechanism of Histamine Oxidation and Electropolymerization at Carbon Electrodes. *Anal. Chem.* **2019**, *91* (13), 8366–8373. https://doi.org/10.1021/acs.analchem.9b01178.

(96) Haase, J.; Brown, E. Integrating the Monoamine, Neurotrophin and Cytokine Hypotheses of Depression - A Central Role for the Serotonin Transporter? *Pharmacol. Ther.* **2015**, *147*, 1–11. https://doi.org/10.1016/j.pharmthera.2014.10.002.

(97) Hersey, M.; Hashemi, P.; Reagan, L. P. Integrating the Monoamine and Cytokine Hypotheses of Depression: Is Histamine the Missing Link? *Eur. J. Neurosci.* **2022**, *55* (9–10), 2895–2911. https://doi.org/10.1111/ejn.15392.

(98) Hersey, M.; Reneaux, M.; Berger, S. N.; Mena, S.; Buchanan, A. M.; Ou, Y.; Tavakoli, N.; Reagan, L. P.; Clopath, C.; Hashemi, P. A Tale of Two Transmitters: Serotonin and Histamine as in Vivo Biomarkers of Chronic Stress in Mice. *J. Neuroinflammation* **2022**, *19* (1), 167. https://doi.org/10.1186/s12974-022-02508-9.

(99) Samaranayake, S.; Abdalla, A.; Robke, R.; Nijhout, H. F.; Reed, M. C.; Best, J.; Hashemi, P. A Voltammetric and Mathematical Analysis of Histaminergic Modulation of Serotonin in the Mouse Hypothalamus. *J. Neurochem.* **2016**, 374–383. https://doi.org/10.1111/jnc.13659.

(100) Hales, K. G.; Korey, C. A.; Larracuente, A. M.; Roberts, D. M. Genetics on the Fly: A Primer on the Drosophila Model System. *Genetics* **2015**, *201* (3), 815–842. https://doi.org/10.1534/genetics.115.183392.

(101) Jennings, B. H. Drosophila-a Versatile Model in Biology & Medicine. *Mater. Today* **2011**, *14* (5), 190–195. https://doi.org/10.1016/S1369-7021(11)70113-4.

(102) Markow, T. A. The Secret Lives of Drosophila Flies. *Elife* **2015**, *4* (JUNE), 1–9. https://doi.org/10.7554/eLife.06793.

(103) Roberts, D. B. Drosophila Melanogaster: The Model Organism. *Entomol. Exp. Appl.* **2006**, *121* (2), 93–103. https://doi.org/10.1111/j.1570-8703.2006.00474.x.

(104) Bellen, H. J.; Levis, R. W.; Liao, G.; He, Y.; Carlson, J. W.; Tsang, G.; Evans-Holm, M.; Hiesinger, P. R.; Schulze, K. L.; Rubin, G. M.; Hoskins, R. A.; Spradling, A. C. The BDGP Gene Disruption Project: Single Transposon Insertions Associated with 40% of Drosophila Genes. *Genetics* **2004**, *167* (2), 761–781. https://doi.org/10.1534/genetics.104.026427.

(105) Perkins, L. A.; Holderbaum, L.; Tao, R.; Hu, Y.; Sopko, R.; McCall, K.; Yang-Zhou, D.; Flockhart, I.; Binari, R.; Shim, H. S.; Miller, A.; Housden, A.; Foos, M.; Randkelv, S.; Kelley, C.; Namgyal, P.; Villalta, C.; Liu, L. P.; Jiang, X.; Huan-Huan, Q.; Wang, X.; Fujiyama, A.; Toyoda, A.; Ayers, K.; Blum, A.; Czech, B.; Neumuller, R.; Yan, D.; Cavallaro, A.; Hibbard, K.; Hall, D.; Cooley, L.; Hannon, G. J.; Lehmann, R.; Parks, A.; Mohr, S. E.; Ueda, R.; Kondo, S.; Ni, J. Q.; Perrimon, N. The Transgenic RNAi Project at Harvard Medical School: Resources and Validation. *Genetics* **2015**, *201* (3), 843–852. https://doi.org/10.1534/genetics.115.180208.

(106) Michael Harnish, J.; Link, N.; Yamamoto, S. Drosophila as a Model for Infectious Diseases. *Int. J. Mol. Sci.* **2021**, *22* (5), 1–42. https://doi.org/10.3390/ijms22052724.

(107) Philyaw, T. J.; Rothenfluh, A.; Titos, I. The Use of Drosophila to Understand Psychostimulant Responses. *Biomedicines* **2022**, *10* (1). https://doi.org/10.3390/biomedicines10010119.

(108) Wang, L.; Kounatidis, I.; Ligoxygakis, P. Drosophila as a Model to Study the Role of Blood Cells in Inflammation, Innate Immunity and Cancer. *Front. Cell. Infect. Microbiol.* **2014**, *3* (JAN), 1–17. https://doi.org/10.3389/fcimb.2013.00113.

(109) Denno, M. E.; Privman, E.; Venton, B. J. Analysis of Neurotransmitter Tissue Content of Drosophila Melanogaster in Different Life Stages. *ACS Chem. Neurosci.* **2015**, *6* (1), 117–123. https://doi.org/10.1021/cn500261e.

(110) Bassett, A. R.; Liu, J. L. CRISPR/Cas9 and Genome Editing in Drosophila. *J. Genet. Genomics* **2014**, *41* (1), 7–19. https://doi.org/10.1016/j.jgg.2013.12.004.

(111) Thibault, S. T.; Singer, M. A.; Miyazaki, W. Y.; Milash, B.; Dompe, N. A.; Singh, C. M.; Buchholz, R.; Demsky, M.; Fawcett, R.; Francis-Lang, H. L.; Ryner, L.; Cheung, L. M.; Chong, A.; Erickson, C.; Fisher, W. W.; Greer, K.; Hartouni, S. R.; Howie, E.; Jakkula, L.; Joo, D.; Killpack, K.; Laufer, A.; Mazzotta, J.; Smith, R. D.; Stevens, L. M.; Stuber, C.; Tan, L. R.; Ventura, R.; Woo, A.; Zakrajsek, I.; Zhao, L.; Chen, F.; Swimmer, C.; Kopczynski, C.; Duyk, G.; Winberg, M. L.; Margolis, J. A Complementary Transposon Tool Kit for Drosophila Melanogaster Using P and PiggyBac. *Nat. Genet.* **2004**, *36* (3), 283–287. https://doi.org/10.1038/ng1314.

(112) Bellen, H. J.; Levis, R. W.; He, Y.; Carlson, J. W.; Evans-Holm, M.; Bae, E.; Kim, J.; Metaxakis, A.; Savakis, C.; Schulze, K. L.; Hoskins, R. A.; Spradling, A. C. The Drosophila Gene Disruption Project: Progress Using Transposons with Distinctive Site Specificities. *Genetics* **2011**, *188* (3), 731–743. https://doi.org/10.1534/genetics.111.126995.

(113) Nagarkar-Jaiswal, S.; Lee, P. T.; Campbell, M. E.; Chen, K.; Anguiano-Zarate, S.; Gutierrez, M. C.; Busby, T.; Lin, W. W.; He, Y.; Schulze, K. L.; Booth, B. W.; Evans-Holm, M.; Venken, K. J. T.; Levis, R. W.; Spradling, A. C.; Hoskins, R. A.; Bellen, H. J. A Library of MiMICs Allows Tagging of Genes and Reversible, Spatial and Temporal Knockdown of Proteins in Drosophila. *Elife* **2015**, *2015* (4), 1–28. https://doi.org/10.7554/eLife.05338.

(114) Deng, B.; Li, Q.; Liu, X.; Cao, Y.; Li, B.; Qian, Y.; Xu, R.; Mao, R.; Zhou, E.; Zhang, W.; Huang, J.; Rao, Y. Chemoconnectomics: Mapping Chemical Transmission in Drosophila. *Neuron* **2019**, *101* (5), 876-893.e4. https://doi.org/10.1016/j.neuron.2019.01.045.

(115) Rio, D. C. Regulation of Drosophila P Element Transposition. *Trends Genet.* **1991**, *7* (9), 282–287. https://doi.org/10.1016/0168-9525(91)90309-E.

(116) Brand, a H.; Perrimon, N. Targeted Gene Expression as a Means of Altering Cell Fates and Generating Dominant

Phenotypes. *Development* **1993**, *118* (2), 401–415.

(117) Bellés, X. Beyond Drosophila: RNAi in Vivo and Functional Genomics in Insects. *Annu. Rev. Entomol.* **2010**, *55*, 111–128. https://doi.org/10.1146/annurev-ento-112408-085301.

(118) Lee, P. T.; Zirin, J.; Kanca, O.; Lin, W. W.; Schulze, K. L.; Li-Kroeger, D.; Tao, R.; Devereaux, C.; Hu, Y.; Chung, V.; Fang, Y.; He, Y.; Pan, H.; Ge, M.; Zuo, Z.; Housden, B. E.; Mohr, S. E.; Yamamoto, S.; Levis, R. W.; Spradling, A. C.; Perrimon, N.; Bellen, H. J. A Gene-Specific T2A-GAL4 Library for Drosophila. *Elife* **2018**, *7* (1993), 1–24. https://doi.org/10.7554/eLife.35574.

(119) Xu, J.; Ren, X.; Sun, J.; Wang, X.; Qiao, H. H.; Xu, B. W.; Liu, L. P.; Ni, J. Q. A Toolkit of CRISPR-Based Genome Editing Systems in Drosophila. *J. Genet. Genomics* **2015**, *42* (4), 141–149. https://doi.org/10.1016/j.jgg.2015.02.007.

(120) Meltzer, H.; Marom, E.; Alyagor, I.; Mayseless, O.; Berkun, V.; Segal-Gilboa, N.; Unger, T.; Luginbuhl, D.; Schuldiner, O. Tissue-Specific (Ts)CRISPR as an Efficient Strategy for in Vivo Screening in Drosophila. *Nat. Commun.* **2019**, *10* (1). https://doi.org/10.1038/s41467-019-10140-0.

(121) Martin, C. A.; Krantz, D. E. Drosophila Melanogaster as a Genetic Model System to Study Neurotransmitter Transporters. *Neurochem. Int.* **2014**, *73* (1), 71–88. https://doi.org/10.1016/j.neuint.2014.03.015.

(122) Barker, E. L.; Blakely, R. D. Structural Determinants of Neurotransmitter Transport Using Cross- Species Chimeras: Studies on Serotonin Transporter. *Methods Enzymol.* **1998**, *296* (1990), 475–498. https://doi.org/10.1016/S0076-6879(98)96035-9.

(123) Lu, Y.; Su, F.; Li, Q.; Zhang, J.; Li, Y.; Tang, T.; Hu, Q.; Yu, X. Q. Pattern Recognition Receptors in Drosophila Immune Responses. *Dev. Comp. Immunol.* **2020**, *102* (July 2019), 103468. https://doi.org/10.1016/j.dci.2019.103468.

(124) Ng, C. T.; Yu, L. E.; Ong, C. N.; Bay, B. H.; Baeg, G. H. The Use of Drosophila Melanogaster as a Model Organism to Study Immune-Nanotoxicity. *Nanotoxicology* **2019**, *13* (4), 429–446. https://doi.org/10.1080/17435390.2018.1546413.

(125) Dietzl, G.; Chen, D.; Schnorrer, F.; Su, K. C.; Barinova, Y.; Fellner, M.; Gasser, B.; Kinsey, K.; Oppel, S.; Scheiblauer, S.; Couto, A.; Marra, V.; Keleman, K.; Dickson, B. J. A Genome-Wide Transgenic RNAi Library for Conditional Gene Inactivation in Drosophila. *Nature* **2007**, *448* (7150), 151–156. https://doi.org/10.1038/nature05954.

(126) Padilla, J. C. A.; Chin, A.; Patel, D.; Wang, X.; Jolivet, P.; Lécuyer, E. RNA Interference (RNAi) Screening in Cultured Drosophila Cells. *Methods Mol. Biol.* **2021**, *2381* (March), 97–112. https://doi.org/10.1007/978-1-0716-1740-3_5.

(127) Majeed, Z. R.; Abdeljaber, E.; Soveland, R.; Cornwell, K.; Bankemper, A.; Koch, F.; Cooper, R. L. Modulatory Action by the Serotonergic System: Behavior and Neurophysiology in Drosophila Melanogaster. *Neural Plast.* **2016**, *2016*. https://doi.org/10.1155/2016/7291438.

(128) Majeed, Z. R.; Stacy, A.; Cooper, R. L. Pharmacological and Genetic Identification of Serotonin Receptor Subtypes on Drosophila Larval Heart and Aorta. *J. Comp. Physiol. B Biochem. Syst. Environ. Physiol.* **2014**, *184* (2), 205–219. https://doi.org/10.1007/s00360-013-0795-7.

(129) Shin, M.; Copeland, J. M.; Venton, B. J. Real-Time Measurement of Stimulated Dopamine Release in Compartments of the Adult Drosophila Melanogaster Mushroom Body. *Anal. Chem.* **2020**, *92* (21), 14398–14407. https://doi.org/10.1021/acs.analchem.0c02305.

(130) Myers Gschweng, K. M.; Sampson, M. M.; Hardcastle, B. J.; Sizemore, T. R.; Dacks, A. M.; Frye, M. A.; Krantz, D. E. Serotonergic Modulation of a Visual Microcircuit in Drosophila Melanogaster. *bioRxiv* **2019**, 1–41. https://doi.org/10.1101/619759.

(131) Pyakurel, P.; Shin, M.; Venton, B. J. Nicotinic Acetylcholine Receptor (NAChR) Mediated Dopamine Release in Larval Drosophila Melanogaster. *Neurochem. Int.* **2018**, *114*, 33–41. https://doi.org/10.1016/j.neuint.2017.12.012.

(132) Kasture, A. S.; Hummel, T.; Sucic, S.; Freissmuth, M. Big Lessons from Tiny Flies: Drosophila Melanogaster as a Model to Explore Dysfunction of Dopaminergic and Serotonergic Neurotransmitter Systems. *Int. J. Mol. Sci.* **2018**, *19* (6). https://doi.org/10.3390/ijms19061788.

(133) Rein, K.; Zöckler, M.; Mader, M. T.; Grübel, C.; Heisenberg, M. The Drosophila Standard Brain. *Curr. Biol.* **2002**, *12* (3), 227–231. https://doi.org/10.1016/S0960-9822(02)00656-5.

(134) Hidalgo, S.; Castro, C.; Zárate, R. V.; Valderrama, B. P.; Hodge, J. J. L.; Campusano, J. M. The Behavioral and Neurochemical Characterization of a Drosophila Dysbindin Mutant Supports the Contribution of Serotonin to Schizophrenia Negative Symptoms. *Neurochem. Int.* **2020**, *138*, 104753. https://doi.org/10.1016/j.neuint.2020.104753.

(135) Narayanan, A. S.; Rothenfluh, A. I Believe I Can Fly!: Use of Drosophila as a Model Organism in Neuropsychopharmacology Research. *Neuropsychopharmacology* **2016**, *41* (6), 1439–1446. https://doi.org/10.1038/npp.2015.322.

(136) Shin, M.; Venton, B. J. Electrochemical Measurements of Acetylcholine-Stimulated Dopamine Release in Adult Drosophila Melanogaster Brains. *Anal. Chem.* **2018**, *90* (17), 10318–10325. https://doi.org/10.1021/acs.analchem.8b02114.

(137) Pyakurel, P.; Privman Champaloux, E.; Venton, B. J. Fast-Scan Cyclic Voltammetry (FSCV) Detection of Endogenous Octopamine in Drosophila Melanogaster Ventral Nerve Cord. *ACS Chem. Neurosci.* **2016**, *7* (8), 1112–1119. https://doi.org/10.1021/acschemneuro.6b00070.

(138) Cooper, S. E.; Venton, B. J. Fast-Scan Cyclic Voltammetry for the Detection of Tyramine and Octopamine. *Anal. Bioanal. Chem.* **2009**, *394* (1), 329–336. https://doi.org/10.1007/s00216-009-2616-0.

(139) Bellen, H. J.; Tong, C.; Tsuda, H. History of Drosophila Neuroscience. *Nat. Rev. Neurosci.* **2010**, *11* (juLy), 514–522.

(140) Donelson, N. C.; Sanyal, S. Use of Drosophila in the Investigation of Sleep Disorders. *Exp. Neurol.* **2015**, *274*, 72–79. https://doi.org/10.1016/j.expneurol.2015.06.024.

(141) Privman Champaloux, E.; Donelson, N.; Pyakurel, P.; Wolin, D.; Ostendorf, L.; Denno, M.; Borman, R.; Burke, C.; Short-Miller, J. C.; Yoder, M. R.; Copeland, J. M.; Sanyal, S.; Venton, B. J. Ring Finger Protein 11 (RNF11) Modulates Dopamine Release in Drosophila. *Neuroscience* **2021**, *452*, 37–48. https://doi.org/10.1016/j.neuroscience.2020.10.021.

(142) Jeibmann, A.; Paulus, W. Drosophila Melanogaster as a Model Organism of Brain Diseases. *Int. J. Mol. Sci.* **2009**, *10* (2), 407–440. https://doi.org/10.3390/ijms10020407.

(143) Xiong, Y.; Yu, J. Modeling Parkinson's Disease in Drosophila: What Have We Learned for Dominant Traits? *Front. Neurol.* **2018**, *9* (APR). https://doi.org/10.3389/fneur.2018.00228.

(144) Aryal, B.; Lee, Y. Disease Model Organism for Parkinson Disease: Drosophila Melanogaster. *BMB Rep.* **2019**, *52* (4), 250–258. https://doi.org/10.5483/BMBRep.2019.52.4.204.

(145) Prusing, K.; Voigt, A.; Schulz, J. B. Drosophila Melanogaster as a Model Organism for Alzheimer's Disease. *Adv. Med. Biol. Vol. 181* **2021**, 179–218.

(146) Ries, A. S.; Hermanns, T.; Poeck, B.; Strauss, R. Serotonin Modulates a Depression-like State in Drosophila Responsive to Lithium Treatment. *Nat. Commun.* **2017**, *8*, 1–11. https://doi.org/10.1038/ncomms15738.

(147) Kishida, K. T.; Saez, I.; Lohrenz, T.; Witcher, M. R.; Laxton, A. W.; Tatter, S. B.; White, J. P.; Ellis, T. L.; Phillips, P. E. M.; Montague, P. R. Subsecond Dopamine Fluctuations in Human Striatum Encode Superposed Error Signals about Actual and Counterfactual Reward. *Proc. Natl. Acad. Sci. U. S. A.* **2016**, *113* (1), 200–205. https://doi.org/10.1073/pnas.1513619112.

(148) Hidalgo, S.; Molina-Mateo, D.; Escobedo, P.; Zárate, R. V.; Fritz, E.; Fierro, A.; Perez, E. G.; Iturriaga-Vasquez, P.; Reyes-Parada, M.; Varas, R.; Fuenzalida-Uribe, N.; Campusano, J. M. Characterization of a Novel Drosophila SERT Mutant: Insights on the Contribution of the Serotonin Neural System to Behaviors. *ACS Chem. Neurosci.* **2017**, *8* (10), 2168–2179. https://doi.org/10.1021/acschemneuro.7b00089.

(149) Araujo, S. M.; Poetini, M. R.; Bortolotto, V. C.; de Freitas Couto, S.; Pinheiro, F. C.; Meichtry, L. B.; de Almeida, F. P.; Santos Musachio, E. A.; de Paula, M. T.; Prigol, M. Chronic Unpredictable Mild Stress-Induced Depressive-like Behavior and Dysregulation of Brain Levels of Biogenic Amines in Drosophila Melanogaster. *Behav. Brain Res.* **2018**, *351* (May), 104–113. https://doi.org/10.1016/j.bbr.2018.05.016.

(150) Hidalgo, S.; Fuenzalida-Uribe, N.; Molina-Mateo, D.; Escobar, A. P.; Oliva, C.; España, R. A.; Andrés, M. E.; Campusano, J. M. Study of the Release of Endogenous Amines in Drosophila Brain in Vivo in Response to Stimuli Linked to Aversive Olfactory Conditioning. *J. Neurochem.* **2020**, 0–1. https://doi.org/10.1111/jnc.15109.

(151) Zeppelin, T.; Ladefoged, L. K.; Sinning, S.; Schiøtt, B. Substrate and Inhibitor Binding to the Serotonin Transporter: Insights from Computational, Crystallographic, and Functional Studies. *Neuropharmacology* **2019**, *161* (February), 107548.

https://doi.org/10.1016/j.neuropharm.2019.02.030.

(152) Davis, B. A.; Nagarajan, A.; Forrest, L. R.; Singh, S. K. Mechanism of Paroxetine (Paxil) Inhibition of the Serotonin Transporter. *Sci. Rep.* **2016**, *6*, 1–13. https://doi.org/10.1038/srep23789.

(153) Lawal, H. O.; Terrell, A.; Lam, H. A.; Djapri, C.; Jang, J.; Hadi, R.; Roberts, L.; Shahi, V.; Chou, M. T.; Biedermann, T.; Huang, B.; Lawless, G. M.; Maidment, N. T.; Krantz, D. E. Drosophila Modifier Screens to Identify Novel Neuropsychiatric Drugs Including Aminergic Agents for the Possible Treatment of Parkinson's Disease and Depression. *Mol. Psychiatry* **2014**, *19* (2), 235–242. https://doi.org/10.1038/mp.2012.170.

(154) He, J.; Hommen, F.; Lauer, N.; Balmert, S.; Scholz, H. Serotonin Transporter Dependent Modulation of Food-Seeking Behavior. *PLoS One* **2020**, *15* (1), 1–23. https://doi.org/10.1371/journal.pone.0227554.

(155) Majeed, Z. R.; Abdeljaber, E.; Soveland, R.; Cornwell, K.; Bankemper, A.; Koch, F.; Cooper, R. L. Modulatory Action by the Serotonergic System: Behavior and Neurophysiology in Drosophila Melanogaster. *Neural Plast.* **2016**, *2016*. https://doi.org/10.1155/2016/7291438.

(156) Clark, M. Q.; Zarin, A. A.; Carreira-Rosario, A.; Doe, C. Q. Neural Circuits Driving Larval Locomotion in Drosophila. *Neural Dev.* **2018**, *13* (1), 1–10. https://doi.org/10.1186/s13064-018-0103-z.

(157) Nichols, C. D.; Becnel, J.; Pandey, U. B. Methods to Assay Drosophila</Em> Behavior. *J. Vis. Exp.* **2012**, No. 61, 3–7. https://doi.org/10.3791/3795.

(158) Heckscher, E. S.; Lockery, S. R.; Doe, C. Q. Characterization of Drosophila Larval Crawling at the Level of Organism, Segment, and Somatic Body Wall Musculature. *J. Neurosci.* **2012**, *32* (36), 12460–12471. https://doi.org/10.1523/JNEUROSCI.0222-12.2012.

(159) Rothenfluh, A.; Heberlein, U. Drugs, Flies, and Videotape: The Effects of Ethanol and Cocaine on Drosophila Locomotion. *Curr. Opin. Neurobiol.* **2002**, *12* (6), 639–645. https://doi.org/10.1016/S0959-4388(02)00380-X.

(160) Flores-Valle, A.; Seelig, J. D. A Place Learning Assay for Tethered Walking Drosophila. *J. Neurosci. Methods* **2022**, *378* (June), 109657. https://doi.org/10.1016/j.jneumeth.2022.109657.

(161) Tadres, D.; Louis, M. PiVR: An Affordable and Versatile Closed-Loop Platform to Study Unrestrained Sensorimotor Behavior. *PLoS Biol.* **2020**, *18* (7), 1–25. https://doi.org/10.1371/journal.pbio.3000712.

(162) Kazama, H. Systems Neuroscience in Drosophila: Conceptual and Technical Advantages. *Neuroscience* **2015**, *296*, 3–14. https://doi.org/10.1016/j.neuroscience.2014.06.035.

(163) Huser, A.; Eschment, M.; Güllü, N.; Collins, K. A. N.; Böpple, K.; Pankevych, L.; Rolsing, E.; Thum, A. S. Anatomy and Behavioral Function of Serotonin Receptors in Drosophila Melanogaster Larvae. *PLoS One* **2017**, *12* (8), 1–27. https://doi.org/10.1371/journal.pone.0181865.

(164) Xiao, N.; Privman, E.; Venton, B. J. Optogenetic Control of Serotonin and Dopamine Release in Drosophila Larvae. *ACS Chem. Neurosci.* **2014**, *5* (8), 666–673. https://doi.org/10.1021/cn500044b.

(165) Klapoetke, N. C.; Murata, Y.; Kim, S. S.; Pulver, S. R.; Birdsey-Benson, A.; Cho, Y. K.; Morimoto, T. K.; Chuong, A. S.; Carpenter, E. J.; Tian, Z.; Wang, J.; Xie, Y.; Yan, Z.; Zhang, Y.; Chow, B. Y.; Surek, B.; Melkonian, M.; Jayaraman, V.; Constantine-Paton, M.; Wong, G. K.-S.; Boyden, E. S. Independent Optical Excitation of Distinct Neural Populations. *Nat. Methods* **2014**, *11* (3), 338–346. https://doi.org/10.1038/nmeth.2836.

(166) Privman, E.; Venton, B. J. Comparison of Dopamine Kinetics in the Larval Drosophila Ventral Nerve Cord and Protocerebrum with Improved Optogenetic Stimulation. *J. Neurochem.* **2015**, *135* (4), 695–704. https://doi.org/10.1111/jnc.13286.

(167) Gambis, A.; Dourlen, P.; Steller, H.; Mollereau, B. Two-Color in Vivo Imaging of Photoreceptor Apoptosis and Development in Drosophila. *Dev. Biol.* **2011**, *351* (1), 128–134. https://doi.org/10.1016/j.ydbio.2010.12.040.

(168) Martin, J. R.; Rogers, K. L.; Chagneau, C.; Brûlet, P. In Vivo Bioluminescence Imaging of Ca2+ Signalling in Brain of Drosophila. *PLoS One* **2007**, *2* (3), 2–9. https://doi.org/10.1371/journal.pone.0000275.

(169) Andlauer, T. F. M.; Sigrist, S. J. In Vivo Imaging of Drosophila Larval Neuromuscular Junctions to Study Synapse Assembly. *Cold Spring Harb. Protoc.* **2012**, *7* (4), 407–413. https://doi.org/10.1101/pdb.top068577.

(170) Johnson, O.; Becnel, J.; Nichols, C. D. Serotonin Receptor Activity Is Necessary for Olfactory Learning and Memory in Drosophila Melanogaster. *Neuroscience* **2011**, *192*, 372–381. https://doi.org/10.1016/j.neuroscience.2011.06.058.

(171) Bacqué-cazenave, J.; Bharatiya, R.; Barrière, G.; Delbecque, J. P.; Bouguiyoud, N.; Di Giovanni, G.; Cattaert, D.; De Deurwaerdère, P. Serotonin in Animal Cognition and Behavior. *Int. J. Mol. Sci.* **2020**, *21* (5), 1–23. https://doi.org/10.3390/ijms21051649.

(172) Yang, Z.; Bertolucci, F.; Wolf, R.; Heisenberg, M. Flies Cope with Uncontrollable Stress by Learned Helplessness. *Curr. Biol.* **2013**, *23* (9), 799–803. https://doi.org/10.1016/j.cub.2013.03.054.

(173) Schmitt, R. E.; Messick, M. R.; Shell, B. C.; Dunbar, E. K.; Fang, H. F.; Shelton, K. L.; Venton, B. J.; Pletcher, S. D.; Grotewiel, M. Dietary Yeast Influences Ethanol Sedation in Drosophila via Serotonergic Neuron Function. *Addict. Biol.* **2020**, *25* (4). https://doi.org/10.1111/adb.12779.

(174) Shell, B. C.; Schmitt, R. E.; Lee, K. M.; Johnson, J. C.; Chung, B. Y.; Pletcher, S. D.; Grotewiel, M. Measurement of Solid Food Intake in Drosophila via Consumption-Excretion of a Dye Tracer. *Sci. Rep.* **2018**, *8* (1), 1–13. https://doi.org/10.1038/s41598-018-29813-9.

(175) Shell, B. C.; Grotewiel, M. Identification of Additional Dye Tracers for Measuring Solid Food Intake and Food Preference via Consumption-Excretion in Drosophila. *Sci. Rep.* **2022**, *12* (1), 1–12. https://doi.org/10.1038/s41598-022-10252-6.

(176) Shell, B. C.; Luo, Y.; Pletcher, S.; Grotewiel, M. Expansion and Application of Dye Tracers for Measuring Solid Food Intake and Food Preference in Drosophila. *Sci. Rep.* **2021**, *11* (1), 1–13. https://doi.org/10.1038/s41598-021-99483-7.

(177) Wu, Q.; Yu, G.; Park, S. J.; Gao, Y.; Ja, W. W.; Yang, M. Excreta Quantification (EX-Q) for Longitudinal Measurements of Food Intake in Drosophila. *iScience* **2020**, *23* (1). https://doi.org/10.1016/j.isci.2019.100776.

(178) Makos, M. A.; Kuklinski, N. J.; Heien, M. L.; Berglund, E. C.; Ewing, A. G. Chemical Measurements in Drosophila. *TrAC - Trends Anal. Chem.* **2009**, *28* (11), 1223–1234. https://doi.org/10.1016/j.trac.2009.08.005.

Chapter 2

Improving serotonin fast-scan cyclic voltammetry detection:
new waveforms to reduce electrode fouling

Abstract

Serotonin is a neuromodulator implicated in depression that is often measured in real-time by fast-scan cyclic voltammetry (FSCV). A specialized “Jackson” waveform (JW, 0.2, 1.0 V, -0.1 V, 0.2 V, 1000 V/s) was developed to reduce serotonin fouling, but the 1.0 V switching potential limits sensitivity and electrodes still foul. The goal of this study was to test the effects of extending the FSCV switching potential to increase serotonin sensitivity and decrease fouling. We compared the Jackson waveform, the dopamine waveform (DA, -0.4 V, 1.3 V, 400 V/s), and two new waveforms: the extended serotonin waveform (ESW, 0.2, 1.3, -0.1, 0.2, 1000 V/s) and extended hold serotonin waveform (EHSW, 0.2, 1.3 (hold 1 ms), -0.1, 0.2, 400 V/s). The EHSW was the most sensitive (LOD = 0.6 nM), and the JW the least sensitive (LOD = 2.4 nM). With the Jackson waveform, electrode fouling was significant with repeated injections of serotonin or exposure to its metabolite, 5-hydroxyindoleacetic acid (5-HIAA). Using the extended waveforms, electrodes fouled 50% less than with the Jackson waveform for both analytes. No electrode fouling was observed with the dopamine waveform because of the negative holding potential. The Jackson waveform was the most selective for serotonin over dopamine (800x), and the ESW was also highly selective. All waveforms were useful for measuring serotonin with optogenetic stimulation in *Drosophila* larvae. These results provide new FSCV waveforms to measure dynamic serotonin changes with different experimental requirements, like high sensitivity (EHSW), high selectivity (ESW, JW), or eliminating electrode fouling (DA).

2.1 Introduction

Serotonin is a major neuromodulator in the brain that is important for mental health by regulating sleep, mood, and appetite.[1,2] The serotonergic system is one of the main targets of antidepressants that treat depression and anxiety disorders, but their efficacies vary in individuals.[3] Serotonin concentrations in the extracellular space are tightly regulated by serotonin receptors and serotonin transporters (SERT).[3–5] Therefore, fast analytical techniques are needed to monitor real-time serotonin changes in the brain. Electrochemical techniques are commonly used to study neurotransmitters *in vivo* in order to understand their effects on specific behaviors and dysfunction in neurological diseases.[1,2,6–8] In particular, fast-scan cyclic voltammetry (FSCV) at carbon-fiber microelectrodes (CFMEs) applies linear ramp potentials at fast scan rates for high sensitivity and rapid temporal resolution detection of neurotransmitter concentration changes.[1,6,9–12] FSCV has revealed the dynamic co-release of serotonin and histamine in mammals[13] and the mechanism of selective serotonin reuptake inhibitors (SSRIs) to increase serotonin concentrations.[14–16] In addition, FSCV has been used to measure rapid release and uptake of serotonin in *Drosophila* larval ventral nerve cords.[17–19] However, serotonin remains difficult to study with FSCV because it's oxidative byproducts foul CFMEs during long-term experiments.[20–23]

Serotonin and its major downstream metabolite, 5-hydroxyindoleacetic acid (5-HIAA), produce highly reactive radicals during oxidation that polymerize to form films on the surface of the CFME.[22,23] These films hinder electron transfer and cause electrode fouling, which decreases sensitivity and limits accurate measurements *in vivo*.[21] The standard FSCV waveform for serotonin, termed the "Jackson" waveform, was proposed to ameliorate these issues and sweeps from 0.2 V to 1.0 V to -0.1 to 0.2 V at 1000 V/s.[20] The Jackson waveform was originally applied to beveled disk electrodes, however, the Hashemi group showed the Jackson waveform can also be applied to cylindrical CFMEs.[21] The Jackson waveform is highly selective for serotonin compared to dopamine, but electrodes still foul with repeated measurements and long exposure to 5-HIAA.[21,24] Surface coatings such as Nafion are commonly used to mitigate this fouling,[21] however they slow electrode responses.[25] A new FSCV waveform that prevents electrode fouling while maintaining high sensitivity and selectivity would be beneficial for studying real-time serotonin release.

Modified FSCV waveforms have been investigated for several neurotransmitters to understand how waveform parameters affect CFME sensitivity and fouling.[8,24,26–28] The Wightman group extended the switching potential of the dopamine waveform from 1.0 V to 1.3 V to increase sensitivity,[27] and later demonstrated higher switching potentials (≥1.3 V) broke carbon-carbon bonds on the surface of the fiber,[29] also increasing surface oxide groups.[8,11,30] The higher switching potential also renews the surface to remove impurities.[29] Likewise, Keithley *et al*. designed "sawhorse" waveforms with an extended hold at 1.3 V and observed greater CFME sensitivity using higher scan rates (≥1000 V/s).[26] Modified sawhorse and extended switching potential waveforms also improved adenosine and

histamine detection.[24,31] Although extending the switching potential enhanced detection of these neurotransmitters, the Jackson waveform has not been revisited in 25 years to improve serotonin detection.[20]

The goal of this study was to develop practical new waveforms for serotonin detection to reduce electrode fouling and increase sensitivity. We hypothesized that extending the switching potential would decrease fouling by renewing the CFME surface, and that holding at a higher switching potential would enhance these effects.[29] We designed new serotonin waveforms to extend the Jackson waveform to 1.3 V with varied scan rates, and tested sawhorse waveforms to hold at 1.3 V. The traditional dopamine waveform was also tested. Electrodes fouled the most using the Jackson waveform with repeated serotonin measurements and long exposure to 5-HIAA, while electrodes using the dopamine waveform did not foul. The extended waveforms with 1.3 V switching potentials had decreased electrode fouling compared to the Jackson waveform and had the highest electrode sensitivity. Waveforms were characterized *in vitro* with optogenetic stimulation in fruit fly larvae and all were useful for stable serotonin detection. Overall, our study develops extended waveforms for serotonin detection that provide high sensitivity and low electrode fouling for measurements *in vivo*.

2.2 Experimental Methods

2.2.1 Chemicals

Serotonin hydrochloride was purchased from Sigma Aldrich (St. Louis, MO). Dopamine hydrochloride and 5-hydroxyindoleacetic acid were purchased from Acros Organics (Morris Plains, NH). A 1 mM stock solution of each chemical was prepared in 0.1 M $HClO_4$. Final working solutions were prepared by diluting a stock in phosphate buffer saline (PBS) (131.25 mM NaCl, 3.00 mM KCl, 10 mM NaH_2PO_4, 1.2 mM $MgCl_2$, 2.0 mM Na_2SO_4, and 1.2 mM $CaCl_2$ with the final pH adjusted to 7.4 with 1 M NaOH).

2.2.2 Microelectrode Preparation

CFMEs were prepared as previously described.[24] A T-650 carbon fiber (Cytec Engineering Materials, West Patterson, NJ) with 7 µm diameter was aspirated into a standard 1.28 mm inner diameter × 0.68 mm outer diameter glass capillary tube (A-M Systems, Sequim, WA) with a vacuum pump. A capillary was then pulled by a vertical puller (Narishige, Tokyo, Japan) to make two electrodes. The exposed fiber was cut to 25-75 µm. The CFME was epoxied by dipping the tip of the fiber into a solution of 14% m-phenylenediamine hardener (Acros Organics, Morris Plains, NH) in Epon Resin 828 (Miller-Stephenson, Danbury, CT) at 80-85 °C for 30-40 seconds. The CFMEs were cured at 100 °C overnight and 150 °C for at least 8 hours.

2.2.3 Electrochemical Instrumentation

Initial flow cell fouling experiments were performed using a two-electrode system with a CFME working electrode backfilled with 1 M KCl.[17,18,24,29] All potential measurements are reported versus a chloridized Ag/AgCl wire reference electrode, and experiments were performed in a grounded Faraday cage. Before experiments, electrode tips were soaked in isopropyl alcohol for a minimum of 10 minutes to clean the surface. Electrodes were connected to a ChemClamp potentiostat and headstage (Dagan, Minneapolis, MN). Data were collected with HDCV Analysis software (Department of Chemistry, University of North Carolina at Chapel Hill). Figure 1 shows background charging currents for each waveform tested and describes background subtraction procedures. The flow-injection system consists of a six-port loop injector with an air actuator (Valco Instruments, Houston, TX). PBS buffer and test solutions were flowed at 2 mL/min using a syringe pump (Harvard Apparatus, Holliston, MA) through a flow cell with the CFME tip inserted in solution. Analyte was flowed by the electrode for 5 seconds. *D. melanogaster in vitro* experiments were performed using the same two-electrode system, except electrodes were connected to a WaveNeuro system (Pine Research, Durham, NC). CFMEs were precalibrated and post calibrated *in vitro* using a flow injection analysis to flow 1 µM serotonin solution by the electrode to determine the current response

(Figure 2). The concentration of serotonin was determined *in vitro* using this calibration factor, since the measured oxidation peak current is linear with the serotonin concentration.[32]

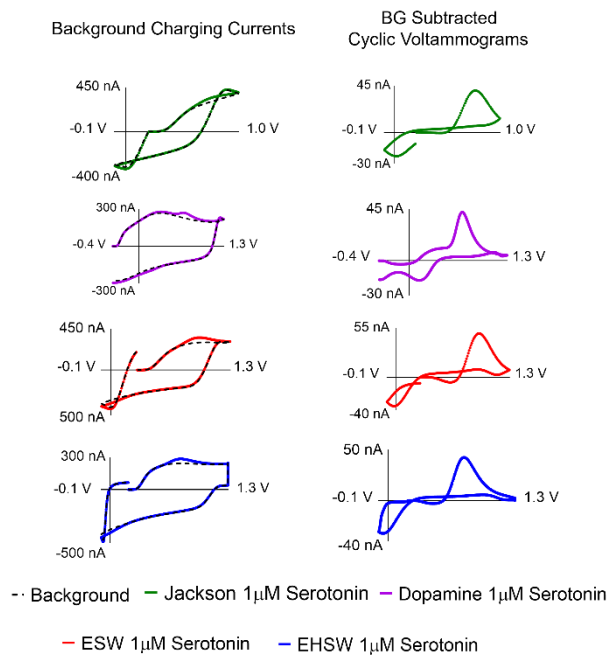

Figure 1. Fast-scan cyclic voltammetry (FSCV) background (BG) charging currents. FSCV cyclic voltammograms on the left column show BG charging currents (dotted line) for each waveform (no analyte) along with BG charging current with 1 μM serotonin (colored). The right column shows BG subtracted cyclic voltammograms for 1μM serotonin with each waveform. When a potential is applied to the CFME, the double layer charges like a capacitor and produces a background (BG) charging current.[11] The charging currents are proportional to the size (surface area) of the CFME and scan rate applied. CFMEs that are 25-75 μm in length usually produce BG currents between 200-800 nA. Larger background currents are observed for the Jackson waveform and ESW with 1000 V/s scan rates. The potential is applied for 10 minutes to allow the BG current to equilibrate before the experiment is run. Ten scans before the serotonin injection were averaged for background currents to subtract, and 5 CVs from when serotonin were injected were averaged for the analyte.

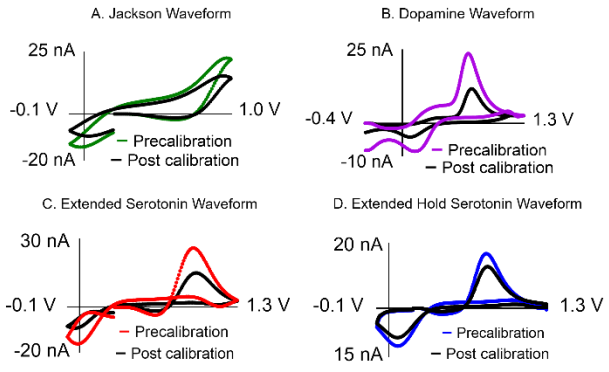

Figure 2. *Drosophila melanogaster in vitro* CFME 1 µM serotonin precalibration and post calibration responses. Figure S2A-D shows example precalibration and post calibration cyclic voltammogram responses with each waveform to 1 µM serotonin flow cell injection. CFMEs foul 20-50% after inserting and removing the electrodes into larval ventral nerve cord tissue. Electrode fouling can be caused by entropy-driven unfolding and adsorption of proteins to the charged electrode surface.[36] Although CFMEs foul from tissue exposure, serotonin detection was stable for each waveform (Fig 7A-D, Fig. S5). On average, CFMEs fouled 40 ± 6% with the Jackson waveform, 43 ± 5% with the Dopamine waveform, ESW 38 ± 4%, and the EHSW 36 ± 3% (*n* = 4).

2.2.4 Waveform Parameters

The traditional serotonin "Jackson" waveform (JW) proposed in Jackson *et al*., scans from 0.2 V to a switching potential of 1.0 V to -0.1 V back to the holding potential of 0.2 V at 1000 V/s (Fig. 3).[20] The traditional dopamine waveform (DA) was tested that scans from -0.4 V to 1.3 V at 400 V/s. The extended serotonin waveform (ESW) extends the Jackson waveform to a switching potential at 1.3 V (0.2 V, 1.3 V, -0.1 V, 0.2 V, 1000 V/s). A sawhorse waveform, known as the extended hold serotonin waveform (EHSW) was similar to the ESW but the switching potential was held for 1 ms at 1.3 V (0.2 V, 1.3 V (1 ms), -0.1 V, 0.2 V, 400 V/s). A frequency of 10 Hz was used for all waveforms. A 2 KHz low-pass filter was applied for 400 V/s scan rates, and 10 kHz filter for 1000 V/s scan rates.

2.2.5 Drosophila melanogaster Experiments

Methods were previously described in Privman *et al*. 2015.[32] Virgin females with UAS-CsChrimson (Stockline #55136, Bloomington Drosophila Stock Center, Bloomington, IN) were crossed with tph-Gal4 (Serotonin driver line), a gift from Dr. Jay Hirsh (University of Virginia, Biology Department) and resulting heterozygous larvae were shielded from light and raised on standard food mixed 250:1 with 100 mM all-trans retinal (Sigma-Aldrich). The ventral nerve cords (VNCs) of third instar "wandering" larvae were dissected out in PBS buffer kept on ice. A VNC was placed on an uncoated Petri dish dorsal side down, and a small slice of the lateral optic lobe was removed using the tip of a 22-gauge hypodermic needle. The electrode was implanted from the lateral edge of the tissue into the dorsal medial protocerebrum. Dissection and electrode insertion were conducted under low light conditions. The electrode was allowed to equilibrate in the tissue for 10 minutes in the dark prior to data collection.

Optogenetic release of serotonin was stimulated by activating CsChrimson ion channels with red light from a 617 nm fiber-coupled high-power LED with a 200 µm core optical cable (ThorLabs, Newton, NJ, USA).[32] The fiber was centered above the VNC using a micromanipulator and the light was modulated with transistor–transistor logic (TTL) inputs to a T-cube LED controller (ThorLabs), which was connected to the FSCV breakout box. TTL input was driven by electrical pulses controlled by the WaveNeuro system and HDCV software, which were used to control frequency, pulse width, and number of pulses. For *in vitro* experiments, 120 biphasic pulses were delivered at 60 Hz and pulse width of 4 ms. Stimulations were repeated every 5 minutes to allow the releasable pool of serotonin to replenish itself.[17]

2.2.6 Serotonin Imaging in Larvae Ventral Nerve Cords

Drosophila were bred to yield a tph-Gal4/CyO; UAS-mCD8-GFP cross, a gift from Dr. Jeffery Copeland (Eastern Mennonite University, Biology Department). Third instar larvae were collected and dissected as stated above but raised in normal light conditions.[32] For imaging preparation, several VNCs were collected and placed in a Petri dish with cold PBS on ice. VNCs were preserved by removing PBS and pipetting 2-3 mL of 4% paraformaldehyde in PBS solution (Alfa Aesar, Ward Hill, MA). The petri dishes were covered in Parafilm (Bemis, Neenah, WI) and gently rocked for 20 minutes on a Nutating Mixer (VWR International, Radnor, PA). Paraformaldehyde was removed and 2 mL PBS was applied for 20 minutes as an initial wash, followed by two 5-minute wash steps. A glass slide was prepared by placing preserved specimens dorsal side up in a 60 µL aliquot of Vectashield (Vector Laboratories, Burlingame, CA). A Zeiss AxioZoom macroscope (Carl Zeiss Microscopy, Germany) was used to image GFP expression with Image J software (National Institutes of Health).

2.2.7 Statistics

Data are the mean ± the standard error of the mean (SEM) for *n* number of electrodes. Statistics were performed in GraphPad Prism 8.0 (GraphPad Software, La Jolla, CA). For One-Way ANOVA, Two-Way ANOVA, and Tukey's post-hoc test, significance was determined at 95% confidence level.

For sensitivity and selectivity determination, the limit of detection (LOD) for serotonin and dopamine were calculated from the lowest concentrations tested: 100 nM serotonin (all waveforms), 100 nM dopamine (DA and EHSW), 1 µM dopamine (ESW), and 10 µM dopamine (JW). LOD is calculated by a ratio method, as the ratio of the measured S/N to the tested concentration is equal to the LOD divided by 3. Noise was determined by calculating the standard deviation (SD) of the baseline current from 0-3 s in the *i* vs t trace (n = 30).

2.3 Results and Discussion

2.3.1 Waveform Characteristics

We designed and tested new serotonin waveforms by varying the switching potential, holding potential, and scan rate to determine their sensitivity, selectivity, and electrode fouling behaviors. Figure 3 shows the main waveforms tested and Table 1 summarizes waveform parameters. The Jackson waveform was compared to the traditional dopamine waveform that uses a negative holding potential and extended switching potential. The extended serotonin waveform (ESW) extends the Jackson waveform to 1.3 V, but uses the same 1000 V/s scan rate. The extended hold serotonin waveform (EHSW) is a sawhorse waveform that extends the applied switching potential at 1.3 V for 1 ms with a slower scan rate at 400 V/s. A 1 ms hold was chosen because holds ≥1 ms do not produce higher or different current responses, but a 1 ms hold oxidizes the surface more than a 0.5 ms hold.[31] Our hypothesis is that extending the switching potential will decrease fouling and increase sensitivity for serotonin by continuously regenerating the carbon fiber surface.[29] In addition to the main waveforms, scan rate was also varied for the ESW and EHSW (Figure 7).

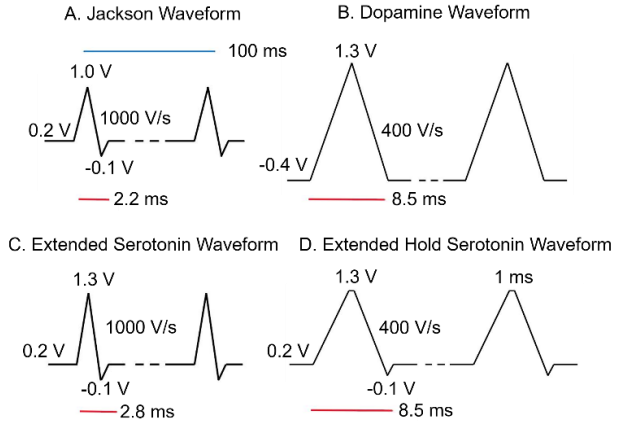

Figure 3. Waveforms tested. **A**. Traditional serotonin "Jackson" waveform with a 1.0 V switching potential and 1000 V/s scan rate. **B**. Traditional dopamine waveform with a -0.4 V holding potential, extended 1.3 V switching potential, and 400 V/s scan rate. **C**. Extended serotonin waveform (ESW) with 1.3 V switching potential and 1000 V/s scan rate. **D**. Extended hold serotonin waveform (EHSW) with a 1 ms hold at 1.3 V and 400 V/s scan rate. All waveforms were repeated at 10 Hz.

Table 1. Summary of waveform parameters.

Waveform	Switching Potential (V)	Holding Potential (V)	Scan Rate (V/s)
Jackson	1.0	0.2	1000
Dopamine	1.3	-0.4	400
ESW	1.3	0.2	1000
EHSW	1.3 (1 ms)	0.2	400

Figure 4 shows example false color plots and cyclic voltammograms (CVs) for each waveform. The Jackson waveform (Fig. 4A) uses a high scan rate that shifts the oxidation peak to approximately 0.9 V. The characteristic reduction peak at 0.0 V is difficult to see on the CV because of the fast scan rate and potential that sweeps to only -0.1 V. However, the reduction peak is observed on the false color plot. The serotonin CV for the dopamine waveform shows full oxidation and reduction peaks at 0.6 V and 0.0 V, respectively (Fig. 4B). The serotonin CV for the ESW is similar to the Jackson waveform; however, the oxidation peak is fully observed because of the extension to 1.3 V (Fig. 4C). The cyclic voltammogram for the EHSW (Fig. 4D) is similar to the dopamine waveform and shows similar oxidation and reduction peaks. The reduction peak is easier to identify than the Jackson waveform and ESW because of the slower scan rate (400 V/s).

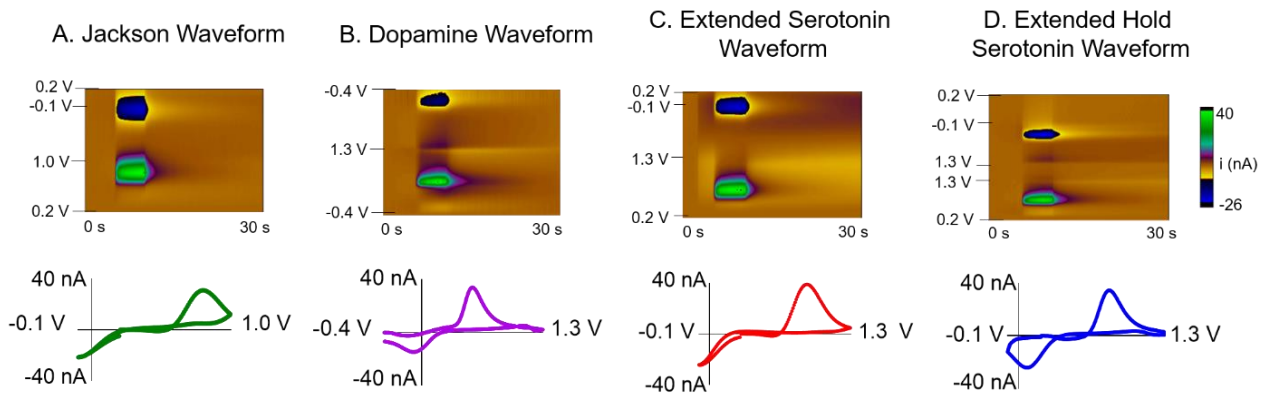

Figure 4. Example false color plots (above) and cyclic voltammograms (CV, below) for all waveforms for 1 µM serotonin injection in a flow cell. Color plots show oxidation (green) and reduction (blue) for serotonin. **A**. The Jackson waveform displays a shifted oxidation peak in the CV, and the reduction peak is harder to see because of the -0.1 V negative potential. Both oxidation and reduction peaks are observed in the color plot. **B**. The dopamine waveform shows a complete CV with fully resolved oxidation and reduction peaks at approximately 0.6 V and 0.0 V, respectively. **C**. The extended serotonin waveform (ESW) extends the switching potential to 1.3 V with 1000 V/s scan rate and thus, the CV is similar to the Jackson waveform, except its oxidation peak is fully resolved. **D**. The extended hold serotonin waveform (EHSW) applies a 1 ms hold at 1.3 V (400 V/s) and the CV shows fully resolved oxidation and reduction peaks similar to the dopamine waveform.

2.3.2 *Repeated serotonin measurement fouling*

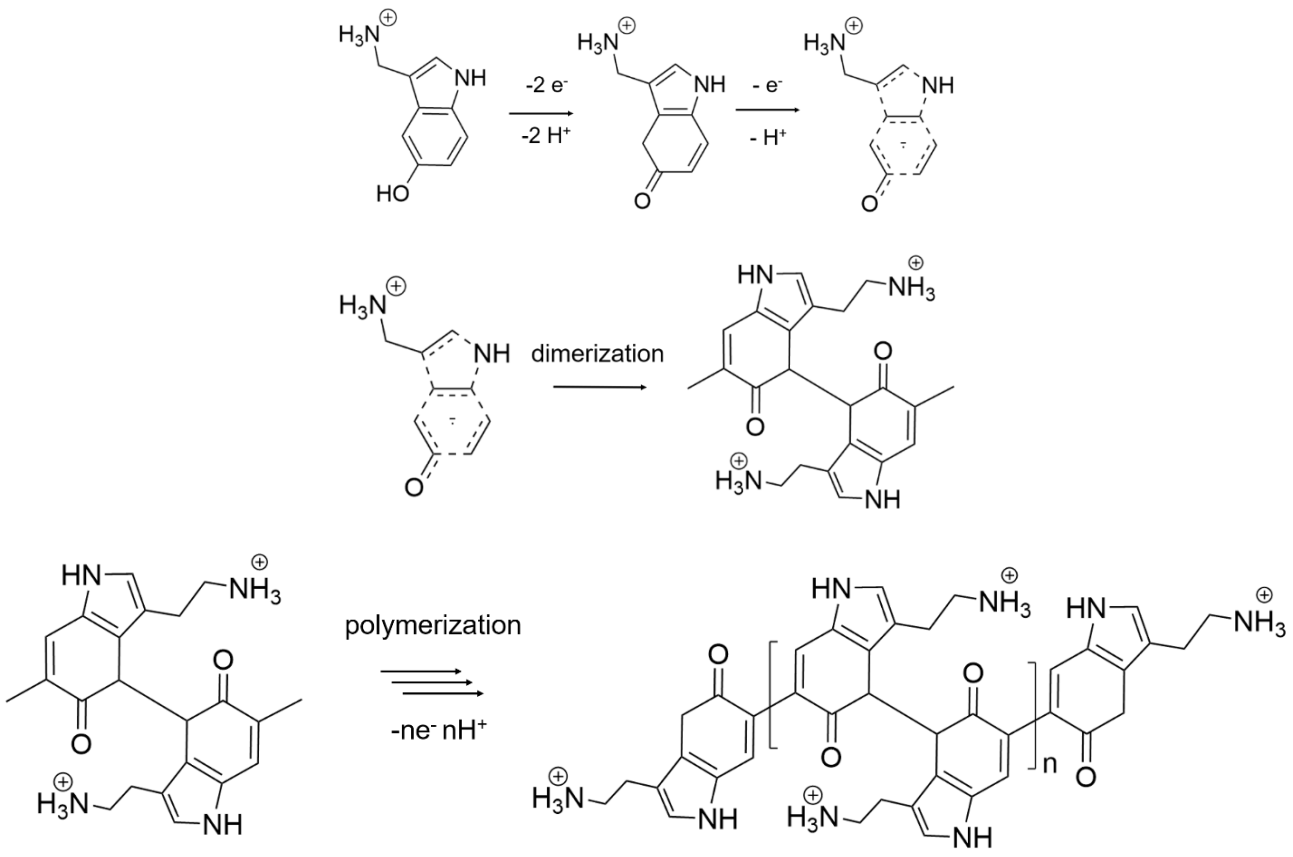

Figure 5. Serotonin and 5-hydroxyindoleacetic acid oxidation scheme. Serotonin undergoes irreversible oxidation after it reaches its quinone form.[22,23] The negatively charged serotonin radical is delocalized over the indole ring structure. Dimerization and extension occur on the alpha carbons located next to serotonin's carbonyl group. 5-hydroxyindole acetic acid (5-HIAA) undergoes a similar irreversible oxidation reaction. 5-HIAA has an identical structure to serotonin, except the ethylamine group is replaced with a negative carboxyl group at physiological pH.

Serotonin undergoes irreversible oxidation and produces a series of radicals that dimerize and extend to form a polymer (Figure 5).[20–23] This serotonin polymer electropolymerizes to the carbon fiber and forms films that hinder electron transfer. To test electrode fouling, 25 repeated serotonin injections were made for 5 seconds every 30 seconds using flow injection analysis. A CFME fouls if the current decreases from the initial current of the first injection. Figure 6A-D shows cyclic voltammograms for the initial (black) and 25th injections (colored) for each waveform. Electrodes using the Jackson waveform (Fig. 6A) fouled the most, with a 39 ± 3% average current decrease after 25 injections (n = 6). No fouling was observed with electrodes using the dopamine waveform (Fig. 6B) and current decreased only 5 ± 2% . Electrode fouling was similar for the ESW (Fig. 6C) and EHSW (Fig. 6D) with 19 ± 2% and 18 ± 4% current decrease, respectively. Fig. 6E compares electrode fouling for the repeated injections among waveforms. There were signficant overall effects of waveform applied (Two-Way ANOVA, $F_{(3,20)} = 26.75$, $p = 0.0001$, $n = 6$) and injection number ($F_{(24,480)} = 66.34$, p =

0.0001) with significant interaction between the groups ($F_{(72,480)}$ = 11.51, p = 0.0001). Tukey's post-hoc test revealed significant differences in electrode fouling with the Jackson waveform compared to the dopamine waveform, ESW, and EHSW (all p = 0.0001). However, no differences in electrode fouling were observed between the other waveforms (p > 0.05). To test the effect of scan rate on electrode fouling, the ESW and EHSW were tested at 400 and 1000 V/s (Fig. 7). No differences were observed with scan rate for the EHSW. However, electrodes using the ESW fouled more at 400 V/s (39 ± 2%) compared to 1000 V/s (19 ± 2%), so 1000 V/s was chosen as the optimal scan rate.

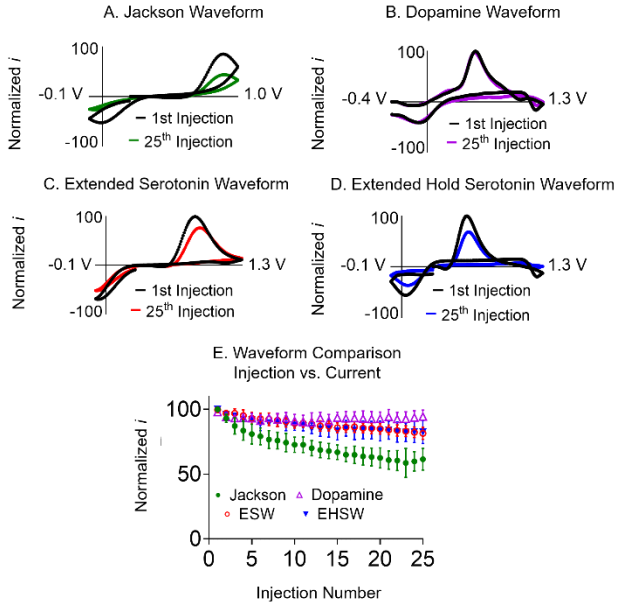

Figure 6. Repeated serotonin measurement electrode fouling was determined by injecting 1 µM serotonin for 5 seconds every 30 seconds repeated 25 times in a flow cell. Cyclic voltammograms show initial (1st, black) and final (25th, color) injections for each waveform. **A**. The current for the 25th CV is significantly reduced with the Jackson waveform. **B**. Electrode current responses using the dopamine waveform were stable. Electrodes using the **C**.ESW and **D**. EHSW had slight decreases in current for the 25th injection. **E**. Comparison of all waveforms for fouling with repeated injections of 1 µM serotonin. Plot shows normalized current (to the first injection) with standard error of the mean (SEM) error bars. There were significant main effects of waveform (Two-Way ANOVA, $F_{(3,20)}$ = 26.75, p = 0.0001, n = 6) and injection number ($F_{(24,480)}$ = 66.34, p = 0.0001) on current detected. Electrode fouling with the Jackson waveform was significantly different compared to electrodes using the dopamine waveform, ESW, and EHSW (Tukey's post-hoc, p = 0.0001). No differences in fouling were observed between the other waveforms (p > 0.05).

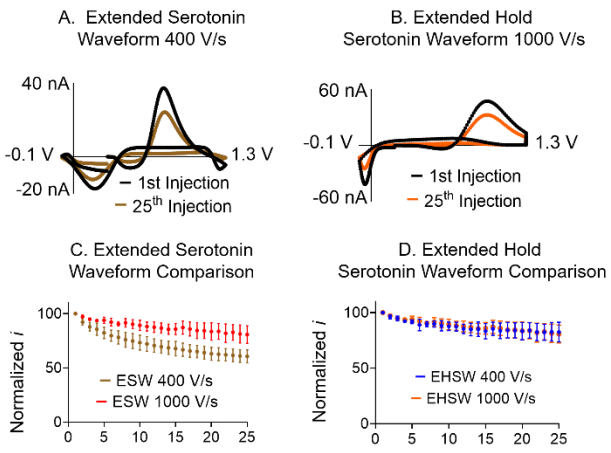

Figure 7. Extended serotonin waveforms scan rate comparison. The extended serotonin (ESW) and extended hold serotonin (EHSW) waveforms were initially tested at 400 and 1000 V/s. The ESW at 400 V/s exhibited similar cyclic voltammograms to the dopamine waveform and EHSW at 400 V/s with oxidation peaks at 0.6 V and reduction peaks at 0.0 to 0.2 V. There was a significant effect of injection number versus normalized current detected comparing the four waveforms (One-way ANOVA, p = 0.0001, n = 6). ESW electrode fouling is significantly different at 400 V/s compared to 1000 V/s with a 39 ± 2% decrease and 19 ± 2%, respectively (Tukey's post-hoc, p = 0.0001). No significant differences in electrode fouling were observed between the ESW 1000 V/s, EHSW 400 V/s, and the EHSW 1000 V/s. The EHSW at 400 and 1000 V/s displayed similar electrode fouling behaviors and suggest extending the switching potential for prolonged periods of time (≥1 ms) compensates for using a slower scan rate.

2.3.3 Fouling after long exposure to 5-hydroxyindoleacetic acid

In mammals, the majority of serotonin in cerebral spinal fluid and blood quickly metabolizes to 5-hydroxyindoleacetaldehyde by monoamine oxidase-A and further oxidizes to 5-hydroxyindoleacetic acid (5-HIAA), which is present in mammalian tissue at concentrations 1000-fold greater than serotonin.[21] 5-HIAA fouls CFMEs through a similar oxidation scheme to serotonin and produces a radical intermediate that dimerizes and electropolymerizes to the CFME (Fig. 5). To determine electrode fouling effects with long 5-HIAA exposure, the current response to a 1 µM 5-HIAA injection was recorded, the CFME was soaked in 5-HIAA for 1 hour with a waveform applied, and then the current response to 5-HIAA was analyzed again. Control experiments were similar, but the electrode was soaked in PBS for an hour with a waveform applied. CFMEs were additionally soaked in 1 µM serotonin for 1 hour to compare fouling behaviors to highly concentrated serotonin for an extended period of time (Fig. 9).

Figure 8A-D shows cyclic voltammograms for the initial and final injections of 5-HIAA for each waveform. In Fig. 8A, electrodes using the Jackson waveform show dramatically reduced currents after the waveform is applied for 1 hour in 5-HIAA. In comparison, using the dopamine waveform, currents are higher after 1 hour of soaking in 5-HIAA (Fig. 8B). For electrodes using the ESW (Fig. 8C) and EHSW (Fig. 8D), currents decreased around a third. Fig. 8E shows a comparison of currents 1 hour after soaking in PBS (control) or 5-HIAA with the different waveforms applied. There were significant effects of waveform (Two-Way ANOVA, $F_{(3,28)}$ = 38.16, p = 0.0001, n = 6 for 5-HIAA, n = 3 for PBS) and soaking in either 5-HIAA and PBS ($F_{(1,28)}$ = 26.47, p = 0.0001) on current response with

significant interaction between the groups ($F_{(3,28)}$ = 14.79, p = 0.0001). Electrodes using the Jackson waveform fouled the most in 5-HIAA with a 65 ± 4% decrease, and current responses were significantly different compared to the control (Fig. 8E, Tukey's post-hoc, p = 0.0001). The ESW and EHSW had similar electrode fouling, with 34 ± 3% and 28 ± 4% current decrease, respectively. However, only EHSW current responses are significantly different in 5-HIAA and PBS (p = 0.01). No electrode fouling was observed with the dopamine waveform, and the final currents were higher than the initial currents (145 ± 11%, p > 0.05), which indicates that the CFME is activated by the waveform. Long exposure to 1 µM serotonin showed similar trends to 5-HIAA even though electrodes fouled severely (Fig. 9). CFMEs using the Jackson waveform fouled the most (85 ± 1%) compared with the ESW (65± 4%) and EHSW (63± 3%), while electrodes showed remarkably less fouling with the dopamine waveform (22 ± 1%).

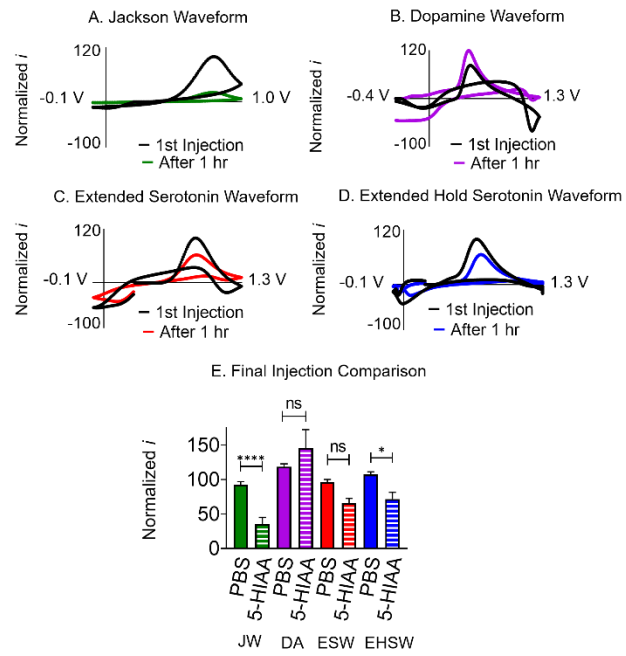

Figure 8. Electrode fouling after long exposure to 5-HIAA. A 1 µM 5-HIAA injection was recorded and the CFME was soaked in 1 µM 5-HIAA for 1 hour with the waveform continuously applied. A final 5-HIAA injection was performed to determine electrode fouling. The control was soaking in PBS for 1 hour between 5-HIAA injections. **A**. Example data using the Jackson waveform shows substantial fouling. **B**. No fouling was observed with the dopamine waveform in 5-HIAA, and final current values were higher than initial currents. Electrodes using the **C**. ESW waveform and **D**. EHSW fouled moderately. **E**. Bar graph compares responses for electrodes soaked in 5-HIAA and PBS. There were significant overall effects of waveform (Two-Way ANOVA, $F_{(3,28)}$ = 38.16, p = 0.0001) and soaking in 5-HIAA (*n* = 6) or PBS (*n* = 3) ($F_{(1,28)}$ = 26.47, p = 0.0001). Electrode fouling was significantly different for the Jackson waveform ($F_{(7,28)}$ = 36.82, Tukey's post-hoc, p = 0.0001) and EHSW (p = 0.01), but not the dopamine waveform (p = 0.1) or ESW (p = 0.055).

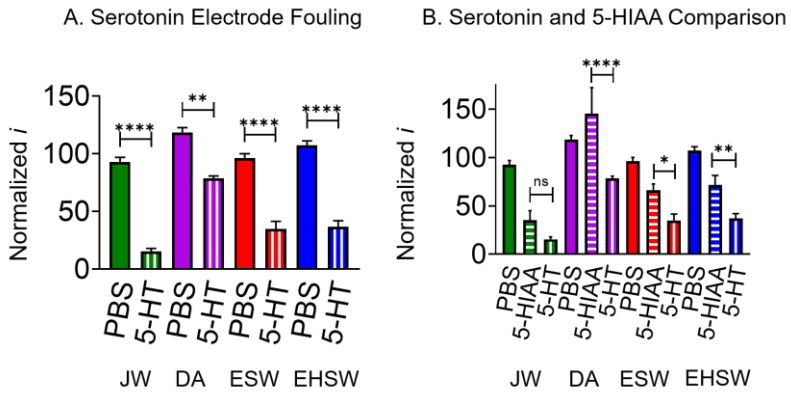

Figure 9. Fouling after long exposure to serotonin. To determine electrode fouling effects with long serotonin exposure, the current response to a 1 µM serotonin injection was recorded, the CFME was soaked in serotonin for 1 hour with a waveform applied, and then the current response to serotonin was analyzed again and compared to the PBS control (Fig. 4E). Long exposure to serotonin causes CFMEs to foul with all waveforms. There were significant effects of waveform (Two-Way ANOVA, $F_{(3,36)} = 60.50$, $p = 0.0001$, $n = 6$ for 5-HIAA, $n = 3$ for PBS, $n = 3$ 5-HT) and soaking in either 5-HT and PBS ($F_{(2,36)} = 84.36$, $p = 0.0001$) on current response with significant interaction between the groups ($F_{(6,36)} = 9.77$, $p = 0.0001$). CFMEs using the Jackson waveform fouled the most with 85 ± 1% current decrease, and responses were significantly different from the PBS control (Fig S4A, Tukey's post-hoc, $p = 0.0001$). However, using the Jackson waveform, CFME fouling with serotonin and 5-HIAA is not significantly different (Fig S4B). Electrodes using the ESW (65 ± 4%) and EHSW (63 ± 3%) fouled similarly and less than the Jackson waveform. Current responses were significantly different in serotonin compared to the control and 5-HIAA (both $p = 0.0001$). However, serotonin electrode fouling responses were not significantly different using the Jackson waveform, ESW, and EHSW ($p \geq 0.5$). Electrodes using the dopamine waveform also fouled with a 22 ± 1% decrease in current, and serotonin responses were significantly different than the control ($p = 0.001$). Though, serotonin electrode fouling with the dopamine waveform was remarkably less and significantly different compared to the Jackson waveform ($p = 0.00001$), ESW ($p = 0.001$), and EHSW ($p = 0.001$). The 1 hour exposure to 1 µM serotonin purposefully fouls electrodes, and may not replicate stimulated responses *in vivo* where it is only subjected to high concentrations over a short period of time, like in our optogenetic experiments. In Abdalla et al. 2017, they estimated the basal concentration of serotonin in mice brain tissue *in vivo* was approximately 60 nM.[39]

For both serotonin and 5-HIAA fouling experiments, extending the switching potential to 1.3 V decreased electrode fouling by removing electropolymerized films.[29] In Jackson *et al*., they proposed using a high scan rate of 1000 V/s to "outrun" serotonin fouling film formation.[20] We observed less electrode fouling using the ESW at 1000 V/s than 400 V/s, but the sawhorse waveform shows no differences with scan rate (Fig. 7). The extended hold at 1.3 V allows more time for the carbon surface to regenerate, so fouling was similar regardless of scan rate.[29] Although electrode fouling was still observed with the new serotonin waveforms, fouling was half that observed using the traditional Jackson waveform for both analytes.

Using the dopamine waveform, electrodes did not foul with repeated serotonin injections or long exposure to 5-HIAA. The holding potential at -0.4 V is applied for over 90% of a waveform cycle and helps attract the positively charged amine group to the electrode.[11,27] However, during serotonin oxidation, the highly reactive radical is delocalized over the indole ring structure.[22,23] This delocalization of the radical gives it a partial negative charge, which could reduce adsorption with a negative holding potential. Likely, serotonin dimers are still produced, but if they polymerize onto the carbon fiber, the higher switching potential regenerates the surface

by continuously breaking carbon-carbon bonds.[29] Similarly, 5-HIAA and its radical possess a negatively charged carboxyl group at physiological pH, which is also repelled by the negative holding potential. In Figure 8E, the dopamine waveform produced higher current responses after 1 hour because the extended switching potential increases surface oxide groups, increasing the current.[29] The waveforms that use a positive holding potential at 0.2 V attract serotonin radicals and 5-HIAA onto the fiber and produce worse electrode fouling (Fig. 6E and Fig. 8E). Although extending the switching potential reduces electrode fouling, a negative holding potential is critical to eliminate it.

2.3.4 Waveform sensitivity and selectivity determination

After understanding electrode fouling behaviors, we investigated CFME responses with serotonin and dopamine for each waveform to determine sensitivity and selectivity. Figure 10 shows example cyclic voltammograms for 100 nM serotonin and dopamine with each waveform and Table 2 gives the average results. Each electrode was used to investigate current responses for both analytes, so responses could be compared (n = 6). Electrodes using all waveforms detected 100 nM serotonin; however, 100 nM dopamine was only detected with electrodes using the dopamine waveform (Fig. 10B) and EHSW (10D) and not with the Jackson waveform (10A) or ESW (10C). Current responses for serotonin were highest using the EHSW, followed by the ESW, dopamine waveform, and Jackson waveform.

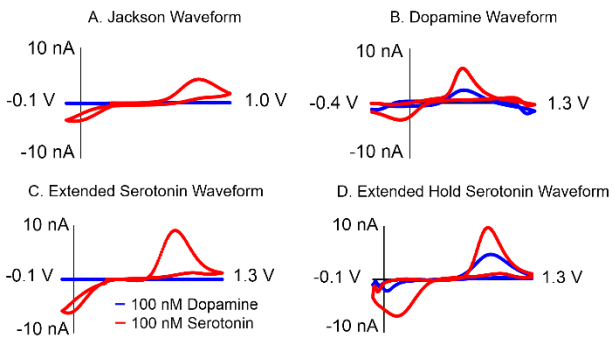

Figure 10. Example current responses for 100 nM serotonin and dopamine (Table 2 shows averaged results from 6 electrodes). **A**. When using the Jackson waveform, the electrode detected 100 nM serotonin, but not 100 nM dopamine. **B**. Both dopamine and serotonin were detected at 100 nM with the dopamine waveform, and the cyclic voltammograms has higher currents for serotonin. **C**. Using the ESW, the CFME detected 100 nM serotonin, but not 100 nM dopamine. **D**. With the EHSW, the electrode detected both 100 nM serotonin and dopamine, and the currents for both analytes were the highest compared to the other waveforms.

Table 2 shows the limit of detection (LOD) for serotonin (5-HT) and dopamine (DA). The limit of detection (LOD) for both analytes was calculated from the lowest concentrations detected, and the LOD for serotonin was lower than dopamine for all waveforms. CFMEs using the Jackson waveform produced the highest LOD for serotonin at 2.4 ± 1.0 nM (n = 6), while the LOD was lowest for the

EHSW (0.6 ± 0.2 nM). Electrodes using the ESW and EHSW were the most sensitive for serotonin, with LODs in the hundreds of picomolar range. Interestingly, with the traditional "dopamine" waveform, CFMEs were 6-times more sensitive for serotonin than dopamine (Fig. 5B). With the Jackson waveform, electrodes showed the greatest selectivity for serotonin, with an 800-fold higher LOD, while electrodes using ESW also had a 200-fold higher LOD for serotonin. With the dopamine waveform and EHSW, electrodes were not highly selective and produced much lower ratios (closer to 1) implying more equal sensitivity to both analytes. The LOD for dopamine with the Jackson waveform is higher than physiological concentrations typically measured *in vivo*, so electrodes should not detect it during experiments.[11]

Table 2. Serotonin and Dopamine limit of detection and selectivity ratio

Waveform	Average LOD 5-HT (nM)	Average LOD DA (nM)	Ratio $\frac{[DA]}{[5\text{-}HT]}$
Jackson	2.4 ± 1.0	2000 ± 600	833
Dopamine	1.5 ± 0.3	9.4 ± 0.2	6.3
ESW	0.8 ± 0.2	189 ± 5	236
EHSW	0.6 ± 0.2	1.4 ± 0.2	2.3

n=6 electrodes each

Extending the switching potential increases CFME sensitivity for both serotonin and dopamine by increasing adsorption through increased oxide groups.[27,29] However, this decreases chemical selectivity. Electrodes using the Jackson waveform showed the greatest selectivity, followed by the ESW. In Jackson *et al*., the -0.1 V potential was designed to allow part of the reduction peak to be observed in the cyclic voltammogram.[20] This limited potential sweep also favors serotonin detection because it reduces around 0.0 V, while dopamine reduces at -0.2 V. When the potential is swept only to -0.1 V, the oxidized dopamine-o-quinone product is not recycled back to dopamine in order to be detected again on the next scan.

Interestingly, with the EHSW, electrodes did not show enhanced selectivity because of their prolonged exposure to the extended switching potential. Electrodes using this sawhorse waveform were the most sensitive to both serotonin and dopamine, however applying 1.3 V for 1 ms or longer compromises selectivity for sensitivity by increasing adsorption.[27,29] Keithley *et al*. examined sawhorse waveforms for dopamine detection and held at the switching potential for 0.55 ms.[26] Their LOD of 0.9 nM for dopamine is similar to our EHSW LOD for dopamine at 1.4 ± 0.2 nM and LOD for serotonin at 0.6 ± 0.2 nM.

2.3.5 Characterization of optogenetically-stimulated serotonin release using various waveforms in Drosophila ventral nerve cords

Previous work in the Venton lab has shown real-time serotonin and dopamine FSCV detection in larvae and adult *Drosophila melanogaster* (fruit flies).[17–19,32] Here, each waveform was investigated for biological applications by detecting serotonin release in isolated fruit fly larvae ventral nerve cords (VNCs). Stimulations were performed with optogenetics by inserting a genetically-encoded, light-sensitive cation channel (CsChrimson)[33] in cells expressing tryptophan hydroxylase (tph).[32] Tryptophan hydroxylase is the rate-determining enzymatic step that converts tryptophan to serotonin. CsChrimson is a form of Channelrhodopsin that responds to red light, causing exocytosis when activated. A short flash of red light onto the larval VNC causes release of only serotonin without interference from dopamine.[34]

Figure 11A shows a confocal image of serotonin neurons in a 5-day old, third-instar larva. Neurons are visualized with GFP expression with a tph-Gal4/CyO; UAS-mCD8-GFP cross. Serotonin cell bodies are located on either side of the midline, although projections fill the neuropil. The CFME was inserted to the side of the midline for optimal serotonin detection and the waveform applied continuously during the experiment (Fig. 11B). The fiber optic cable was positioned above the VNC to deliver red light (617 nm) stimulations, which were 2 seconds long and delivered every 5 minutes to allow the releasable pool of serotonin to replenish itself.[17]

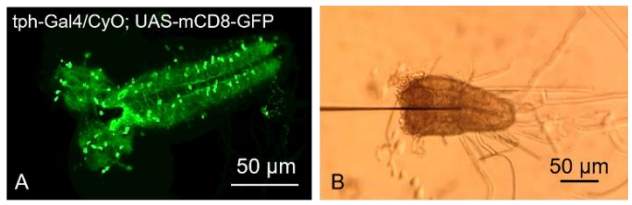

Figure 11. Serotonin neuron imaging and CFME placement in *Drosophila* larvae ventral nerve cords (VNC). **A**. A tph-Gal4/CyO; UAS-mCD8-GFP cross shows GFP expression of serotonin neuron clusters in the larva VNC. **B**. Image shows optimal CFME placement in the neuropil of the VNC to detect the highest concentrations of serotonin.

Figure 12A-D shows example false color plots, *i* vs *t* plots, and serotonin cyclic voltammograms (inset) for the initial (colored) and final (6th, black) optogenetic stimulations for each waveform. The false color plots and cyclic voltammograms for each waveform are similar to their corresponding examples in Figure 4A-D. The *i* vs *t* plots show stable electrode current responses when stimulations are repeated every 5 minutes, regardless of the waveform used. There was no significant effect of waveform on current stability for repeated injections in *Drosophila* (Fig. 13, One-Way ANOVA, $F_{(3,20)} = 1.747$, $p = 0.1897$, $n = 4$). Ambient levels of serotonin did not foul electrodes and stable serotonin detection was achieved because the 5 minute wait period between stimulations allows the releasable pool to replenish itself.[17] Monoamine oxidase-A, which catalyzes the breakdown of serotonin to 5-HIAA, has not been identified in

Drosophila.[35] Instead, serotonin undergoes sugar-conjugated acetylation reactions and is recycled into the larva's body and chitin in the adult's exoskeleton. Thus, fouling during *in vitro* detection may not be as much of a prevalent problem in this model organism compared to mammals.[21] Future experiments should compare the waveforms in more complex *in vivo* mammalian models to determine stability where 5-HIAA fouling is more prevalent.[21] Although detection was stable, a comparison of pre and post-calibrated electrodes show CFMEs foul 20-50% due to protein adsorption onto the CFME from inserting and removing it into the VNC tissue (Fig. 2).[36]

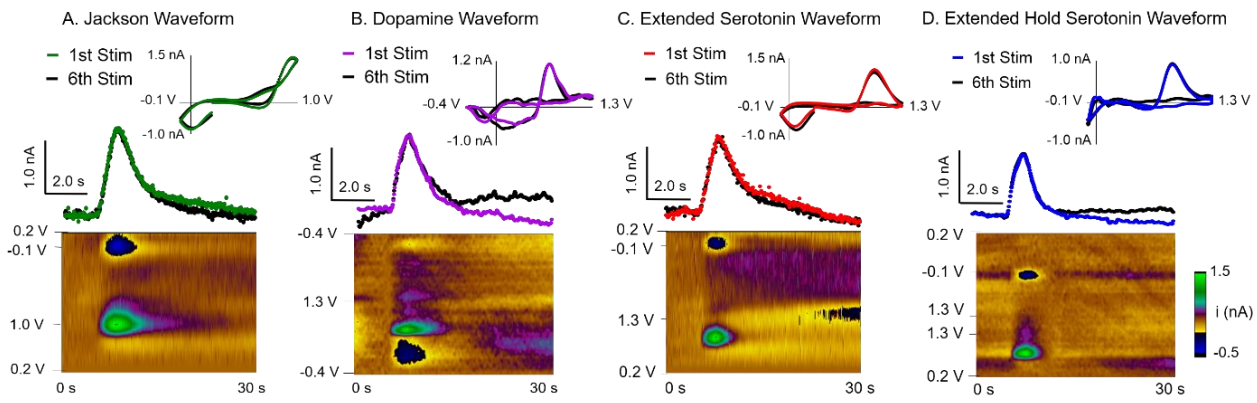

Figure 12. Optogenetic stimulation of serotonin in *Drosophila* with different waveforms. Repeated stimulations were performed by shining a red light on the ventral nerve cord for 2 seconds every 5 minutes. False color plots show serotonin release on the first stimulation. Current responses were compared for the first and final (6th) stimulations. Electrodes using the (**A**) Jackson waveform, (**B**) dopamine waveform, (**C**) ESW, and (**D**) EHSW all produced stable measurements (n = 4).

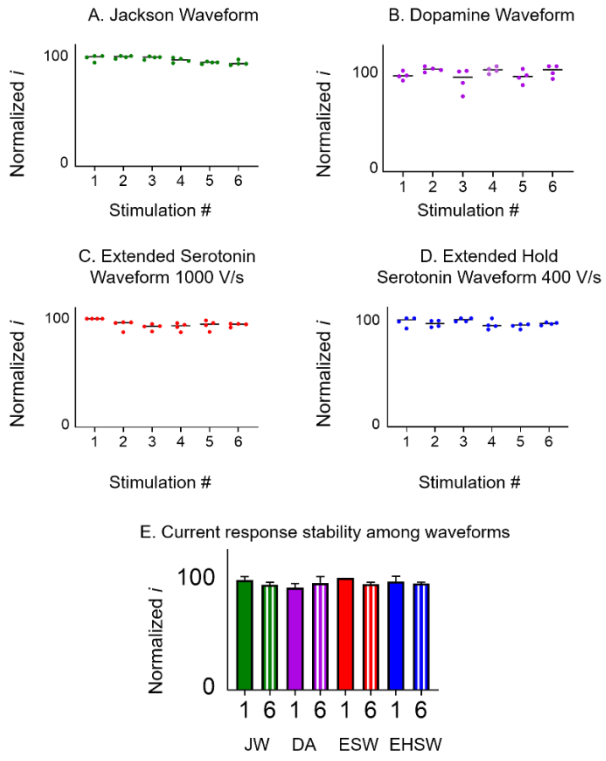

Figure 13. Optogenetic stimulation waveform stability. A 5 minute wait period was applied between stimulations and six stimulations were applied. Electrode response stability was determined by comparing normalized currents for the 1st (solid) and 6th stimulations (*n* = 4). The Jackson waveform (green) had an average first stimulation stability of 95.4 ± 1.1%. The dopamine waveform (purple) at 104 ± 3%, the ESW (red) 94.3 ± 1.7%, the EHSW (blue) 98.1 ± 1.9%. All waveforms remained above 90% stable after six repeated stimulations.

2.3.6 Comparison of serotonin waveforms and future applications

Our results show electrodes foul severely when the Jackson waveform is used to detect repeated serotonin measurements or when 5-HIAA is present. However, the Jackson waveform is highly selective for serotonin and does not detect physiological concentrations of dopamine.[11] The Jackson waveform is best suited for complex *in vivo* experiments where serotonin is detected with the possible interference of dopamine; for example, in regions like the striatum where interference needs to be avoided.[1] With the Jackson waveform, Nafion-coated electrodes are required to mitigate serotonin and 5-HIAA fouling.[21] Nafion is a cation-exchange polymer that shields serotonin and 5-HIAA from electropolymerizing to the surface of the fiber. Although it reduces electrode fouling, thick Nafion layers decrease response times *in vivo*, so caution is necessary when determining kinetic information during these experiments.[25]

Our work also shows that changing the applied FSCV waveform reduces electrode fouling without applied polymer coatings. With the extended serotonin waveform (ESW), electrodes had comparable selectivity to the Jackson waveform with reduced fouling

and higher sensitivity. The ESW could be applied *in vivo* without Nafion if selectivity and faster responses are required. Nafion coatings may not be stable with a 1.3 V switching potential because of surface regeneration.[29] With the extended hold serotonin waveform (EHSW), electrode responses were not as selective, but were the most sensitive for both serotonin and dopamine. The EHSW would be beneficial for optogenetic experiments where either serotonin or dopamine was specifically stimulated, especially if high sensitivity was necessary.

A major finding in this work is that there is no electrode fouling for serotonin with the dopamine waveform. Further, with the dopamine waveform, electrodes were more sensitive for serotonin than dopamine, but they were not highly selective. The dopamine waveform's anti-fouling nature is due to its extended switching potential, which renews the carbon electrode surface, and negative holding potential, which reduces adsorption of serotonin and its oxidation products. In Moran *et al*., a unique waveform (-0.6 V to 1.4 V and back, 400 V/s) was used to detect both serotonin and dopamine in a single cyclic voltammogram, with machine learning to distinguish the compounds.[1,37] Serotonin and dopamine are usually identified by their different reduction peaks (0.0 V and -0.2 V, respectively), but these can shift *in vivo* from tissue fouling and protein adsorption.[36,38] While the sensitivity of CFMEs with the dopamine waveform has been investigated previously,[27,29] it should be recognized that the CFME is more sensitive to serotonin with this waveform and that small concentrations of serotonin will easily interfere with dopamine measurements. Ultimately, using the dopamine waveform is beneficial because it produces high sensitivity and causes less electrode fouling, and it is useful in experiments where selectivity is not a problem. For example, the dopamine waveform is useful for detecting serotonin in optogenetic experiments, where the channel is genetically targeted to one cell type, so selectivity is not an issue.[17,32]

Overall, this work shows many waveforms can be applied to CFMEs to detect serotonin. Electrodes using the Jackson waveform are the most selective for serotonin, but electrodes using the ESW show higher sensitivity than the Jackson waveform while maintaining high selectivity. With the EHSW and dopamine waveform, electrodes also have excellent sensitivity. All extended waveforms show less (ESW, EHSW) or no (DA) electrode fouling. Each waveform can be applied to *Drosophila* for stable serotonin detection; however, future *in vivo* applications of each waveform should be based on the properties desired for an experiment.

2.4 Conclusions

Overall, this work evaluated different FSCV waveforms for serotonin detection and detailed different advantages and disadvantages for each waveform. Detection using the Jackson waveform is the most selective for serotonin but fouling is the most problematic. The ESW shows higher electrode sensitivity while maintaining high selectivity. With the EHSW and dopamine waveform, electrodes have excellent sensitivity. All extended waveforms show reduced electrode fouling compared to the Jackson waveform, and the dopamine waveform shows no electrode fouling with serotonin or 5-HIAA. Each waveform can be applied to CFMEs for stable serotonin detection in *Drosophila*; however, future *in vivo* applications should be based on experimental designs. For example, the dopamine waveform can be used in experiments where fouling is an issue if the analyte being detected is known to be serotonin, so selectivity is not a concern. The ESW is a better choice for experiments requiring selectivity between dopamine and serotonin, and will limit fouling. All waveforms should be further investigated in mammalian models, but this work developed a toolkit of serotonin waveforms that can be tuned to the requirements of an individual experiment, and will facilitate a better understanding of the role of serotonin in illnesses such as depression.

2.5 References

(1) Moran, R. J.; Kishida, K. T.; Lohrenz, T.; Saez, I.; Laxton, A. W.; Witcher, M. R.; Tatter, S. B.; Ellis, T. L.; Phillips, P. E.; Dayan, P.; Montague, P. R. The Protective Action Encoding of Serotonin Transients in the Human Brain. *Neuropsychopharmacology* **2018**, *43* (6), 1425–1435. https://doi.org/10.1038/npp.2017.304.

(2) Shin, M.; Wang, Y.; Borgus, J. R.; Venton, B. J. Electrochemistry at the Synapse. *Annu. Rev. Anal. Chem.* **2019**, *12* (1), 297–321. https://doi.org/10.1146/annurev-anchem-061318-115434.

(3) Fakhoury, M. Revisiting the Serotonin Hypothesis: Implications for Major Depressive Disorders. *Mol. Neurobiol.* **2016**, *53* (5), 2778–2786. https://doi.org/10.1007/s12035-015-9152-z.

(4) Wood, K. M.; Zeqja, A.; Nijhout, H. F.; Reed, M. C.; Best, J.; Hashemi, P. Voltammetric and Mathematical Evidence for Dual Transport Mediation of Serotonin Clearance in Vivo. *J. Neurochem.* **2014**, *130* (3), 351–359. https://doi.org/10.1111/jnc.12733.

(5) Saylor, R. A.; Hersey, M.; West, A.; Buchanan, A. M.; Berger, S. N.; Nijhout, H. F.; Reed, M. C.; Best, J.; Hashemi, P. In Vivo Hippocampal Serotonin Dynamics in Male and Female Mice: Determining Effects of Acute Escitalopram Using Fast Scan Cyclic Voltammetry. *Front. Neurosci.* **2019**, *13* (APR), 1–13. https://doi.org/10.3389/fnins.2019.00362.

(6) Venton, B. J.; Wightman, R. M. Psychoanalytical Electrochemistry: Dopamine and Behavior. *Anal. Chem.* **2003**, *75* (19).

(7) Ganesana, M.; Lee, S. T.; Wang, Y.; Venton, B. J. Analytical Techniques in Neuroscience: Recent Advances in Imaging, Separation, and Electrochemical Methods. *Anal. Chem.* **2017**, *89* (1), 314–341. https://doi.org/10.1021/acs.analchem.6b04278.

(8) Puthongkham, P.; Venton, B. J. Recent Advances in Fast-Scan Cyclic Voltammetry. *Analyst* **2020**, *145* (4), 1087–1102. https://doi.org/10.1039/c9an01925a.

(9) Lama, R. D.; Charlson, K.; Anantharam, A.; Hashemi, P. Ultrafast Detection and Quantification of Brain Signaling Molecules with Carbon Fiber Microelectrodes. *Anal. Chem.* **2012**, *84* (19), 8096–8101. https://doi.org/10.1021/ac301670h.

(10) Huffman, M. L.; Venton, B. J. Carbon-Fiber Microelectrodes for in Vivo Applications. *Analyst* **2009**, *134* (1), 18–24.

https://doi.org/10.1039/b807563h.

(11) Venton, B. J.; Cao, Q. Fundamentals of Fast-Scan Cyclic Voltammetry for Dopamine Detection. *Analyst* **2020**, *145* (4), 1158–1168. https://doi.org/10.1039/c9an01586h.

(12) Andrews, A. M. Why Monitor Molecules in Neuroscience? *ACS Chem. Neurosci.* **2017**, *8* (2), 211–212. https://doi.org/10.1021/acschemneuro.7b00052.

(13) Hashemi, P.; Dankoski, E. C.; Wood, K. M.; Ambrose, R. E.; Wightman, R. M. In Vivo Electrochemical Evidence for Simultaneous 5-HT and Histamine Release in the Rat Substantia Nigra Pars Reticulata Following Medial Forebrain Bundle Stimulation. *J. Neurochem.* **2011**, *118* (5), 749–759. https://doi.org/10.1111/j.1471-4159.2011.07352.x.

(14) Dankoski, E. C.; Carroll, S.; Wightman, R. M. Acute Selective Serotonin Reuptake Inhibitors Regulate the Dorsal Raphe Nucleus Causing Amplification of Terminal Serotonin Release. *J. Neurochem.* **2016**, *136* (6), 1131–1141. https://doi.org/10.1111/jnc.13528.

(15) Dankoski, E. C.; Agster, K. L.; Fox, M. E.; Moy, S. S.; Wightman, R. M. Facilitation of Serotonin Signaling by SSRIs Is Attenuated by Social Isolation. *Neuropsychopharmacology* **2014**, *39* (13), 2928–2937. https://doi.org/10.1038/npp.2014.162.

(16) Wood, K. M.; Hashemi, P. Fast-Scan Cyclic Voltammetry Analysis of Dynamic Serotonin Reponses to Acute Escitalopram. *ACS Chem. Neurosci.* **2013**, *4* (5), 715–720. https://doi.org/10.1021/cn4000378.

(17) Borue, X.; Condron, B.; Venton, B. J. Both Synthesis and Reuptake Are Critical for Replenishing the Releasable Serotonin Pool in Drosophila. *J. Neurochem.* **2010**, *113* (1), 188–199. https://doi.org/10.1111/j.1471-4159.2010.06588.x.

(18) Borue, X.; Cooper, S.; Hirsh, J.; Condron, B.; Venton, B. J. Quantitative Evaluation of Serotonin Release and Clearance in Drosophila. *J. Neurosci. Methods* **2009**, *179* (2), 300–308. https://doi.org/10.1016/j.jneumeth.2009.02.013.

(19) Xiao, N.; Privman, E.; Venton, B. J. Optogenetic Control of Serotonin and Dopamine Release in Drosophila Larvae. *ACS Chem. Neurosci.* **2014**, *5* (8), 666–673. https://doi.org/10.1021/cn500044b.

(20) Jackson, B. P.; Dietz, S. M.; Wightman, R. M. Fast-Scan Cyclic Voltammetry of 5-Hydroxytryptamine. *Anal. Chem.* **1995**, *67* (6), 1115–1120. https://doi.org/10.1021/ac00102a015.

(21) Hashemi, P.; Dankoski, E. C.; Petrovic, J.; Keithley, R. B.; Wightman, R. M. Voltammetric Detection of 5-Hydroxytryptamine Release in the Rat Brain. *Anal. Chem.* **2009**, *81* (22), 9462–9471. https://doi.org/10.1021/ac9018846.

(22) Wrona, M. Z.; Dryhurst, G. Electrochemical Oxidation of 5-Hydroxytryptamine in Aqueous Solution at Physiological PH. *Bioorg. Chem.* **1990**. https://doi.org/10.1016/0045-2068(90)90005-P.

(23) Anne, A.; Lemordant, D.; Dryhurst, G.; Wrona, M. Z. Mechanism and Products of Electrochemical Oxidation of 5, 7-Dihydroxytryptamine. *J. Am. Chem. Soc.* **1989**, *111* (2), 719–726. https://doi.org/10.1021/ja00184a050.

(24) Puthongkham, P.; Lee, S. T.; Jill Venton, B. Mechanism of Histamine Oxidation and Electropolymerization at Carbon Electrodes. In *Analytical Chemistry*; 2019. https://doi.org/10.1021/acs.analchem.9b01178.

(25) Ross, A. E.; Venton, B. J. Nafion-CNT Coated Carbon-Fiber Microelectrodes for Enhanced Detection of Adenosine. *Analyst* **2012**, *137* (13), 3045–3051. https://doi.org/10.1039/c2an35297d.

(26) Keithley, R. B.; Takmakov, P.; Bucher, E. S.; Belle, A. M.; Owesson-White, C. A.; Park, J.; Wightman, R. M. Higher Sensitivity Dopamine Measurements with Faster-Scan Cyclic Voltammetry. *Anal. Chem.* **2011**. https://doi.org/10.1021/ac200143v.

(27) Heien, M. L. A. V.; Phillips, P. E. M.; Stuber, G. D.; Seipel, A. T.; Wightman, R. M. Overoxidation of Carbon-Fiber Microelectrodes Enhances Dopamine Adsorption and Increases Sensitivity. *Analyst* **2003**, *128* (12), 1413–1419. https://doi.org/10.1039/b307024g.

(28) Robinson, D. L.; Venton, B. J.; Heien, M. L. A. V.; Wightman, R. M. Detecting Subsecond Dopamine Release with Fast-Scan Cyclic Voltammetry in Vivo. In *Clinical Chemistry*; 2003. https://doi.org/10.1373/49.10.1763.

(29) Takmakov, P.; Zachek, M. K.; Keithley, R. B.; Walsh, P. L.; Donley, C.; McCarty, G. S.; Wightman, R. M. Carbon Microelectrodes with a Renewable Surface. *Anal. Chem.* **2010**, *82* (5), 2020–2028. https://doi.org/10.1021/ac902753x.

(30) Mccreery, R. L.; Mccreery, R. L. Advanced Carbon Electrode Materials for Molecular Electrochemistry Advanced Carbon

Electrode Materials for Molecular Electrochemistry. *2646 Chem. Rev.* **2008**, *108* (June), 2646–2687. https://doi.org/10.1021/cr068076m.

(31) Ross, A. E.; Venton, B. J. Sawhorse Waveform Voltammetry for Selective Detection of Adenosine, ATP, and Hydrogen Peroxide. *Anal. Chem.* **2014**, *86* (15), 7486–7493. https://doi.org/10.1021/ac501229c.

(32) Privman, E.; Venton, B. J. Comparison of Dopamine Kinetics in the Larval Drosophila Ventral Nerve Cord and Protocerebrum with Improved Optogenetic Stimulation. *J. Neurochem.* **2015**, *135* (4), 695–704. https://doi.org/10.1111/jnc.13286.

(33) Klapoetke, N. C.; Murata, Y.; Kim, S. S.; Pulver, S. R.; Birdsey-Benson, A.; Cho, Y. K.; Morimoto, T. K.; Chuong, A. S.; Carpenter, E. J.; Tian, Z.; Wang, J.; Xie, Y.; Yan, Z.; Zhang, Y.; Chow, B. Y.; Surek, B.; Melkonian, M.; Jayaraman, V.; Constantine-Paton, M.; Wong, G. K.-S.; Boyden, E. S. Independent Optical Excitation of Distinct Neural Populations. *Nat. Methods* **2014**, *11* (3), 338–346. https://doi.org/10.1038/nmeth.2836.

(34) Shin, M.; Copeland, J. M.; Venton, B. J. Drosophila as a Model System for Neurotransmitter Measurements. *ACS Chem. Neurosci.* **2018**, *9* (8), 1872–1883. https://doi.org/10.1021/acschemneuro.7b00456.

(35) Dewhurst, S. A.; Croker, S. G.; Ikeda, K.; Mccaman, R. E. METABOLISM OF BIOGENIC NERVOUS TISSUE IN DROSOPHILA E Metabolism in Insect Tissues Has Received Little Attention Compared with Acetylcholine Metabolism (Metcalf & March , 1950 ; Colhoun , 1958 ; Dewhurst et Al ., 1970). In 1954 Adrenalin , Noradrenalin. *Comp. Biochem. Physiol.* **1972**, *43* (1966), 975–981.

(36) Norde, W. Driving Forces for Protein Adsorption at Solid Surfaces. *Macromol. Symp.* **1996**, *103*, 5–18. https://doi.org/10.1002/masy.19961030104.

(37) Kishida, K. T.; Saez, I.; Lohrenz, T.; Witcher, M. R.; Laxton, A. W.; Tatter, S. B.; White, J. P.; Ellis, T. L.; Phillips, P. E. M.; Montague, P. R. Subsecond Dopamine Fluctuations in Human Striatum Encode Superposed Error Signals about Actual and Counterfactual Reward. *Proc. Natl. Acad. Sci. U. S. A.* **2016**, *113* (1), 200–205. https://doi.org/10.1073/pnas.1513619112.

(38) Seaton, B. T.; Hill, D. F.; Cowen, S. L.; Heien, M. L. Mitigating the Effects of Electrode Biofouling-Induced Impedance for Improved Long-Term Electrochemical Measurements In Vivo. *Anal. Chem.* **2020**, No. 2. https://doi.org/10.1021/acs.analchem.9b05194.

(39) Abdalla, A.; Atcherley, C. W.; Pathirathna, P.; Samaranayake, S.; Qiang, B.; Peña, E.; Morgan, S. L.; Heien, M. L.; Hashemi, P. In Vivo Ambient Serotonin Measurements at Carbon-Fiber Microelectrodes. *Anal. Chem.* **2017**, *89* (18), 9703–9711. https://doi.org/10.1021/acs.analchem.7b01257.

Chapter 3

SSRI antidepressants differentially modulate serotonin reuptake and release in *Drosophila*

Abstract

Selective serotonin reuptake inhibitor (SSRI) antidepressants are commonly prescribed treatments for depression, but their effects on serotonin reuptake and release are not well understood. *Drosophila melanogaster*, the fruit fly, expresses the serotonin transporter (dSERT), the major target of SSRIs, but real-time serotonin changes after SSRIs have not been characterized in this model. The goal of this study was to characterize effects of SSRIs on serotonin concentration and reuptake in *Drosophila* larvae. We applied various doses (0.1 – 100 µM) of fluoxetine (Prozac), escitalopram (Lexapro), citalopram (Celexa), and paroxetine (Paxil), to ventral nerve cord (VNC) tissue and measured optogenetically-stimulated serotonin release with fast-scan cyclic voltammetry (FSCV). Fluoxetine increased reuptake from 1-100 µM, but serotonin concentration only increased at 100 µM. Thus, fluoxetine occupies dSERT and slows clearance, but does not affect concentration. Escitalopram and paroxetine increased serotonin concentrations at all doses, but escitalopram increased reuptake more. Citalopram showed lower concentration changes and faster reuptake profiles compared to escitalopram, so the racemic mixture of citalopram does not change reuptake as much as the *S*-isomer. Dose response curves were constructed to compare dSERT affinities and paroxetine showed the highest affinity and fluoxetine the lowest. These data demonstrate SSRI mechanisms are complex, with separate effects on reuptake or release. Further, dynamic serotonin changes in *Drosophila* are similar to previous studies in mammals. This work establishes how antidepressants affect serotonin in real-time, which is useful for future studies that will investigate pharmacological effects of SSRIs with different genetic mutations in *Drosophila.*

3.1 Introduction

Drosophila melanogaster, the fruit fly, is a versatile model organism that is useful to study the genetic basis of diseases, including illnesses like depression.[1–5] *Drosophila* show many depressive behaviors, including learned helplessness and changes to locomotion and feeding,[6–8] and the Krantz group created genetic screens to test neuropsychiatric drugs that target monoamine neurotransmitters with this model.[5] Although fruit flies possess simpler neural circuitry than mammals, they use the same neurotransmitters, like serotonin, that are implicated in depression.[1,2,8] Flies have all the major components of the serotonergic system, including the serotonin transporter (dSERT), which is targeted by selective serotonin reuptake inhibitor (SSRI) antidepressants.[1,8–10] SERT reuptakes serotonin back into the presynaptic neuron as part of a negative feedback loop, and SSRIs bind to SERT to inhibit this mechanism.[9,11,12] Behavioral research reveals that the serotonin system controls depressive behaviors in flies,[7,8] since mutations to serotonin receptors and serotonin biosynthesis pathways directly affect larval locomotion and feeding.[7] The Campusano group found a new dSERT mutant that displayed increased body movements, and that fluoxetine increased biogenic amine reuptake in that mutant.[8] While behavioral studies show the downstream effects of genetic mutations, *Drosophila* could also be a good model system to study how neurotransmitters regulate depression and change during administration of SSRIs. However, there is little basic research on the real-time effects of SSRIs on serotonin changes in *Drosophila*.

SSRIs are the most commonly prescribed antidepressants; however, their efficacies vary greatly in individuals. One major issue is that many SSRI antidepressants possess different chemical structures and binding affinities to SERT.[8,13–16] Prozac (fluoxetine), Lexapro (escitalopram), Celexa (citalopram), and Paxil (paroxetine) are common SSRIs that do not share chemical structural motifs (Figure 1), and molecular modeling and docking simulation studies show they have different binding affinities to SERT.[11,13,15,16] Historically, the x-ray crystal structure of human SERT (hSERT) was not collected until 2016,[17] and dSERT was used before that to understand the binding affinities and activities of these drugs. Thus, dSERT is a good model to understand hSERT.[11,18,19] and pharmaceutical screens of SSRIs in *Drosophila* would be beneficial for future studies of how mutations in SERT affect neurotransmission.

To monitor neurotransmitters in real-time *in vitro*, electrochemical detection using fast-scan cyclic voltammetry (FSCV) at carbon fiber microelectrodes (CFMEs) has been used to measure fast neurotransmitter release and reuptake changes.[1,20–22] With FSCV, the potential is linearly ramped positively to directly oxidize and then negatively to then reduce electroactive neurotransmitters.[21–23] Unique potential waveforms such as the Jackson waveform or extended serotonin waveform (ESW) are more selective for serotonin detection over dopamine.[20,24] Previously, FSCV and other electrochemical techniques have been used to understand serotonin dynamics in

mammals.[25–27] The Hashemi group demonstrated citalopram and escitalopram increase extracellular serotonin,[28,29] and Wightman's group found that serotonin was stored in dense core vesicles.[25] The Daws group also found serotonin reuptake did not significantly change in SERT KO mice,[27] which implies compensation by other neurotransmitter systems. Our group has adapted FSCV to measure neurotransmitter dynamics in *Drosophila*.[1,30–32] Serotonin release is stimulated using optogenetics, as the UAS/Gal4 system is used to express CsChrimson with a tryptophan hydroxylase (trh-Gal4) driver that localizes it in serotonin neurons.[20,33] This stimulation protocol selectively releases only serotonin and is used to study serotonin changes in *Drosophila* to understand how concentration and reuptake are affected by SSRIs *in vitro*.

The goal of this study is to explore how SSRIs work at dSERT to change serotonin in real-time, so that *Drosophila* can be used as a model organism to study these antidepressants with simple pharmacological assays. We hypothesized that the concentration of serotonin and the rate of reuptake would vary due to the unique structures of each drug and their affinities for dSERT. At low doses (<1 µM), escitalopram and paroxetine were the only drugs that increased serotonin concentration. Escitalopram showed the largest change in reuptake, followed by fluoxetine, citalopram, and paroxetine. These results indicate that stereochemistry for escitalopram and citalopram contribute to their activity. Additionally, fluoxetine affects serotonin reuptake without changes in concentration, while paroxetine elicits large changes in serotonin concentration without noticeable changes in reuptake. Our results show serotonin concentration and reuptake changes are different with each SSRI and suggest unique mechanisms of action that need to be explored in the future. With this knowledge of how different SSRIs act at dSERT to change serotonin, *Drosophila* can be used to study how genetic mutations affect SSRI efficacy and behavior.

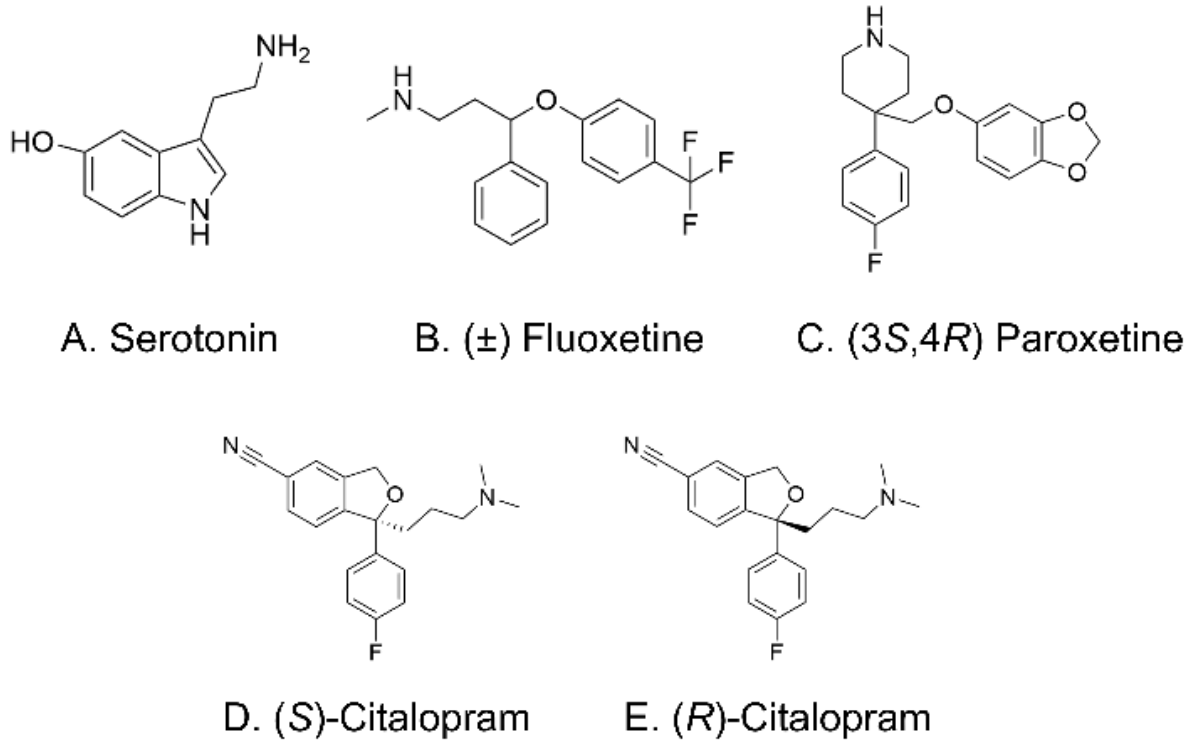

Figure 1. Chemical structures of serotonin and common selective serotonin reuptake inhibitor (SSRI) antidepressants. **A.** Serotonin has an indole ring structure. **B.** Fluoxetine (Prozac) is a racemic mixture of (*S*) and (*R*)-fluoxetine. It possesses a very different ring structure than serotonin and other SSRI antidepressants. **C.** Paroxetine (Paxil) contains a benzodioxole group on a piperdine ring that bears substitutes at the 3 and 4 positions for a (3*S*,4*R*)-diastereomer. **D.** (*S*)-Citalopram is the (S)-enantiomer of citalopram and is exclusively produced as escitalopram (Lexapro). **E.** (*R*)-Citalopram is the (*R*)-enantiomer of citalopram. Citalopram (Celexa) is a racemic mixture of the (*S*) and (*R*)-enantiomers.

3.2 Experimental Methods

3.2.1 Chemicals

Serotonin hydrochloride (CAS Number: 153-98-0), fluoxetine hydrochloride (56296-78-7), escitalopram oxalate (219861-08-2), paroxetine hydrochloride (110429-35-1), citalopram hydrobromide (59729-32-7), and all-trans retinal (116-31-4) were purchased from Sigma Aldrich (St Louis, MO). For pre- and post-calibrations, a 1 mM stock solution of serotonin was prepared in 0.1 M $HClO_4$. A final working solution of 1 µM serotonin was prepared by diluting the stock in phosphate buffer saline (PBS, 131.25 mM NaCl, 3.00 mM KCl, 10 mM NaH_2PO_4, 1.2 mM $MgCl_2$, 2.0 mM Na_2SO_4, and 1.2 mM $CaCl_2$ with the final pH adjusted to 7.4 with 1 M NaOH).[20] A 1 mM stock solution of SSRI antidepressant was prepared in PBS and made fresh daily. Drugs were then diluted to 4x the final dose, and a syringe was used to slowly add 1 mL of the SSRI dropwise to 3 mL of PBS for *in vitro* optogenetic experiments to make a final solution bathing the larval VNC in the desired dose.

3.2.2 Microelectrode Preparation

CFMEs were prepared as previously described.[20,34] Briefly, a T-650 carbon fiber (Cytec Engineering Materials, West Patterson, NJ) with a 7 µm diameter was aspirated into a standard 1.28 mm inner diameter x 0.69 mm outer diameter glass capillary tube (A-M Systems, Sequim, WA) with a vacuum pump. A capillary was then pulled by a Flaming Brown micropipette horizontal puller (Sutter Instrument, Novato, CA) to make two electrodes. Fibers were cut to 25-75 µm and epoxied by dipping the tip of the electrode into a solution of 14% m-phenylenediamine hardener (108-45-2, Acros Organics, Morris Plains, NH) in Epon Resin 828 (25068-38-6, Miller Stephenson, Danbury, CT) at 80–85 °C for 35 seconds. The CFMEs were cured at 100 °C overnight and 150 °C for at least 4 hours the next day.

3.2.3 Electrochemical Instrumentation

Electrochemical experiments were performed using a two-electrode system with a CFME working electrode backfilled with 1 M KCl.[20,30,33,35] All potential measurements are reported versus a chloridized Ag/AgCl wire reference electrode. Experiments were conducted in a covered, grounded Faraday cage to block out light. Before experiments, electrode tips were soaked in isopropyl alcohol for at least 10 minutes to clean the surface. The extended serotonin waveform (ESW, 0.2 V, 1.3 V, -0.1 V, 0.2 V, 1000 V/s) was continuously applied to electrodes using a WaveNeuro system (Pine Research, Durham, NC).[20] Data were collected with HDCV Analysis software (Department of Chemistry, University of North Carolina at Chapel Hill). A flow-injection system with a six-port loop injector and air actuator (Valco Instruments, Houston, TX) was used to pre- and post-calibrate CFMEs for *in vitro* experiments. PBS buffer was flowed at 2 mL/min using a syringe pump (Harvard Apparatus, Holliston, MA) through a flow cell with the CFME tip inserted in solution. For calibration, 1 □M serotonin was injected for 5 seconds to determine current response. The concentration of serotonin released during *in vitro* experiments was determined using this calibration factor.

3.2.4 Tissue Preparation for in vitro Experiments

Methods were previously described in Dunham and Venton 2020.[20] UAS-CsChrimson (Stockline BL#55136, Bloomington *Drosophila* Stock Center, Bloomington, IN) virgin females were crossed with trh-Gal4 (BL#38389) flies and resulting heterozygous larvae were kept in the dark and raised on standard food mixed 250:1 with 100 mM all-trans retinal.[20] The ventral nerve cords (VNCs)

of third instar “wandering” larvae were dissected in PBS kept on ice. A VNC was placed in an uncoated Petri dish dorsal side down containing 3 mL of room temperature PBS. A small slice of the lateral optic lobe was removed using the tip of a 22-gauge hypodermic needle. A CFME was implanted from the lateral edge of the tissue into the dorsal medial protocerebrum using a micromanipulator. Dissection and electrode insertion were performed under low light conditions to reserve the pools of releasable serotonin.[35] CFMEs were allowed to equilibrate for 10 minutes in tissue in the dark prior to data collection. Institutional ethical approval was not required for this study. Randomization procedures were not applied for allocation of different treatments. No exclusion criteria for samples were predetermined. No blinding was performed during data analysis.

3.2.5 Optogenetic Serotonin Release

Optogenetic release of serotonin was stimulated by activating CsChrimson ion channels with red light from a 617 nM fiber-coupled high-power LED with a 200 µm core optical cable (ThorLabs, Newton, NJ, USA).[20] A micromanipulator was used to center the fiber above the VNC tissue, and transistor-transistor logic (TTL) inputs to a T-cube LED controller (ThorLabs) were connected to the FSCV breakout box to control the light. TTL input was driven by electrical pulses from the WaveNeuro system and HDCV software to control frequency, pulse width, and number of pulses. For *in vitro* experiments, 120 biphasic pulses were delivered at 60 Hz with pulse width of 4 ms. An initial stimulation was recorded and 1 mL of SSRI was slowly added to the Petri dish to not move the tissue or CFME. Stimulations were repeated every 5 minutes for 15 minutes after the SSRI was added to allow the releasable pool of serotonin to replenish itself.

3.2.6 Serotonin GFP Imaging in Larvae Ventral Nerve Cords

Drosophila were bred to yield a trh-Gal4/Cyo; UAS-mcD8-GFP cross (Dr. Jeffery Copeland, Eastern Mennonite University, Biology Department). GFP was used to visualize serotonin neurons in the fruit fly larva VNC. Flies and larvae were raised in normal light conditions.[20] Several VNCs were dissected out and placed in a Petri dish with PBS kept on ice. PBS was removed and VNCs were preserved with 1-2 mL of 4% paraformaldehyde in PBS solution (30525-89-4, Alfa Aesar, Ward Hill, MA). The Petri dishes were coved in Parafilm (Bemis, Neenah, WI) and rocked for 20 minutes on a Nutating Mixer (VWR International, Radnor, PA). Paraformaldehyde was removed and an initial wash of 2 mL of PBS was applied for 20 minutes, followed by two 5 minute washes. The specimens were placed on a glass slide dorsal side up in 60 µL of Vectashield (Vector Laboratories, Burlingame, CA). GFP expression

was imaged using a Zeiss AxioZoom macroscope (Carl Zeiss Microscopy, Germany) with Image J software (National Institutes of Health).

3.2.7 Statistics

Data are the mean ± the standard error of the mean (SEM) for *n* number of *Drosophila* larvae. For 100 nM, 1, 10, and 100 µM dosage experiments, *n* = 6 larvae (larvae were not sexed, so both males and females were used). For drug dose response curve experiments, each dose is at least *n* = 4 larvae. For a sample calculation, we performed power analysis in MedCalc (MedCalc Statistical Software, Ostend, Belgium) using the paired sample t-test where = 0.05, 1-β = 0.1, mean difference in current detected = 0.45 nA, and standard deviation of differences = 0.2 nA, which results in *n* = 4 larvae.[30,33,35,36] Statistics were performed in GraphPad Prism 8.0 (GraphPad Software, La Jolla, CA). Data were normally-distributed for multiple drug comparisons (all KS distance ≥ 0.1719, Kolmogrorov-Smirnov, p > 0.1000). Significance was determined at a 95% confidence level for One-Way ANOVA, Two-Way ANOVA, Tukey's post-hoc test, and comparison of fits. No test for outliers was performed.

3.3 Results

3.3.1 Characterization of SSRI antidepressants in Drosophila with fast-scan cyclic voltammetry

The goal of this study was to understand serotonin changes with different SSRI antidepressants in *Drosophila* larvae. Figure 2A-D illustrates the experimental overview. Serotonin was measured electrochemically using FSCV. A new serotonin FSCV waveform, the extended serotonin waveform (ESW), was applied because it has high serotonin sensitivity and high selectivity for serotonin over dopamine detection.[20] Here, a VNC was dissected out from a third instar lava, and a CFME was inserted into the dissected-out VNC tissue to detect serotonin, while a reference electrode was placed in the bath. To visualize serotonin neurons, we expressed GFP in tryptophan hydroxylase neurons, the enzyme that makes serotonin (trh-Gal4/Cyo; UAS-mcD8-GFP, Fig. 2B). Serotonin neuron clusters surround the mid-line of the VNC and Figure 2C shows optimal CFME placement to measure optogenetically-released serotonin with FSCV. However, for optogenetic experiments, flies were crossed to yield heterozygous trh-Gal4/UAS-CsChrimson larvae.

Figure 2D shows serotonin release before and after administration of a high (100 M) dose of fluoxetine. Data are shown as concentration versus time plots (above, black) and false color plots (below). The FSCV color plot verifies serotonin is detected as serotonin oxidation (green) appears around 0.6 V and reduction (blue) around 0.0 V to -0.1 V. An initial red-light stimulation was applied

for 2 seconds to stimulate serotonin detection before the SSRI. Then fluoxetine was applied to the bath and stimulations repeated every 5 minutes. Figure 3 displays example repeated stimulations with the other SSRIs and high doses of escitalopram, paroxetine, and citalopram show changes around 5 minutes. Stimulated serotonin concentration increases 10 minutes after the drug. Serotonin reuptake also starts to increase at 10 minutes and is visualized as the elongated oxidation and reduction peaks on the color plot and a longer time to half max decay (t_{50}) on the traces. Although these changes start at 10 minutes, serotonin concentration and reuptake changes increase at 15 minutes. Here, we chose 15 minutes for all experiments to ensure that each drug had full effects.

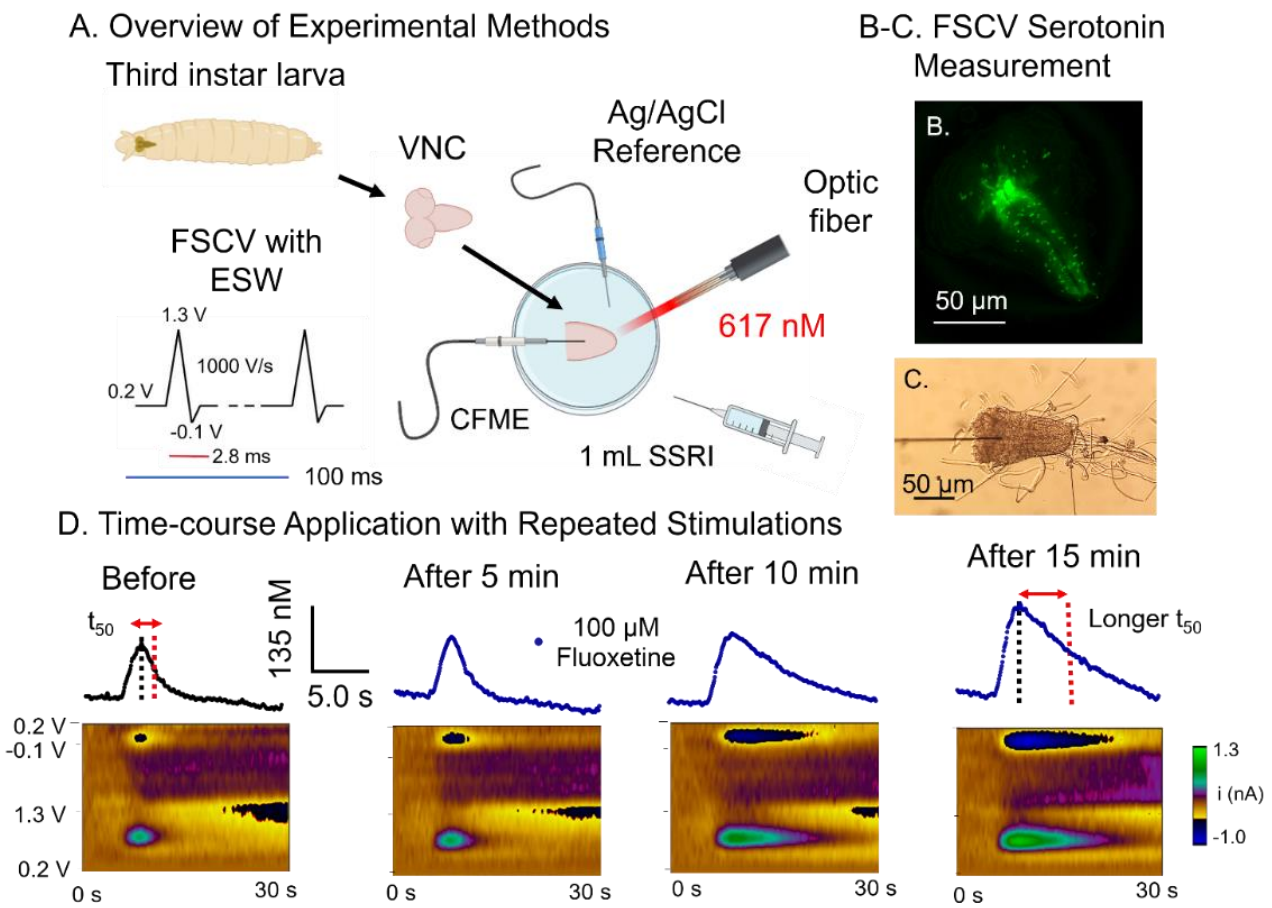

Figure 2. Serotonin measurements in *Drosophila* larval nerve cord after SSRIs. **A.** Experimental overview. From counterclockwise, a third instar larva ventral nerve cord (VNC) is dissected out and placed in a Petri dish. A carbon fiber microelectrode (CFME) is inserted and an optical fiber placed over the VNC. Fast-scan cyclic voltammetry (FSCV) with extended serotonin waveform (ESW) is applied to the CFME continuously to measure serotonin that is released after a 2-second red light (617 nm) stimulation that opens an optogenetic channel. Then, an SSRI is added to the bath. Cartoon was created in BioRender. **B.** Location of serotonin neurons in *Drosophila*. GFP expression of serotonin neuron clusters from a trh-Gal4/Cyo; UAS-mcD8-GFP fly. Serotonin neurons flank the midline of the VNC and the optic lobes. **C.** Microscope image shows optimal placement of the CFME into the midline of the VNC to detect the highest concentrations of serotonin near serotonin neurons. **D.** SSRI application with repeated stimulations. Example FSCV conc. versus *t* and color plots show serotonin detected before and after 100 µM fluoxetine (*n* = 6 larvae). Optogenetic stimulations are repeated every 5 minutes. Current detected is converted to serotonin concentration using a post-calibration factor, and reuptake is characterized by the time to half max decay (t_{50}) of the peak detected in the trace, which increases from before and after 15 minutes.

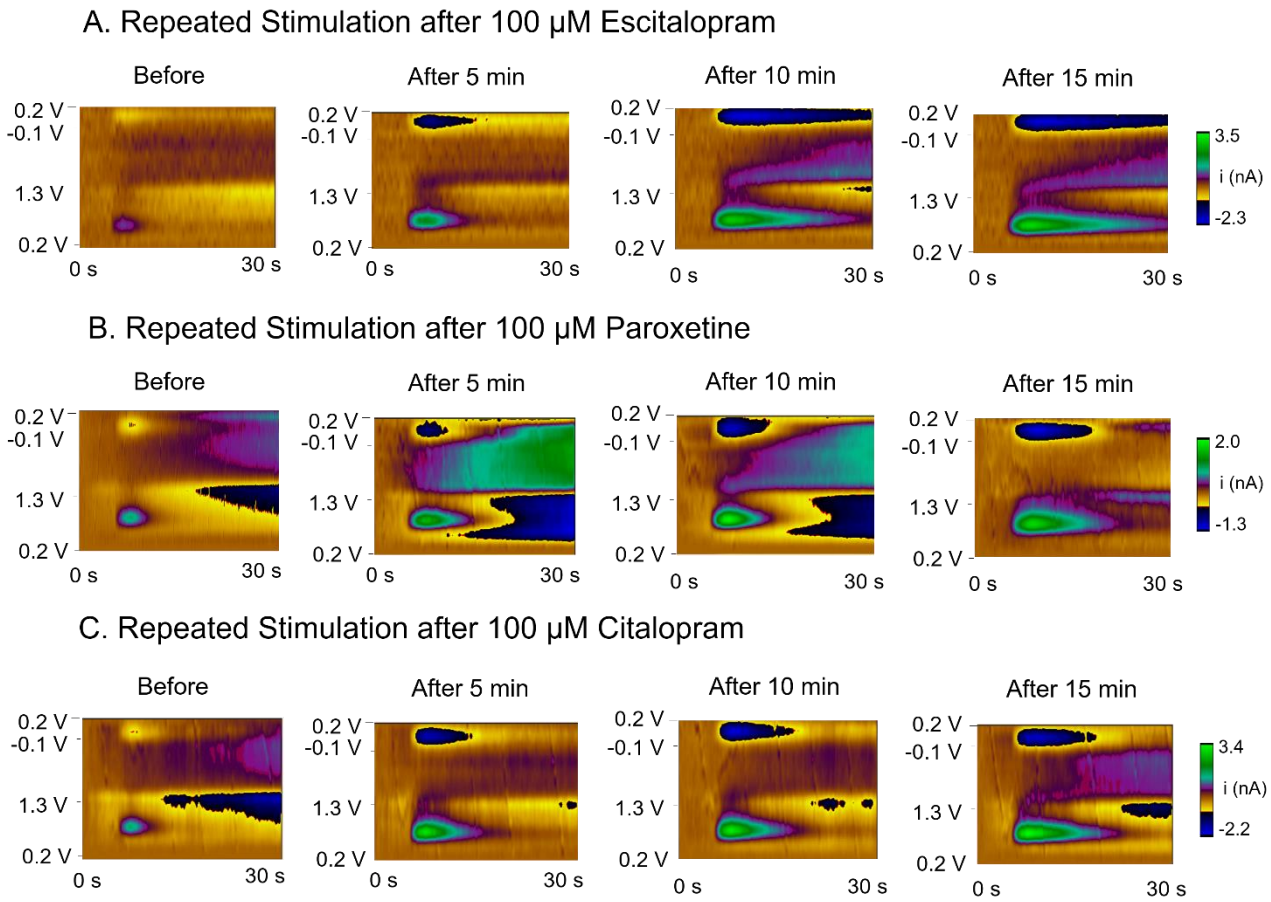

Figure 3. FSCV serotonin detection after repeated 5 minute stimulations with other SSRI antidepressants (*n* = 6 larvae). Figure 2D shows example FSCV color plots before and after 100 µM fluoxetine was applied with characteristic serotonin oxidation and reduction changes once a red-light, optogenetic stimulation is applied every 5 minutes. Fig. 3A, B, C also show example FSCV color plots before and after 100 µM escitalopram, paroxetine, and citalopram, respectively. Red-light stimulations were also applied every 5 minutes. Escitalopram, paroxetine, and citalopram start to show changes in serotonin concentration and reuptake after 5 minutes, but the largest changes in concentration and reuptake are noticeable after 15 minutes.

3.3.2 Escitalopram increases serotonin reuptake and concentration more than citalopram

Lexapro (escitalopram) and Celexa (citalopram) are commonly prescribed SSRI antidepressants to treat depression. Lexapro is the (*S*)-enantiomer of citalopram, while Celexa is a 50:50 racemic mixture of (*S*)- and (*R*)-citalopram.[15,37,38] Figure 4A-D shows serotonin concentration and reuptake changes with escitalopram. Figure 4A-B shows concentration versus *t* plots before (black) and after a low dose, 100 nM (A), and a high dose, 10 µM (B), of escitalopram. Serotonin concentration and reuptake increased, which is visualized with the longer traces and increase in current, even at a lower dose. There was a significant overall effect of escitalopram dose on serotonin concentration (Fig. 4C, One-Way ANOVA $F_{(4,43)} = 74.05$, $p < 0.0001$, $n = 6$). Tukey's post-hoc test revealed serotonin concentrations were significantly different from pre-drug for every dose ($p^{**} < 0.01$, $p^{***} < 0.001$, and $p^{****} < 0.0001$). Likewise, there was a significant overall effect of escitalopram dose on t_{50} (Fig. 4D, one-Way ANOVA $F_{(4,43)} = 189.4$, $p < 0.0001$) and

reuptake was different after each dose than pre-drug. Figure 5A displays example traces for 100 µM doses, and escitalopram approximately tripled with this dose.

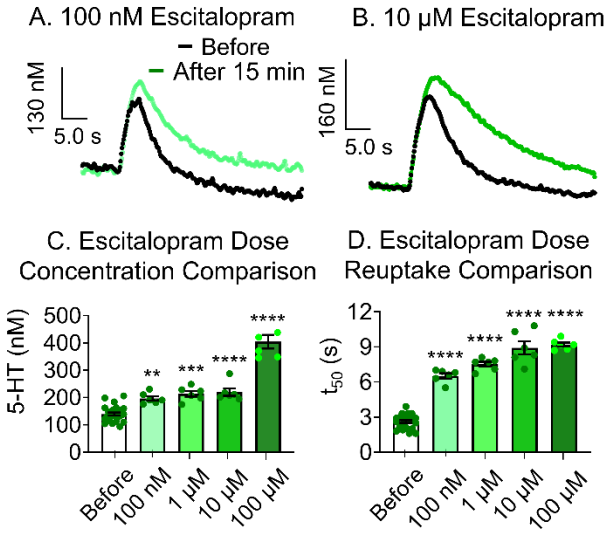

Figure 4. Effects of escitalopram. Traces before (black) and after (green) escitalopram (Lexapro, *n* = 6 larvae). **A-B**. Example FSCV conc. versus *t* traces before and after (A) 100 nM and (B) 10 µM escitalopram. **C.** Concentration changes by dose. One-Way ANOVA with Tukey's post-hoc comparisons show each dose is significantly different than pre-drug (before) ($p^{**} < 0.01$, $p^{***} < 0.001$, and $p^{****} < 0.0001$). **D.** Serotonin reuptake (t_{50}) changes. Reuptake significantly increased with all doses (One-way ANOVA, Tukey's post-test, $p^{****} < 0.0001$).

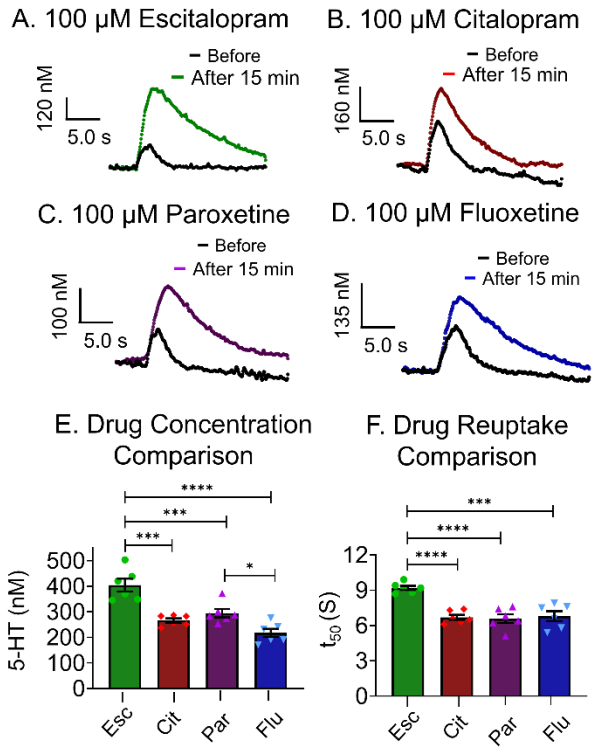

Figure 5. SSRI comparisons at 100 µM (*n* = 6 larvae). Serotonin concentration and reuptake are characterized by conc. versus *t* plots before (black) and after 100 µM escitalopram (A, green), citalopram (B, red), paroxetine (C, purple), and fluoxetine (D, blue) were applied for 15 minutes with methods previously described. Each SSRI increased serotonin concentrations and slowed reuptake. High-doses of fluoxetine, paroxetine, and citalopram were similar in release and reuptake. However, serotonin concentrations were higher with escitalopram and reuptake was longer than the other SSRIs. There were signficant effects with the 100 □M dose of each drug on serotonin concentration (Fig 5E, One-Way ANOVA, $F_{(3,20)} = 20.26$, $p \leq 0.0001$, $n = 6$). Serotonin concentrations were significantly higher with paroxetine and escitalopram, and Tukey's post-hoc test determined both were different to fluoxetine ($p \leq 0.0256$ and $p \leq 0.0001$, respectively). There was also a significant effect of the 100 □M dose of each drug with serotonin reuptake (Fig 5F, One-Way ANOVA, $F_{(3,20)} = 16.00$, $p \leq 0.0001$, $n = 6$). Serotonin uptake was significantly different with escitalopram compared to the other drugs (Tukey's post-hoc, all $p \leq 0.0001$). However, there were no differences between paroxetine, fluoxetine, and citalopram (all $p \geq 0.9609$).

Figure 6A-E displays serotonin concentration and reuptake changes with citalopram. Citalopram did not increase serotonin concentrations or reuptake at 100 nM (Fig. 6A), but did increase concentration and reuptake at 10 µM (Fig. 6B). There was a significant overall effect of citalopram dose on serotonin concentration (Fig. 6C, One-Way ANOVA, $F_{(4,43)} = 68.14$, $p < 0.0001$, $n = 6$). Tukey's post-hoc showed serotonin concentrations were not significantly different after 100 nM ($p = 0.9965$) or 1 µM ($p = 0.5098$), but concentrations increased at 10 and 100 µM (both $p < 0.0001$). Additionally, there was a significant overall effect of citalopram dose on serotonin reuptake (Fig. 6D, One-Way ANOVA $F_{(4,43)} = 114.3$, $p < 0.0001$), and Tukey's post-hoc revealed reuptake after 100 nM citalopram was not different than before the drug ($p = 0.8687$), but reuptake was increased significantly with 1, 10, and 100 µM doses ($p < 0.0001$).

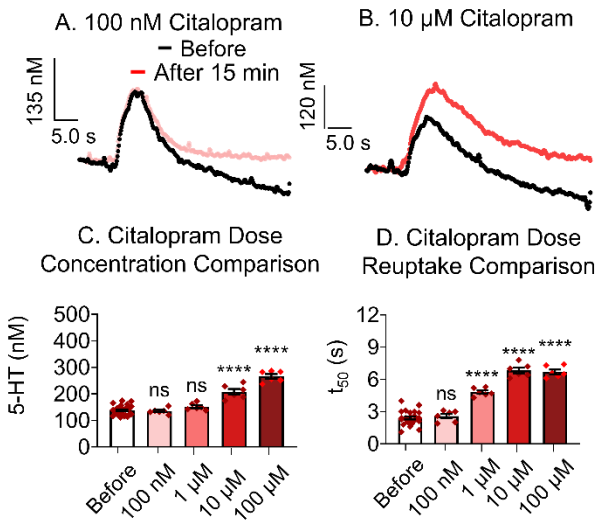

Figure 6. Effects of citalopram. Traces are before (black) and after (red) citalopram (Celexa, *n* = 6 larvae). **A-B**. Plots show serotonin current and t_{50} changes before and after (A) 100 nM and (B) 10 µM. **C.** Bar graph shows serotonin concentration by dose. Serotonin only significantly increased with 10 and 100 µM citalopram (One-Way ANOVA, Tukey's post-hoc, *p***** ≤ 0.0001). **D.** Changes in serotonin reuptake (t_{50}). Reuptake was not affected at the lowest dose, 100 nM (One-way ANOVA, Tukey's post-test, $p < 0.8687$), but was significantly greater at the larger doses, (*p***** < 0.0001).

3.3.3 Paroxetine elicits high serotonin concentration changes, but less change in reuptake

Figure 7A-D shows serotonin concentration and reuptake changes with paroxetine. Paroxetine increased serotonin concentrations at 100 nM and even more at 10 µM. However, serotonin reuptake was fast, with shorter t_{50} values than the other SSRIs. There was a significant overall effect of paroxetine dose on serotonin concentration (Fig. 7C, One-Way ANOVA $F_{(4,43)} = 47.85$, $p < 0.0001$, $n = 6$), and Tukey's post-hoc determined serotonin concentrations were significantly different than pre-drug after all doses (100 nM $p < 0.001$, all other doses $p < 0.0001$). There was also a significant overall effect of paroxetine dose on serotonin reuptake (Fig. 7D, One-Way ANOVA $F_{(4,43)} = 68.51$, $p < 0.0001$), and Tukey's post-hoc test determined reuptake was significantly different with each dose (all $p < 0.0001$).

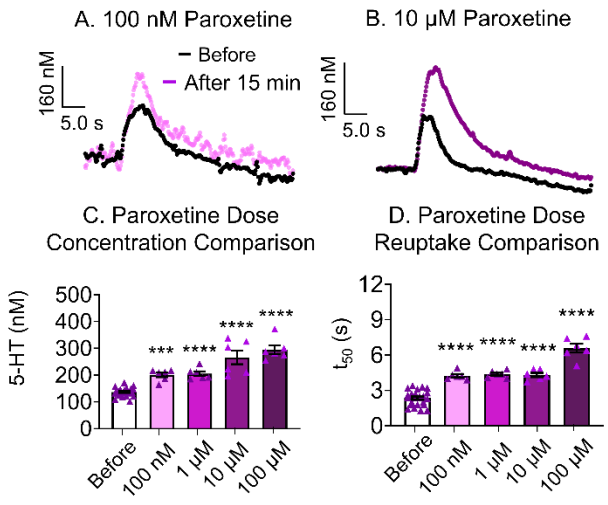

Figure 7. Effects of paroxetine. Traces are before (black) and after (purple) paroxetine (Paxil, *n* = 6 larvae). **A-B**. Example FSCV conc. versus *t* plots before and after (A) 100 nM and (B) 10 µM paroxetine. **C.** Concentration changes by dose. One-Way ANOVA with Tukey's post-hoc comparisons show each dose is significantly different than pre-drug (before) (*p***** < 0.0001). **D.** Serotonin reuptake (t_{50}) changes. Reuptake significantly increased with all doses (One-way ANOVA, Tukey's post-test, *p***** < 0.0001). However, uptake was faster than with escitalopram or citalopram.

3.3.4 Fluoxetine slows serotonin reuptake, but does not affect serotonin concentration

Figure 8A-D displays serotonin concentration and reuptake changes with fluoxetine. Serotonin concentrations did not increase at 100 nM or 10 µM, but reuptake noticeably increased at 10 µM (Fig. 8A, B). Serotonin concentrations did not increase except with 100 µM (Fig. 8C), even though reuptake started to change at doses ≥ 1 µM (Fig. 8D). There was a significant overall effect of fluoxetine dose on serotonin concentration (Fig 8C, One-Way ANOVA $F_{(4,43)} = 19.38$, $p < 0.0001$, $n = 6$), and Tukey's post-hoc test showed concentration was different than pre-drug at 100 µM ($p < 0.0001$, other doses all $p \geq 0.9264$). For reuptake, there was a significant overall effect of fluoxetine dose on serotonin reuptake (Fig 8D, One-Way ANOVA $F_{(4,43)} = 41.67$, $p < 0.0001$). With Tukey's post-hoc test, serotonin reuptake was not significantly different with 100 nM ($p = 0.7102$), but was significant for the doses 1-100 µM (all $p < 0.0001$).

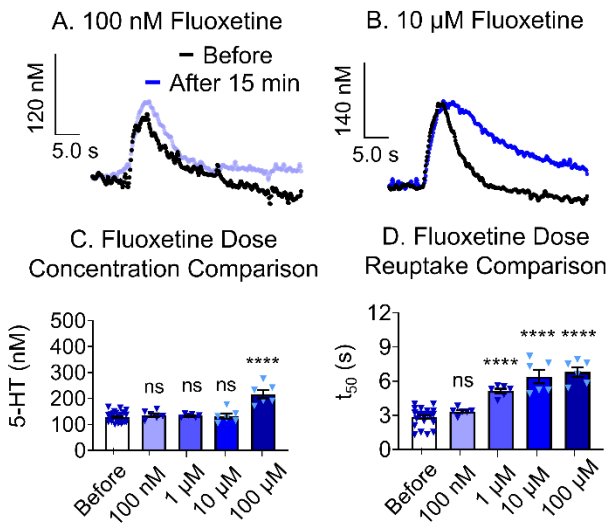

Figure 8. Effects of Fluoxetine. Traces are before (black) and after (blue) fluoxetine (Prozac, *n* = 6 larvae). **A-B**. Example FSCV conc. versus *t* traces before and after (A) 100 nM and (B) 10 µM fluoxetine. **C.** Concentration changes by dose. One-Way ANOVA with Tukey's post-hoc comparisons show concentration is not significantly different from 100 nM to 10 µM compared to pre-drug (before, all $p \geq 0.9264$). Only serotonin concentrations with 100 µM were different ($p^{****} < 0.0001$). **D.** Serotonin reuptake (t_{50}) changes. Reuptake was not significantly different with 100 nM fluoxetine (One-way ANOVA, Tukey's post-test, $p < 0.7102$). However, reuptake was significantly different from 1-100 µM ($p^{****} < 0.0001$).

3.3.5 SSRIs show differences in serotonin concentration, reuptake, and SERT affinity

To compare different SSRIs, we first chose a middle dose (1 □M) to understand serotonin concentration and reuptake changes (Figure 9A-F). Figure 7A-D shows concentration versus time traces before (black) and after 1 µM escitalopram (Fig. 9A, green), citalopram (Fig. 9B, red), paroxetine (Fig. 9C, purple), and fluoxetine (Fig. 9D, blue). Paroxetine and escitalopram were the only drugs that increased concentration at 1 □M, but escitalopram displayed slower reuptake, while reuptake with paroxetine was much faster. With citalopram and fluoxetine, concentrations did not increase, but both displayed longer reuptakes. However, both were faster than escitalopram. There were signficant effects with the 1 □M dose of each drug on serotonin concentration (Fig 9E, One-Way ANOVA, $F_{(3,40)} = 18.37$, $p < 0.0001$, $n = 6$). Serotonin concentrations were significantly higher with paroxetine and escitalopram, and Tukey's post-hoc test determined both were different to fluoxetine (both $p < 0.0001$). There was also a significant effect of the 1 □M dose of each drug with serotonin reuptake (Fig 9F, One-Way ANOVA, $F_{(3,40)} = 63.92$, $p < 0.0001$, $n = 6$). Serotonin reuptake was significantly different with escitalopram compared to the other drugs (Tukey's post-hoc, all $p < 0.0001$). However, there were no differences between paroxetine, fluoxetine, and citalopram (all $p \geq 0.4572$).

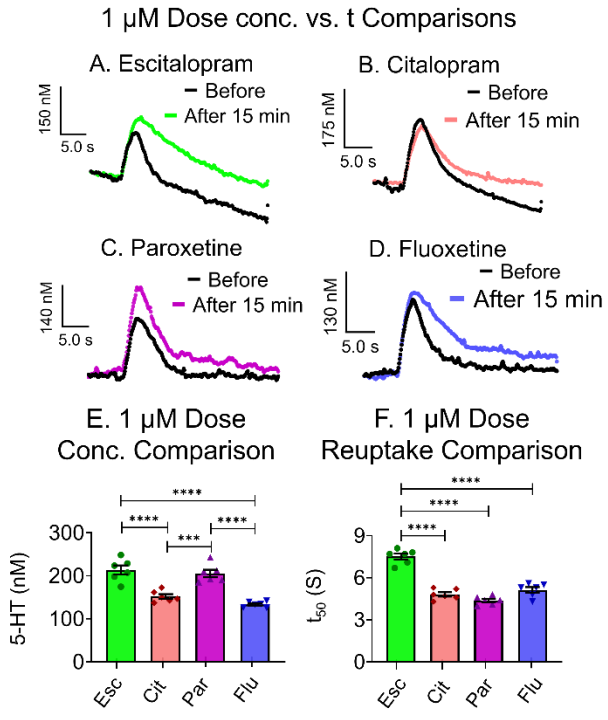

Figure 9. Comparison of SSRIs at 1 µM (*n* = 6 larvae). **A-D.** Conc. versus *t* plots show serotonin concentration and reuptake changes before (black) and after 1 µM escitalopram (A, green), citalopram (B, red), paroxetine (C, purple), and fluoxetine (D, blue) **E.** Serotonin concentration comparisons (One-Way ANOVA, Tukey's post-hoc, *p**** < 0.001, *p***** < 0.0001). **F.** Reuptake differences (t_{50}) by drug type (One-way ANOVA, Tukey's post-test, *p***** < 0.0001). Data were normally-distributed (all KS distance ≥ 0.1719, Kolmogrorov-Smirnov, p > 0.1000).

Figure 10A shows dose response curves for each drug, which plots the peak concentration versus dose. All drugs were tested at 100 nM, 1 µM, 10 µM, 50 µM, 100 µM, and 1 mM, and additional doses were added as needed to define the curves (Fig. 11-14, *n* = at least 4 larvae). The SSRIs were very different in their slopes and EC_{50} values, which describe their affinity to dSERT.[39] Table 1 summarizes serotonin release with EC_{50} values for each SSRI. Fluoxetine (blue) showed the highest EC_{50} of 87 µM and steepest slope since concentrations did not increase below 100 µM, which suggests that it does not have a high affinity for dSERT. Escitalopram (green) had the largest changes in serotonin release from 75 to 100 µM, but showed a more gradual change with a lower EC_{50} of 28 µM. Citalopram (red) had an EC_{50} of 17 µM, and shows the most gradual slope, which implies serotonin release is proportional to dose applied. It's EC_{50} is similar to escitalopram. The curve for paroxetine curve (purple) showed the lowest EC_{50} at 6.6 µM and gradually changed from 1 to 10 µM. Comparison of fits determined that EC_{50} values were different for each drug (Fig. 10A, $F_{(6,104)} = 17.97$, $p < 0.0001$). Paroxetine exhibited the highest affinity to dSERT, which has also been described in other studies.[14,40] Although these responses are useful, they only describe normalized changes in concentration and not reuptake.

Table 1. Summary of drug dose response curve data with initial reuptake and concentration changes

SSRI	Release EC_{50} (µM)	Reuptake EC_{50} (µM)	Max. t_{50} (s)*
Escitalopram	28	54	11.2 ± 0.6
Citalopram	17	36	8.6 ± 0.2
Paroxetine	6.6	44	7.9 ± 0.3
Fluoxetine	87	2.7	7.8 ± 0.4

* t_{50} at 1 mM, the maximum dosage tested

In Figure 10B, we plotted dose response curves with t_{50} on the y-axis and log concentration on the x-axis. The average pre-drug t_{50} is shown as the dashed, black line. Table 1 also summarizes the normalized EC_{50} reuptake change and maximum concentration t_{50} for each SSRI. Escitalopram (green) showed large increases even at lower doses, while fluoxetine (blue) and citalopram (red) showed gradual increases at 1 µM. Paroxetine (purple) displayed faster reuptake from 1-10 µM, but slowed at 50-100 µM. Each SSRI exhibited longer reuptake at extremely high doses (100 µM and 1 mM), except fluoxetine, which experienced the greatest change in reuptake from 100 nM-10 µM and shows a lower EC_{50} value. There were signficant overall effects of the type of drug (Two-Way ANOVA, $F_{(3,72)} = 149.1$, $p < 0.0001$) and dose applied ($F_{(5,72)} = 90.48$, $p < 0.0001$) on serotonin reuptake with significant interaction between the groups ($F_{(15,72)} = 5.2999$, $p < 0.0001$). Tukey's post-hoc test showed reuptake with escitalopram was significantly longer compared to the other SSRIs at all doses tested (all $p < 0.0001$). Interestingly at 10 µM, paroxetine displayed faster reuptake that was significantly different from fluoxetine ($p \leq 0.01$) and citalopram ($p \leq 0.001$). However, at doses ≥ 50 µM there were no differences in reuptake for fluoxetine, citalopram, or paroxetine (all $p \geq 0.6143$).

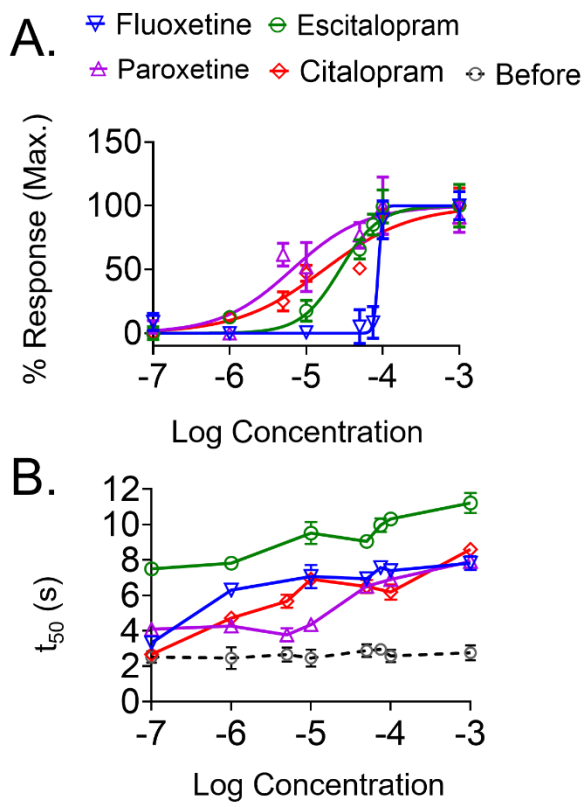

Figure 10. Dose response curves for serotonin concentration and reuptake changes. **A.** Concentration curve. Normalized drug response curves show serotonin concentration changes after a drug is applied for 15 minutes. Fluoxetine (blue), escitalopram (green), paroxetine (purple), and citalopram (red, *n* = at least 4 larvae). EC_{50} values for each drug were different (Comparison of Fits, $F_{(6,104)} = 17.97$, $p < 0.0001$). Paroxetine's EC_{50} value was the lowest and fluoxetine the highest. Paroxetine displayed the highest affinity for dSERT, followed by escitalopram and citalopram with similar affinity, and fluoxetine the lowest. **B**. Uptake curve. Serotonin t_{50} values before (black dotted line) and after each concentration. Escitalopram showed large changes in reuptake, even at lower doses, while fluoxetine and citalopram start to increase t_{50} at doses ≥ 1 μM. Paroxetine t_{50} only increases with higher doses ≥ 50 μM. Data were normally-distributed for multiple drug comparisons (all KS distance ≥ 0.1719, Kolmogrorov-Smirnov, p > 0.1000).

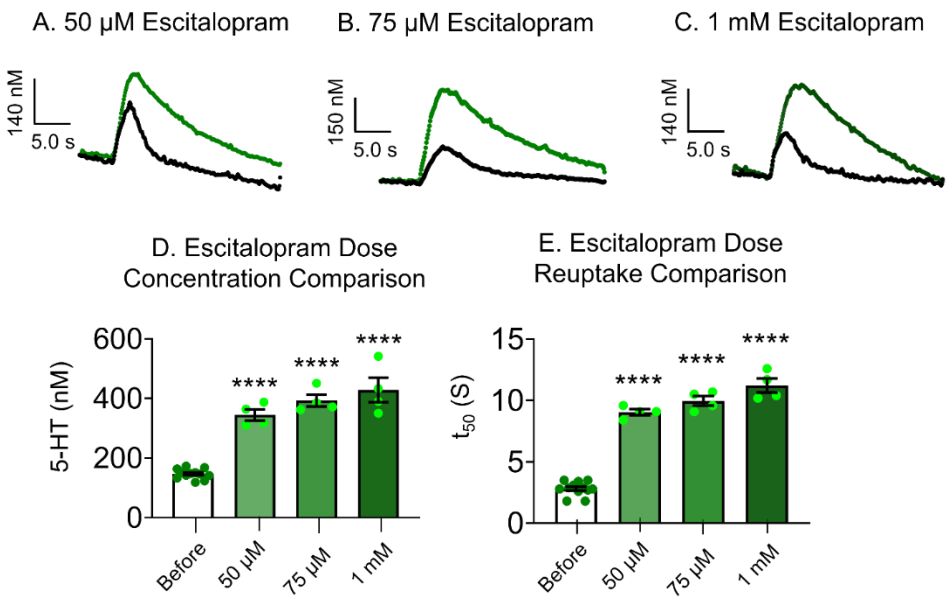

Figure 11. Serotonin release and reuptake effects for additional escitalopram doses tested (Lexapro, at least *n* = 4 larvae). Serotonin concentration and reuptake are characterized by conc. versus *t* plots before (black) and after 50 µM (A), 75 µM (B), and 1 mM escitalopram (C). There was a significant overall effect of escitalopram dose on serotonin concentration (Fig. 11D, One-Way ANOVA, $F_{(3,20)} = 75.58$, $p \leq 0.0001$, $n = 6$), and Tukey's post-hoc determined serotonin concentrations were significantly different with all doses (all $p \leq 0.0001$). For serotonin reuptake, there was a significant overall effect of escitalopram dose on serotonin reuptake (Fig. 11E, One-Way ANOVA $F_{(3,20)} = 222.4$, $p \leq 0.0001$). Tukey's post-hoc revealed reuptake increased significantly each dose (all $p \leq 0.0001$).

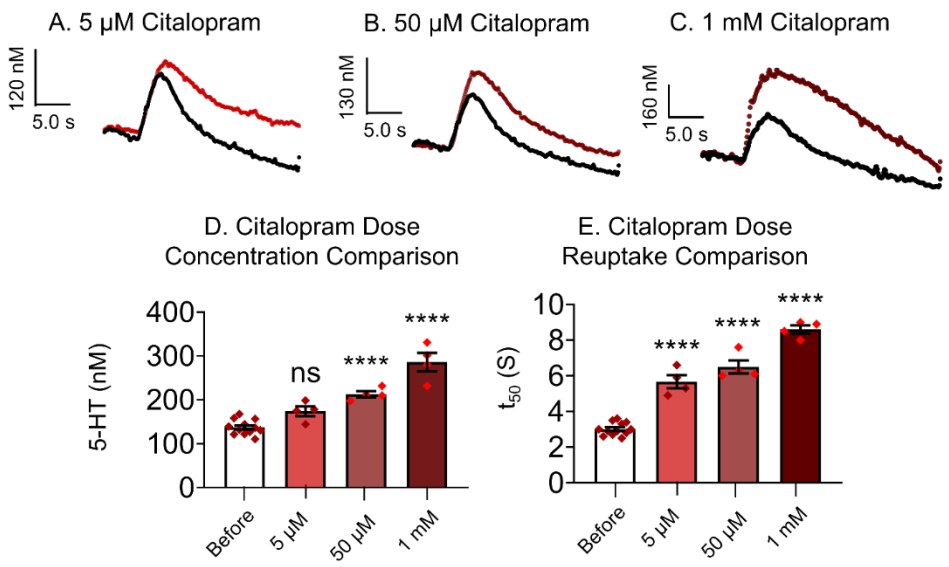

Figure 12. Serotonin release and reuptake effects for additional citalopram doses tested (Celexa, *n* = at least 4 larvae). Serotonin concentration and reuptake are characterized by conc. versus *t* plots before (black) and after 5 µM (A), 50 µM (B), and 1 mM citalopram (C). Serotonin concentrations start to increase at 5 µM, but gradually increase more at 50 µM and 1 mM citalopram. With serotonin reuptake, each dose gradually slowed reuptake, but 1 mM showed the greatest change. There was a significant overall effect of citalopram dose on serotonin concentration (Fig. 12D, One-Way ANOVA, $F_{(3,20)} = 45.57$, $p \leq 0.0001$, $n = 6$), and Tukey's post-hoc determined serotonin concentrations were significantly different with 50 µM and 1 mM (both $p \leq 0.0001$). Although serotonin concentration increased at 5 µM, it was not significantly different compared to pre-drug ($p = 0.0505$). For serotonin reuptake, there was a significant overall effect of citalopram dose on serotonin reuptake (Fig. 12E, One-Way ANOVA $F_{(3,20)} = 137.0$, $p \leq 0.0001$). Tukey's post-hoc revealed reuptake increased significantly each dose (all $p \leq 0.0001$).

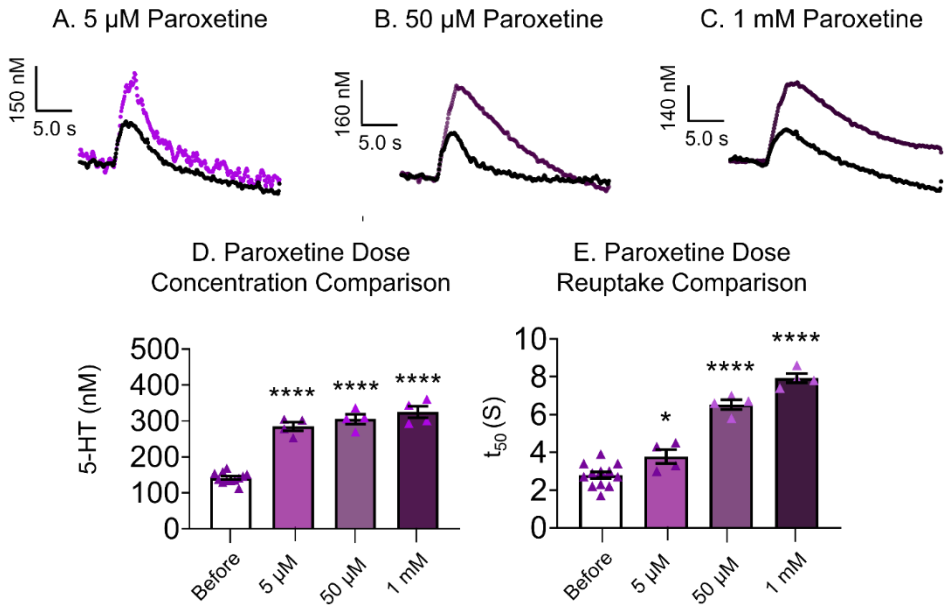

Figure 13. Serotonin release and reuptake effects for additional paroxetine doses tested (Paxil, *n* = at least 4 larvae). Serotonin concentration and reuptake are characterized by conc. versus *t* plots before (black) and after 5 µM (A), 50 µM (B), and 1 mM paroxetine (C). Serotonin concentrations increased with each dose and were similar. However, serotonin reuptake was similar to pre-drug for 5 µM paroxetine. Reuptake noticeably increased at 50 µM and 1 mM. There was a significant overall effect of paroxetine dose on serotonin concentration (Fig. 13D, One-Way ANOVA $F_{(3,20)} = 111.5$, $p \leq 0.0001$, $n = 6$), and Tukey's post-hoc determined serotonin concentrations were significantly different than pre-drug at each doses (all $p \leq 0.0001$). For serotonin reuptake, there was a significant overall effect of paroxetine dose on serotonin reuptake (Fig. 13E, One-Way ANOVA $F_{(3,20)} = 90.95$, $p \leq 0.0001$), and Tukey's post-hoc test determined reuptake was significantly different with each dose (5 µM = 0.0471, 50 µM and 1 mM $p \leq 0.0001$).

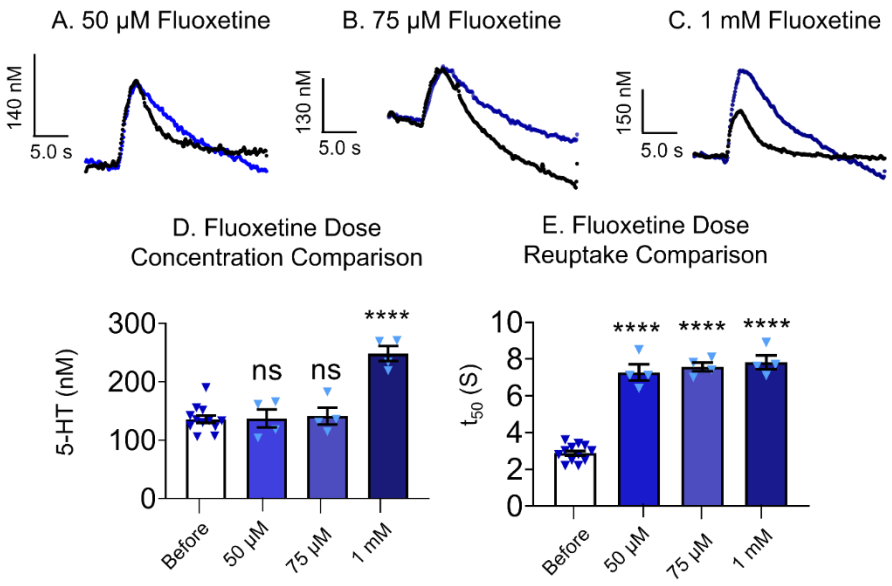

Figure 14. Serotonin release and reuptake effects for additional fluoxetine doses tested (Prozac, *n* = at least 4 larvae). Serotonin concentration and reuptake are characterized by *conc.* versus *t* plots before (black) and after 50 µM (A), 75 µM (B), and 1 mM fluoxetine (C). Serotonin concentrations did not increase, except with 1 mM fluoxetine. However, serotonin reuptake was longer and similar with each dose. There was a significant overall effect of fluoxetine dose on serotonin concentration (Fig 14D, One-Way ANOVA $F_{(3,20)} = 20.92$, $p \leq 0.0001$, $n = 6$), and Tukey's post-hoc determined concentration was different than pre-drug at 1 mM ($p \leq 0.0001$, other doses all $p \geq 0.9858$). For reuptake, there was a significant overall effect of fluoxetine dose on serotonin reuptake (Fig 14E, One-Way ANOVA $F_{(3,20)} = 124.4$, $p \leq 0.0001$). With Tukey's post-hoc test, serotonin reuptake was significant for each dose (all $p \leq 0.0001$).

3.4 Discussion

Our results show that SSRIs in *Drosophila* larvae differentially regulate reuptake and release. For example, paroxetine increases serotonin concentrations at the lowest doses, which implies high affinity, but does not slow reuptake at those doses. In comparison, escitalopram increases serotonin concentration and reuptake at low doses, while citalopram and fluoxetine only affect reuptake at low doses. Escitalopram is only the *S*-enantiomer of citalopram and has more effects than citalopram, a 50:50 racemic mixture, which implies the *S*-enantiomer is more active. Altogether, our data show SSRIs have different mechanisms of action to modulate both release and reuptake.

3.4.1 SSRIs differ in their effects on serotonin reuptake

Each SSRI affected serotonin reuptake, but their affinities differed. At lower doses (≤ 10 µM), escitalopram (Lexapro) elicited longer serotonin reuptake compared to the other SSRIs. Meanwhile, paroxetine (Paxil) showed much faster reuptake that was similar

to pre-drug reuptake. Interestingly, citalopram (Celexa) and fluoxetine (Prozac) slowed reuptake more than paroxetine, but did not affect serotonin concentration. However, at higher doses (≥ 50 μM), escitalopram still showed the longest reuptake, but there were no differences between paroxetine, citalopram and fluoxetine. Previously, both slow and fast reuptake modes have been identified due to different binding sites on SERT, intracellular signaling cascades, and different kinetic models of uptake for these SSRIs.[26,28,41]

Historically, dSERT and dDAT (dopamine transporter) were used in substrate binding or molecular modeling and docking simulation studies to understand the binding affinities of SSRIs and other psychoactive drugs until the structure of hSERT was determined with x-ray crystallography in 2016.[11,17–19,42] Previous studies from the Barker and Blakely labs found that dSERT and human SERT (hSERT) show 51% sequence identity and similar structures with active sites.[18,19,40,43,44] They also explored hSERT/dSERT chimeras where they used site-specific mutagenesis to understand genetic differences to citalopram.[18] Although dSERT shows lower affinity for many drugs compared to hSERT, they show equivalent translocation kinetics with Km binding affinities of 490 nM for serotonin for both hSERT and dSERT.[19] Thus, dSERT is a good model for understanding possible SSRI effects that are similar to humans.

dSERT also possesses two binding sites, a primary binding site (S1) located in the center of its transmembrane domain that binds SSRIs with high affinity, and another binding site in the extracellular vestibule (S2), that binds with low affinity, similar to hSERT.[40,45] In several studies, escitalopram binds to the primary S1 site with high affinity and also the S2 site with an allosteric mechanism.[41,45] Escitalopram elicits longer t_{50} profiles compared to the other SSRIs because of complete inhibition of serotonin reuptake with its dual activity at the primary and allosteric binding sites, even at lower doses (100 nM). Meanwhile, *R*-citalopram (Celexa) causes reuptake changes at higher doses (≥ 1 μM), because *R*-citalopram does not bind to the S2 allosteric site with the same affinity. Fluoxetine also does not bind to this S2 allosteric site, and only increases serotonin reuptake at does ≥ 1 μM. Thus, binding at the different allosteric sites affects reuptake, and different SSRIs blocked reuptake with different affinities.

Paroxetine differs from the other SSRIs in that it shows very fast reuptake, except with high doses. Paroxetine binds to the SERT primary and allosteric sites,[41] but it could affect different down-stream signaling cascades that result in faster serotonin reuptake. Zhong et al. discovered several SERT interacting proteins (SIPs) that directly interact with SERT and regulate specific downstream, intracellular signaling cascades that impact SERT's uptake function and density on the cell surface.[41] One SIP that increases SERT's uptake is neuronal nitric oxide synthase (nNOS),[41] which is widely expressed in the brain. Nitric oxide (NO) acts as a chemical messenger in the presynaptic serotonin neuron and increased NO causes faster reuptake by SERT. Likewise, another SIP, protein

interacting with C kinase 1 (PICK1), also increases SERT's uptake function.[41] It is possible that when paroxetine binds to dSERT with high affinity, it induces downstream effects with nNOS or PICK1 as they interact with dSERT.

Other studies have also focused on different reuptake mechanisms for SSRIs in mammals. Historically, Shaskan and Snyder were the first to suggest two reuptake mechanisms, slow and fast, that were affected by antidepressants.[26] They coined these mechanisms "Uptake 1," which is high affinity and low efficiency uptake and "Uptake 2," which is low affinity and high efficiency uptake. The Daws group further investigated reuptake in mammals and found with pharmacology experiments that Uptake 1 primarily relied on SERT, while Uptake 2 relied on other neurotransmitter transporters like the dopamine transporter (DAT) and norepinephrine transporter (NET).The Hashemi group elaborated on this research using FSCV and serotonin kinetic models in mice and proposed hybrid clearance of serotonin with SSRIs, like escitalopram, that show initial fast uptake that then slows.[26] Our data for escitalopram in *Drosophila* does not show a hybrid uptake mechanism and relies more on the slow, Uptake 1 mechanism. Interestingly, in several previous studies in Hashemi lab, they looked at serotonin reuptake dynamics for citalopram,[29] escitalopram,[28] and fluoxetine,[46] and our t_{50} values in *Drosophila* are very similar to their *in vivo* data in mice, which is shown in Table 2. They also saw similar trends where fluoxetine requires higher doses to elicit concentration changes compared to citalopram and escitalopram.[28,29,46] Thus, reuptake and turnover kinetics are equivalent and concentration changes are similar, which indicates that *Drosophila* can be used in pharmacological assays to understand reuptake and concentration changes with genetic mutants that are easier to create with this model. Still, these Uptake 1 and Uptake 2 mechanisms have not been investigated yet in *Drosophila*, and future studies should model serotonin reuptake changes with different antidepressants, like atypical antidepressants, that affect dSERT and dDAT.

Table 2. Summary of reuptake (t_{50}) comparisons for dSERT and mSERT/rSERT for SSRIs

	dSERT		**mSERT or rSERT**	
Drug	**t_{50} (s)**	**Dose**	**t_{50} (s)**	**Dose**
Escitalopram	7.5 ± 0.2	1 µM	7.1 ± 1.1[28]	10 mg/kg
Citalopram	6.8 ± 0.3	10 µM	7.4 ± 1.5[29]	10 mg/kg
Fluoxetine	5.1 ± 0.2	1 µM	4.0 ± 0.7[46]	20 mg/kg

t_{50} is the time it takes to clear serotonin to 50% of its peak level.

3.4.2 Serotonin concentration changes are coupled with reuptake for some SSRIs, but independent for others

SSRIs also affected serotonin concentrations, but the increase in reuptake was sometimes decoupled from changes in concentration. When reuptake is blocked, the concentration often increases because slow reuptake allows serotonin to build up in the extracellular space. Escitalopram and paroxetine increased serotonin concentrations at all doses, including the lowest concentration tested, 100 nM. However, interestingly, paroxetine does not affect reuptake at those low doses while escitalopram slowed reuptake dramatically. Thus, increases in concentration were not simply due to changes in reuptake allowing serotonin to accumulate. Meanwhile, citalopram increased serotonin at doses ≥ 5 μM (Fig. S4A), and fluoxetine increased serotonin only at doses ≥ 100 μM (Fig. S6C). We saw obvious trends with dSERT affinity, where paroxetine and escitalopram increased serotonin concentrations at low doses, which may be related to them binding to dSERT at its primary and allosteric sites with high affinity. Likewise, citalopram and fluoxetine show lower affinity to dSERT and do not change concentrations until higher doses are applied.

3.4.3 Comparison of SSRIs

Celexa (citalopram) was first marketed in 1998, but the (*S*)-enantiomer was more effective than the (*R*)-enantiomer, so Lexapro (escitalopram) was introduced in 2002.[37,38] Citalopram, is a 50:50 racemic mixture of the (*R*)- and (*S*)-enantiomer of citalopram, while Lexapro is exclusively produced as the (*S*)-enantiomer.[38] With escitalopram, serotonin concentrations increased with low doses, but reuptake was also significantly longer than the other SSRIs at all doses (Fig. 3 A-D and 8A-B). It is possible that escitalopram reuptake is so slow that it causes serotonin to accumulate outside of the cell, which increases serotonin concentrations detected with FSCV. Unlike escitalopram, citalopram displayed faster reuptake and did not increase serotonin concentrations at doses ≤ 5 μM. Our data indicate that there are stereochemistry effects with these enantiomers and that the (*S)*-enantiomer causes larger changes in both reuptake and concentration, especially at lower doses.

Paxil (paroxetine) was first marketed in North America in the early 1990s. However, since the early 2000s, it has been more closely regulated because of severe side effects and birth defects reported in pregnant women.[47] Paroxetine does not slow reuptake as much as other SSRIs, but serotonin concentrations increase at lower doses because of its high dSERT affinity. Zhong et al., suggested that SNARE complex proteins, like secretory carrier-associated membrane protein 2 (SCAMP2) and syntaxin-1A, interact directly with SERT as SIPs.[41] SCAMP2 aids in vesicle transport to the cell membrane with endocytosis and exocytosis, while syntaxin-1A is a membrane protein that works with SNAP-25, synaptobrevin, and others to dock and fuse vesicles and open pores for

exocytosis.[41] Thus, paroxetine may increase serotonin release through proteins such as SCAMP2 or syntaxin-1A when it binds to dSERT, even though it does not slow reuptake.

Historically, Prozac (fluoxetine) was the first SSRI antidepressant to undergo clinical trials in the 1980s, and was marketed to replace monoamine oxidase inhibitors (MAOIs) and tricyclic antidepressants (TCAs).[37,38] Initially, fluoxetine had less severe side effects compared to MAOIs and TCAs. However, it produces extremely variable efficacies.[9,48,49] Serotonin concentrations did not increase at doses ≤ 100 µM in *Drosophila,* which implies a dose dependency. Fluoxetine displayed the lowest affinity for dSERT, but increased serotonin reuptake at doses ≥ 1 µM (Fig. 6B, 6D, and 8A-B). Our data imply that fluoxetine binds to dSERT and slows reuptake, but does not cause accumulation of serotonin in the extracellular space that increases concentration, which is different than other SSRIs. Thus, fluoxetine may use a desensitization mechanism that primarily changes serotonin reuptake more than concentration, which has been suggested in the past.[48,50] Previously, the Campusano group characterized biogenic amine (serotonin, dopamine, and octopamine) concentration and reuptake changes with fluoxetine in a new dSERT mutant.[8] They found that concentrations only increased at 50 and 100 µM fluoxetine and reuptake (t_{50}) was slower, almost doubling in time, which is similar to our data from 1 µM-1 mM fluoxetine.[8]

3.4.4 Future applications in Drosophila to understand genetic effects on SSRI efficacy

Although *Drosophila* possesses exquisite genetic and behavioral toolboxes to understand depression, the lack of real-time measurements of serotonin and other neurotransmitters limit pharmacology applications to understand differences with antidepressants without genetic manipulations. *Drosophila* show many depressive behaviors with changes in appetite, locomotion, and motivation,[6–8] which are affected by serotonin. Further, when fluoxetine is administered to flies with mutated dSERT or serotonin receptors, it changes these behaviors.[7,8] *Drosophila* is a key model to study behavioral changes with depression and antidepressants, and FSCV and optogenetics will enable a better understanding of real-time serotonin concentration and reuptake changes. Our data imply that SSRIs differentially modulate serotonin reuptake and concentration. All the SSRIs affected serotonin reuptake, but some impacted serotonin concentration and release. Future studies need to consider not just serotonin reuptake, but also how serotonin is accumulated or released with each antidepressant. Also, our data imply that each SSRI regulates unique downstream signaling cascades that affect SERT. Several studies indicate SIPs change the density of SERT on the cell surface or its uptake function.[41] These cascades also influence calcium signaling, which directly impacts serotonin release with exocytosis.[25,51,52] *Drosophila* is a prime model to study changes in calcium signaling because of the wide array of genetic tools available to target genetically-encoded sensors.[1,2,20,53] Several novel dSERT mutants with point mutations recently became publicly available, which can be utilized to understand serotonin changes

with FSCV.[8,54,55] New dSERT mutants can also be made to characterize how changes in dSERT structure impact SSRI antidepressant responses. Mutants that alter SNARE complex proteins or other SIPs could also be explored to better understand these mechanisms of action. Additionally, hSERT/dSERT chimeras could be created to investigate real-time serotonin changes with pharmacology or to make better dSERT mutants more similar to hSERT.[18,19,44] Since some antidepressants also affect dDAT and the glutamatergic system, those systems could also be studied.[1,33,44,48,56–58] Thus, this work facilitates depression research in *Drosophila* by establishing the different effects of SSRIs in WT flies. Ultimately, these techniques can be applied to new antidepressant drugs to understand how specific dSERT mutations impact real-time serotonin release and reuptake, and correlate those changes with efficacies in mitigating depression behaviors.

3.5 Conclusions

Overall, this work describes fundamental comparisons of several common SSRI antidepressants in *Drosophila* using FSCV. FSCV and *Drosophila* are useful to characterize real-time serotonin release and reuptake with antidepressants. Escitalopram and paroxetine were the only drugs that increased serotonin release with low doses (< 1 µM), but they showed different serotonin reuptake profiles as paroxetine did not affect reuptake while escitalopram greatly slowed reuptake. Citalopram did not have the same effect on release and reuptake as escitalopram, which is exclusively the *S*-enantiomer. Interestingly, fluoxetine did not increase serotonin release with doses ≤ 100 µM, but serotonin reuptake was significantly longer at doses ≥ 1 µM. Dose response concentration curves determined paroxetine showed the highest affinity to dSERT, while fluoxetine showed the lowest. Our data suggest that the effects of SSRI on serotonin release and reuptake are independent, and that different binding sites or different downstream protein activation causes variable effects on release and reuptake. Future studies could characterize new antidepressant drugs and dSERT mutations to understand how genetic changes impact real-time serotonin release and reuptake, which will facilitate a better understanding of each SSRI in their treatment of depression.

3.6 References

(1) Shin, M.; Copeland, J. M.; Venton, B. J. Drosophila as a Model System for Neurotransmitter Measurements. *ACS Chem. Neurosci.* **2018**, *9* (8), 1872–1883. https://doi.org/10.1021/acschemneuro.7b00456.

(2) Kasture, A. S.; Hummel, T.; Sucic, S.; Freissmuth, M. Big Lessons from Tiny Flies: Drosophila Melanogaster as a Model to Explore Dysfunction of Dopaminergic and Serotonergic Neurotransmitter Systems. *International Journal of Molecular Sciences*. MDPI AG June 2018. https://doi.org/10.3390/ijms19061788.

(3) Ries, A.-S.; Hermanns, T.; Poeck, B.; Strauss, R. Serotonin Modulates a Depression-like State in Drosophila Responsive to

Lithium Treatment. *Nat. Commun.* **2017**, *8*, 15738. https://doi.org/10.1038/ncomms15738.

(4) Narayanan, A. S.; Rothenfluh, A. I Believe I Can Fly!: Use of Drosophila as a Model Organism in Neuropsychopharmacology Research. *Neuropsychopharmacology* **2016**, *41* (6), 1439–1446. https://doi.org/10.1038/npp.2015.322.

(5) Lawal, H. O.; Terrell, A.; Lam, H. A.; Djapri, C.; Jang, J.; Hadi, R.; Roberts, L.; Shahi, V.; Chou, M. T.; Biedermann, T.; Huang, B.; Lawless, G. M.; Maidment, N. T.; Krantz, D. E. Drosophila Modifier Screens to Identify Novel Neuropsychiatric Drugs Including Aminergic Agents for the Possible Treatment of Parkinson's Disease and Depression. *Mol. Psychiatry* **2014**, *19* (2), 235–242. https://doi.org/10.1038/mp.2012.170.

(6) Yang, Z.; Bertolucci, F.; Wolf, R.; Heisenberg, M. Flies Cope with Uncontrollable Stress by Learned Helplessness. *Curr. Biol.* **2013**, *23* (9), 799–803. https://doi.org/10.1016/j.cub.2013.03.054.

(7) Majeed, Z. R.; Abdeljaber, E.; Soveland, R.; Cornwell, K.; Bankemper, A.; Koch, F.; Cooper, R. L. Modulatory Action by the Serotonergic System: Behavior and Neurophysiology in Drosophila Melanogaster. *Neural Plast.* **2016**, *2016*. https://doi.org/10.1155/2016/7291438.

(8) Hidalgo, S.; Molina-Mateo, D.; Escobedo, P.; Zárate, R. V; Fritz, E.; Fierro, A.; Perez, E. G.; Iturriaga-Vasquez, P.; Reyes-Parada, M.; Varas, R.; Fuenzalida-Uribe, N.; Campusano, J. M. Characterization of a Novel Drosophila SERT Mutant: Insights on the Contribution of the Serotonin Neural System to Behaviors. *ACS Chem. Neurosci.* **2017**, *8* (10), 2168–2179. https://doi.org/10.1021/acschemneuro.7b00089.

(9) Fakhoury, M. Revisiting the Serotonin Hypothesis: Implications for Major Depressive Disorders. *Mol. Neurobiol.* **2016**, *53* (5), 2778–2786. https://doi.org/10.1007/s12035-015-9152-z.

(10) Araujo, S. M.; Poetini, M. R.; Bortolotto, V. C.; de Freitas Couto, S.; Pinheiro, F. C.; Meichtry, L. B.; de Almeida, F. P.; Santos Musachio, E. A.; de Paula, M. T.; Prigol, M. Chronic Unpredictable Mild Stress-Induced Depressive-like Behavior and Dysregulation of Brain Levels of Biogenic Amines in Drosophila Melanogaster. *Behav. Brain Res.* **2018**, *351* (May), 104–113. https://doi.org/10.1016/j.bbr.2018.05.016.

(11) Zeppelin, T.; Ladefoged, L. K.; Sinning, S.; Schiøtt, B. Substrate and Inhibitor Binding to the Serotonin Transporter: Insights from Computational, Crystallographic, and Functional Studies. *Neuropharmacology* **2019**, *161* (February), 107548. https://doi.org/10.1016/j.neuropharm.2019.02.030.

(12) Schloss, P.; Williams, D. C. The Serotonin Transporter: A Primary Target for Antidepressant Drugs. *J. Psychopharmacol.* **1998**, *12* (2), 115–121. https://doi.org/10.1177/026988119801200201.

(13) Coleman, J. A.; Gouaux, E. Structural Basis for Recognition of Diverse Antidepressants by the Human Serotonin Transporter. *Nat. Struct. Mol. Biol.* **2018**, *25* (2), 170–175. https://doi.org/10.1038/s41594-018-0026-8.

(14) Coleman, J. A.; Navratna, V.; Antermite, D.; Yang, D.; Bull, J. A.; Gouaux, E. Chemical and Structural Investigation of the Paroxetine-Human Serotonin Transporter Complex. *Elife* **2020**, *9*, 1–38. https://doi.org/10.7554/eLife.56427.

(15) Rannversson, H.; Andersen, J.; Bang-Andersen, B.; Strømgaard, K. Mapping the Binding Site for Escitalopram and Paroxetine in the Human Serotonin Transporter Using Genetically Encoded Photo-Cross-Linkers. *ACS Chem. Biol.* **2017**, *12* (10), 2558–2562. https://doi.org/10.1021/acschembio.7b00338.

(16) Andersen, J.; Stuhr-Hansen, N.; Zachariassen, L. G.; Koldsø, H.; Schiøtt, B.; Strømgaard, K.; Kristensen, A. S. Molecular Basis for Selective Serotonin Reuptake Inhibition by the Antidepressant Agent Fluoxetine (Prozac). *Mol. Pharmacol.* **2014**, *85* (5), 703–714. https://doi.org/10.1124/mol.113.091249.

(17) Coleman, J. A.; Green, E. M.; Gouaux, E. X-Ray Structures and Mechanism of the Human Serotonin Transporter. *Nature* **2016**, *532* (7599), 334–339. https://doi.org/10.1038/nature17629.

(18) Barker, E. L.; Perlman, M. A.; Adkins, E. M.; Houlihan, W. J.; Pristupa, Z. B.; Niznik, H. B.; Blakely, R. D. High Affinity Recognition of Serotonin Transporter Antagonists Defined by Species-Scanning Mutagenesis. An Aromatic Residue in Transmembrane Domain I Dictates Species-Selective Recognition of Citalopram and Mazindol. *J. Biol. Chem.* **1998**, *273* (31), 19459–19468. https://doi.org/10.1074/jbc.273.31.19459.

(19) Barker, E. L.; Blakely, R. D. Structural Determinants of Neurotransmitter Transport Using Cross- Species Chimeras: Studies on Serotonin Transporter. *Methods Enzymol.* **1998**, *296* (1990), 475–498. https://doi.org/10.1016/S0076-6879(98)96035-9.

(20) Dunham, K. E.; Venton, B. J. Improving Serotonin Fast-Scan Cyclic Voltammetry Detection: New Waveforms to Reduce Electrode Fouling. *Analyst* **2020**, *145* (22), 7437–7446. https://doi.org/10.1039/D0AN01406K.

(21) Puthongkham, P.; Venton, B. J. Recent Advances in Fast-Scan Cyclic Voltammetry. *Analyst* **2020**, *145*, 1087–1102. https://doi.org/10.1039/C9AN01925A.

(22) Venton, B. J.; Cao, Q. Fundamentals of Fast-Scan Cyclic Voltammetry for Dopamine Detection. *Analyst* **2020**, *145*, 1158–1168. https://doi.org/10.1039/C9AN01586H.

(23) Shin, M.; Wang, Y.; Borgus, J. R.; Venton, B. J. Electrochemistry at the Synapse. *Annu. Rev. Anal. Chem.* **2019**, *12* (1), 297–321. https://doi.org/10.1146/annurev-anchem-061318-115434.

(24) Jackson, B. P.; Dietz, S. M.; Wightman, R. M. Fast-Scan Cyclic Voltammetry of 5-Hydroxytryptamine. *Anal. Chem.* **1995**, *67* (6), 1115–1120. https://doi.org/10.1021/ac00102a015.

(25) Kile, B. M.; Guillot, T. S.; Venton, B. J.; Wetsel, W. C.; Augustine, G. J.; Wightman, R. M. Synapsins Differentially Control Dopamine and Serotonin Release. *J. Neurosci.* **2010**, *30* (29), 9762–9770. https://doi.org/10.1523/JNEUROSCI.2071-09.2010.

(26) Wood, K. M.; Zeqja, A.; Nijhout, H. F.; Reed, M. C.; Best, J.; Hashemi, P. Voltammetric and Mathematical Evidence for Dual Transport Mediation of Serotonin Clearance in Vivo. *J. Neurochem.* **2014**, *130* (3), 351–359. https://doi.org/10.1111/jnc.12733.

(27) Bowman, M. A.; Vitela, M.; Clarke, K. M.; Koek, W.; Daws, L. C. Serotonin Transporter and Plasma Membrane Monoamine Transporter Are Necessary for the Antidepressant-like Effects of Ketamine in Mice. *Int. J. Mol. Sci.* **2020**, *21* (20), 1–22. https://doi.org/10.3390/ijms21207581.

(28) Wood, K. M.; Hashemi, P. Fast-Scan Cyclic Voltammetry Analysis of Dynamic Serotonin Reponses to Acute Escitalopram. *ACS Chem. Neurosci.* **2013**, *4* (5), 715–720. https://doi.org/10.1021/cn4000378.

(29) Hashemi, P.; Dankoski, E. C.; Lama, R.; Wood, K. M.; Takmakov, P.; Wightman, R. M. Brain Dopamine and Serotonin Differ in Regulation and Its Consequences. *Proc. Natl. Acad. Sci. U. S. A.* **2012**, *109* (29), 11510–11515. https://doi.org/10.1073/pnas.1201547109.

(30) Borue, X.; Cooper, S.; Hirsh, J.; Condron, B.; Venton, B. J. Quantitative Evaluation of Serotonin Release and Clearance in Drosophila. *J. Neurosci. Methods* **2009**, *179* (2), 300–308. https://doi.org/10.1016/j.jneumeth.2009.02.013.

(31) Vickrey, T. L.; Condron, B.; Venton, B. J. Detection of Endogenous Dopamine Changes in Drosophila Melanogaster Using Fast-Scan Cyclic Voltammetry. *Anal. Chem.* **2009**, *81* (22), 9306–9313. https://doi.org/10.1021/ac901638z.

(32) Shin, M.; Copeland, J. M.; Venton, B. J. Real-Time Measurement of Stimulated Dopamine Release in Compartments of the Adult Drosophila Melanogaster Mushroom Body. *Anal. Chem.* **2020**, *92* (21), 14398–14407. https://doi.org/10.1021/acs.analchem.0c02305.

(33) Privman, E.; Venton, B. J. Comparison of Dopamine Kinetics in the Larval Drosophila Ventral Nerve Cord and Protocerebrum with Improved Optogenetic Stimulation. *J. Neurochem.* **2015**, *135* (4), 695–704. https://doi.org/10.1111/jnc.13286.

(34) Puthongkham, P.; Lee, S. T.; Venton, B. J. Mechanism of Histamine Oxidation and Electropolymerization at Carbon Electrodes. *Anal. Chem.* **2019**, *91* (13), 8366–8373. https://doi.org/10.1021/acs.analchem.9b01178.

(35) Borue, X.; Condron, B.; Venton, B. J. Both Synthesis and Reuptake Are Critical for Replenishing the Releasable Serotonin Pool in Drosophila. *J. Neurochem.* **2010**, *113* (1), 188–199. https://doi.org/10.1111/j.1471-4159.2010.06588.x.

(36) Xiao, N.; Privman, E.; Venton, B. J. Optogenetic Control of Serotonin and Dopamine Release in Drosophila Larvae. *ACS Chem. Neurosci.* **2014**, *5* (8), 666–673. https://doi.org/10.1021/cn500044b.

(37) Hayes, B. D.; Klein-Schwartz, W.; Clark, R. F.; Muller, A. A.; Miloradovich, J. E. Comparison of Toxicity of Acute Overdoses with Citalopram and Escitalopram. *J. Emerg. Med.* **2010**, *39* (1), 44–48. https://doi.org/10.1016/j.jemermed.2008.06.030.

(38) Owens, M. J.; Knight, D. L.; Nemeroff, C. B. Second-Generation SSRIs: Human Monoamine Transporter Binding Profile of Escitalopram and R-Fluoxetine. *Biol. Psychiatry* **2001**, *50* (5), 345–350. https://doi.org/10.1016/S0006-3223(01)01145-3.

(39) Currie, G. M. Pharmacology, Part 1: Introduction to Pharmacology and Pharmacodynamics. *J. Nucl. Med. Technol.* **2018**, *46* (2), 81–86. https://doi.org/10.2967/jnmt.117.199588.

(40) Davis, B. A.; Nagarajan, A.; Forrest, L. R.; Singh, S. K. Mechanism of Paroxetine (Paxil) Inhibition of the Serotonin Transporter. *Sci. Rep.* **2016**, *6*, 1–13. https://doi.org/10.1038/srep23789.

(41) Zhong, H.; Sánchez, C.; Caron, M. G. Consideration of Allosterism and Interacting Proteins in the Physiological Functions of the Serotonin Transporter. *Biochem. Pharmacol.* **2012**, *83* (4), 435–442. https://doi.org/10.1016/j.bcp.2011.09.020.

(42) Roman, D. L.; Saldaña, S. N.; Nichols, D. E.; Carroll, F. I.; Barker, E. L. Distinct Molecular Recognition of Psychostimulants by Human and Drosophila Serotonin Transporters. *J. Pharmacol. Exp. Ther.* **2004**, *308* (2), 679–687. https://doi.org/10.1124/jpet.103.057836.

(43) Demchyshyn, L. L.; Pristupa, Z. B.; Sugamori, K. S.; Barker, E. L.; Blakely, R. D.; Wolfgang, W. J.; Forte, M. A.; Niznik, H. B. Cloning, Expression, and Localization of a Chloride-Facilitated, Cocaine-Sensitive Serotonin Transporter from Drosophila Melanogaster. *Proc. Natl. Acad. Sci. U. S. A.* **1994**, *91* (11), 5158–5162. https://doi.org/10.1073/pnas.91.11.5158.

(44) Rodriguez, G. J.; Roman, D. L.; White, K. J.; Nichols, D. E.; Barker, E. L. Distinct Recognition of Substrates by the Human and Drosophila Serotonin Transporters. *J. Pharmacol. Exp. Ther.* **2003**, *306* (1), 338–346. https://doi.org/10.1124/jpet.103.048751.

(45) Plenge, P.; Abramyan, A. M.; Sørensen, G.; Mørk, A.; Weikop, P.; Gether, U.; Bang-Andersen, B.; Shi, L.; Loland, C. J. The Mechanism of a High-Affinity Allosteric Inhibitor of the Serotonin Transporter. *Nat. Commun.* **2020**, *11* (1), 1–12. https://doi.org/10.1038/s41467-020-15292-y.

(46) Ribaudo, G.; Bortoli, M.; Witt, C. E.; Parke, B.; Mena, S.; Oselladore, E.; Zagotto, G.; Hashemi, P.; Orian, L. ROS-Scavenging Selenofluoxetine Derivatives Inhibit In Vivo Serotonin Reuptake. *ACS Omega* **2021**. https://doi.org/10.1021/acsomega.1c05567.

(47) Nevels, R. M.; Gontkovsky, S. T.; Williams, B. E. Paroxetine—the Antidepressant from Hell? Probably Not, but Caution Required. *Psychopharmacol. Bull.* **2016**, *46* (1), 77–104.

(48) Commons, K. G.; Linnros, S. E. Delayed Antidepressant Efficacy and the Desensitization Hypothesis. *ACS Chem. Neurosci.* **2019**, *10* (7), 3048–3052. https://doi.org/10.1021/acschemneuro.8b00698.

(49) Perez-Caballero, L.; Torres-Sanchez, S.; Bravo, L.; Mico, J. A.; Berrocoso, E. Fluoxetine: A Case History of Its Discovery and Preclinical Development. *Expert Opin. Drug Discov.* **2014**, *9* (5), 567–578. https://doi.org/10.1517/17460441.2014.907790.

(50) Neumaier, J. F.; Root, D. C.; Hamblin, M. W. Chronic Fluoxetine Reduces Serotonin Transporter MRNA and 5-HT(1B) MRNA in a Sequential Manner in the Rat Dorsal Raphe Nucleus. *Neuropsychopharmacology* **1996**, *15* (5), 515–522. https://doi.org/10.1016/S0893-133X(96)00095-4.

(51) Nurrish, S. Dense Core Vesicle Release: Controlling the Where as Well as the When. *Genetics* **2014**, *196* (3), 601–604. https://doi.org/10.1534/genetics.113.159905.

(52) Wong, M. Y.; Shakiryanova, D.; Levitan, E. S. Presynaptic Ryanodine Receptor-CamKII Signaling Is Required for Activity-Dependent Capture of Transiting Vesicles. *J. Mol. Neurosci.* **2009**, *37* (2), 146–150. https://doi.org/10.1007/s12031-008-9080-8.

(53) Wan, J.; Peng, W.; Li, X.; Qian, T.; Song, K.; Zeng, J.; Deng, F.; Hao, S.; Feng, J.; Zhang, P.; Zhang, Y.; Zou, J.; Pan, S.; Shin, M.; Venton, B. J.; Zhu, J. J.; Jing, M.; Xu, M.; Li, Y. A Genetically Encoded Sensor for Measuring Serotonin Dynamics. *Nat. Neurosci.* **2021**, *24* (5), 746–752. https://doi.org/10.1038/s41593-021-00823-7.

(54) Bellen, H. J.; Levis, R. W.; He, Y.; Carlson, J. W.; Evans-Holm, M.; Bae, E.; Kim, J.; Metaxakis, A.; Savakis, C.; Schulze, K. L.; Hoskins, R. A.; Spradling, A. C. The Drosophila Gene Disruption Project: Progress Using Transposons with Distinctive Site Specificities. *Genetics* **2011**, *188* (3), 731–743. https://doi.org/10.1534/genetics.111.126995.

(55) Nagarkar-Jaiswal, S.; Lee, P. T.; Campbell, M. E.; Chen, K.; Anguiano-Zarate, S.; Gutierrez, M. C.; Busby, T.; Lin, W. W.; He, Y.; Schulze, K. L.; Booth, B. W.; Evans-Holm, M.; Venken, K. J. T.; Levis, R. W.; Spradling, A. C.; Hoskins, R. A.; Bellen, H. J. A Library of MiMICs Allows Tagging of Genes and Reversible, Spatial and Temporal Knockdown of Proteins in Drosophila. *Elife* **2015**, *2015* (4), 1–28. https://doi.org/10.7554/eLife.05338.

(56) Shin, M.; Venton, B. J. Electrochemical Measurements of Acetylcholine-Stimulated Dopamine Release in Adult Drosophila Melanogaster Brains. *Anal. Chem.* **2018**, *90* (17), 10318–10325. https://doi.org/10.1021/acs.analchem.8b02114.

(57) Pyakurel, P.; Shin, M.; Venton, B. J. Nicotinic Acetylcholine Receptor (NAChR) Mediated Dopamine Release in Larval Drosophila Melanogaster. *Neurochem. Int.* **2018**, *114*, 33–41. https://doi.org/10.1016/j.neuint.2017.12.012.

(58) Li, Y. F. A Hypothesis of Monoamine (5-HT) – Glutamate/GABA Long Neural Circuit: Aiming for Fast-Onset Antidepressant Discovery. *Pharmacol. Ther.* **2020**, *208*, 107494. https://doi.org/10.1016/j.pharmthera.2020.107494.

Chapter 4

Microdosing ketamine increases locomotion and feeding in *Drosophila*, but does not affect serotonin like SSRIs

Abstract

Recently, the FDA approved microdosing ketamine for treatment resistant depression. Traditional antidepressants, like selective serotonin reuptake inhibitors (SSRIs), act on serotonin, but it is not clear how ketamine affects serotonin. *Drosophila melanogaster*, the fruit fly, has similar neurotransmitters to mammals, and is a good model system to study depression behaviors, such as locomotion and feeding. The goal of this study was to compare changes in serotonin, locomotion, and feeding behaviors in *Drosophila* larvae after feeding ketamine or SSRIs. We used fast-scan cyclic voltammetry (FSCV) to measure optogenetically-stimulated serotonin changes, as well as locomotion tracking software and blue dye feeding tracers to monitor behavior. Initially, we created dose-response curves comparing ketamine and SSRIs (escitalopram, paroxetine, and fluoxetine) and found that ketamine did not affect serotonin at low doses (≤ 5 μM), but inhibited SERT at higher doses (1 mM). We then fed larvae various doses (1 – 100 mM) of antidepressants for 24 hours and found that 1 mM ketamine also did not affect serotonin, but increased locomotion and feeding. Low doses (≤ 10 mM) of escitalopram and fluoxetine also increased feeding and locomotion behaviors, but inhibited SERT without affecting concentration. At 100 mM, ketamine inhibited SERT, increased serotonin, but decreased locomotion and feeding, similar to fluoxetine. Altogether, these data suggest that microdosing ketamine increases locomotion and feeding, but does not work through serotonergic mechanisms, while higher doses inhibit SERT and decrease these behaviors. Ultimately, this work shows that *Drosophila* is a good model to discern antidepressant mechanisms with ketamine and SSRIs.

4.1 Introduction

In 2019, the FDA approved microdosing ketamine to treat major depressive disorder (MDD) and treatment resistant depression (TRD).[1–3] Patients with these diagnoses often fail to positively respond to at least 2 antidepressants, which are commonly selective serotonin reuptake inhibitor (SSRIs). For ketamine treatments, patients are given intravenous ketamine at low doses (0.5-1.0 mg/kg) over a period of several hours.[2] Interestingly, rapid-onset positive effects have been reported within 4 hours that persist for up to 1-2 weeks,[2] which is remarkably different than conventional SSRIs that take many weeks to see initial improvements.[4] Since this discovery, several studies have explored the mechanism of action for ketamine to understand its effects on depression behaviors.[2,4–6] Formally, ketamine is classified as a noncompetitive NMDA antagonist that affects the glutamatergic system.[2,4] However, it also shows weak agonism to mu, delta, and kappa opioid receptors,[2,7] and binds to a variety of receptors and transporters in the brain, including serotonin.[2,4,5] Here, ketamine initiates different signaling cascades (i.e., AKT/ERK, MAPK, HOMER/ SHANK, or RAS/ RAF)[2] that result in the rapid translation of brain-derived neurotrophic factor (BDNF), which increases dendritic spine density formation [2,4,6,8] and alleviates depression symptoms.[2] In comparison, SSRIs bind to the serotonin transporter (SERT) to inhibit serotonin reuptake and increase extracellular serotonin concentrations.[9–12] However, it is still unclear how ketamine affects serotonin in real-time and whether it modifies serotonin dynamics similar to SSRIs (i.e., inhibits SERT). Furthermore, it is not understood how different doses of these antidepressants affect behaviors that are impacted by depression, such as feeding and locomotion.[13–15] Real-time measurements of serotonin and analytical behavioral assays can be used in *Drosophila melanogaster* (the fruit fly) to compare the effects of ketamine and SSRIs on feeding and locomotion.

Previously, electrochemical techniques have been used to measure rapid serotonin with ketamine and SSRIs in mice and *Drosophila*.[5,9,11,16–19] The Daws group used chronoamperometry to measure serotonin with SERT double knockout (-/-) mice and found that high doses of ketamine (32 mg/kg) slowed serotonin reuptake,[5] which led them to conclude that SERT inhibition was required for ketamine's antidepressant effects. However, they only measured serotonin changes with a single dose and did not investigate lower doses similar to a microdose treatment. Using fast-scan cyclic voltammetry, the Hashemi group also characterized serotonin concentration and reuptake changes with escitalopram and fluoxetine in mice *in vivo*,[9,10,18,20] while our lab also investigated optogenetically-stimulated serotonin changes with escitalopram, citalopram, fluoxetine, and paroxetine in *Drosophila* larvae and found their responses were similar to mammals.[9–11,20] Previously, we found differences in how each SSRI affected serotonin, since some had more effects on release while others only inhibited dSERT to inhibit reuptake.[10,11,21,22] Similarly, FSCV could be used to compare ketamine to SSRIs in *Drosophila* to clarify how serotonin changes at antidepressant or anesthetic doses to explain effects on behavior.

Fruit flies are capable of performing complex behavioral tasks that can be studied with simple behavioral assays.[23] For example, video tracking software can be used to compare locomotion changes with different drugs or genetic mutations, including climbing assays in adults and crawling in larvae, to understand their downstream effects. Previously, the Louis lab also created the Raspberry Pi virtual reality system (PiVR) that monitors the movements of *Drosophila* larvae in an arena with video tracking equipment.[24] Additionally, several analytical assays have also been created to measure feeding in *Drosophila*.[13–15,25] For example, the Grotewiel and Pletcher labs pioneered UV-Visible spectroscopy assays in *Drosophila* with simple blue food dye tracers to measure how much food was consumed based on the concentration of dye collected in adult flies.[25–27] With depression, flies can also exhibit depression-like states from uncontrollable mechanical stress, which result in decreased climbing in adults, and this depressive behavior can be alleviated with fluoxetine.[23,28] Together, these behavioral assays in larvae can be used to measure how feeding and locomotion are modified with different doses of antidepressants.

The goal of this study was to compare changes in serotonin, locomotion, and feeding behaviors in *Drosophila* larvae with bath-applying and feeding ketamine versus SSRIs. Here, we found that ketamine did not inhibit serotonin reuptake at acute doses ≤ 5 μM with bath-application. However, the highest 1 mM ketamine dose increased serotonin concentration and reuptake by inhibiting SERT. When *Drosophila* larvae were fed antidepressants for 24 hours, a low dose of ketamine (1 mM) also did not affect serotonin concentration or reuptake, while all SSRIs slowed serotonin reuptake, and paroxetine increased serotonin concentrations. Additionally, feeding 10 mM ketamine increased serotonin concentrations, but did not affect reuptake, whereas a 100 mM ketamine dose dramatically inhibited dSERT with slower reuptake and higher concentrations. Feeding low doses (≤ 10 mM) of ketamine, escitalopram, and fluoxetine also caused feeding and locomotion behavior to increase, while higher doses (100 mM) of ketamine and fluoxetine decreased them. Altogether, these data suggest that ketamine and SSRIs affect serotonin differently, but behavior similarly. Specifically, low doses of ketamine do not affect serotonin, but high, anesthetic doses of ketamine inhibit dSERT. Thus, ketamine does not affect serotonin release or reuptake at microdoses, although it does affect behavior, and its mechanism of action is different from SSRIs at low doses. Ultimately, our work shows that *Drosophila* is a good model to determine different antidepressant mechanisms of action, and other genetic applications should be explored to understand serotonin and behavior effects with ketamine and SSRIs.

4.2 Experimental Methods

4.2.1 Chemicals

Serotonin hydrochloride, ketamine hydrochloride, fluoxetine hydrochloride, escitalopram oxalate, paroxetine hydrochloride, and all-trans retinal were purchased from Sigma Aldrich (St Louis, MO, USA).[11] FD&C Blue No. 1 food dye powder (Flavors and Color, Diamond Bar, CA, USA) was purchased on Amazon. For pre- and post-calibrations, a 1 mM stock solution of serotonin was prepared in 0.1 M $HClO_4$. A final working solution of 1 µM serotonin was prepared by diluting the stock in phosphate buffer saline (PBS, 131.25 mM NaCl, 3.00 mM KCl, 10 mM NaH_2PO_4, 1.2 mM $MgCl_2$, 2.0 mM Na_2SO_4, and 1.2 mM $CaCl_2$ with the final pH adjusted to 7.4 with 1 M NaOH).[16] Drugs were prepared in PBS and made fresh daily.

4.2.2 Microelectrode preparation

CFMEs were prepared as previously described.[11,16] Briefly, a T-650 carbon fiber (Cytec Engineering Materials, West Patterson, NJ, USA) with a 7 µm diameter was aspirated into a standard 1.28 mm inner diameter x 0.69 mm outer diameter glass capillary tube (A-M Systems, Sequim, WA) with a vacuum pump. A capillary was then pulled by a Flaming Brown micropipette horizontal puller (Sutter Instrument, Novato, CA) to make two electrodes.[11] Fibers were cut to 25-75 µm and epoxied by dipping the tip of the electrode into a solution of 14% m-phenylenediamine hardener (108-45-2, Acros Organics, Morris Plains, NH, USA) in Epon Resin 828 (25068-38-6, Miller Stephenson, Danbury, CT, USA) at 80–85 °C for 35 seconds. The CFMEs were cured at 100°C overnight and 150°C for at least 4 hours the next day.

4.2.3 Electrochemical instrumentation

Electrochemical experiments were performed using a two-electrode system with a CFME working electrode backfilled with 1 M KCl.[16,29–31] All potential measurements are reported versus a chloridized, Ag/AgCl wire reference electrode. Experiments were conducted in a covered, grounded Faraday cage to block out light. Before experiments, electrode tips were soaked in isopropyl alcohol for at least 10 minutes to clean the surface. The extended serotonin waveform (ESW, 0.2 V, 1.3 V, -0.1 V, 0.2 V, 1000 V/s) was continuously applied to electrodes using a WaveNeuro system (Pine Research, Durham, NC, USA).[16] Data were collected with HDCV Analysis software (Department of Chemistry, University of North Carolina at Chapel Hill, USA). A flow-injection system with a six-port loop injector and air actuator (Valco Instruments, Houston, TX, USA) was used to pre- and post-calibrate CFMEs for *in vitro* experiments. PBS buffer was flowed at 2 mL/min using a syringe pump (Harvard Apparatus, Holliston, MA, USA) through a flow cell

with the CFME tip inserted in solution. For calibration, 1 μM serotonin was injected for 5 seconds to determine current response. The concentration of serotonin released during *in vitro* experiments was determined using this calibration factor.

4.2.4 Ventral nerve cord tissue preparation for optogenetic in vitro experiments

Methods for larva VNC dissection were previously described.[11] UAS-CsChrimson (Stockline BL#55136, Bloomington *Drosophila* Stock Center, Bloomington, IN, USA) virgin females were crossed with trh-Gal4 (BL#38389) flies and progeny heterozygous larvae were kept in the dark and raised on standard food mixed 250:1 with 100 mM all-trans retinal (ATR) until drug feeding was applied.[16] The ventral nerve cords (VNCs) of third instar “wandering” larvae were dissected in PBS kept on ice. A VNC was placed in an uncoated Petri dish dorsal side down containing 3 mL of room temperature PBS. A small slice of the lateral optic lobe was removed using the tip of a 22-gauge hypodermic needle. A CFME was implanted from the lateral edge of the tissue into the dorsal medial protocerebrum using a micromanipulator. Dissection and electrode insertion were performed under low light conditions to reserve the pools of releasable serotonin.[29] CFMEs were allowed to equilibrate for 10 minutes in tissue in the dark prior to data collection.[11,16]

4.2.5 Optogenetic serotonin release

Optogenetic release of serotonin was stimulated by activating CsChrimson ion channels with red light from a 617 nM fiber-coupled high-power LED with a 200 μm core optical cable (ThorLabs, Newton, NJ, USA).[11,16] A micromanipulator was used to center the fiber above the VNC tissue, and transistor-transistor logic (TTL) inputs to a T-cube LED controller (ThorLabs) were connected to the FSCV breakout box to control the light. TTL input was driven by electrical pulses from the WaveNeuro system and HDCV software to control frequency, pulse width, and number of pulses. For *in vitro* ketamine dose-response experiments, 120 biphasic pulses were delivered at 60 Hz with pulse width of 4 ms. An initial stimulation was recorded and 1 mL of the drug was slowly added to the Petri dish to not move the tissue or CFME. Stimulations were repeated every 5 minutes for 30 minutes after a drug was added to allow the releasable pool of serotonin to replenish itself. For antidepressant feeding experiments for 24 hours, 30 biphasic pulses were applied with the same parameters.

4.2.6 Feeding antidepressants to larvae for FSCV optogenetic experiments

Heterozygous progeny larvae (trh-Gal4; UAS-CsChrimson) were collected on day 5 after eating standard food (Food “J” for Janelia, Lab Express, Ann Arbor, MI, USA) mixed 250:1 with 100 mM ATR since birth. A stock drug solution that was 2x as concentrated as the final desired dose was made in PBS. Larvae were scooped out with food and gently mixed with an equal volume of drug. ATR was then added again in the same 250:1 ratio. Larvae were allowed to eat the food with drug for 24 hours before FSCV experiments (Figure 1, *n* = 6 larvae). The control larvae were mixed with only PBS.

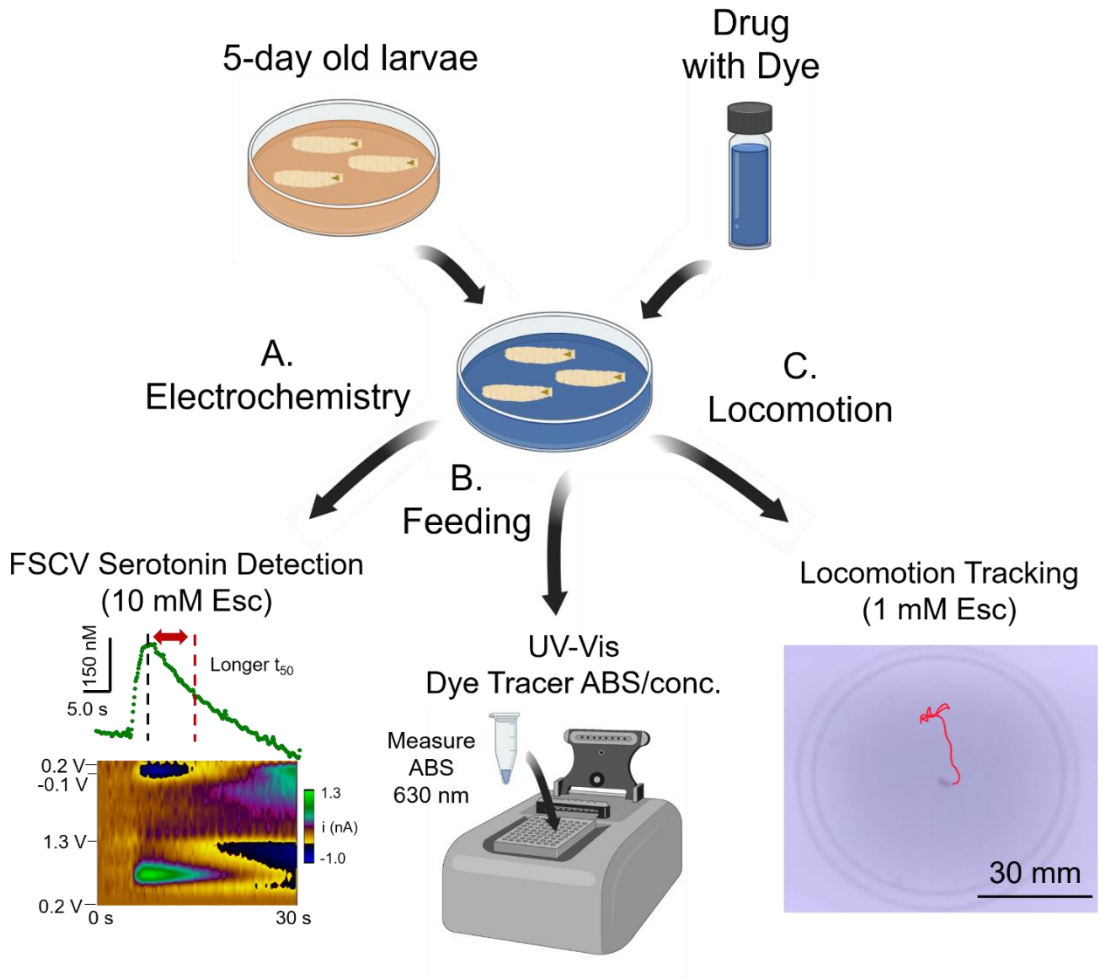

Figure 1. Feeding antidepressants to *Drosophila* larvae to measure real-time serotonin changes with feeding and locomotion behaviors. Larvae were collected on day 5 and ate antidepressants for 24 hrs. **A.** Fast-scan cyclic voltammetry (FSCV) and optogenetics were used to measure serotonin concentration and reuptake changes. Example FSCV conc. versus time and color plot show serotonin detected after feeding 10 mM escitalopram. Current was converted to serotonin conc. using a post-calibration factor, and reuptake is characterized by the time to half max decay (t_{50}) of the peak detected in the trace (*n* = 6 larvae/ drug dose). **B.** Blue dye internal food consumption was measured with a UV-Vis spectrophotometer from a tissue homogenate of *n* = 30 larvae. Blue dye absorbance was measured at 630 nm. **C.** Locomotion was tracked using PiVR and LoliTrack. A larva was placed on a 60 mm Petri dish. PiVR recorded a 60 sec video of the larva (*n* = 30 larvae/drug and dose), and LoliTrack was used to track their movement. Cartoons created in BioRender.

4.2.7 UV-Vis dye tracer food consumption determination with different antidepressants

A 1% w/v FD&C Blue No. 1 solution was made by adding food dye powder to PBS. Methods are adapted from Shell et al.[32] For drug feeding experiments, an antidepressant drug was added to the blue dye solution. On day 5, larvae were scooped with their food and mixed with the blue dye drug solution. Larvae ate the drug and blue dye tracer for 24 hours. After 24 hours, 30 larvae were collected and placed into 500 µL of deionized (DI) water in an Eppendorf tube and centrifuged at 13,000 rpm for 30 mins using an AccuSpin Micro 17 Centrifuge (Fisher Scientific, Waltham, MA, USA). A micro spatula was then used to crush the larvae into a tissue homogenate and centrifuged again for 15 mins. Tissue homogenates were discarded and 50 µL of the blue dye tracer supernatant was added to 200 µL DI water to make a 1:5 dilution. The absorbance of the blue dye sample was measured at 630 nm using a Tecan plate reader Ultraviolet-Visible spectrophotometer (Tecan, Männedorf, Switzerland). For each drug, n = 5 samples (n = 30 larvae/sample) were collected and measured with 3 technical replicates. A calibration curve was constructed from 5 – 250 µM dye, and the slope of the calibration graph was used to determine the concentration of dye in the supernatant to calculate the mass of food eaten per larva per day.[32]

4.2.8 Real-time Drosophila larvae locomotion tracking

The Raspberry Pi based Virtual Reality system (PiVR, v. 3) was constructed following the methods in Tadres and Louis 2020 and the “Build your own PiVR” section on their website.[24] The computer casing parts and camera tower were printed using a Stratasys F170 3D Printer (Strartasys, Eden Prairie, MN, USA) at UVA’s MAE Rapid Prototyping and Machine labs using the files from the Louis Lab GitLab. The camera resolution was set to 640x480, and the animal detection method was set for third instar *Drosophila* larvae. After eating a drug for 24 hours, a larva was placed in the center of a 60 mm Petri dish and their movements were recorded for 60 s (n = 30 larvae). The individual recording files were then converted from h2p6 format to MPEG4 format using File Viewer Plus (Sharpened Productions, Minneapolis, MN, USA, v. 4.3.). LoliTrack software (Loligo Systems, Viborg, Denmark, v. 5.2.0) was used to track the distance the larvae traveled from the video recordings using their “Tracking 2D” setting.

4.2.9 Statistics and data analysis

Data are the mean ± the standard error of the mean (SEM) for n number of *Drosophila* larvae. For SSRI and ketamine feeding electrochemistry experiments, n = 6 larvae (larvae were not sexed, so both males and females were used). For drug dose response curve experiments, each dose is at least n = 4 larvae. For a sample calculation, we performed power analysis in MedCalc (MedCalc

Statistical Software, Ostend, Belgium) using the paired sample t-test where ɒ = 0.05, 1-β = 0.1, mean difference in current detected = 0.45 nA, and standard deviation of differences = 0.2 nA, which results in *n* = 4 larvae.[29–31,33] Statistics were performed in GraphPad Prism 8.0 (GraphPad Software, La Jolla, CA). Data were normally-distributed for multiple drug comparisons (all KS distance ≥ 0.1980, Kolmogrorov-Smirnov, p > 0.1000). Significance was determined at a 95% confidence level for One-Way ANOVA, Tukey's post-hoc test, and comparison of fits. No test for outliers was performed.

4.3 Results

4.3.1 Ketamine and SSRIs show differences in serotonin release, reuptake, and dSERT affinity

Initially, we bath-applied a variety of ketamine doses directly to larva VNC tissue to understand how ketamine affected serotonin. Figure 2A-G shows FSCV serotonin concentration versus time plots before (black) and after 15 minutes of bath-application of (A) 100 nM, (B) 1 µM, (C) 5 µM, (D) 10 µM, (E) 50 µM, (F) 100 µM, and (G) 1 mM ketamine. Serotonin concentration starts to increase with the 5 µM dose; however reuptake is not changed. Starting at 10 µM ketamine, serotonin reuptake was slightly slower and concentrations increased. This trend was also similar for the 50 µM and 100 µM dose. However, serotonin concentrations and reuptake dramatically increased with the highest, 1 mM ketamine dose. There was a significant overall effect of ketamine dose on serotonin concentration (Fig. 3H, One-Way ANOVA, $F_{(7,40)} = 20.51$, $p \leq 0.0001$, $n = 6$), and Tukey's post-hoc test revealed serotonin concentrations were significantly different with 10 µM, 50 µM, 100 µM, and 1 mM ketamine (all $p \leq 0.0029$). Likewise, there was a significant overall effect of ketamine dose on t_{50} (Fig. 3I, One-Way ANOVA $F_{(7,40)} = 24.48$, $p \leq 0.0001$, $n = 6$), and reuptake was significantly longer with 10 µM, 50 µM, 100 µM, and 1 mM ketamine (Tukey's post-hoc, all $p \leq 0.0058$).

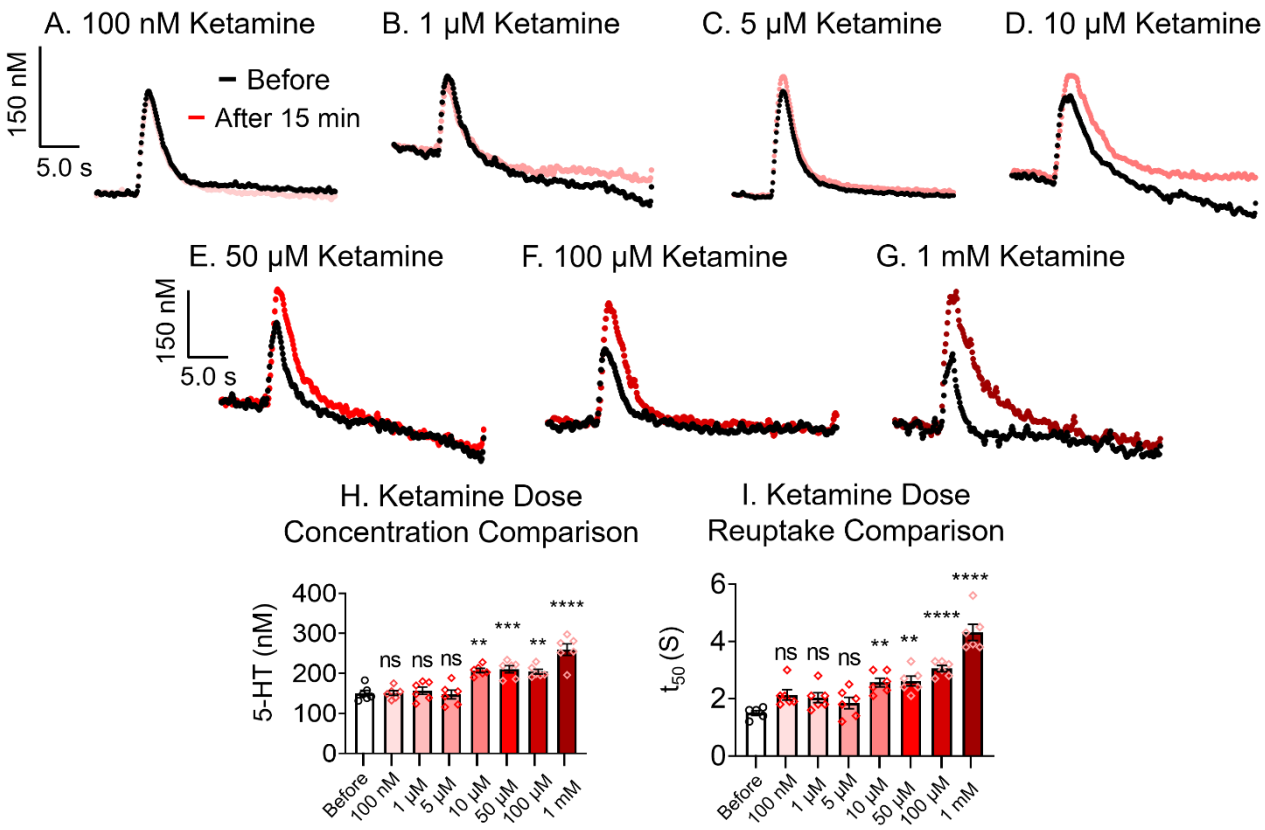

Figure 2. Serotonin release and reuptake effects for acute ketamine (*n* = 6 larvae each). Ketamine was bath-applied to *Drosophila* larvae VNC tissue and optogenetic stimulation repeated every 5 mins for 15 mins. Serotonin concentration and reuptake are characterized by conc. versus *t* plots before (black) and after (A) 100 nM, (B) 1 μM, (C) 5 μM, (D) 10 μM, (E) 50 μM, (F) 100 μM, and (G) 1 mM ketamine. (H) Evoked concentration of serotonin vs ketamine dose. There was a significant overall effect of ketamine dose on serotonin concentration (One-Way ANOVA, $F_{(7,40)} = 20.51$, $p \leq 0.0001$, $n = 6$), and Tukey's post-hoc determined serotonin concentrations were significantly different than pre-drug at 10 μM ($p < 0.0014$), 50 μM ($p < 0.0007$), 100 μM ($p < 0.0029$), and 1 mM ketamine ($p \leq 0.0001$). (I) For serotonin reuptake, there was a significant overall effect of ketamine dose on serotonin reuptake (One-Way ANOVA $F_{(7,40)} = 24.48$, $p \leq 0.0001$, $n = 6$). Tukey's post-hoc revealed reuptake increased significantly with 10 μM ($p < 0.0058$), 50 μM ($p < 0.0034$), 100 μM ($p \leq 0.0001$), and 1 mM ketamine ($p \leq 0.0001$).

Next, we constructed dose response curves to compare the effect of ketamine on dSERT with SSRI antidepressants (Fig. 3A). Here, drugs were bath-applied to tissue and serotonin stimulations were recorded after 15 minutes.[11] All drugs were tested at 100 nM, 1 μM, 10 μM, 50 μM, 100 μM, and 1 mM, and additional doses were added as needed to define the curves (Fig. 4, *n* = at least 4 larvae). The slopes and EC_{50} values, which describe their affinity to dSERT, were different for each antidepressant.[34] Table 1 summarizes serotonin release with EC_{50} values for each drug. Ketamine had the largest changes in concentration between 10 and 100 μM, which produced an EC_{50} of 36 μM. Paroxetine (purple) had the lowest EC_{50} at 1.5 μM, gradually changing from 1 to 10 μM, and showed the highest affinity to dSERT. Meanwhile, escitalopram (green) had the largest changes in serotonin release from 10 to 50 μM, with a lower EC_{50} of 17 μM that was similar to ketamine. Fluoxetine (blue) had the highest EC_{50} of 87 μM, which suggests that it does not have a high affinity for dSERT. Comparison of fits determined that EC_{50} values were different for each drug (Fig. 3A, $F_{(3, 129)} = 41.26$, $p <$

0.0001). With these responses, ketamine exhibited a higher affinity to SERT than fluoxetine, and was similar to escitalopram. Although these responses are useful, they only describe changes in concentration and not reuptake.

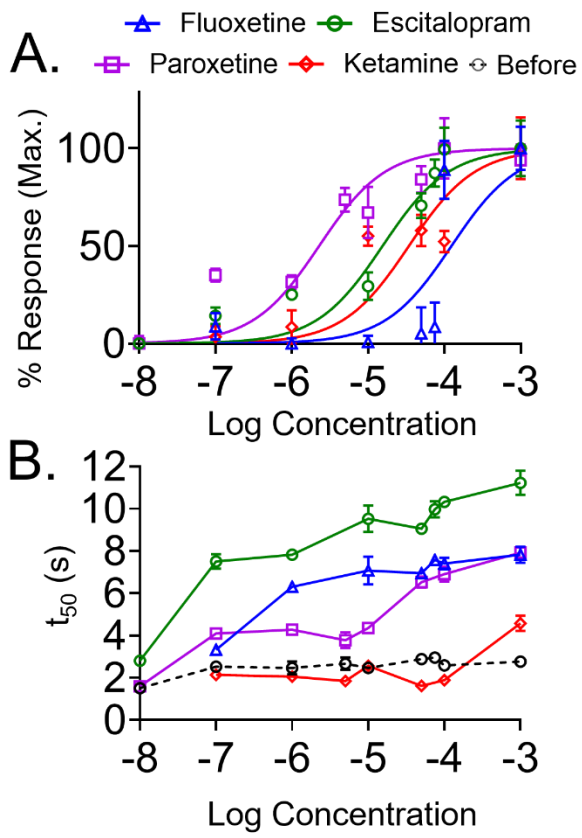

Figure 3. Dose-response curves for serotonin concentration and reuptake changes with antidepressants. **A.** Concentration curve. Normalized drug response curves show serotonin concentration changes after a drug is bath-applied for 15 min. Escitalopram (green), paroxetine (purple), fluoxetine (blue), and ketamine (red, *n* = at least 4 larvae per dose). EC50 values for each drug were different (comparison of fits, $F_{(3, 129)} = 41.26$, $p < 0.0001$, *n* ≥4 larvae). Paroxetine displayed the highest affinity for dSERT, followed by escitalopram, ketamine, and fluoxetine the lowest. **B.** Uptake curve. Serotonin t_{50} values. Control, no drug, is black dotted line. Escitalopram showed large changes in reuptake, even at lower doses. Paroxetine and fluoxetine showed reuptake smaller changes at lower doses, but increased with higher doses. Ketamine did not slow reuptake, except at the highest dose. Data were normally-distributed for multiple drug comparisons (all KS distance ≥ 0.1980, Kolmogrorov-Smirnov, $p > 0.1000$).

Table 1. Summary drug dose-response curve and reuptake data

Antidepressant	Release, EC_{50} (μM)	Reuptake, EC_{50} (μM)	Max t_{50} (s)
Escitalopram	17	4.5	11.2 ± 0.6
Paroxetine	1.5	47	7.9 ± 0.3
Fluoxetine	87	8.3	7.8 ± 0.4
Ketamine	36	134	4.3 ± 0.3

* t_{50} at 1 mM, the maximum dosage tested

To compare serotonin reuptake changes between ketamine and SSRIs at different doses, we constructed log dose-response uptake curves. In Figure 3B, we plotted dose response curves with t_{50} on the y-axis and log concentration on the x-axis. The average pre-drug t_{50} is shown as the dashed, black line. Table 1 also summarizes the normalized EC_{50} reuptake change and maximum concentration t_{50} for each drug. Ketamine (red) did not increase reuptake, except at the highest 1 mM dose. Escitalopram (green) showed large increases in t_{50} even at the lowest, 10 nM dose, while fluoxetine (blue) showed gradual increases at 1 μM. Paroxetine (purple) displayed faster reuptake from 1-10 μM, but slowed at 50-100 μM. Each drug exhibited longer reuptake at extremely high doses (100 μM and 1 mM), but escitalopram and fluoxetine had the greatest change in reuptake at lower doses and had lower EC_{50} values. There were signficant overall effects of antidepressant on serotonin reuptake (One-Way ANOVA, $F_{(4,34)} = 18.91$, $p < 0.0001$). Tukey's post-hoc test showed reuptake with SSRIs was significantly longer compared to pre-drug (escitalopram $p^{****} < 0.0001$, paroxetine $p^{*} < 0.01$, fluoxetine $p^{***} < 0.001$). However, there was no significant difference between ketamine and pre-drug ($p > 0.1$).

4.3.2 Ketamine does not affect serotonin release or reuptake at low doses compared to SSRIs after 24 hours

Next, we fed larvae low doses of ketamine and different SSRI antidepressants to characterize serotonin changes with chronic consumption. Figure 4A-G shows serotonin concentration and reuptake changes after feeding lower doses of antidepressants for 24 hours. Figure 4A-E shows FSCV serotonin conc. versus *t* plots after feeding larvae (A) PBS only, (B) 1 mM ketamine, (C) 1 mM escitalopram, (D) 1 mM paroxetine, and (E) 1 mM fluoxetine. One-Way ANOVA and Tukey's post-hoc test showed that feeding low

doses of ketamine and SSRIs significantly affected serotonin concentration (Fig. 4F, $F_{(4,25)} = 8.217$, $p \leq 0.001$, $n = 6$) and reuptake (Fig. 4G, $F_{(4,25)} = 136.3$, $p \leq 0.0001$, $n = 6$) after 24 hours. Ketamine did not affect serotonin concentration or reuptake (both $p \geq 0.85$). Escitalopram and fluoxetine also did not significantly increase serotonin concentrations ($p \geq 0.056$). However, serotonin reuptake was significantly slower with both of these SSRIs ($p \leq 0.0001$). In comparison, paroxetine significantly increased serotonin concentration and reuptake (both $p \leq 0.0001$) at this low dose because of its high dSERT affinity. Thus, at the lowest feeding dose, ketamine did not affect serotonin release or reuptake, although other SSRIs did change serotonin at these doses.

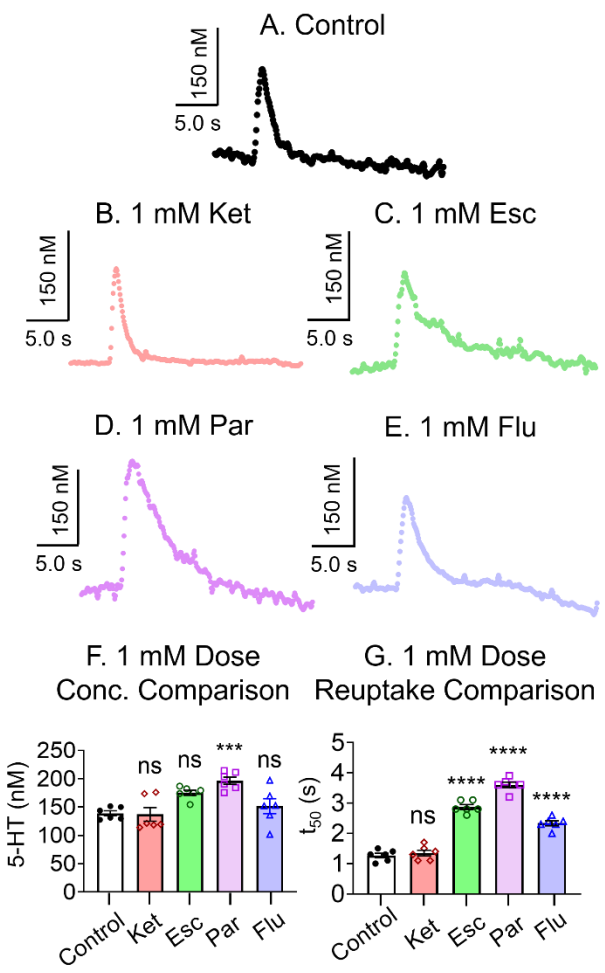

Figure 4. Low doses (1 mM) feeding ketamine and SSRIs show differences in serotonin (5-HT) release and reuptake. *Drosophila* larvae were fed (**A**, black) PBS only, (**B**, red) 1 mM ketamine, (**C**, green) 1 mM escitalopram, (**D**, purple) 1 mM paroxetine, and (**E**, blue) 1 mM fluoxetine for 24 hours ($n = 6$ larvae). Changes in serotonin (**F**) concentration and (**G**) reuptake were measured using FSCV with optogenetics. One-Way ANOVA and Tukey's post-hoc test showed significant effects of drug on serotonin concentration ($F_{(4,25)} = 8.217$, $p \leq 0.001$, $n = 6$) and reuptake ($F_{(4,25)} = 136.3$, $p \leq 0.0001$, $n = 6$). Ketamine did not affect serotonin concentration or reuptake at 1 mM. Paroxetine was the only SSRI that increased serotonin concentrations, but reuptake increased with paroxetine, escitalopram, and fluoxetine.

4.3.3 Ketamine mainly affects serotonin release at mid-doses, while SSRIs affect reuptake after 24 hours

After comparing low-doses of antidepressants, we fed a higher, 10 mM dose to *Drosophila* larvae (Fig. 5A-G). Figure 5A-E shows FSCV serotonin conc. versus *t* plots after feeding larvae for 24 hours (A) PBS only, (B) 10 mM ketamine, (C) 10 mM escitalopram, (D) 10 mM paroxetine, and (E) 10 mM fluoxetine. One-Way ANOVA and Tukey's post-hoc test showed a significant effect of antidepressant type on serotonin concentration ($F_{(4,25)} = 24.76$, $p \leq 0.0001$, $n = 6$) and reuptake ($F_{(4,25)} = 331.5$, $p \leq 0.0001$, $n = 6$). Similar to the 1 mM dose, ketamine did not affect serotonin reuptake at 10 mM ($p \geq 0.3022$), but serotonin concentrations did increase ($p \leq 0.0001$), which suggests a release mechanism instead of SERT inhibition. Compared to ketamine, the other SSRIs all significantly increased serotonin reuptake (all $p \leq 0.0001$), but they were different in how they affected serotonin concentrations. Both escitalopram and paroxetine increased serotonin concentrations at 10 mM (both $p \leq 0.0001$), but fluoxetine did not ($p \geq 0.99$). Thus, fluoxetine binds to dSERT and inhibits serotonin clearance without affecting concentration. Altogether, ketamine releases higher serotonin at mid-doses without affecting SERT, while SSRIs inhibit serotonin reuptake and have different effects on concentrations depending on their dSERT affinity.

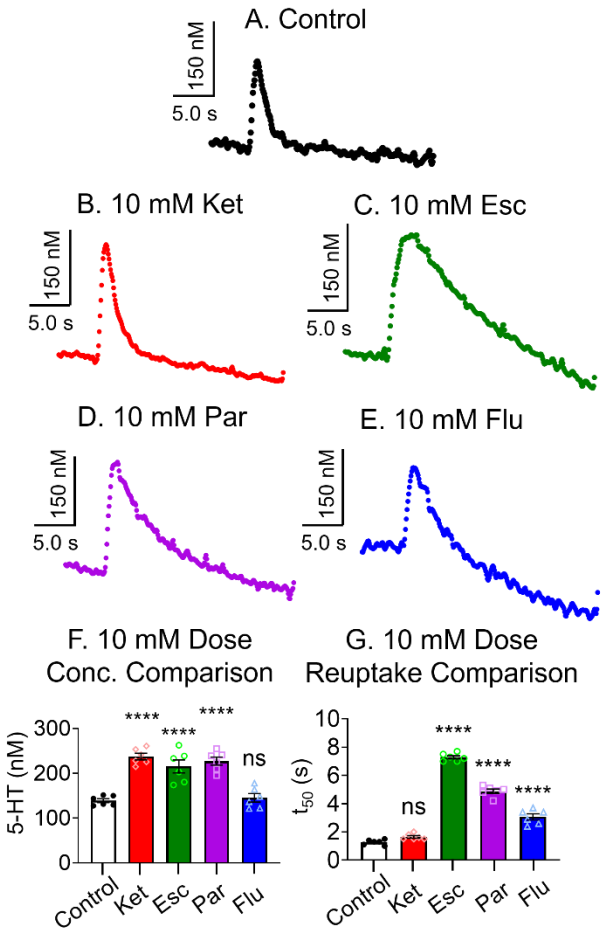

Figure 5. Ketamine mainly affects serotonin release at 10 mM, while SSRIs affect reuptake. *Drosophila* larvae were fed (**A**, black) PBS only, (**B**, red) 10 mM ketamine, (**C**, green) 10 mM escitalopram, (**D**, purple) 10 mM paroxetine, and (**E**) 10 mM fluoxetine for 24 hours (n = 6 larvae). One-Way ANOVA and Tukey's post-hoc test showed that 5-HT concentration (**F**, $F_{(4,25)} = 24.76$, $p \leq 0.0001$, n = 6) and reuptake (**G**, $F_{(4,25)} = 331.5$, $p \leq 0.0001$, n = 6) were significantly different with drug. At 10 mM, ketamine did not affect serotonin reuptake ($p \geq 0.3022$), however concentrations were significantly higher ($p \leq 0.0001$). With the SSRIs, each significantly slowed reuptake ($p \leq 0.0001$). However, fluoxetine did not increase serotonin concentrations ($p \geq 0.9900$) like escitalopram or paroxetine (both $p \leq 0.0001$).

4.3.4 High doses of ketamine and fluoxetine inhibit SERT to increase serotonin after 24 hours

Next, we fed larvae a higher, 100 mM dose to monitor serotonin dynamics changes. Figure 6A-E shows FSCV serotonin conc. versus *t* plots after feeding larvae (A) PBS only, (B) 100 mM ketamine, and (C) 100 mM fluoxetine. We chose to only investigate fluoxetine because it was the only SSRI that did not increase serotonin concentrations at lower doses. One-Way ANOVA and Tukey's post-hoc test showed a significant effect of antidepressants on serotonin concentration ($F_{(2,15)} = 20.52$, $p \leq 0.0001$, n = 6) and reuptake ($F_{(2,15)} = 112.6$, $p \leq 0.0001$, n = 6). With ketamine, the 100 mM dose significantly increased serotonin concentrations and slowed reuptake (both $p \leq 0.0001$), which is different than the 1 mM and 10 mM doses, which did not affect serotonin reuptake.

Additionally, 100 mM fluoxetine also significantly increased serotonin concentrations ($p \leq 0.001$) and slowed reuptake ($p \leq 0.0001$), which shows that higher concentrations of fluoxetine are needed to increase serotonin concentrations.

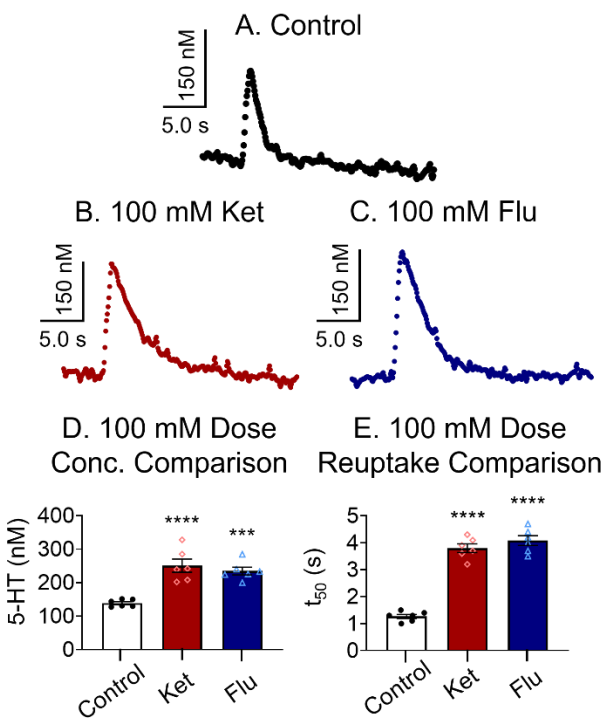

Figure 6. High doses of ketamine and fluoxetine increase serotonin (5-HT) by dSERT inhibition. *Drosophila* larvae were fed (**A**, black) PBS only, (**B**, red) 100 mM ketamine, and (**C**, blue) 100 mM fluoxetine for 24 hours ($n = 6$ larvae). One-Way ANOVA and Tukey's post-hoc test showed that 5-HT concentration (**D**, $F_{(2,15)} = 20.52$, $p \leq 0.0001$, $n = 6$) and reuptake (**E**, $F_{(2,15)} = 112.6$, $p \leq 0.0001$, $n = 6$) were different. Ketamine and fluoxetine both dramatically slowed serotonin reuptake ($p \leq 0.0001$) and increased serotonin concentrations ($p \leq 0.0001$ and $p \leq 0.001$, respectively) with high doses.

4.3.5 Low doses of ketamine and escitalopram increase feeding behaviors

A common symptom of depression and side effect of antidepressants is weight gain or loss.[35,36] To understand how SSRIs and ketamine affect feeding behaviors, we used blue food dye tracers with UV-Vis spectroscopy to measure the amount of food *Drosophila* larvae ate after 24 hours. A linear calibration curve of absorbance vs. dye concentration was made to calculate the dye consumed by a larva (Figure 7). Figure 8 compares the mass of food eaten (µg) per larva per day ($n = 5$ collection samples/dose with $n = 30$ larvae/sample). Overall, there was a significant effect of antidepressant type and dose on food consumption (Fig. 8, One-Way ANOVA, $F_{(10,44)} = 238.5$, $p \leq 0.0001$, $n = 6$), and Tukey's post-hoc test showed that larvae significantly consumed more food with 1 mM ketamine, 1 mM escitalopram, and 10 mM ketamine ($p^{****} < 0.0001$), but less food was consumed with 100 mM ketamine ($p^{*} < 0.05$).

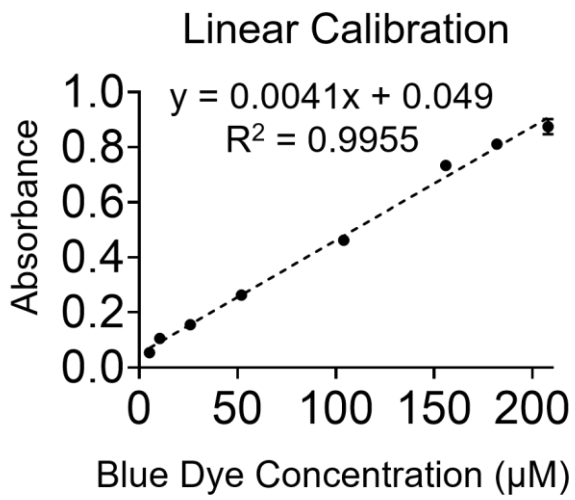

Figure 7. Blue dye linear calibration for Drosophila larvae food consumption (*n* = 3 replicates/ concentration). The linear equation was used to back-calculate the mass (µg) of food eaten per larva per day.

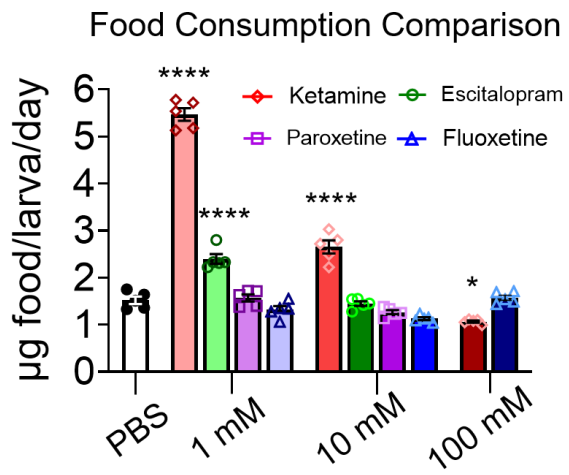

Figure 8. Food consumption for different antidepressant drugs (*n* = 5 samples/dose with *n* = 30 larvae/sample). One-Way ANOVA ($F_{(10,44)}$ = 238.5, $p \leq 0.0001$, *n* = 6) and Tukey's post-hoc comparisons found the amount of blue food eaten significantly increased with 1 mM ketamine, 10 mM ketamine, and 1 mM escitalopram (all *p*****< 0.0001). However, the amount of food consumed significantly decreased with 100 mM ketamine (*p* = 0.0134).

4.3.6 Low doses of ketamine, escitalopram, and fluoxetine increase locomotion behaviors

In addition to changes in appetite and feeding, antidepressants have been previously shown to affect locomotion.[13–15] Here, we used PiVR to record *Drosophila* larvae and LoliTrack tracking software to characterize how 24 hours of feeding ketamine and SSRIs affect locomotion. Figure 9A-K shows still images with the path the larva traveled drawn in red after eating food mixed with (A) PBS only, (B) 1 mM ketamine, (C) 1 mM escitalopram, (D) 1 mM paroxetine, (E) 1 mM fluoxetine, (F) 10 mM ketamine, (G) 10 mM

escitalopram, (H) 10 mM paroxetine, (I) 10 mM fluoxetine, (J) 100 mM ketamine, and (K) 100 mM fluoxetine. There was a significant overall effect of antidepressant on distance traveled (Fig. 9, One-Way ANOVA, $F_{(10,319)} = 72.35$, $p \leq 0.0001$, $n = 6$), and Tukey's post-hoc test showed that distance traveled significantly increased with 1 mM ketamine, 1 mM escitalopram, 1 mM fluoxetine, and 10 mM fluoxetine (all p**** < 0.0001). However, distance traveled significantly decreased with 100 mM fluoxetine (p** < 0.01).

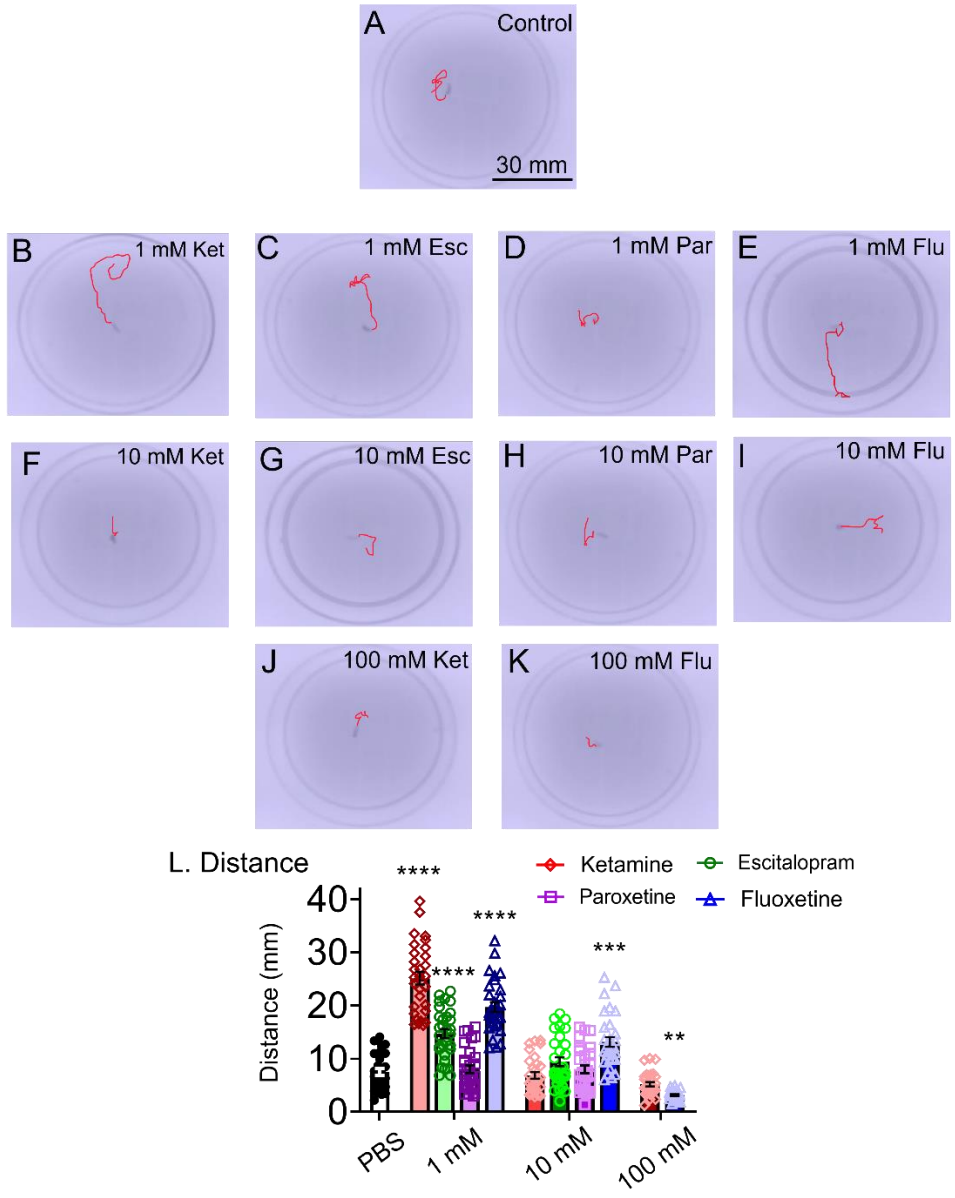

Figure 9. Locomotion tracking comparison after *Drosophila* larvae ate different antidepressant drugs for 24 hours ($n = 30$ larvae/dose). A larva's locomotion was tracked for 60 s after (**A**) PBS, (**B**) 1 mM ketamine, (**C**) 1 mM escitalopram, (**D**) 1 mM paroxetine, I 1 mM fluoxetine, (**F**) 10 mM ketamine, (**G**) 10 mM escitalopram, (**H**) 10 mM paroxetine, (**I**) 10 mM fluoxetine, (**J**) 100 mM ketamine, and (**K**) 100 mM fluoxetine. Larvae showed increased locomotion with 1 mM ketamine, 1 mM escitalopram, 1 mM fluoxetine, and 10 mM fluoxetine. However, locomotion decreased with 100 mM fluoxetine. **L.** One-Way ANOVA ($F_{(10,319)} = 72.35$, $p \leq 0.0001$, $n = 6$) and Tukey's post-hoc comparisons found the distance traveled significantly increased with 1 mM ketamine, 1 mM escitalopram, 1 mM fluoxetine, and 10 mM fluoxetine (all p****< 0.0001). However, distance significantly decreased with 100 mM fluoxetine ($p \geq 0.0020$).

4.4 Discussion

Our results show that feeding ketamine to *Drosophila* larvae does not affect serotonin at low, microdoses, but promotes changes in serotonin release at mid-doses and inhibits serotonin reuptake at higher, anesthetic doses. In contrast, all SSRI doses slowed serotonin reuptake, but they affected serotonin concentrations differently based on their dSERT affinities. Interestingly, we saw similar dose-dependent effects on behavior where low doses (1 mM) of ketamine, escitalopram, and fluoxetine increased feeding and locomotion behaviors, while higher doses (100 mM) of ketamine and fluoxetine decreased them. Together, these electrochemical and behavioral data indicate that other neurotransmitters or membrane transport proteins may contribute to increased feeding and locomotion with ketamine instead of dSERT. Altogether, this work shows that *Drosophila* is a good model to rapidly study pharmacological mechanisms with serotonin, especially promiscuous drugs like ketamine that have a wide-range of behavioral effects and other molecular targets.

4.4.1 Ketamine and SSRIs show different serotonin changes that are dose-dependent

In Dunham and Venton 2022,[11] we previously measured real-time serotonin concentration and reuptake changes by bath-applying SSRIs to *Drosophila* larvae VNCs. Here, we bath-applied different doses of ketamine to understand how ketamine regulated serotonin compared to SSRIs. Ketamine did not affect serotonin concentration or reuptake at doses ≤ 5 µM. However, ketamine subtly increased serotonin at 10, 50, and 100 µM, but the largest changes were with the highest, 1 mM dose. Together, these data indicate that microdoses of ketamine do not affect serotonin, while higher doses inhibit dSERT to increase serotonin concentrations and slow reuptake. Thus, the mechanism of action for ketamine is different compared to the SSRIs (i.e., escitalopram, paroxetine, and fluoxetine),[11] which mainly increased serotonin uptake.

After comparing dose-responses with bath-application, we fed larvae different doses of these antidepressants for 24 hours to more closely replicate how they cross the blood-brain barrier in humans.[37] For ketamine, we saw that the lowest, 1 mM dose did not affect serotonin, which was similar to the low (≤ 1 µM) bath application doses. A 10 mM mid-dose only increased serotonin concentrations and did not inhibit reuptake, which was similar to the 5 µM dose. After feeding larvae 100 mM ketamine, serotonin concentrations dramatically increased and reuptake slowed by inhibiting dSERT, which is similar to the 1 mM bath application. Similar results were also seen with feeding SSRIs, as data had similar dose responses to bath-application data.[11] For example,

fluoxetine slowed serotonin reuptake at the lowest 1 mM and 10 mM feeding doses, which is similar to bath applied doses < 100 µM but concentration was not affected and required the highest 100 mM dose to increase serotonin, similar to higher doses (≥ 100 µM) with bath applications.[11] Additionally, 10 mM paroxetine showed high concentration changes and slow reuptake that was similar to the higher doses (≥ 50 µM) we bath-applied.[11] Feeding 10 mM escitalopram also caused serotonin concentrations to increase with dramatically slower serotonin reuptake, which is similar to a 10 µM bath-applied dose and other FSCV data that has also been previously reported in mice.[9,18,20]

4.4.2 Ketamine and SSRIs change feeding and locomotion similarly, even though serotonin changes are different

Common symptoms of depression include weight gain or loss from changes in appetite and activity, which can be affected by taking antidepressants. However, it is not understood whether these behaviors are caused by serotonin changes from these drugs only. Here, we measured feeding and locomotion changes with serotonin after feeding larvae ketamine and SSRIs for 24 hours without genetic mutations. Primarily, we saw the low doses (1 mM) of ketamine, escitalopram, and fluoxetine increased both feeding and locomotion (Figure 8 and 9). Although locomotion effects have not been previously characterized in *Drosophila*, several new clinical studies have shown that microdosing ketamine increases appetite and positive effects for patients with co-morbid eating disorders and depression,[38–40] and low doses of ketamine cause hyperlocomotion in mammals.[41] Additionally, Hidalgo et al. also investigated locomotion changes after feeding *Drosophila* larvae a high dose of fluoxetine,[13] and found that fluoxetine decreased locomotion, which is similar to our 100 mM fluoxetine data.

Altogether, these results show that antidepressants change feeding and locomotion behaviors without genetic manipulations, and that they seem to increase or decrease in a dose-dependent manner, regardless of the antidepressant. Specifically, our electrochemistry data shows that serotonin is different with each antidepressant, but behavior changes are similar. For instance, 1 and 10 mM ketamine, as well as 1 mM escitalopram increased feeding. At 1 mM, neither ketamine and escitalopram significantly increased serotonin concentrations, but escitalopram did inhibit dSERT to increase reuptake. Additionally, 10 mM ketamine also increased feeding, and we saw that this dose increased serotonin concentration, but reuptake was not affected, which further suggests a release mechanism instead of dSERT inhibition. Interestingly, only high doses of ketamine caused SERT inhibition and feeding were actually decreased, likely due to its anesthetic effects. Likewise, we saw similar effects with locomotion, where 1 mM ketamine, 1 mM escitalopram, 1 mM fluoxetine, and 10 mM fluoxetine increased locomotion, but serotonin concentrations were not significantly different at these doses. However, escitalopram and fluoxetine significantly increased reuptake, unlike ketamine. Interestingly, we saw that

higher dose of each drug increased serotonin concentrations and slowed reuptake by dSERT inhibition, and decreased both feeding and locomotion. For example, 100 mM fluoxetine significantly decreased locomotion and its serotonin dynamics are very similar to 100 mM ketamine (Figure 7A-E). Thus, there is no correlation between serotonin and increased feeding and locomotion, which suggests serotonin is not the primary neurotransmitter controlling these behaviors. It is important to note that only low doses of ketamine produce antidepressant effects because higher doses act as an anesthetic.[2,42,43]

4.4.3 Comparison of ketamine and SSRI behavioral data to the literature

From our electrochemical and behavioral data, low doses of ketamine used for depression treatments do not rely on serotonin or use a SERT inhibition mechanism in *Drosophila*. Previously, the Daws group investigated the role of SERT with ketamine in mice using *in vivo* amperometry to measure serotonin changes.[44] They compared how serotonin changed in real-time with wild type (wt) mice versus SERT double knockout (-/-) mice by injecting a high dose of 32 mg/kg ketamine. This high dose did not cause serotonin concentrations to increase, but did significantly slow serotonin reuptake in the wt mice. Meanwhile, the SERT -/- mice were not affected. Low doses were not explored with either genotype. Overall, our results in *Drosophila* were similar to this mammalian data as serotonin reuptake only significantly increased with higher doses. Additionally, tail suspension tests and forced swim tests in mammals showed different effects with ketamine doses for the wt and SERT (-/-), but only the highest dose (32 mg/kg) decreased locomotion. This is similar to our higher, 100 mM dose ketamine data. The Daws group also tried a lower, 3.2 mg/kg ketamine dose and found no changes in locomotion, which is similar to our 10 mM feeding dose data. Thus, our data are similar to mammals, but also show that microdosing ketamine's antidepressant effects do not rely on serotonin or dSERT inhibition.

Compared to SSRIs, ketamine has many different effects on neuromodulatory systems, which are outlined in Table 2. Formally, ketamine is described as an NDMA receptor antagonist, which affects the glutamatergic system.[2] Although glutamate is an excitatory molecule in mammals,[45] it shows excitatory and inhibitory effects in *Drosophila* in their neuromuscular junction[46] and olfactory system,[47] respectively. Ketamine also has broad effects on mu, delta, and kappa opioid receptors in mammals that prolong its positive effects for long periods of time, as well as unclear effects on serotonin.[7] For instance, some literature suggests microdosing ketamine relies on SERT inhibition to increase serotonin concentrations after 24 hours,[2,4,8,48] while others suggest that immediate responses (≤ 24 hours) may rely more on serotonin (5-$HT_{1A,2A,2C}$) receptor inhibition or activation. However, another study with PET imaging in humans saw that SERT was 70-80% occupied by various SSRIs, but not affected by low doses of ketamine.[48] Here, the authors also suggested SERT may be inhibited by higher, anesthetic ketamine doses. Our results show that feeding larvae doses ≤ 10 mM for 24 hours does

not inhibit dSERT, and that these doses either do not affect serotonin (1 mM) or rely on a serotonin release mechanism (10 mM). Thus, future studies should also examine changes in other neurotransmitters, like glutamate and dopamine, or membrane transport proteins, like serotonin receptors.

Table 2. Antidepressant types and their mechanisms of action by neurotransmitter system or molecular target

Antidepressant	Neurotransmitter or membrane transport protein	Citation
Escitalopram	SERT 5-HT_{1A}	Mansari 2005[49]
Paroxetine	SERT Nitric oxide synthase	Stahl 1998[22]
Fluoxetine	SERT 5-HT_{2C} NET	Wong 2005[50] Owen 2001[12]
Ketamine	NMDA, AMPA receptors 5-HT_{2C} μ, δ, κ opiate receptors SERT, DAT, and NET	Kraus et al. 2019[2]

Although they are labeled as selective serotonin reuptake inhibitors, many SSRIs also modulate serotonin receptors, including receptor 5-HT_{1A} and 5-HT_{2C} (Table 2). For example, escitalopram desensitizes 5-HT_{1A} receptors over long periods of time in humans,[49,51] while fluoxetine has been shown to block 5-HT_{2C} receptors.[52] In *Drosophila*, they possess similar serotonin receptor homology to mammals, except they have fewer subtypes that include 5-$HT_{1A,\ 1B,\ 2,\ 7}$.[14,15,53,54] Previously, Silva et al. 2014 found that RNAi knockdown mutations to receptors 5-HT_{1A} and 5-HT_{7} decreased locomotion in *Drosophila* larvae, while mutations to 5-HT_{1B} did not cause any changes.[14] Additionally, Majeed et al. 2016 found through evoked excitatory postsynaptic measurements in muscle fibers that 5-HT_{2} receptor activation plays a role in sensory motor neuron circuits in *Drosophila* larvae.[15] Although we did not explore antidepressant effects with serotonin receptor mutants, our results suggest that low doses of escitalopram and fluoxetine may have downstream effects on these receptors that impact locomotion and feeding behaviors, even though they also slowed reuptake and were different from ketamine. Interestingly, our data showed that 1 mM escitalopram significantly increased feeding and locomotion, while 1 mM and 10 mM fluoxetine only increased locomotion and did not affect feeding. These data suggest that escitalopram and fluoxetine may have similar downstream effects on a specific serotonin receptor that affects locomotion, but differential effects on another target that influences feeding behaviors. Ultimately, SSRIs and ketamine may use different mechanisms, respectively, but both affect feeding and locomotion behaviors that would alleviate depression symptoms.

4.4.4 Future applications in Drosophila to understand serotonin receptor and dSERT effects with antidepressants

Although microdosing ketamine has been found to be beneficial for those who suffer from TRD,[8,43,55] it is not understood how serotonin changes over time with this treatment or in comparison to conventional SSRIs. *Drosophila melanogaster* is a beneficial model organism that can be used to measure real-time changes in serotonin with these different antidepressants without genetic manipulations to understand their individual mechanisms of action.[11,23,56] *Drosophila* is also a key model to study behavioral changes with these treatments to fundamentally understand their effects on the serotonergic system.[13–15] Our data imply that low doses of ketamine do not change serotonin, but mid-doses increase serotonin release, and do not rely on SERT inhibition except at high, anesthetic doses.[44,57] Likewise, low doses of escitalopram and fluoxetine only slowed reuptake, and showed similar feeding and locomotion effects to ketamine. It is possible that these SSRIs may have downstream effects on other neurotransmitters or membrane transport proteins that should be investigated in the future using *Drosophila* and FSCV.[4,49,51,52] Particularly, *in vivo* FSCV measurements in adult *Drosophila* could be explored to measure serotonin in 5-$HT_{1A,\ 2A,\ 2B,\ 7}$ receptor RNAi knockdowns to clarify how ketamine and SSRIs change serotonin with these genetic mutations.[58–60] In this setup, real-time locomotion and feeding behaviors could still also be investigated.[58] Novel glutamate genetic sensors, such as iGluSNFR, could also be utilized to understand how glutamate changes in real-time with these antidepressants in *Drosophila* coupled with real-time FSCV serotonin measurements.[61] In addition to serotonin receptor mutations, dSERT genetic mutations should also be considered to decipher these changes with escitalopram and fluoxetine.[13,62,63] Regardless, our work shows that ketamine's antidepressant effects do not rely on serotonin or dSERT inhibition,[44,57] which helps determine different antidepressant mechanisms that will facilitate a better understanding for their use in the treatment of depression.[64,65]

4.5 Conclusions

Overall, this work compares real-time serotonin changes with ketamine versus SSRI antidepressants, as well as changes in feeding and locomotion in *Drosophila* using FSCV and analytical behavior assays to help discern their different mechanisms of action. Initially, we constructed dose-response curves by bath-applying ketamine to *Drosophila* larvae VNC tissue compared to SSRIs (escitalopram, paroxetine, and fluoxetine) and found that it did not affect serotonin at low doses (≤ 5 μM), but inhibited SERT at higher doses (1 mM). We then fed larvae various doses (1 – 100 mM) of antidepressants for 24 hours and found that 1 mM ketamine also did not affect serotonin, but increased locomotion and feeding at this dose. At 100 mM, however, it inhibited SERT to increase serotonin and decreased locomotion and feeding, which was also similar with SSRIs. Additionally, these data suggest our

bath-application data is similar to feeding ketamine and SSRIs, as well as previous electrochemistry data collected in mammals. Low doses (≤ 10 mM) of escitalopram and fluoxetine also increased feeding and locomotion behaviors, but mainly affected reuptake without increasing serotonin. Altogether, these data suggest that increasing serotonin and SERT inhibition do not correlate to increased locomotion and feeding behavior, and that microdosing ketamine works through a different mechanism than SSRIs. Ultimately, this work shows that *Drosophila* is a good model to discern antidepressant and behavioral mechanisms with ketamine and SSRIs and future studies should investigate other neurotransmitters, such as glutamate or dopamine, as well as serotonin receptor and dSERT mutations to further understand their mechanisms of action.

4.6 References

(1) Ruberto, V. L.; Jha, M. K.; Murrough, J. W. Pharmacological Treatments for Patients with TRD. *Pharmaceuticals* **2020**, *13*, 116.
(2) Kraus, C.; Wasserman, D.; Henter, I. D.; Acevedo-Diaz, E.; Kadriu, B.; Zarate, C. A. The Influence of Ketamine on Drug Discovery in Depression. *Drug Discovery Today* **2019**, *24* (10), 2033–2043. https://doi.org/10.1016/j.drudis.2019.07.007.
(3) Berman, R. M.; Cappiello, A.; Anand, A.; Oren, D. A.; Heninger, G. R.; Charney, D. S.; Krystal, J. H. Antidepressant Effects of Ketamine in Depressed Patients. *Biological Psychiatry* **2000**, *47* (4), 351–354. https://doi.org/10.1016/S0006-3223(99)00230-9.
(4) Li, Y. F. A Hypothesis of Monoamine (5-HT) – Glutamate/GABA Long Neural Circuit: Aiming for Fast-Onset Antidepressant Discovery. *Pharmacology and Therapeutics* **2020**, *208*, 107494. https://doi.org/10.1016/j.pharmthera.2020.107494.
(5) Bowman, M. A.; Vitela, M.; Clarke, K. M.; Koek, W.; Daws, L. C. Serotonin Transporter and Plasma Membrane Monoamine Transporter Are Necessary for the Antidepressant-like Effects of Ketamine in Mice. *International Journal of Molecular Sciences* **2020**, *21* (20), 1–22. https://doi.org/10.3390/ijms21207581.
(6) Maynard, K. R.; Hill, J. L.; Calcaterra, N. E.; Palko, M. E.; Kardian, A.; Paredes, D.; Sukumar, M.; Adler, B. D.; Jimenez, D. V.; Schloesser, R. J.; Tessarollo, L.; Lu, B.; Martinowich, K. Functional Role of BDNF Production from Unique Promoters in Aggression and Serotonin Signaling. *Neuropsychopharmacology* **2016**, *41* (8), 1943–1955. https://doi.org/10.1038/npp.2015.349.
(7) West, A. M.; Holleran, K. M.; Jones, S. R. Kappa Opioid Receptors Reduce Serotonin Uptake and Escitalopram Efficacy in the Mouse Substantia Nigra Pars Reticulata. *IJMS* **2023**, *24* (3), 2080. https://doi.org/10.3390/ijms24032080.
(8) Pham, T. H.; Mendez-David, I.; Defaix, C.; Guiard, B. P.; Tritschler, L.; David, D. J.; Gardier, A. M. Ketamine Treatment Involves Medial Prefrontal Cortex Serotonin to Induce a Rapid Antidepressant-like Activity in BALB/CJ Mice. *Neuropharmacology* **2017**, *112*, 198–209. https://doi.org/10.1016/j.neuropharm.2016.05.010.
(9) Wood, K. M.; Zeqja, A.; Nijhout, H. F.; Reed, M. C.; Best, J.; Hashemi, P. Voltammetric and Mathematical Evidence for Dual Transport Mediation of Serotonin Clearance in Vivo. *Journal of Neurochemistry* **2014**, *130* (3), 351–359. https://doi.org/10.1111/jnc.12733.
(10) Ribaudo, G.; Bortoli, M.; Witt, C. E.; Parke, B.; Mena, S.; Oselladore, E.; Zagotto, G.; Hashemi, P.; Orian, L. ROS-Scavenging Selenofluoxetine Derivatives Inhibit In Vivo Serotonin Reuptake. *ACS Omega* **2021**. https://doi.org/10.1021/acsomega.1c05567.
(11) Dunham, K. E.; Venton, B. J. SSRI Antidepressants Differentially Modulate Serotonin Reuptake and Release in Drosophila. *Journal of Neurochemistry* **2022**, No. June, 1–13. https://doi.org/10.1111/jnc.15658.
(12) Owens, M. J.; Knight, D. L.; Nemeroff, C. B. Second-Generation SSRIs: Human Monoamine Transporter Binding Profile of Escitalopram and R-Fluoxetine. *Biological Psychiatry* **2001**, *50* (5), 345–350. https://doi.org/10.1016/S0006-3223(01)01145-3.
(13) Hidalgo, S.; Molina-Mateo, D.; Escobedo, P.; Zárate, R. V.; Fritz, E.; Fierro, A.; Perez, E. G.; Iturriaga-Vasquez, P.; Reyes-Parada, M.; Varas, R.; Fuenzalida-Uribe, N.; Campusano, J. M. Characterization of a Novel Drosophila SERT Mutant: Insights on the Contribution of the Serotonin Neural System to Behaviors. *ACS Chemical Neuroscience* **2017**, *8* (10), 2168–2179. https://doi.org/10.1021/acschemneuro.7b00089.
(14) Silva, B.; Goles, N. I.; Varas, R.; Campusano, J. M. Serotonin Receptors Expressed in Drosophila Mushroom Bodies Differentially Modulate Larval Locomotion. *PLoS ONE* **2014**, *9* (2). https://doi.org/10.1371/journal.pone.0089641.

(15) Majeed, Z. R.; Abdeljaber, E.; Soveland, R.; Cornwell, K.; Bankemper, A.; Koch, F.; Cooper, R. L. Modulatory Action by the Serotonergic System: Behavior and Neurophysiology in Drosophila Melanogaster. *Neural Plasticity* **2016**, *2016*. https://doi.org/10.1155/2016/7291438.
(16) Dunham, K. E.; Venton, B. J. Improving Serotonin Fast-Scan Cyclic Voltammetry Detection: New Waveforms to Reduce Electrode Fouling. *Analyst* **2020**, *145* (22), 7437–7446. https://doi.org/10.1039/d0an01406k.
(17) Hashemi, P.; Dankoski, E. C.; Lama, R.; Wood, K. M.; Takmakov, P.; Wightman, R. M. Brain Dopamine and Serotonin Differ in Regulation and Its Consequences. *Proceedings of the National Academy of Sciences of the United States of America* **2012**, *109* (29), 11510–11515. https://doi.org/10.1073/pnas.1201547109.
(18) Saylor, R. A.; Hersey, M.; West, A.; Buchanan, A. M.; Berger, S. N.; Nijhout, H. F.; Reed, M. C.; Best, J.; Hashemi, P. In Vivo Hippocampal Serotonin Dynamics in Male and Female Mice: Determining Effects of Acute Escitalopram Using Fast Scan Cyclic Voltammetry. *Frontiers in Neuroscience* **2019**, *13* (APR), 1–13. https://doi.org/10.3389/fnins.2019.00362.
(19) Hashemi, P.; Dankoski, E. C.; Petrovic, J.; Keithley, R. B.; Wightman, R. M. Voltammetric Detection of 5-Hydroxytryptamine Release in the Rat Brain. *Analytical Chemistry* **2009**, *81* (22), 9462–9471. https://doi.org/10.1021/ac9018846.
(20) Wood, K. M.; Hashemi, P. Fast-Scan Cyclic Voltammetry Analysis of Dynamic Serotonin Reponses to Acute Escitalopram. *ACS Chemical Neuroscience* **2013**, *4* (5), 715–720. https://doi.org/10.1021/cn4000378.
(21) Zhong, H.; Sánchez, C.; Caron, M. G. Consideration of Allosterism and Interacting Proteins in the Physiological Functions of the Serotonin Transporter. *Biochemical Pharmacology* **2012**, *83* (4), 435–442. https://doi.org/10.1016/j.bcp.2011.09.020.
(22) Stahl, S. M. Mechanism of Action of Serotonin Selective Reuptake Inhibitors. *Journal of Affective Disorders* **1998**, *51* (3), 215–235. https://doi.org/10.1016/S0165-0327(98)00221-3.
(23) Kasture, A. S.; Hummel, T.; Sucic, S.; Freissmuth, M. Big Lessons from Tiny Flies: Drosophila Melanogaster as a Model to Explore Dysfunction of Dopaminergic and Serotonergic Neurotransmitter Systems. *International Journal of Molecular Sciences* **2018**, *19* (6). https://doi.org/10.3390/ijms19061788.
(24) Tadres, D.; Louis, M. PiVR: An Affordable and Versatile Closed-Loop Platform to Study Unrestrained Sensorimotor Behavior. *PLoS Biology* **2020**, *18* (7), 1–25. https://doi.org/10.1371/journal.pbio.3000712.
(25) Shell, B. C.; Schmitt, R. E.; Lee, K. M.; Johnson, J. C.; Chung, B. Y.; Pletcher, S. D.; Grotewiel, M. Measurement of Solid Food Intake in Drosophila via Consumption-Excretion of a Dye Tracer. *Scientific Reports* **2018**, *8* (1), 1–13. https://doi.org/10.1038/s41598-018-29813-9.
(26) Shell, B. C.; Luo, Y.; Pletcher, S.; Grotewiel, M. Expansion and Application of Dye Tracers for Measuring Solid Food Intake and Food Preference in Drosophila. *Scientific Reports* **2021**, *11* (1), 1–13. https://doi.org/10.1038/s41598-021-99483-7.
(27) Shell, B. C.; Grotewiel, M. Identification of Additional Dye Tracers for Measuring Solid Food Intake and Food Preference via Consumption-Excretion in Drosophila. *Scientific Reports* **2022**, *12* (1), 1–12. https://doi.org/10.1038/s41598-022-10252-6.
(28) Ries, A. S.; Hermanns, T.; Poeck, B.; Strauss, R. Serotonin Modulates a Depression-like State in Drosophila Responsive to Lithium Treatment. *Nature Communications* **2017**, *8*, 1–11. https://doi.org/10.1038/ncomms15738.
(29) Borue, X.; Condron, B.; Venton, B. J. Both Synthesis and Reuptake Are Critical for Replenishing the Releasable Serotonin Pool in Drosophila. *Journal of Neurochemistry* **2010**, *113* (1), 188–199. https://doi.org/10.1111/j.1471-4159.2010.06588.x.
(30) Borue, X.; Cooper, S.; Hirsh, J.; Condron, B.; Venton, B. J. Quantitative Evaluation of Serotonin Release and Clearance in Drosophila. *Journal of Neuroscience Methods* **2009**, *179* (2), 300–308. https://doi.org/10.1016/j.jneumeth.2009.02.013.
(31) Privman, E.; Venton, B. J. Comparison of Dopamine Kinetics in the Larval Drosophila Ventral Nerve Cord and Protocerebrum with Improved Optogenetic Stimulation. *Journal of Neurochemistry* **2015**, *135* (4), 695–704. https://doi.org/10.1111/jnc.13286.
(32) Shell, B. C.; Schmitt, R. E.; Lee, K. M.; Johnson, J. C.; Chung, B. Y.; Pletcher, S. D.; Grotewiel, M. Measurement of Solid Food Intake in Drosophila via Consumption-Excretion of a Dye Tracer. *Scientific Reports* **2018**, *8* (1), 1–13. https://doi.org/10.1038/s41598-018-29813-9.
(33) Xiao, N.; Privman, E.; Venton, B. J. Optogenetic Control of Serotonin and Dopamine Release in Drosophila Larvae. *ACS Chemical Neuroscience* **2014**, *5* (8), 666–673. https://doi.org/10.1021/cn500044b.
(34) Currie, G. M. Pharmacology, Part 1: Introduction to Pharmacology and Pharmacodynamics. *Journal of Nuclear Medicine Technology* **2018**, *46* (2), 81–86. https://doi.org/10.2967/jnmt.117.199588.
(35) De Vry, J.; Schreiber, R. Effects of Selected Serotonin 5-HT1 and 5-HT2 Receptor Agonists on Feeding Behavior: Possible Mechanisms of Action. *Neuroscience and Biobehavioral Reviews* **2000**, *24* (3), 341–353. https://doi.org/10.1016/S0149-7634(99)00083-4.
(36) Keszthelyi, D.; Troost, F. J.; Masclee, A. A. M. Understanding the Role of Tryptophan and Serotonin Metabolism in Gastrointestinal Function. *Neurogastroenterology and Motility* **2009**, *21* (12), 1239–1249. https://doi.org/10.1111/j.1365-2982.2009.01370.x.
(37) Reis, M.; Aamo, T.; Spigset, O.; Ahlner, J. Serum Concentrations of Antidepressant Drugs in a Naturalistic Setting: Compilation Based on a Large Therapeutic Drug Monitoring Database. *Therapeutic Drug Monitoring* **2009**, *31* (1), 42–56. https://doi.org/10.1097/FTD.0b013e31819114ea.

(38) Robison, R.; Lafrance, A.; Brendle, M.; Smith, M.; Moore, C.; Ahuja, S.; Richards, S.; Hawkins, N.; Strahan, E. A Case Series of Group-Based Ketamine-Assisted Psychotherapy for Patients in Residential Treatment for Eating Disorders with Comorbid Depression and Anxiety Disorders. *Journal of Eating Disorders* **2022**, *10* (1), 1–9. https://doi.org/10.1186/s40337-022-00588-9.
(39) Schwartz, T.; Trunko, M. E.; Feifel, D.; Lopez, E.; Peterson, D.; Frank, G. K. W.; Kaye, W. A Longitudinal Case Series of IM Ketamine for Patients with Severe and Enduring Eating Disorders and Comorbid Treatment-Resistant Depression. *Clinical Case Reports* **2021**, *9* (5), 1–7. https://doi.org/10.1002/ccr3.3869.
(40) Ragnhildstveit, A.; Slayton, M.; Jackson, L. K.; Brendle, M.; Ahuja, S.; Holle, W.; Moore, C.; Sollars, K.; Seli, P.; Robison, R. Ketamine as a Novel Psychopharmacotherapy for Eating Disorders: Evidence and Future Directions. *Brain Sciences* **2022**, *12* (3). https://doi.org/10.3390/brainsci12030382.
(41) Irifune, M.; Shimizu, T.; Nomoto, M. Ketamine-Induced Hyperlocomotion Associated with Alteration of Presynaptic Components of Dopamine Neurons in the Nucleus Accumbens of Mice. *Pharmacology Biochemistry and Behavior* **1991**, *40* (2), 399–407. https://doi.org/10.1016/0091-3057(91)90571-I.
(42) Stahl, S. M. Mechanism of Action of Ketamine. *CNS Spectrums* **2013**, *18* (4), 171–174. https://doi.org/10.1017/S109285291300045X.
(43) Zanos, P.; Thompson, S. M.; Duman, R. S.; Zarate, C. A.; Gould, T. D. Convergent Mechanisms Underlying Rapid Antidepressant Action. *CNS Drugs* **2018**, *32* (3), 197–227. https://doi.org/10.1007/s40263-018-0492-x.
(44) Bowman, M. A.; Vitela, M.; Clarke, K. M.; Koek, W.; Daws, L. C. Serotonin Transporter and Plasma Membrane Monoamine Transporter Are Necessary for the Antidepressant-like Effects of Ketamine in Mice. *International Journal of Molecular Sciences* **2020**, *21* (20), 1–22. https://doi.org/10.3390/ijms21207581.
(45) Galvanho, J. P.; Manhães, A. C.; Carvalho-Nogueira, A. C. C.; Silva, J. de M.; Filgueiras, C. C.; Abreu-Villaça, Y. Profiling of Behavioral Effects Evoked by Ketamine and the Role of 5HT2 and D2 Receptors in Ketamine-Induced Locomotor Sensitization in Mice. *Progress in Neuro-Psychopharmacology and Biological Psychiatry* **2020**, *97*, 109775. https://doi.org/10.1016/j.pnpbp.2019.109775.
(46) Zimmerman, J. E.; Chan, M. T.; Lenz, O. T.; Keenan, B. T.; Maislin, G.; Pack, A. I. Glutamate Is a Wake-Active Neurotransmitter in Drosophila Melanogaster. *Sleep* **2017**, *40* (2). https://doi.org/10.1093/sleep/zsw046.
(47) Liu, W. W.; Wilson, R. I. Glutamate Is an Inhibitory Neurotransmitter in the *Drosophila* Olfactory System. *Proc. Natl. Acad. Sci. U.S.A.* **2013**, *110* (25), 10294–10299. https://doi.org/10.1073/pnas.1220560110.
(48) Spies, M.; James, G. M.; Berroterán-Infante, N.; Ibeschitz, H.; Kranz, G. S.; Unterholzner, J.; Godbersen, M.; Gryglewski, G.; Hienert, M.; Jungwirth, J.; Pichler, V.; Reiter, B.; Silberbauer, L.; Winkler, D.; Mitterhauser, M.; Stimpfl, T.; Hacker, M.; Kasper, S.; Lanzenberger, R. Assessment of Ketamine Binding of the Serotonin Transporter in Humans with Positron Emission Tomography. *International Journal of Neuropsychopharmacology* **2018**, *21* (2), 145–153. https://doi.org/10.1093/ijnp/pyx085.
(49) El Mansari, M.; Sánchez, C.; Chouvet, G.; Renaud, B.; Haddjeri, N. Effects of Acute and Long-Term Administration of Escitalopram and Citalopram on Serotonin Neurotransmission: An In Vivo Electrophysiological Study in Rat Brain. *Neuropsychopharmacol* **2005**, *30* (7), 1269–1277. https://doi.org/10.1038/sj.npp.1300686.
(50) Wong, D. T.; Perry, K. W.; Bymaster, F. P. The Discovery of Fluoxetine Hydrochloride (Prozac). *Nature Reviews Drug Discovery* **2005**, *4* (12), 950. https://doi.org/10.1038/nrd1821.
(51) Fakhoury, M. Revisiting the Serotonin Hypothesis: Implications for Major Depressive Disorders. *Molecular Neurobiology* **2016**, *53* (5), 2778–2786. https://doi.org/10.1007/s12035-015-9152-z.
(52) Ni, Y. G.; Miledi, R. Blockage of 5HT $_{2C}$ Serotonin Receptors by Fluoxetine (Prozac). *Proc. Natl. Acad. Sci. U.S.A.* **1997**, *94* (5), 2036–2040. https://doi.org/10.1073/pnas.94.5.2036.
(53) Tierney, A. J. Invertebrate Serotonin Receptors: A Molecular Perspective on Classification and Pharmacology. *Journal of Experimental Biology* **2018**, *221* (19), 1–11. https://doi.org/10.1242/jeb.184838.
(54) Hauser, F.; Cazzamali, G.; Williamson, M.; Blenau, W.; Grimmelikhuijzen, C. J. P. A Review of Neurohormone GPCRs Present in the Fruitfly Drosophila Melanogaster and the Honey Bee Apis Mellifera. *Progress in Neurobiology* **2006**, *80* (1), 1–19. https://doi.org/10.1016/j.pneurobio.2006.07.005.
(55) Mathew, S. J.; Zarate, C. A. Ketamine for Treatment-Resistant Depression: The First Decade of Progress. *Ketamine for Treatment-Resistant Depression: The First Decade of Progress* **2016**, 1–155. https://doi.org/10.1007/978-3-319-42925-0.
(56) Yang, Z.; Bertolucci, F.; Wolf, R.; Heisenberg, M. Flies Cope with Uncontrollable Stress by Learned Helplessness. *Current Biology* **2013**, *23* (9), 799–803. https://doi.org/10.1016/j.cub.2013.03.054.
(57) Stahl, S. M. Mechanism of Action of Ketamine. *CNS Spectrums* **2013**, *18* (4), 171–174. https://doi.org/10.1017/S109285291300045X.
(58) Shin, M.; Venton, B. J. Fast-Scan Cyclic Voltammetry (FSCV) Reveals Behaviorally-Evoked Dopamine Release by Sugar Feeding in Adult Drosophila Mushroom Body. *Angewandte Chemie International Edition* **2022**, *n/a* (n/a). https://doi.org/10.1002/anie.202207399.

(59) Perkins, L. A.; Holderbaum, L.; Tao, R.; Hu, Y.; Sopko, R.; McCall, K.; Yang-Zhou, D.; Flockhart, I.; Binari, R.; Shim, H. S.; Miller, A.; Housden, A.; Foos, M.; Randkelv, S.; Kelley, C.; Namgyal, P.; Villalta, C.; Liu, L. P.; Jiang, X.; Huan-Huan, Q.; Wang, X.; Fujiyama, A.; Toyoda, A.; Ayers, K.; Blum, A.; Czech, B.; Neumuller, R.; Yan, D.; Cavallaro, A.; Hibbard, K.; Hall, D.; Cooley, L.; Hannon, G. J.; Lehmann, R.; Parks, A.; Mohr, S. E.; Ueda, R.; Kondo, S.; Ni, J. Q.; Perrimon, N. The Transgenic RNAi Project at Harvard Medical School: Resources and Validation. *Genetics* **2015**, *201* (3), 843–852. https://doi.org/10.1534/genetics.115.180208.

(60) Hidalgo, S.; Fuenzalida-Uribe, N.; Molina-Mateo, D.; Escobar, A. P.; Oliva, C.; España, R. A.; Andrés, M. E.; Campusano, J. M. Study of the Release of Endogenous Amines in Drosophila Brain in Vivo in Response to Stimuli Linked to Aversive Olfactory Conditioning. *Journal of Neurochemistry* **2020**, 0–1. https://doi.org/10.1111/jnc.15109.

(61) Richter, F. G.; Fendl, S.; Haag, J.; Drews, M. S.; Borst, A. Glutamate Signaling in the Fly Visual System. *iScience* **2018**, *7*, 85–95. https://doi.org/10.1016/j.isci.2018.08.019.

(62) Murphy, S. E.; Norbury, R.; Godlewska, B. R.; Cowen, P. J.; Mannie, Z. M.; Harmer, C. J.; Munafò, M. R. The Effect of the Serotonin Transporter Polymorphism (5-HTTLPR) on Amygdala Function: A Meta-Analysis. *Molecular Psychiatry* **2013**, *18* (4), 512–520. https://doi.org/10.1038/mp.2012.19.

(63) Murphy, D. L.; Li, Q.; Engel, S.; Wichems, C.; Andrews, A.; Lesch, K. P.; Uhl, G. Genetic Perspectives on the Serotonin Transporter. *Brain Research Bulletin* **2001**, *56* (5), 487–494. https://doi.org/10.1016/S0361-9230(01)00622-0.

(64) Ruberto, V. L.; Jha, M. K.; Murrough, J. W. Pharmacological Treatments for Patients with TRD. *Pharmaceuticals* **2020**, *13*, 116.

(65) Coplan, J. D.; Gopinath, S.; Abdallah, C. G.; Berry, B. R. A Neurobiological Hypothesis of Treatment-Resistant Depression-Mechanisms for Selective Serotonin Reuptake Inhibitor Non-Efficacy. *Frontiers in Behavioral Neuroscience* **2014**, *8* (MAY), 1–16. https://doi.org/10.3389/fnbeh.2014.00189.

Chapter 5

Conclusions and Future Directions

5.1 Contributions of this dissertation to the field

In this thesis, we improved serotonin fast-scan cyclic voltammetry (FSCV) detection at carbon-fiber microelectrodes and used these methods to elucidate different antidepressant mechanisms of action in *Drosophila*. This chapter summarizes major conclusions from these works and proposes future studies in *Drosophila* that will utilize new tools for *in vivo* adult FSCV detection and imaging with genetic sensors to further investigate antidepressants and downstream behaviors with genetic mutations to the serotonergic system.

5.1.1 Improved fast-scan cyclic voltammetry waveforms for serotonin and dopamine detection

In Chapter 2, we used different FSCV waveforms to improve electrode fouling by serotonin and its major metabolite, 5-hydroxyindoleacetic acid (5-HIAA). In previous FSCV research, modified dopamine waveforms with extended switching potentials (≥ 1.3 V)[1] and extended holds (≥ 1 ms)[2,3] increased dopamine sensitivity and reduced electrode fouling. However, the Jackson waveform that is commonly used for serotonin detection had not been revisited in more than 25 years.[4,5] In this chapter, we analyzed repeated measurement and long-term electrode fouling to serotonin and 5-HIAA with four waveforms. [6] We found that the extended 1.3 V waveforms decreased electrode fouling by 50% for both serotonin and dopamine. However, the dopamine waveform eliminated electrode fouling because of its negative holding potential and 1.3 V switching potential.[1,7] Additionally, all extended switching potential waveforms increased both serotonin and dopamine sensitivity,[1] but the Jackson waveform was the most selective for serotonin.[5] We also characterized serotonin detection *in vitro* in fruit fly larvae VNC tissue and found that electrodes do not foul with repeated optogenetic stimulations,[8,9] which shows that *Drosophila melanogaster* is a beneficial model to measure serotonin. This work provides a tool-box of serotonin waveforms to measure serotonin in different experiments where high sensitivity or selectivity is needed, or no electrode fouling is required.[6]

Several groups have been inspired by our extended serotonin waveform work, either to use the new waveform for biological applications or to study new electrochemical waveforms for serotonin. Stucky and Johnson found that our new extended serotonin waveform did not foul electrodes with the SSRIs fluoxetine, escitalopram, or sertraline.[12] However, the typical Jackson waveform with bare and Nafion-coated CFMEs fouled electrodes significantly with these SSRIs. In Movassaghi *et al.* 2021,[10] they used rapid pulse voltammetry and FSCV waveforms to monitor both dopamine and serotonin across different timescales and saw that the extended 1.3 V switching potential was required to increase serotonin sensitivity compared to dopamine. Likewise, in Shin *et al.* 2021,[11] they created new N-shaped multiple square wave voltammetry waveforms and found that applying a negative holding potential decreased electrode fouling. Together, these works show that serotonin and dopamine can be measured simultaneously with different waveform

parameters, and that our new extended serotonin waveform is useful for pharmacology studies because of its anti-fouling properties and increased sensitivity.

5.1.2 Using serotonin FSCV detection to elucidate different antidepressant mechanisms of action and their downstream effects on behaviors

In Chapter 3, we used FSCV and optogenetics to compare serotonin concentration and reuptake changes with four common SSRIs: fluoxetine, escitalopram, paroxetine, and citalopram in *Drosophila* larvae.[13] We found that fluoxetine increased reuptake from 1-100 µM, but serotonin concentrations only increase at 100 µM.[13–15] Thus, fluoxetine occupies dSERT and slows clearance, but does not affect concentration. Escitalopram and paroxetine increased serotonin concentrations at all doses, but escitalopram dramatically increased reuptake more.[13,16,17] Citalopram showed lower concentration changes and faster reuptake profiles compared to escitalopram, so the racemic mixture of citalopram does not change reuptake as much as the *S*-isomer.[18,19] Dose-response curves also showed paroxetine displayed the highest dSERT affinity and fluoxetine the lowest.[20,21] These data demonstrate SSRI mechanisms are complex, with separate effects on reuptake or release. Previous FSCV data collected in mammals also showed similar serotonin changes in both models.[15–17] This work establishes how antidepressants affect serotonin in real-time, which is useful for future studies that will investigate pharmacological effects of SSRIs with different genetic mutations in *Drosophila*.

Chapter 4 explores changes in real-time serotonin dynamics with ketamine compared to SSRIs to determine how they contribute to their different mechanisms of action.[22–24] Formally, ketamine is classified as an NMDA antagonist, but it has unclear effects on the serotonergic system.[22] It is not understood how serotonin changes in real-time or how real-time locomotion and feeding behaviors change with these treatments.[14,22,25,26] In this chapter, we measured and characterized serotonin changes with FSCV, and tracked real-time locomotion and feeding behaviors with Raspberry Pi Virtual Reality (PiVR)[27] and Ultraviolet-Visible (UV-Vis) Spectroscopy.[28] We fed larvae various doses (1 – 100 mM) of antidepressants (ketamine, escitalopram, paroxetine, and fluoxetine) for 24 hours. Here, we found that ketamine does not affect serotonin concentration or reuptake at low doses (1 mM). However, ketamine does increase serotonin release at mid-doses and inhibits serotonin reuptake at higher, anesthetic doses.[29] Additionally, all SSRIs inhibited dSERT to increase serotonin reuptake, but yielded different concentration changes because of their different SERT affinities that were similar to our previous bath-applications in Chapter 3.[13] There were also dose-dependent effects, as low doses of escitalopram and fluoxetine inhibited dSERT, but did not affect serotonin concentrations. For behavior, low doses of ketamine, escitalopram, and fluoxetine (1 mM) significantly increased feeding and locomotion behaviors, while higher doses (100 mM) of

ketamine and fluoxetine decreased them.[14,29] These data suggest ketamine's mechanism of action is complex and different from SSRI antidepressants. Specifically, ketamine does not increase serotonin release or inhibit dSERT at micro-doses. Additionally, the locomotion and feeding behavior changes suggest different downstream effects with glutamate, 5-HT receptors, or dSERT.[14,25,26] Ultimately, this work shows that *Drosophila* is a good model system to study complex mechanisms of different types of antidepressants, and future studies should investigate real-time, multiplexed changes in glutamate and serotonin for these antidepressants.[30,31]

5.2 Challenges and future directions

5.2.1 Investigating D. melanogaster serotonin transporter mutations to understand genetic and behavior effects with ketamine and SSRIs

From our research in Chapters 3-4, a logical next step would be to investigate serotonin dynamic changes from SSRIs and ketamine with serotonin transporter (SERT) mutations in *Drosophila* larvae. Currently, we have two *Drosophila* SERT mutants that are illustrated in Figure 1 and described in Table 1. Previously, the Bellen group created a SERT mutant that features a Minos Transposon cassette with 3 stop codons that do not allow the gene to be translated after exon 2, which we denote as mutant #1.[32] Meanwhile, our collaborator, Jeff Copeland (Eastern Mennonite University, Biology) has created a partial SERT knockout using CRISPR Cas9 that is denoted as mutant #2. Here, CRISPR was used to remove the transcribed gene after exon 3. For both mutants, they possess one copy and are heterozygous because the homozygous phenotype is lethal. These mutants can be easily crossed with balancer fly lines (i.e., curly wings and tubby larvae on chromosomes 2 and 3, respectively) to make UAS-CsChrimson and Trh-Gal4 lines that contain the serotonin transporter mutation on chromosome 2. These flies could then be utilized to measure serotonin dynamic changes with these mutations using FSCV and optogenetics similar to Chapters 3-4.

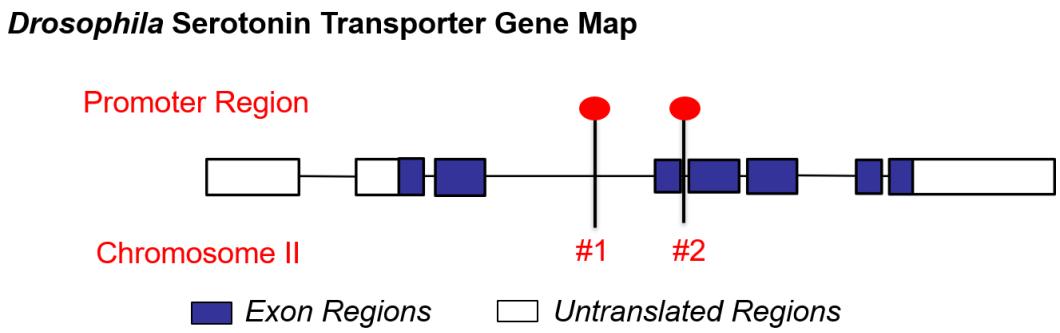

Figure 1. *Drosophila* serotonin transporter (SERT) gene map. Map shows placement of genetic mutations on chromosome 2. Mutation 1 was created by the Bellen lab and features a Minos Transposon cassette with 3 stop codons that do not allow the gene to be translated after exon 2. Mutation 2 is a partial knock out designed by Jeff Copeland (Easter Mennonite University) created with CRISPR Cas9. It only allows transcription and translation to exon 3.

Table 1. *Drosophila* serotonin transporter mutant characterizations

Mutant #	Genetic characterization	Reference
1 BL #36004	MI02578 (Minos Transposon) Splice acceptor with 3 STOP Codons	Nagar-Jaiswal et al. 2015[32] Hidalgo et al. 2017[14]
2	CRISPR-Cas9 Partial Knock Out	Dr. Jeff Copeland Eastern Mennonite University

We have also performed preliminary feeding and locomotion assays in mutant #1 using the methods described in Chapter 4. Figure 2A shows the mass of food eaten per larva per day for mutant #1 with 1 mM ketamine, escitalopram, and fluoxetine compared to a control genotype (Trh-Gal4, data in Chapter 4). There were significant effects of drug type (Two-Way ANOVA, $F_{(3,32)} = 553.5$, $p \leq 0.0001$, $n = 5$) and genotype ($F_{(3,32)} = 132.0$, $p \leq 0.0001$) on the amount of food eaten. Tukey's post-hoc test revealed there were no significant differences in food eaten with the control (PBS) between the genotypes ($p \geq 0.6305$). Additionally, the SERT mutants ate less food with 1 mM ketamine ($p \leq 0.0001$) and escitalopram ($p \leq 0.01$) compared to the control. However, the mutants also ate more food with 1 mM fluoxetine compared to the control ($p \leq 0.0001$). Although the amount of food eaten was different for each drug, the SERT mutant followed the same general trend with 1 mM ketamine and escitalopram where it increased the amount of food eaten, even though it was less than the control. Together, this data implies that this partial dSERT knockout does not change feeding without antidepressants (PBS), but does decrease feeding compared to the control genotype with ketamine and escitalopram.

Possible, SERT inhibition or concentration may change, which could decrease this behavior, similar to what we saw with higher antidepressant doses. Interestingly, fluoxetine increased feeding in the mutant compared to the control genotype, which should be explored with serotonin and other neurotransmitter measurements to understand how this behavior changed.

Figure 2B compares the distance traveled for mutant #1 with 1 mM ketamine, escitalopram, and fluoxetine compared to the control genotype. There were significant effects of drug type (Two-Way ANOVA, $F_{(3,232)} = 136.2$, $p \leq 0.0001$, $n = 30$) and genotype ($F_{(3,232)} = 176.1$, $p \leq 0.0001$) on distance traveled. Tukey's post-hoc test revealed the SERT mutant traveled significantly less than the control with only PBS (control, $p \leq 0.01$). Similarly, locomotion also significantly decreased with the SERT mutant with ketamine, escitalopram, and fluoxetine (all $p \leq 0.0001$) compared to the control genotype. Although the SERT mutant decreased locomotion compared to the control genotype, it follows the same trend where the distance traveled increased with each drug, even though it was less than the control. Ultimately, these preliminary results show that dSERT plays a role in locomotion. Specifically, this dSERT partial knockout significantly decreases locomotion with and without antidepressants, which should be characterized in the future by measuring serotonin changes with *Drosophila* larvae and FSCV with optogenetics.

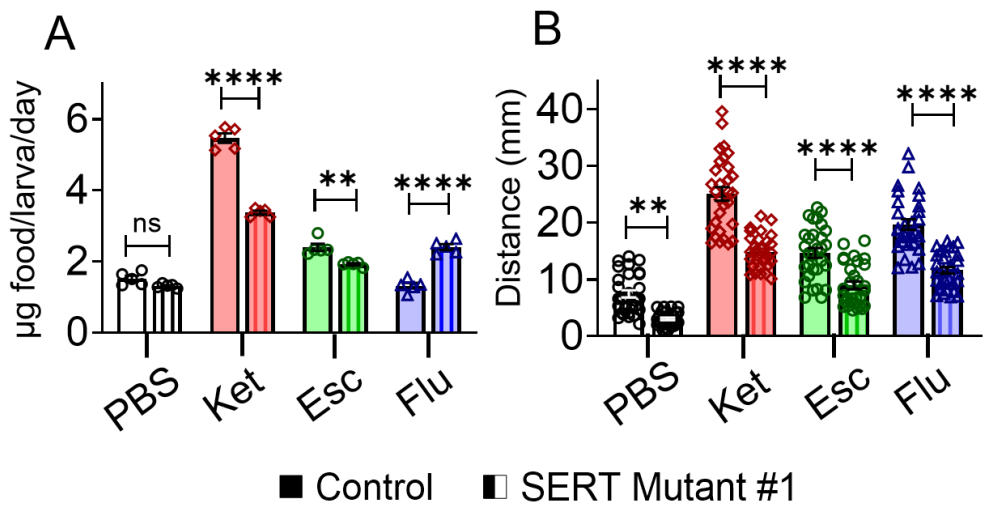

Figure 2. Feeding and locomotion behavior comparisons between SERT mutant #1 and control genotype (Trh-Gal4, Chapter 4). A. Feeding data. B. Locomotion data

5.2.2 Using in vivo FSCV serotonin detection and glutamate genetic sensors to explore SERT and serotonin receptor genetic effects with ketamine and SSRIs

Along with the experiments described previously in *Drosophila* larvae, a logical next step for our research would be to measure serotonin in *Drosophila* adults. Figure 3A-C shows Trh-Gal4 driven GFP expression (green), as well as 5-HT immunostaining (red) in a *Drosophila* adult.[33] Figure 3A shows serotonin neurons innervate the gut and olfactory regions in the adult brain and ventral nerve

cord.[33] Likewise, Figure 3B-C show anterior and posterior images of the adult brain where most serotonin neurons are located in the mushroom body, antennal lobes, and sub-esophageal ganglion region.[33,34] Initial experiments will use acetylcholine to stimulate serotonin release that will be measured with FSCV.[35] Acetylcholine-stimulated neurotransmitter release is not specific and other analytes, like dopamine and octopamine, may be released with serotonin.[35–37] A selective waveform, such as the extended serotonin waveform or Jackson waveform,[6] will be able to differentiate serotonin from these analytes. These experiments will enable real-time, selective serotonin detection in the adult fly brain for the first time, and these methods could be used for a variety of pharmacological and behavioral studies. For example, serotonin measurements could be linked to feeding or locomotion to understand its fundamental role in these processes. Likewise, depression-related aging effects could be investigated more easily in *Drosophila* adults that include changes in sleep-wake cycles or with downstream behaviors in feeding and locomotion.

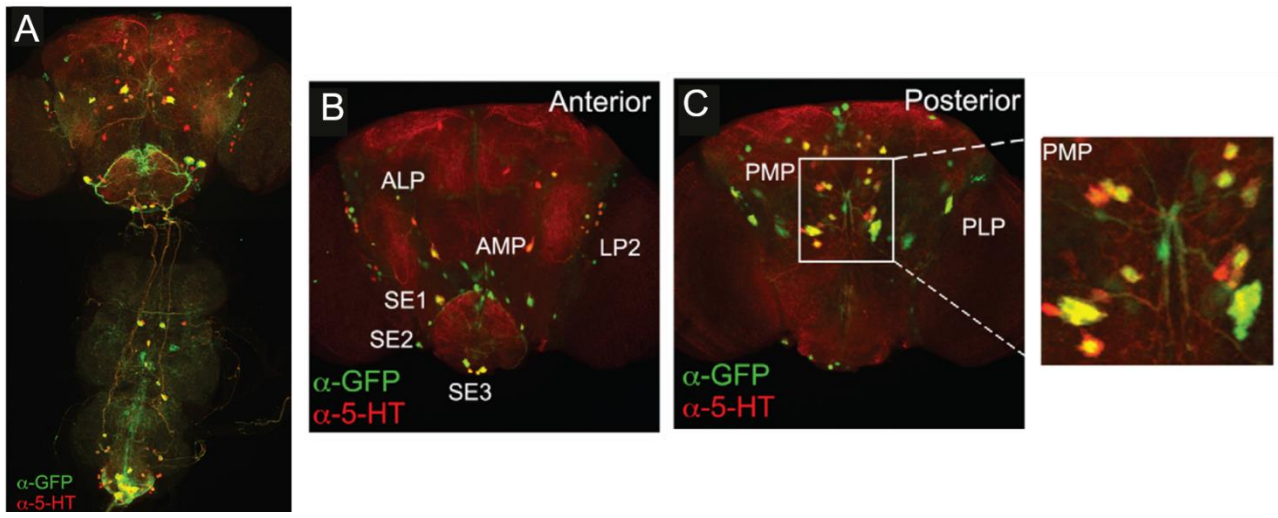

Figure 3. Trh-Gal4 driven GFP expression and 5-HT immunostaining in adult *Drosophila*. **A.** Trh-Gal4 (3rd chromosome) driven mCD8:GFP signals (green) and 5-HT immunostaining (red) in an adult male brain. Serotonin neuron locations in adult *Drosophila* brain in the **(B)** anterior adult brain **(C)** posterior positions. Taken from Alekseyenko OV, Lee C, Kravitz EA (2010) Targeted Manipulation of Serotonergic Neurotransmission Affects the Escalation of Aggression in Adult Male Drosophila melanogaster. PLoS ONE 5(5): e10806. doi:10.1371/journal.pone.0010806

After successfully measuring acetylcholine-stimulated serotonin release in adult *Drosophila*, the next step of our research will be *in vivo* serotonin detection with FSCV. Figure 4A-B shows the setup and CFME implantation into an awake, immobilized adult *Drosophila* fly.[38] Here, a fly is immobilized in a chamber that allows for real-time monitoring of locomotion or feeding behaviors (Fig. 4A). A part of the cuticle is carefully removed and a capillary with acetylcholine and a CFME are inserted into the brain. *In vivo* detection will allow us to monitor real-time behavioral changes that are coupled to serotonin. This methodological setup will also allow us to more easily investigate 5-HT 1A, 1B, 2A, 2B, and 7 RNAi receptor knockdowns and their effects on serotonin and these

behaviors.[25,39,40] In addition to 5-HT receptor mutations, dSERT mutants could be studied. With these genetic mutants, SSRIs and ketamine should be explored to understand their effects on lower, micro-doses to elucidate if they play a role in their mechanisms of action and downstream behaviors.[22] Compared to larvae, adult experiments will also allow monitoring long-term changes of feeding antidepressants or age-related effects.[41]

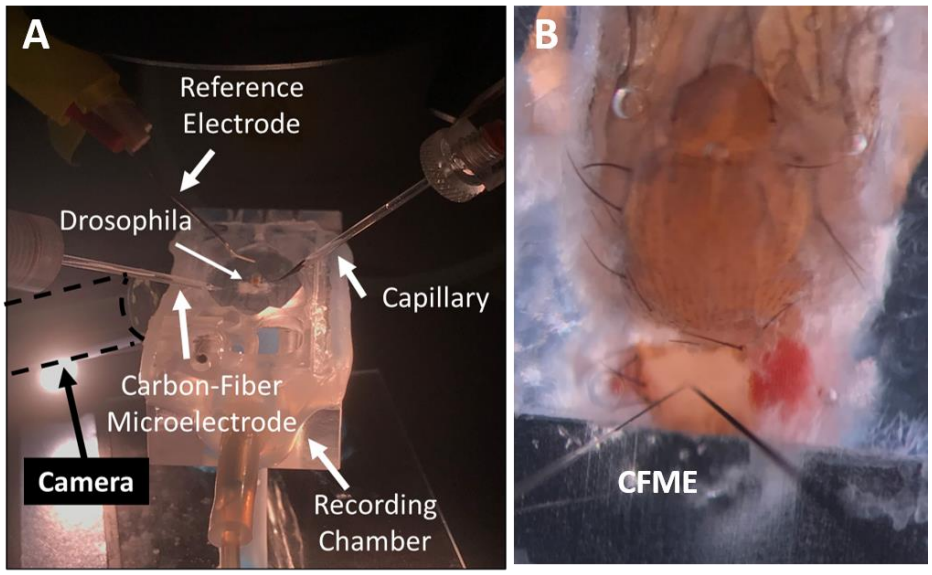

Figure 4. *In vivo* FSCV adult *Drosophila* brain preparation. **A.** Picture of setup of *in vivo* FSCV measurements in adult fly brain. **B.** An anesthetized fly was immobilized in a recording chamber, and the cuticle of dorsal head was removed to expose the brain. A CFME and a capillary filled with acetylcholine were implemented in the medial tip of the MB. Taken from Shin and Venton. *Angew. Chem. Int.* Ed. 2022, 61, doi.org/10.1002/anie.202207399

In addition to FSCV serotonin measurement in adult *Drosophila*, a next step would be to multiplex FSCV measurement with the glutamate fluorescent sensor, iGluSnFR.[42,43] Compared to other neurotransmitters, glutamate is not electroactive and cannot be measured with FSCV. However, the iGluSnFR genetic sensor allows for the temporal and spatial measurement of glutamate from a glutamate-binding protein coupled to a fluorescence signal, which is shown in Figure 5. Here, 2-photon microscopy is used to allow fast, high-resolution imaging *in vitro* or *in vivo* in *Drosophila*. In these experiments, the FSCV extended serotonin or Jackson waveform could be used to measure serotonin and microscopy to measure iGluSnFR fluorescence. This will also be used to explore the genetic mutations described previously with micro-doses of ketamine and SSRIs with their mechanisms and behaviors. Altogether, these novel methods will allow us to discern how glutamate modulates serotonin in *Drosophila* with different antidepressant treatments, which will be useful in understanding how ketamine is different to SSRIs, especially at low doses, and effects with genetic mutations to the

serotonergic system. Ultimately, this work is valuable because it is easier to create genetic mutations and use genetic sensors in *Drosophila*, which will benefit future research with glutamate and serotonin in mammals.

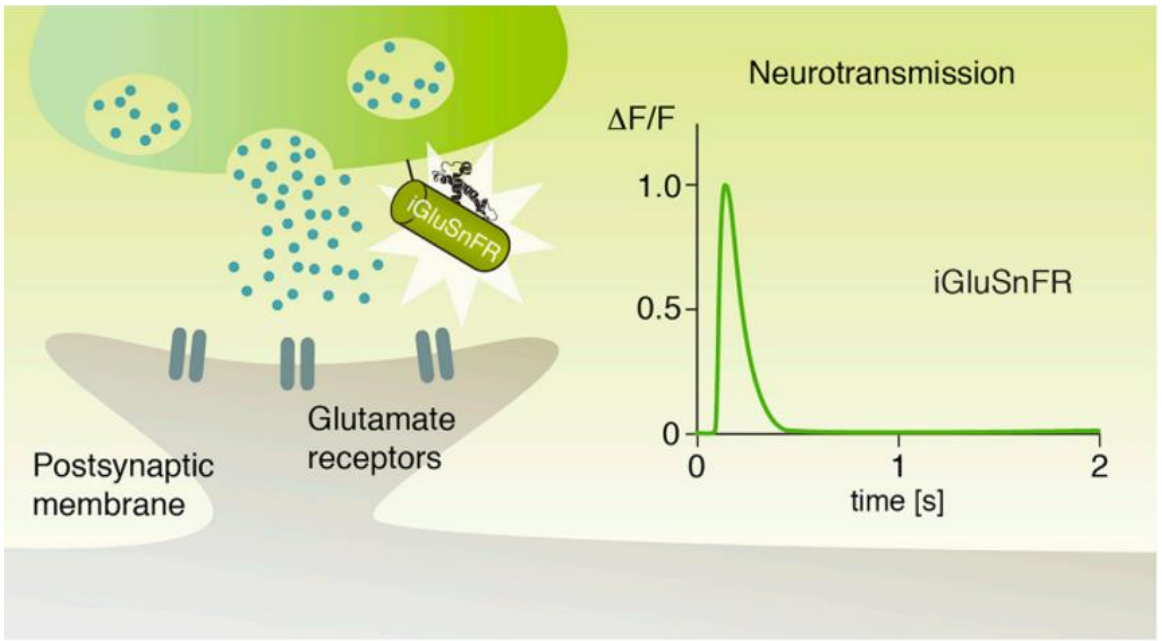

Figure 5. Overview of iGluSnFR fluorescence detection. The iGluSnFR genetic sensor allows for high temporal and spatial measurement of glutamate from a glutamate-binding protein coupled to a fluorescence signal. Typically, a 2-photon microscope is used to allow fast, high-resolution imaging *in vitro* or *in vivo* in *Drosophila*. Taken from Richter et al., iScience 7, 85–95 September 28, 2018 https://doi.org/10.1016/ j.isci.2018.08.019

5.3 Final Remarks

Overall, this dissertation improved serotonin FSCV detection and demonstrated how FSCV and optogenetics could be used to elucidate different antidepressant mechanisms of action in *Drosophila*. Previously, the Jackson waveform and Nafion-coated CFMEs were used to explore basic SSRI concentration and release changes in mammals. However, they caused severe electrode fouling and limited temporal resolution. In this thesis, Chapter 2 improved serotonin FSCV detection by investigating different waveform parameters and offering a tool-box of waveforms to measure serotonin in different experiments. With Chapters 3 and 4, we used our improved extended serotonin waveform to compare antidepressant mechanisms of action for SSRIs and ketamine. Specifically, we found that each SSRI antidepressant had individual effects on serotonin release and reuptake based on their SERT affinity. Meanwhile, ketamine did not affect serotonin concentration or release at micro-, sub-asthenic doses, but higher anesthetic doses inhibited SERT to increase serotonin concentrations. Here, our work also shows that serotonin changes are similar to previous data collected in mammals, and that *Drosophila* is a good model to study serotonin and behavior changes with depression because it is easier and faster to create

genetic mutations in this model. Altogether, these works create a variety of FSCV serotonin waveforms that can be used to understand the neurochemistry and neurobiology of depression treatments and behaviors in *Drosophila*. Additionally, our work creates a cornerstone of real-time serotonin and behavioral measurement in *Drosophila* larvae that can be expanded upon in the future to understand age-related depression and neurodegenerative effects with novel techniques in adult *Drosophila* that will help research in mammals. Ultimately, these technological developments will facilitate new and exciting research on the neuromodulatory roles of serotonin and its genetic effects on pharmacological treatments for depression and other important illnesses.

5.4 References

(1) Takmakov, P.; Zachek, M. K.; Keithley, R. B.; Walsh, P. L.; Donley, C.; McCarty, G. S.; Wightman, R. M. Carbon Microelectrodes with a Renewable Surface. *Analytical chemistry* **2010**, *82* (5), 2020–2028. https://doi.org/10.1021/ac902753x.

(2) Ross, A. E.; Venton, B. J. Sawhorse Waveform Voltammetry for Selective Detection of Adenosine, ATP, and Hydrogen Peroxide. *Analytical Chemistry* **2014**, *86* (15), 7486–7493. https://doi.org/10.1021/ac501229c.

(3) Keithley, R. B.; Takmakov, P.; Bucher, E. S.; Belle, A. M.; Owesson-White, C. A.; Park, J.; Wightman, R. M. Higher Sensitivity Dopamine Measurements with Faster-Scan Cyclic Voltammetry. *Analytical Chemistry* **2011**. https://doi.org/10.1021/ac200143v.

(4) Jackson, B. P.; Dietz, S. M.; Wightman, R. M. Fast-Scan Cyclic Voltammetry of 5-Hydroxytryptamine. *Analytical Chemistry* **1995**, *67* (6), 1115–1120. https://doi.org/10.1021/ac00102a015.

(5) Hashemi, P.; Dankoski, E. C.; Petrovic, J.; Keithley, R. B.; Wightman, R. M. Voltammetric Detection of 5-Hydroxytryptamine Release in the Rat Brain. *Analytical Chemistry* **2009**, *81* (22), 9462–9471. https://doi.org/10.1021/ac9018846.

(6) Dunham, K. E.; Venton, B. J. Improving Serotonin Fast-Scan Cyclic Voltammetry Detection: New Waveforms to Reduce Electrode Fouling. *Analyst* **2020**, *145* (22), 7437–7446. https://doi.org/10.1039/d0an01406k.

(7) Heien, M. L. A. V.; Phillips, P. E. M.; Stuber, G. D.; Seipel, A. T.; Wightman, R. M. Overoxidation of Carbon-Fiber Microelectrodes Enhances Dopamine Adsorption and Increases Sensitivity. *Analyst* **2003**, *128* (12), 1413–1419. https://doi.org/10.1039/b307024g.

(8) Borue, X.; Cooper, S.; Hirsh, J.; Condron, B.; Venton, B. J. Quantitative Evaluation of Serotonin Release and Clearance in Drosophila. *Journal of Neuroscience Methods* **2009**, *179* (2), 300–308. https://doi.org/10.1016/j.jneumeth.2009.02.013.

(9) Borue, X.; Condron, B.; Venton, B. J. Both Synthesis and Reuptake Are Critical for Replenishing the Releasable Serotonin Pool in Drosophila. *Journal of Neurochemistry* **2010**, *113* (1), 188–199. https://doi.org/10.1111/j.1471-4159.2010.06588.x.

(10) Movassaghi, C. S.; Perrotta, K. A.; Yang, H.; Iyer, R.; Cheng, X.; Dagher, M.; Fillol, M. A.; Andrews, A. M. Simultaneous Serotonin and Dopamine Monitoring across Timescales by Rapid Pulse Voltammetry with Partial Least Squares Regression. *Anal Bioanal Chem* **2021**, *413* (27), 6747–6767. https://doi.org/10.1007/s00216-021-03665-1.

(11) Shin, H.; Goyal, A.; Barnett, J. H.; Rusheen, A. E.; Yuen, J.; Jha, R.; Hwang, S. M.; Kang, Y.; Park, C.; Cho, H.-U.; Blaha, C. D.; Bennet, K. E.; Oh, Y.; Heien, M. L.; Jang, D. P.; Lee, K. H. Tonic Serotonin Measurements *In Vivo* Using N-Shaped Multiple Cyclic Square Wave Voltammetry. *Anal. Chem.* **2021**, *93* (51), 16987–16994. https://doi.org/10.1021/acs.analchem.1c02131.

(12) Stucky, C.; Johnson, M. A. Improved Serotonin Measurement with Fast-Scan Cyclic Voltammetry: Mitigating Fouling by SSRIs. *Journal of The Electrochemical Society* **2022**, *169* (4), 045501. https://doi.org/10.1149/1945-7111/ac5ec3.

(13) Dunham, K. E.; Venton, B. J. SSRI Antidepressants Differentially Modulate Serotonin Reuptake and Release in Drosophila. *Journal of Neurochemistry* **2022**, No. June, 1–13. https://doi.org/10.1111/jnc.15658.

(14) Hidalgo, S.; Molina-Mateo, D.; Escobedo, P.; Zárate, R. V.; Fritz, E.; Fierro, A.; Perez, E. G.; Iturriaga-Vasquez, P.; Reyes-Parada, M.; Varas, R.; Fuenzalida-Uribe, N.; Campusano, J. M. Characterization of a Novel Drosophila SERT Mutant: Insights on the Contribution of the Serotonin Neural System to Behaviors. *ACS Chemical Neuroscience* **2017**, *8* (10), 2168–2179. https://doi.org/10.1021/acschemneuro.7b00089.

(15) Ribaudo, G.; Bortoli, M.; Witt, C. E.; Parke, B.; Mena, S.; Oselladore, E.; Zagotto, G.; Hashemi, P.; Orian, L. ROS-Scavenging Selenofluoxetine Derivatives Inhibit In Vivo Serotonin Reuptake. *ACS Omega* **2021**. https://doi.org/10.1021/acsomega.1c05567.

(16) Wood, K. M.; Hashemi, P. Fast-Scan Cyclic Voltammetry Analysis of Dynamic Serotonin Reponses to Acute Escitalopram. *ACS Chemical Neuroscience* **2013**, *4* (5), 715–720. https://doi.org/10.1021/cn4000378.

(17) Wood, K. M.; Zeqja, A.; Nijhout, H. F.; Reed, M. C.; Best, J.; Hashemi, P. Voltammetric and Mathematical Evidence for Dual Transport Mediation of Serotonin Clearance in Vivo. *Journal of Neurochemistry* **2014**, *130* (3), 351–359. https://doi.org/10.1111/jnc.12733.
(18) Owens, M. J.; Knight, D. L.; Nemeroff, C. B. Second-Generation SSRIs: Human Monoamine Transporter Binding Profile of Escitalopram and R-Fluoxetine. *Biological Psychiatry* **2001**, *50* (5), 345–350. https://doi.org/10.1016/S0006-3223(01)01145-3.
(19) Rannversson, H.; Andersen, J.; Bang-Andersen, B.; Strømgaard, K. Mapping the Binding Site for Escitalopram and Paroxetine in the Human Serotonin Transporter Using Genetically Encoded Photo-Cross-Linkers. *ACS Chemical Biology* **2017**, *12* (10), 2558–2562. https://doi.org/10.1021/acschembio.7b00338.
(20) Rodriguez, G. J.; Roman, D. L.; White, K. J.; Nichols, D. E.; Barker, E. L. Distinct Recognition of Substrates by the Human and Drosophila Serotonin Transporters. *Journal of Pharmacology and Experimental Therapeutics* **2003**, *306* (1), 338–346. https://doi.org/10.1124/jpet.103.048751.
(21) Demchyshyn, L. L.; Pristupa, Z. B.; Sugamori, K. S.; Barker, E. L.; Blakely, R. D.; Wolfgang, W. J.; Forte, M. A.; Niznik, H. B. Cloning, Expression, and Localization of a Chloride-Facilitated, Cocaine-Sensitive Serotonin Transporter from Drosophila Melanogaster. *Proceedings of the National Academy of Sciences of the United States of America* **1994**, *91* (11), 5158–5162. https://doi.org/10.1073/pnas.91.11.5158.
(22) Kraus, C.; Wasserman, D.; Henter, I. D.; Acevedo-Diaz, E.; Kadriu, B.; Zarate, C. A. The Influence of Ketamine on Drug Discovery in Depression. *Drug Discovery Today* **2019**, *24* (10), 2033–2043. https://doi.org/10.1016/j.drudis.2019.07.007.
(23) Stahl, S. M. Mechanism of Action of Ketamine. *CNS Spectrums* **2013**, *18* (4), 171–174. https://doi.org/10.1017/S109285291300045X.
(24) Pham, T. H.; Mendez-David, I.; Defaix, C.; Guiard, B. P.; Tritschler, L.; David, D. J.; Gardier, A. M. Ketamine Treatment Involves Medial Prefrontal Cortex Serotonin to Induce a Rapid Antidepressant-like Activity in BALB/CJ Mice. *Neuropharmacology* **2017**, *112*, 198–209. https://doi.org/10.1016/j.neuropharm.2016.05.010.
(25) Majeed, Z. R.; Abdeljaber, E.; Soveland, R.; Cornwell, K.; Bankemper, A.; Koch, F.; Cooper, R. L. Modulatory Action by the Serotonergic System: Behavior and Neurophysiology in Drosophila Melanogaster. *Neural Plasticity* **2016**, *2016*. https://doi.org/10.1155/2016/7291438.
(26) Huser, A.; Eschment, M.; Güllü, N.; Collins, K. A. N.; Böpple, K.; Pankevych, L.; Rolsing, E.; Thum, A. S. Anatomy and Behavioral Function of Serotonin Receptors in Drosophila Melanogaster Larvae. *PLoS ONE* **2017**, *12* (8), 1–27. https://doi.org/10.1371/journal.pone.0181865.
(27) Tadres, D.; Louis, M. PiVR: An Affordable and Versatile Closed-Loop Platform to Study Unrestrained Sensorimotor Behavior. *PLoS Biology* **2020**, *18* (7), 1–25. https://doi.org/10.1371/journal.pbio.3000712.
(28) Shell, B. C.; Schmitt, R. E.; Lee, K. M.; Johnson, J. C.; Chung, B. Y.; Pletcher, S. D.; Grotewiel, M. Measurement of Solid Food Intake in Drosophila via Consumption-Excretion of a Dye Tracer. *Scientific Reports* **2018**, *8* (1), 1–13. https://doi.org/10.1038/s41598-018-29813-9.
(29) Bowman, M. A.; Vitela, M.; Clarke, K. M.; Koek, W.; Daws, L. C. Serotonin Transporter and Plasma Membrane Monoamine Transporter Are Necessary for the Antidepressant-like Effects of Ketamine in Mice. *International Journal of Molecular Sciences* **2020**, *21* (20), 1–22. https://doi.org/10.3390/ijms21207581.
(30) Wan, J.; Peng, W.; Li, X.; Qian, T.; Song, K.; Zeng, J.; Deng, F.; Hao, S.; Feng, J.; Zhang, P.; Zhang, Y.; Zou, J.; Pan, S.; Zhu, J. J.; Jing, M.; Xu, M.; Li, Y. A Genetically Encoded GRAB Sensor for Measuring Serotonin Dynamics in Vivo. *bioRxiv* **2020**, 2020.02.24.962282. https://doi.org/10.1101/2020.02.24.962282.
(31) Hamdan, S. K.; Zain, Z. M. In Vivo Electrochemical Biosensor for Brain Glutamate Detection: A Mini Review. *Malaysian Journal of Medical Sciences* **2014**, *21*, 11–25.
(32) Nagarkar-Jaiswal, S.; Lee, P. T.; Campbell, M. E.; Chen, K.; Anguiano-Zarate, S.; Gutierrez, M. C.; Busby, T.; Lin, W. W.; He, Y.; Schulze, K. L.; Booth, B. W.; Evans-Holm, M.; Venken, K. J. T.; Levis, R. W.; Spradling, A. C.; Hoskins, R. A.; Bellen, H. J. A Library of MiMICs Allows Tagging of Genes and Reversible, Spatial and Temporal Knockdown of Proteins in Drosophila. *eLife* **2015**, *2015* (4), 1–28. https://doi.org/10.7554/eLife.05338.
(33) Alekseyenko, O. V.; Lee, C.; Kravitz, E. A. Targeted Manipulation of Serotonergic Neurotransmission Affects the Escalation of Aggression in Adult Male Drosophila Melanogaster. *PLoS ONE* **2010**, *5* (5), e10806. https://doi.org/10.1371/journal.pone.0010806.
(34) Jenett, A.; Rubin, G. M.; Ngo, T.-T. B.; Shepherd, D.; Murphy, C.; Dionne, H.; Pfeiffer, B. D.; Cavallaro, A.; Hall, D.; Jeter, J.; Iyer, N.; Fetter, D.; Hausenfluck, J. H.; Peng, H.; Trautman, E. T.; Svirskas, R. R.; Myers, E. W.; Iwinski, Z. R.; Aso, Y.; DePasquale, G. M.; Enos, A.; Hulamm, P.; Lam, S. C. B.; Li, H.-H.; Laverty, T. R.; Long, F.; Qu, L.; Murphy, S. D.; Rokicki, K.; Safford, T.; Shaw, K.; Simpson, J. H.; Sowell, A.; Tae, S.; Yu, Y.; Zugates, C. T. A GAL4-Driver Line Resource for Drosophila Neurobiology. *Cell Reports* **2012**, *2* (4), 991–1001. https://doi.org/10.1016/j.celrep.2012.09.011.
(35) Shin, M.; Venton, B. J. Electrochemical Measurements of Acetylcholine-Stimulated Dopamine Release in Adult Drosophila Melanogaster Brains. *Analytical Chemistry* **2018**, *90* (17), 10318–10325. https://doi.org/10.1021/acs.analchem.8b02114.

(36) Hidalgo, S.; Fuenzalida-Uribe, N.; Molina-Mateo, D.; Escobar, A. P.; Oliva, C.; España, R. A.; Andrés, M. E.; Campusano, J. M. Study of the Release of Endogenous Amines in Drosophila Brain in Vivo in Response to Stimuli Linked to Aversive Olfactory Conditioning. *Journal of Neurochemistry* **2020**, 0–1. https://doi.org/10.1111/jnc.15109.
(37) Pyakurel, P.; Shin, M.; Venton, B. J. Nicotinic Acetylcholine Receptor (NAChR) Mediated Dopamine Release in Larval Drosophila Melanogaster. *Neurochemistry International* **2018**, *114*, 33–41. https://doi.org/10.1016/j.neuint.2017.12.012.
(38) Shin, M.; Venton, B. J. Fast-Scan Cyclic Voltammetry (FSCV) Reveals Behaviorally-Evoked Dopamine Release by Sugar Feeding in Adult Drosophila Mushroom Body. *Angewandte Chemie International Edition* **2022**, *n/a* (n/a). https://doi.org/10.1002/anie.202207399.
(39) Silva, B.; Goles, N. I.; Varas, R.; Campusano, J. M. Serotonin Receptors Expressed in Drosophila Mushroom Bodies Differentially Modulate Larval Locomotion. *PLoS ONE* **2014**, *9* (2). https://doi.org/10.1371/journal.pone.0089641.
(40) Fakhoury, M. Revisiting the Serotonin Hypothesis: Implications for Major Depressive Disorders. *Molecular Neurobiology* **2016**, *53* (5), 2778–2786. https://doi.org/10.1007/s12035-015-9152-z.
(41) Dumitrescu, E.; Copeland, J. M.; Venton, B. J. *Parkin* Knockdown Modulates Dopamine Release in the Central Complex, but Not the Mushroom Body Heel, of Aging *Drosophila*. *ACS Chem. Neurosci.* **2023**, *14* (2), 198–208. https://doi.org/10.1021/acschemneuro.2c00277.
(42) Marvin, J. S.; Scholl, B.; Wilson, D. E.; Podgorski, K.; Kazemipour, A.; Muller, J. A.; Schoch, S.; Quiroz, F. J. U.; Rebola, N.; Bao, H.; Little, J. P.; Tkachuk, A. N.; Cai, E.; Hantman, A. W.; Wang, S. S.-H.; DePiero, V. J.; Borghuis, B. G.; Chapman, E. R.; Dietrich, D.; DiGregorio, D. A.; Fitzpatrick, D.; Looger, L. L. Stability, Affinity, and Chromatic Variants of the Glutamate Sensor IGluSnFR. *Nature methods* **2018**, *15* (11), 936–939. https://doi.org/10.1038/s41592-018-0171-3.
(43) Richter, F. G.; Fendl, S.; Haag, J.; Drews, M. S.; Borst, A. Glutamate Signaling in the Fly Visual System. *iScience* **2018**, *7*, 85–95. https://doi.org/10.1016/j.isci.2018.08.019.

Appendix

List of publications for this dissertation

1. **Dunham, K.E**. and Venton, B.J. 2020. Improving serotonin fast-scan cyclic voltammetry detection: new waveforms to reduce electrode fouling. *Analyst*. DOI: 10.1039/d0an01406k

2. **Dunham, K.E**. and Venton, B.J. 2022. SSRI antidepressants differentially modulate serotonin reuptake and release in *Drosophila*. 2022. *Journal of Neurochemistry*. DOI: 10.1111/jnc.15658.

List of fly lines used in this dissertation

1. UAS-CsChrimson (III) – Stockline #55136 Bloomington (BL) Drosophila Stock Center, Bloomington, IN, Ch. 2-4
2. Tph-Gal4 (II) – Dr. Jay Hirsh, UVA Biology, Charlottesville, VA, Ch. 2
3. Trh-Gal4 (III) – #38389 BL, Ch. 3-4
4. Trh-Gal4 (II) - Dr. Jay Hirsh, UVA Biology, Charlottesville, VA (balanced crosses for Ch. 5)
5. SERT Mutant #1 (II) – #36004 BL, Ch. 5
6. 5-HT1A RNAi knockdown (III) – #25834 BL, Ch. 5
7. 5-HT1A RNAi knockdown (III) – #33885 BL, Ch. 5
8. 5-HT1A RNAi knockdown (III) – #25834 BL, Ch. 5
9. 5-HT1B RNAi knockdown (III) – #25833 BL, Ch. 5
10. 5-HT1B RNAi knockdown (III) – #33418 BL, Ch. 5
11. 5-HT1B RNAi knockdown (II) – #51842 BL, Ch. 5
12. 5-HT1B RNAi knockdown (II) – #54006 BL, Ch. 5
13. UAS-iGluSnFR (III) – #59609 BL, Ch. 5
14. UAS-iGluSnFR (III) – #59610 BL, Ch. 5
15. UAS-5-HT1 GRAB sensor (III) – #90874 BL, Ch. 5